DOCTORAL THESIS

Regulation of MHC II protein expression by lysosomal degradation and vitamin D

Shah, Nakul

Award date:
2019

Awarding institution:
University of Roehampton

Regulation of MHC II protein expression by lysosomal degradation and vitamin D

by

Nakul Shah (B-tech, M-tech)

A thesis submitted in partial fulfilment of the requirements for the degree of PhD

Department of Life Sciences

Roehampton University

2018

Abstract

Major histocompatibility complex class II (MHC II) proteins display peptides to CD4+ T cells. Their regulation of expression is important for normal immune function and autoimmunity. Two aspects of this were explored here. Expression of HLA-DR, the major human MHCII isoform, was manipulated in immortalised antigen-presenting cells (APCs), and characterised by qRT-PCR, flow cytometry and Western blot. Mass spectrometry was used to quantify expression changes of polymorphic HLA-DR beta chain variants. First, the mechanism of DR proteolysis was elucidated. MHCII degradation had been shown to be regulated by ubiquitylation and peptide loading. This study showed that cathepsin D (Cat D), a lysosomal aspartyl protease, degrades DR molecules not associated with peptide or invariant chain. Interestingly, when Cat D activity was ablated, APCs eventually restored wild-type DR levels, using feedback mechanisms that remain to be explored. Secondly, the effects of vitamin D and retinoic acid (RA) on DR expression were explored. Previous work had shown both indirect effects on DR levels and transactivation of some DRB allelic variants by vitamin D. This study revealed synergistic actions of RA and vitamin D on DR expression by myeloid model APCs but mutual antagonism in lymphoblastoid cells, and suggested that DR beta-chain copy number variants may be regulated discordantly. This work suggests that in physiological DR protein turnover, Cat D attacks the groove of DR molecules that lost bound peptide, mediating quality control of antigen presentation. This could mitigate against autoimmunity by limiting unconventional presentation pathways independent of invariant chain or HLA-DM. The small size of the vitamin D and RA effects on DR argues against a major role in autoimmunity, with the possible exception of the unusual DRB1*15-DRB5*01 MS risk haplotype. Novel tools were generated for the quantification of codominant expression of DR allelic and copy number variants, which will be useful in extending this work to primary APCs.

Contents

List of Figures

List of Tables

List of Abbreviations

1, 25(OH) D3- 1, 25 dihydroxyvitamin D

AEBSF- 4-(2-aminoethyl) benzenesulfonyl fluoride hydrochloride

AEP- Asparaginyl endopeptidase

AGE- Agarose gel electrophoresis

AML- Acute myeloid leukemia

APC - Antigen-presenting cell

APS- Ammonium per Sulphate

ATPase- Adenylpyrophosphatase

BBB- Blood Brain Barrier

BCA - Bicinchoninic acid assay

Cat – Cathepsin

CLIP - Class II-associated invariant chain peptides

CIITA- Class II transactivator

CNS- Central Nervous System

Ct- Cycle threshold

CSF- Cerebrospinal Fluid

DCs- Dendritic cells

DMSO- Dimethyl sulfoxide

DMTs- Disease Modifying Therapies

DNA- Deoxyribonucleic acid

EAE- Experimental Autoimmune Encephalomyelitis

EBV - Epstein-Barr virus

ER- Endoplasmic reticulum

FACS- Fluorescence-activated cell sorting

FBS- Fetal Bovine Serum

FITC- Fluorescein isothiocyanate

GILT- Gamma-interferon Inducible Lysosomal Thiol reductase

GWAS- Genome-wide association studies

HLA - Human leukocyte antigen

HIFBS- Heat-inactivated fetal bovine serum

HTCs- Homozygote Typing Cells

HRP- Horseradish Peroxidase

ICAT- Isotope-Coded protein labels

Ii - Invariant chain

IMDM- Iscove's Modified Dulbecco's Medium

kDa - Kilo Dalton

LCMS- Liquid Chromatography–Mass Spectrometry

MARCH - Membrane-associated really interesting new gene protein

MBP - Myelin Basic Protein

MHC - Major histocompatibility complex molecules

MIIC- MHC class II compartment

MFI- Mean Fluorescence Intensity

MMP- Matrix Metalloproteinase

MoDCs- Monocyte-derived dendritic cells

MOG- Myelin Oligodendrocyte Glycoprotein

MOI- Multiplicity of infection

MRI- Magnetic Resonance Imaging

MS- Multiple Sclerosis

MQ- MaxQuant

NMS- Normal mouse serum

Pep A- Pepstatin A

Pep a-p- Pepstatin A penetratin

PBS- Phosphate buffer saline

PD – Proteome Discover

PLPs- Proteolipid Proteins

PMSF- Phenylmethylsulfonyl fluoride

PVDF- Polyvinylidene difluoride

qRTPCR – Real time reverse transcription polymerase chain reaction

RA- Retinoic Acid

RAR- Retinoic A Receptor

RIPA-Radio-immunoprecipitation assay buffer

RNA - Ribonucleic acid

RPMI- Roswell Park Memorial Institute medium

RXR- Retinoic X Receptor

SILAC- Stable Isotope Labelling of Amino acid in Cultures

SD- Standard Deviation

SDS-PAGE - Sodium Dodecyl Sulphate-Polyacrylamide Gel Electrophoresis

US- Unstained

TECs- Thymic epithelial cells

TEMED- Tetramethylethylenediamine

TCR - T-cell receptor

TNF - Tumour Necrosis Factor

VDR- Vitamin D receptor

VDRE- Vitamin D response element

VDP- Vitamin D Binding Protein

VSVG- Vesicular stomatitis virus glycoprotein

WB - Western blot

Acknowledgement

"*If I have seen further, it is only by standing on the shoulders of giants.*"
– Sir Isaac Newton, 1676

The completion of this thesis would not have been possible without the contributions and support of so many others. First and foremost, I would like to thank my supervisors, Dr Robert Busch and Professor Jolanta Opacka-Juffry. I feel incredibly privileged to have benefited from the mentorship of such accomplished and wonderfully complementary supervisors.

I thank Dr Busch for providing me the opportunity to undertake my PhD in his lab. He has provided invaluable guidance and direction while also affording me a great deal of independence. I am also thankful to him for instilling in me a deep respect and interest in both statistical methods and scientific rigour. His open door policy has resulted in countless thought-provoking conversations that have both motivated me to challenge commonly held opinions and shaped the way I approach new research questions.

I am also very grateful to Professor Opacka-Juffry for her unceasing encouragement and enthusiasm. She is a generous, caring, visionary mentor who sets a high standard for achievement. I thank her for inspiring me to strive and also settling for nothing less than excellence in my endeavours.

I gratefully acknowledge the organizations that have provided financial support for this work: Multiple Sclerosis Society of the UK (MS Society), MS International Federation (MSIF) and Roehampton University for the grants that supported my research. I am also thankful to Graduate School at Roehampton University for all the research and training network programmes which provided numerous resources and opportunities throughout my doctorate journey for which I am especially grateful.

Thank you to all of our collaborators at Cambridge Centre for Proteomics and Anthony Nolan Cancer Institute. I would like to offer specific thanks to all members of Dr Mike Deery's

team at the Cambridge Centre for Proteomics for being prompt in running samples through the mass spectrometer. I am grateful of Professor Steve Marsh and Dr Neema Mayor from the Anthony Nolan Cancer Institute for providing homozygous typing cells for the work and their valuable advice.

I would also like to take opportunity to thank all the members of the Health Science Research Centre (HSRC) at Roehampton University for their thoughtful feedback during lab meetings and in the seminar series. I am also pleased to acknowledge the contributions of Research Student Review Board (RSRB) and thank them for their guidance and for bringing focus to my pursuits.

I wish to thank the technical staff at HSRC for their support in maintaining the lab standards and also for their kind help in fulfilling my lab needs and supplies. I would also like to thank the past members of Dr Busch's lab for providing some of the foundations of this work. I would also like to thank Dr Sandeepan Mukherjee from Haffkine Institute, India for providing inspirational first research experiences during my early work days. I thank all of those with whom I have maintained friendships from my days in Roehampton; the many fun times we have shared during my PhD have left me refreshed and ready to return to my lab with renewed focus and drive. So many others have contributed in making my dreams come true I take this opportunity to express my sincere thanks to all of them.

I can never thank my family, especially my MA and PAA for their support in getting me to this stage and also shaping who I am today. They were always with me during the difficult times and many things would have been left incomplete without their help. I also would like to thanks Dhwani for tolerating me, for always being there when I needed you.

Above all I submit myself to the Almighty who has been with me in this endeavour and showered me with His bountiful blessings.

Gratitude is the memory of the heart and thanks to you all for giving such wonderful memories…

Chapter 1: General Introduction

1.1 Scope of thesis

This thesis investigates the regulation of antigen presentation to helper T cells. This is an important process in immune recognition that bridges innate and adaptive immunity, whereby antigen presenting cells (APCs) capture antigens and display them in peptide form on the cell surface in association with major histocompatibility complex class II (MHC II) molecules (Penn and Ilmonen, 2001). The resultant complex can be recognised by helper T cells via their T cell antigen receptor (Neefjes et al., 2011). This process provides a mechanism of communication between innate and adaptive immune cells about the presence of specific pathogens in the context of normal host defence and also seems to be the focus of disease mechanisms in auto-immunity. In both contexts it is very important to know how the expression of MHC II molecules is regulated by transcriptional and post transcriptional mechanisms and by their extensive genetic polymorphism.

The first part of this thesis characterises the specific enzymes involved in the breakdown process of MHC II molecules and its relation to peptide binding. The second part explores the effects of vitamin D and retinoic acid on the expression of HLA-DR allelic and gene variants. Both processes are of potential relevance to the pathogenesis of autoimmune diseases. Previous work has postulated links mechanisms of autoimmunity with aberrant turnover of MHC II molecules (Busch et al., 2005) or to the effects of vitamin D on MHC II protein expression (Ramagopalan and Ebers, 2009). The work set out in this thesis informs such hypotheses.

1.2 Immune System

The human body is continuously challenged by infectious agents, such as bacteria, viruses, fungi, parasitic worms, etc., of which some are pathogenic, and their own survival can lead to the disease or death of the host. A defence network has evolved in living organisms, including humans, ensuring protection against such foreign agents, commonly known as the immune system (Barber, 1980, Travis, 2009). It is able to generate an enormous diversity of cells and molecules capable of specifically recognizing the large variety of such invading pathogens. Generally it is divided into two branches, the innate immune system and the adaptive immune system (Warrington et al., 2011), but it consists of several biological effector mechanisms. The major agents of both the branches are shown in Figure 1.1.

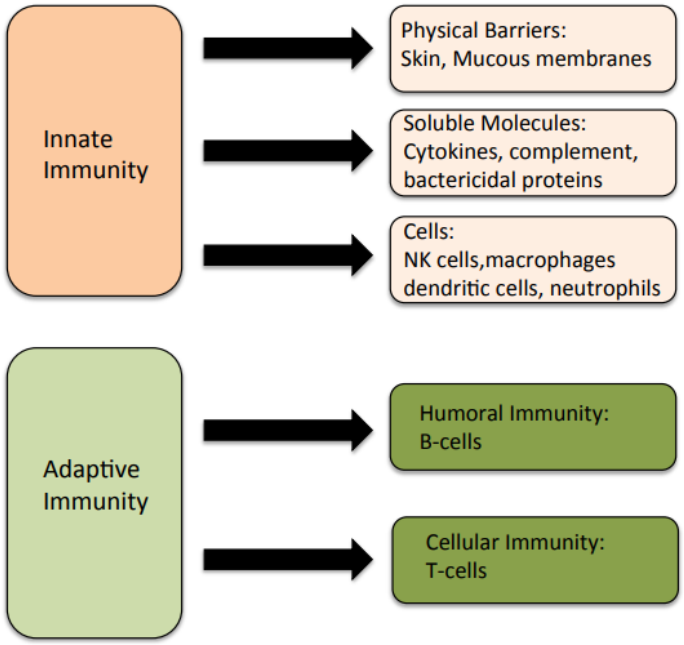

Figure 1.1 Overview of the Innate and Adaptive Immune Systems. The main elements of both the innate and adaptive arms of the human immune system.

Host defence begins with physical barriers such as the skin and mucous membranes, which form the first line of defence and are fundamental to innate immunity (Turvey and Broide, 2010). Additionally, barrier immunity employs chemical defences, such as antibacterial

enzymes in secretions (mucus, saliva, tears) and stomach acid, which produce an environment that is difficult for pathogenic organisms to infiltrate. If pathogens do breach the body's physical and chemical barriers, the innate immune system can launch a prompt non-specific response (Turvey and Broide, 2010). Immune cells such as neutrophils, macrophages, and natural killer (NK) cells are recruited to the primary infection site (Hoffmann and Akira, 2013). The role of these cells is to capture and destroy invading pathogens and to clear damaged or infected host cells. The innate immune system uses germline-encoded pattern recognition receptors (PRRs) that survey both the extracellular and intracellular space for conserved microbial determinants to detect pathogens (Brubaker et al., 2015).

If the innate response cannot clear the pathogen, then cells of the adaptive immune system are recruited. A hallmark of the adaptive immune system is the ability to identify specific antigens, which are unique structures found within pathogens or their products (Mackay and von Andrian, 2001). The adaptive immune cells responsible for this specific recognition are lymphocytes (Wherry and Masopust, 2016). Lymphocytes are divided into B and T cells, based on their locations during development and maturation, and their antigen recognition. Both B and T cells recognize specific antigens (Ag) via clonally variable cell surface receptors. The B cell receptor is a cell surface bound antibody and can recognize whole antigen. In contrast, the αβ-T cell receptor (TCR) can only recognize processed antigens when bound to molecules known as major histocompatibility complex (MHC) molecules (Davis and Bjorkman, 1988). An alternative γδ-TCR exists but its main focus does not seem to be MHC molecules (Vantourout and Hayday, 2013). Unlike innate immune cells, this antigen receptors are not fixed by germ-line encoded sequences; instead, they are somatically generated or 'custom made' via gene-shuffling events that occur during their development (Bonilla and Oettgen, 2010).

Immune cells that take up an Ag and process it into a form recognized by, or serve to activate, specific helper T cells are known as professional antigen presenting cells (APCs). B cells function as APCs by processing whole Ag into antigenic fragments and displaying those fragments via MHC molecules to T cells (Chaplin, 2010). Other APCs that play critical roles in the immune system are macrophages and dendritic cells (DCs). DCs play a crucial role in linking innate and adaptive immunity. Immature DCs migrate from the blood into various tissues and specialize in phagocytosis (Alvarez et al., 2008). When they encounter an antigen, they rapidly mature and migrate to lymphoid tissues where they carry out antigen presentation to T cells (Sallusto and Lanzavecchia, 2002).

1.3 Major histocompatibility complex (MHC)

MHC glycoproteins are a family of cell surface molecules, which are encoded by MHC genes (Penn and Ilmonen, 2001). The major function of MHC glycoproteins is to bind peptides derived from pathogens in a groove-shaped peptide-binding site and display them on the cell surface for recognition by T cells (Holling et al., 2004). The MHC molecules thus play a fundamental role in the immune system (Mak and Saunders, 2006). The importance of MHC genes in the immune response was first determined from studies using inbred mouse strains performed by George Snell (Snell, 1948) and inspired by earlier investigations by Peter Gorer (Gorer, 1937, Gorer and Schütze, 1938). Jean Dausset subsequently described the human MHC (Dausset, 1981).

The MHC is a 7.6 Mbp multi-locus region of the genome, located on the short arm of chromosome 6 in humans (Mungall et al., 2003, Horton et al., 2004). In humans, MHC molecules are also known as human leukocyte antigens (HLA). This term was coined due to the observation that antibodies identifying MHC molecules targeted polymorphic antigens on leukocytes (Thorsby, 2009). There are more than 200 genes in the coding region, which can

be categorized into three basic groups: MHC class I (MHC I), MHC class II (MHC II) and MHC class III (MHC III) (Erickson, 1987). MHC I molecules are expressed by most nucleated cells, where they present mainly endogenous peptide on the cell surface to CD8+ T cells (cytotoxic T lymphocytes) (Natarajan et al., 1999a). MHC II molecules are presented on specialized APCs like macrophages, dendritic cells and B cells. During infection, they present exogenous peptides to CD4+ T cells (Pulendran, 2005). Lastly, the MHC III region plays a role in various aspects of innate immunity by encoding complement proteins, inflammatory cytokines such as tumour necrosis factor α, and heat shock proteins (Hauptmann and Bahram, 2004).

1.3.1 Structure of MHC II molecules

MHC II molecules contain two different polypeptide chains, a 33 kDa α chain and a 28 kDa β chain, which are associated by noncovalent interactions (Cole, 2013). MHC II molecules are membrane-bound glycoproteins that contain external domains, a transmembrane segment, and a cytoplasmic anchor segment as shown in Figure 1.2. Each chain in a MHC II molecule contains two external domains: α1 and α2 domains in one chain and β1 and β2 domains in the other chain. The membrane-proximal α2 & β2 domains bear sequence homology to the immunoglobulin fold structure (Kaufman et al., 1984). The membrane-distal portion of a MHC II molecule is composed of the α1 & β1 domains and forms the antigen binding cleft for processed antigen (Ferrante, 2013). MHC II proteins possess a single, open-ended peptide binding groove, which accommodates peptides with a 9-amino acid central core and C- and N- terminal overhangs of varying lengths (Brown et al., 1993). Most peptides naturally binding to MHC II molecules are approximately 13-25 residues in length (Jardetzky et al., 1991, Chicz et al., 1992). Certain anchor residues are preferentially found within the core (typically at relative positions 1, 4, 6, 7 and 9 depending on the allele), where they make

complementary contacts with specificity pockets lining the groove. Other residues may vary widely, thus allowing MHC II molecules to bind thousands of peptides, so long as they satisfy the binding preferences of the anchor residues (Rammensee, 1995). Allelic variants of MHC II molecules diversify the peptide binding groove with little impact on the tertiary structure, thus giving each variant a unique peptide binding repertoire (albeit with some overlap).

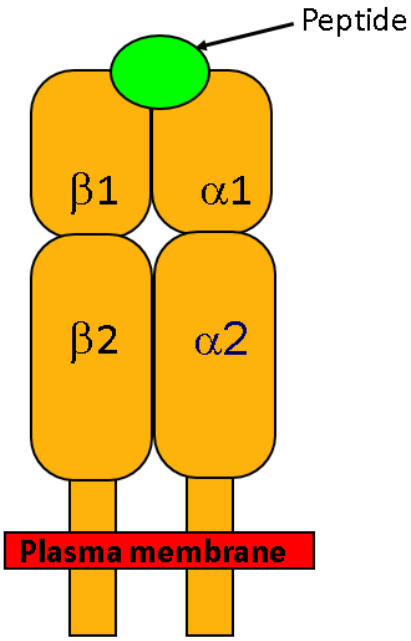

Figure 1.2 Basic structure of a MHC II molecule. MHC class II molecules consist of two non-covalently associated non-identical polypeptide chains, the α-chain and the β-chain.

MHC class II molecules have a relatively restricted pattern of expression due to the regulation by Class II transactivator (CIITA) (Masternak et al., 2000, LeibundGut-Landmann et al., 2004) which limits the expression MHC II to APCs or tissue cells that have been induced with pro-inflammatory cytokines. CIITA controls the gene transcription by a complex of DNA-binding proteins in the promoter region. Vitamin D can also modify the expression of MHC II transcriptionally by binding to the vitamin D response element

(VDRE) also present in the promoter region (Ramagopalan et al., 2009). This aspect of regulation is discussed further in the introduction towards Chapter 5.

1.3.2 MHC II Antigen processing and presentation

Classical MHC II molecules bind peptides generated in endocytic compartments of APCs and present them at the cell surface, where they engage with clonally variable T cell receptors (TCRs) on T cells expressing the co-receptor CD4 (Neefjes et al., 2011). This is critical in the generation of an effective adaptive immune response, with CD4+ T helper cells acting to co-ordinate and activate other immune effectors (Zhu and Paul, 2010); during positive and negative selection of thymocytes in the thymus (central tolerance); as well as in peripheral tolerance and immune regulation (Morris and Allen, 2012). The generation of peptides from native protein antigens is commonly referred to as antigen processing, whereas the display of the peptides at the cell surface by the MHC molecule is referred to as antigen presentation (Mellman et al., 1998).

The individual α and β chains of MHC II are synthesised and assembled in the endoplasmic reticulum (ER), where they associate with invariant chain (Ii) (Roche and Cresswell, 1990, Cosson and Bonifacino, 1992). The peptide binding groove of the MHC II molecule is blocked by a disordered region of Ii, thus preventing ER polypeptides from associating with the groove (Busch et al., 1996). MHC II/Ii complexes then exit the ER and accumulate transiently in late endosomal compartments under the direction of the cytoplasmic tail of Ii (Busch and Mellins, 1996). Earlier work suggested that an Ii trimer associates with three αβ heterodimers to form a nonamer, but more recent evidence suggests that once a pentameric complex has formed (an Ii trimer and a single αβ heterodimer), binding of additional MHC II is inhibited as the complex bends towards the cell membrane (Koch et al., 2011). In any case, MHC II/Ii complexes are transported to endocytic compartments, where Ii chain is

sequentially degraded, first by aspartic proteases to give the p22 degradation intermediate, and then by the cysteine proteases, cathepsin L and S, to yield both the p10 intermediate and, finally, class II-associated Ii peptides (CLIP) (Marić et al., 1994, Hsing and Rudensky, 2005). However, the initiating role of aspartyl proteases in Ii removal is not universally accepted and may differ between cell types (Villadangos et al., 1997, Deussing et al., 1998).The terminal Ii degradation fragments, CLIP, continue to block the peptide binding groove and must dissociate to allow presentation of antigen.

Although spontaneous CLIP release may occur (Kropshofer et al., 1995), the non-classical MHC II molecule, HLA-DM, which is structurally similar to HLA DR but lacks a peptide binding groove, accelerates the process (Sloan et al., 1995, Denzin and Cresswell, 1995). Recent crystallographic studies of DM in complex with the MHC II molecule, HLA-DR, have elucidated a mechanism for this catalysis (Pos et al., 2012). HLA-DM interacts laterally with MHC II-CLIP complexes, causing a tryptophan to flip away from the HLA-DR P1 pocket, enabling major conformational changes that position hydrophobic HLA-DR residues in the P1 pocket. Furthermore, initially incoming peptides have only partial access to the peptide-binding groove and must compete with HLA-DR residue for access to the P1 pocket, as well as the P2 site. This provides an energetic barrier and creates a stringent selection process for the highest affinity peptides (Vogt et al., 1999, Painter and Stern, 2012). Once a peptide has bound P1 and P2, the conformational changes are reversed and thus peptide selection is terminated through HLA-DM dissociation (Busch et al., 2005). Hence, HLA-DM establishes an affinity based hierarchy for peptide binding. Once stably loaded with peptides, MHC II molecules are shuttled to the cell surface, allowing antigen presentation to CD4+ T cells. The process of antigen presentation by MHC II molecules is depicted in Figure 1.3.

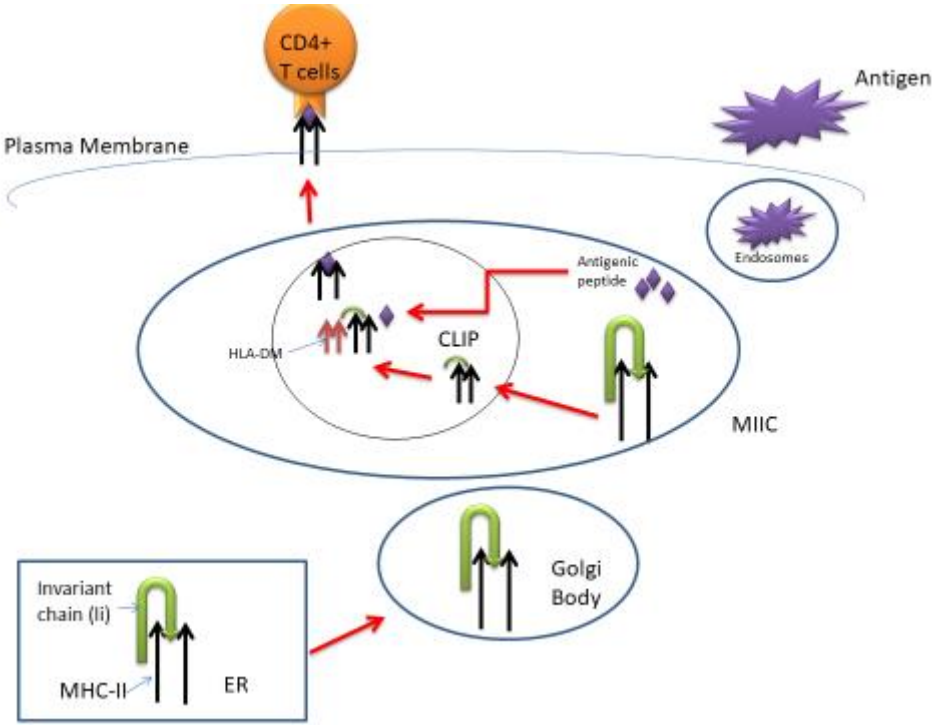

Figure 1.3 Antigen presentation by MHC II molecules. MHC II dimers assemble with the invariant chain (Ii) in the endoplasmic reticulum (ER). This complex is then transported to specialized lysosomal compartment known as the MHC class II compartment (MIIC), through the Golgi body. In the MIIC, the Iichain is hydrolysed to leave MHC II bound to an Iifragment, called class II-associated invariant chain peptide (CLIP). Simultaneously, the exogenous antigens on internalization are fragmented into small peptides for presentation. Peptide exchange is catalysed by the non-classical MHC II molecule, HLA DM. The peptide-loaded MHC II can then transported to the cell surface, where antigen presentation takes place. Figure adapted from Neefjes et al (2011).

The peptide is an integral part of the MHC molecule, as it stabilizes the structure. In the absence of bound peptide or chaperones, MHC II molecules readily aggregate (Kropshofer et al., 1997). This ensures that only stable MHC II/peptide complexes are transported to the cell surface and MHC II molecules present peptides that were processed within the cell. Nevertheless, the peptide binding specificity of MHC II molecule is not the only factor affecting antigen presentation.

The physiology of antigen presentation is complicated by differential expression of endosomal proteases in different APCs. Cathepsins are lysosomal proteases consisting of at least 15 members (Stoka et al., 2016). Most of these are ubiquitously expressed, although some have more tissue- or cell type-specific expression profiles. This affects the processing of Ii, MHC II and protein antigens. There is some level of redundancy to this system (Reich et al., 2011). Lysosomal processing of antigen involves many different exopeptidases, endopeptidases and reductases, such as the γ-interferon (IFN)-induced lysosomal thiol reductase (GILT), which is required for the degradation of protein antigens containing disulphide bonds (Haque et al., 2002, Maric et al., 2001). The presence of different proteases can alter the peptide repertoire that binds to MHC II molecules (Hsieh et al., 2002) . Moreover, different proteases can play the same role in different cell types; for example, cathepsin L and S (Cat L/S) can play the same role in the degradation of Ii, with Cat L being abundantly expressed in thymic epithelial cells (TECs), whereas B cells and DCs express Cat S (Hsing and Rudensky, 2005, Reich et al., 2011). This makes it difficult to pinpoint particular enzymes responsible for a defined role/s. More details about function of cathepsins are explained in the introduction to Chapter 3.

Another important criterion for the efficient working of these enzymes is maintenance of a low pH in the lysosomes. The pH within lysosomes is acidic (less than 5), whereas the pH in the cytoplasm is neutral (around 7.2). This low pH is essential for most proteases found within lysosomes to function optimally. This low lysosomal pH is maintained by an adenylpyrophosphatase (ATPase) that utilizes the energy liberated by ATP hydrolysis to pump protons into the lumen of the lysosome (Mindell, 2012, Ishida et al., 2013).

1.3.3 MHC II degradation

Expression levels of MHC II at the cell surface are determined by their rates of synthesis, internalization, intracellular retention, recycling and degradation. Several mechanisms that control MHC II degradation have been investigated. Cell surface expression of MHC II increases during DC maturation. The synthesis of MHC II increases in response to maturation signals, but only temporarily, and is virtually absent in fully matured DCs (Granucci et al., 2001, Wilson et al., 2004). MHC II complexes that are formed from newly synthesized MHC II during DC activation become long-lived, generating a pool of stable MHC II complexes potentially displaying antigen from the pathogen. On the other hand, MHC II molecules that were synthesised prior to DC activation are irreversibly sorted in the lysosomes/endosomes (Walseng et al., 2010). MHC II synthesis is shut down after DCs have matured.

Ubiquitination is a post-translational modification that, amongst others functions in cell homeostasis and signalling, mediates sorting of integral membrane proteins to lysosomes for their degradation. A highly conserved unique lysine at position 225 in the cytoplasmic tail of the MHC II β chain can be ubiquitinated (Ohmura-Hoshino et al., 2006). Lysine at position 219 in the cytoplasmic tail of DR α can also be ubiquitinated but other features of DR α limit the process to a certain extent (Lapaque et al., 2009). This is a variant of the default ubiquitination pathway which is responsible for the majority of intracellular protein degradation in eukaryotic cells by the proteasome (Finley, 2009). In both of these pathways, the specificity is ensured by conjugating substrates to a chain of ubiquitin moieties. This polyubiquitination process requires a cascade of three types of enzymes: E1, E2, and E3 (Iiand Ye, 2008). First, ubiquitin is bound and activated by the E1 ubiquitin-activating enzyme. Then the activated ubiquitin moiety is transferred to the E2 ubiquitin conjugating enzyme, which finally, via the E3 ubiquitin-protein ligase, transfers ubiquitin to the target

protein, which can be rapidly degraded (Pickart, 2001). The schematic representation of the ubiquitination process is shown in Figure 1.4.

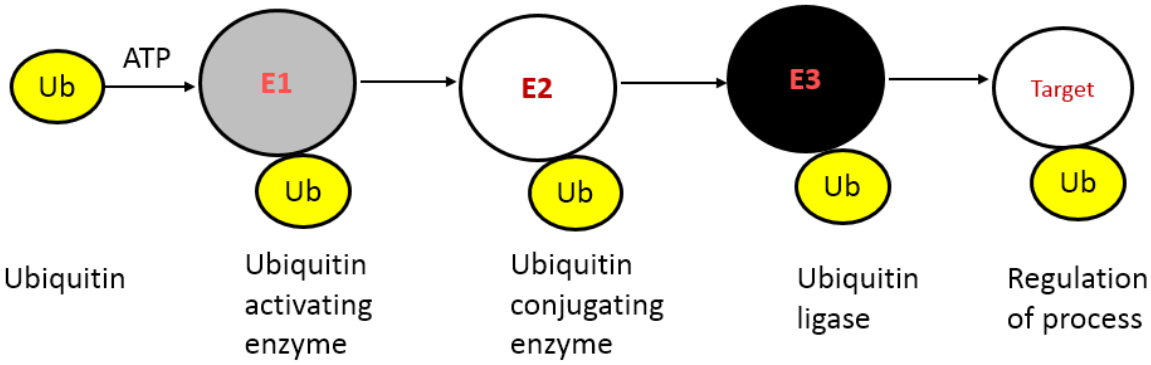

Figure 1.4 Enzymatic steps in protein ubiquitination. Protein degradation through ubiquitin requires sequential action of three enzymes. Free ubiquitin (Ub) is activated by ubiquitin activating enzyme (E1) using ATP to form E1-Ub complex. Activated Ub is transferred to a carrier protein (E2), and then transferred to a ligase (E3). This will allow the polymerization of one or more ubiquitin molecules on target proteins. Figure adapted from Jesenberger and Jentsch (2002)

Ubiquitination of MHC II in APCs is driven by membrane associated ring finger protein I (MARCH I), a member of the E3 ligases (De Gassart et al., 2008). More evidence of the association of MARCH I with MHC II was found in co-immunoprecipitation studies (Tze et al., 2011). The pivotal role of MARCH I in regulating MHC II mediated antigen presentation is further illustrated by observations that the anti-inflammatory cytokine IL-10 induces MARCH I expression in primary human monocytes (Thibodeau et al., 2008), thereby promoting MHC II degradation under immunosuppressive conditions. Down-regulation of MARCH I transcription was demonstrated in maturing DCs (De Gassart et al., 2008, Young et al., 2008). The half-life of MARCH I is claimed to be shorter than 30 minutes (Jabbour et al., 2009), thus explaining the loss of ubiquitination in maturing DCs. Thus, ubiquitination of

MHC II regulates its cell surface expression by providing a signal for efficient sorting towards degradation in the lysosome (Shin et al., 2006, van Niel et al., 2006). In DCs where lysine at 225 position of HLA-DR β was mutated to prevent ubiquitination, there was a reduction of endocytosis by 20-fold when compared to wild type MHC II (De Gassart et al., 2008). However, ubiquitination of MHC II might involve, in addition to MARCH I, also other E3 ligases. In MARCH I knockout mice, ubiquitination of MHC II was absent in B cells but remained intact in DCs (Matsuki et al., 2007) indicating overlapping specificities of the E3 ligases.

In summary, MHC II molecules are extraordinarily stable but still display cell type-specific half-lives. Factors affecting the degradation of MHC II molecules following internalisation are not well understood. It is most likely that MHC II molecules are degraded in a similar way to any other lysosomal proteins, but the specific protease(s) involved remain unidentified and are investigated in this thesis.

1.3.4 MHC II polymorphism and inheritance

The entire MHC region is one of the most highly polymorphic gene complexes known and is not only multi-allelic, but also multigenic (Trowsdale and Knight, 2013). The genetic diversity of MHC II molecules arises from the presence of numerous genes encoding the α- and β-chains and extensive allelic polymorphism. There are three classical isotypes of MHC II molecules, called HLA-DP, HLA-DQ, and HLA-DR, which have different specificity of peptide binding (Penn and Ilmonen, 2001). Secondly, the genes constituting the HLA region are highly polymorphic; i.e., many alternative forms of the gene called alleles exist at each locus (Klein and Sato, 2000). The polymorphism and co-dominant expression of MHC molecules results in great genetic diversity among humans with regard to their HLA type.

Of the MHC II molecules, HLA-DR is the most widely studied isotype (van Lith et al., 2010). It is subject to the largest extent of allelic polymorphism and is characterized by having a monomorphic α-chain and a highly polymorphic β-chain, which determines the diversity of HLA-DR antigens (van Lith et al., 2010). Only one gene exists for the α-chain (HLA-DRA) whereas four different loci encode functional HLA-DR β-chains (HLA-DRB). These are HLA-DRB1, HLA-DRB3, HLADR-B4, and HLA-DRB5 (Figure 1.5). Five additional pseudogenes exist, encoding non-expressed β-chains; HLA-DRB2, HLA-DRB6, HLA-DRB7, HLA-DRB8, and HLA-DRB9 (Handunnetthi et al., 2010b). All humans carry HLA-DRB1, while the presence of any of the three remaining functional genes varies from individual to individual, which is referred gene varaition (Schaschl et al., 2009, Gamazon and Stranger, 2015).

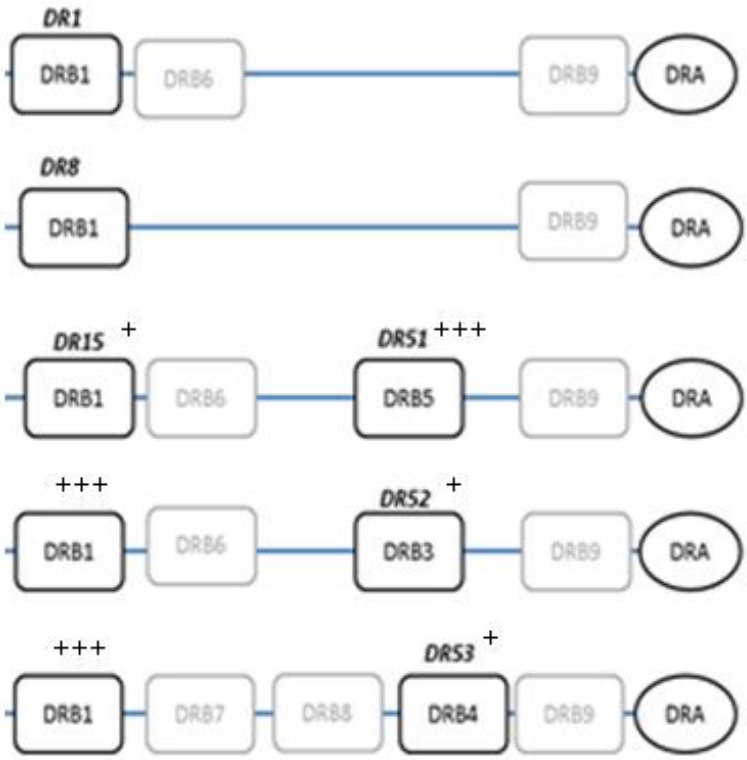

Figure 1.5 Schematic representation of the five human HLA-DRB haplotypes. Adapted from Anderson (1998). Genes and pseudogenes are shown in dark and light colour.

Furthermore, the HLA-DRB1 locus has the most identified alleles of all HLA class II loci. Any of the functional HLA-DR β-chains can pair up with an HLA-DR α-chain to form a heterodimeric HLA-DR molecule. Despite the diversity of HLA-DRB, it is possible to divide individuals into five different HLA-DR haplotypes, which denote a particular combination of HLA-DRB1 alleles and their linked gene variant (Figure 1.5) (Handunnetthi et al., 2010b). These groups are characterized by their sole expression of HLA-DRB1 or HLA-DRB1 in combination with HLA-DRB3, HLADR-B4, or HLA-DRB5. Since inheritance of HLA antigens is codominant (Choo, 2007), an individual may produce up to four different DR protein variants: two from the maternally and paternally derived DRB1 alleles, and up to two more from the alternate DRB gene loci.

Henceforth, in the thesis, I will be using the nomenclature of the XVth Histocompatibility Workshop (Marsh et al., 2010). Briefly, allelic variation will be represented by two-digit numbers following the gene name (e.g. HLA-DRB1*15). The first two digits correspond to the type of serological antigen presented by the HLA-DRB1. Each allele can be further resolved in to subgroups that differ due to nonsynonymous nucleotide substitutions represented, by the addition of further digits (e.g. HLA-DRB1*15:01). This are used to list the subtypes, numbers being assigned in the order in which DNA sequences have been determined. Alleles whose numbers differ in the first four digits must differ in one or more nucleotide substitutions that change the amino acid sequence of the encoded protein. Lastly, differences in the nucleotide sequence of the HLA-DRB1 DNA that do not actually result in amino acid differences within the gene product, i.e. synonymous substitutions, are represented by an additional two digits (e.g. HLA-DRB1*15:01:01) (Marsh et al., 2010). Further digits can be added to indicate the promoter polymorphism.

1.3.5 Role of MHC II in self-tolerance and auto immunity

As implied Section 1.1, the purpose of the immune system is to destroy, isolate, and/or remove any pathogens and the toxic substances they produce, which may harm the homeostasis of the host. It is therefore crucial that the adaptive immune response is directed specifically against the pathogens and not against the host. Occasionally, the immune system fails in making this distinction and reacts destructively against particular host-antigens, resulting in autoimmunity (Smith and Germolec, 1999). Antigen presentation is not only crucial for the regulation of protective immune responses against invading pathogens, but is also necessary for the maintenance of self-tolerance.

MHC II expression directs positive selection (selection of T cells which can recognise MHC molecules) and negative selection (deletion of self-reactive T cells (Klein et al., 2014));which shape the specificity of the T-cell-receptor repertoire of the CD4+ T-cell population during its development in the thymus (Kyewski and Klein, 2006). Nevertheless, T cells with an autoreactive repertoire still escape from the thymus, since not all self-antigens are expressed in the thymus. To prevent this auto-reactive leakage, a peripheral T cell tolerance process exists, whereby self-reactive T cells are physically kept away from self-antigens, are deleted e.g. by apoptotic stimuli, suppressed or inhibited, or simply ignore the antigens due to their low concentration (Kamradt and Mitchison, 2001). Despite all the existing tolerance mechanisms, auto-reactive cells can still break tolerance and cause autoimmunity. There can be several reasons for this, including incomplete expression of self-antigens during T cell education, structural similarity between microbial and self-antigens (known as molecular mimicry) (Albert and Inman, 1999), the presence of co-stimulatory signals during inflammation (Kamradt et al., 1991), infectious agents (Christen et al., 2012), post

translational modifications which can generate neo-epitopes from self-proteins, and thus result in the breaking of self-tolerance (Anderton, 2004).

It is therefore perhaps not surprising to find that the human MHC II gene region holds the largest number, and some of the longest recognised associations with autoimmune diseases of any similar-sized region across the genome. The involvement of the MHC II in many complex diseases is confirmed further by Genome-wide association studies (GWAS) (WTCCC, 2007), and some examples are listed in Table 1.1.

Table 1.1 Genes in the MHC II in which variation has a relationship to disease.

Disease	HLA locus	Comments	Reference
Rheumatoid arthritis	*HLA-DRB1,HLA-DP*	HLA-DRB1*04 alleles confer high risk and the rest exhibit a more moderate risk	(Fernando et al., 2008, Raychaudhuri, 2010)
Type 1 Diabetes	*HLA-DRB1, HLADQB1,* *HLA-DQA1,HLA-A, HLA-B*	Heterozygosity for both European haplotypes confers the greatest risk for Type 1 Diabetes	WTCCC, (2007), (Howson et al., 2009)
Ulcerative colitis	*HLA-DRB1, HLADQB1,* *HLA-DRA*	HLA-DRB1*0103 is the most reproducible association	(Fernando et al., 2008, Silverberg et al., 2009)
Crohn's disease	*HLA-DQA, HLA-DRB1*	HLA-DRB1*0701 is the most reproducible association	(Stokkers et al., 1999, Barrett et al., 2008)
Multiple sclerosis	*HLA-DRB1, HLA-A,HLA-DQ*	The most consistently reproducible finding is HLA-DRB1*1501 in Northern Europeans	(Modin et al., 2004, Ramagopalan et al., 2008, Sawcer et al., 2011)
Systemic Lupus Erythematosus	*HLA-DRB1, HLADQB1* *HLA-DRA*		(Sestak et al., 2011)

Table modified from Handunnetthi et al (2010b)

It is not just the MHC molecule but environmental factors also have an impact on the development of auto immune disease (Dankers et al., 2016). Pathogens like viruses and bacteria have been implicated in autoimmunity (Ercolini and Miller, 2009). Recently there is also growing evidence that the gut microbiota influence the development of autoimmunity (Rosser and Mauri, 2016). Dietary components are also linked with the development of auto immune disease conditions (Vojdani et al., 2014). Of these, vitamin D, because of its immunomodulating effects, also has an impact on the development of autoimmune diseases, has been discussed in detail.

1.4 Vitamin D

Vitamin D is an essential nutrient compound, best known for its role in calcium homeostasis and bone mineralization (Veldurthy et al., 2016). The discovery that the vitamin D receptor (VDR) is expressed in many human cells, including immune cells, has directed the attention to the extra skeletal effects of vitamin D (Morgan et al., 2000). Vitamin D is involved in numerous other functions such as modulating immune function, and regulating cellular proliferation, differentiation, and apoptosis (Maruotti and Cantatore, 2010) and then in development of autoimmune disease (Handel et al., 2013). In addition, vitamin D is neuro-protective (Wrzosek et al., 2013).

1.4.1 Production and metabolism

In humans, vitamin D is obtained either through synthesis in the skin or through dietary ingestion. Ergocalciferol (vitamin D2) can only be obtained via oral consumption through dietary intake of oily fish or UV irradiated mushrooms (Kamweru and Tindibale, 2016). Cholecalciferol (vitamin D3) is produced in the skin following exposure of 7-dehydrocholesterol to UVB radiation (sunlight) (Holick, 1981). However, the majority of

vitamin D in humans is obtained through synthesis in the skin (Calvo et al., 2005). Vitamin D metabolism is a sequential process as shown in Figure 1.6. The first step is the hydroxylation of vitamin D_3 or vitamin D_2 in the liver, performed by the cytochrome P450 mixed-function oxidases (CYPs), of which CYP2R1 is the most important one (Zhu et al., 2013). This yields 25-hydroxy-vitamin D (25-OH-D), the metabolite measured in the blood to evaluate vitamin D status. A second hydroxylation step then takes place in the kidney, resulting in 1,25-dihydroxyvitamin D (1,25-OH_2-D). This is the active form of vitamin D and is also referred as calcitriol. The enzyme responsible for this is 1 α-hydroxylase (CYP27B1) (Prosser and Jones, 2004). Calcitriol is then transported in the blood by the vitamin D binding protein and, on reaching the target cell, it dissociates, binds to vitamin D receptor (VDR) within the cytoplasm, and mediates its biological actions (Haussler et al., 1997). This complex enters the nucleus and forms a heterodimer with a nuclear receptor, the retinoid X receptor (RXR) (Thompson et al., 1998, Thompson et al., 1999). The heterotrimer calcitriol–VDR–RXR lastly binds to vitamin D-responsive elements (VDREs) (White, 2004), which are made up of a sequence of DNA within the promoter region of the target genes. The complete system thus regulates (by activation or suppression) gene transcription and thereby protein synthesis (Niino et al., 2008). Thus, calcitriol, secreted into the bloodstream by the kidney and exerting its actions in various other tissues by binding to a specific receptor, can be considered as a hormone..

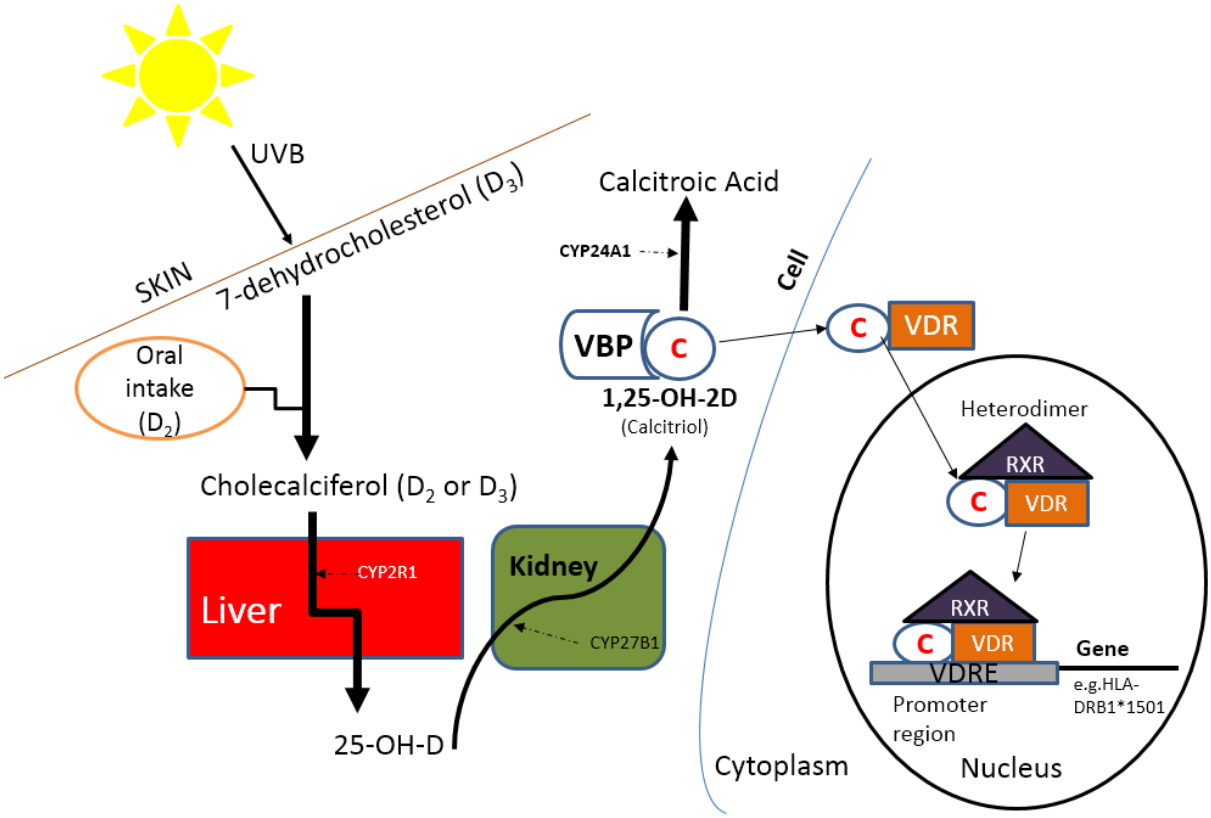

Figure 1.6 A schematic representation showing the pathway of vitamin D metabolism and action. During exposure to sunlight 7-dehydrocholesterol in the skin is converted to Cholecalciferol D3. Vitamin D in the circulation is bound to the vitamin D binding protein which transports it to the liver where vitamin D is converted to 25-OH-D. It is biologically inactive and must be converted in the kidneys to its biologically active form 1, 25-OH-2D. Active vitamin D can then enter cells and stimulate the vitamin D receptor protein to bind to DNA in the nucleus via RXR nuclear receptor, acting as a regulator for hundreds of genes. At the gene level, the heterodimer comprising calcitriol may stimulate or repress protein synthesis, depending on the cell. Abbreviations: C, calcitriol; CYP2R1, vitamin D-25-hydroxylase; CYP27B1, 1α-hydroxylase; RXR, retinoid X receptor; UVB, ultraviolet B radiation; VDR, vitamin D receptor; VDRE, vitamin D-responsive element; VBP vitamin D binding protein. Figure adapted from Charles Pierrot-Deseilligny (2013)

Moreover, various immune cells, including monocytes, dendritic cells, macrophages, B cells, and T cells, also have the capability to convert 25-OH-D into 1,25-OH_2-D (Heine et al., 2008, Jeffery et al., 2012, Bakdash et al., 2014). This allows for local regulation of the concentration of 1,25-OH_2-D.

RXR is a shared nuclear hormone receptor as, it can also bind as a homodimer or as a heterodimer with retinoic A receptor (RAR) (Blomhoff and Blomhoff, 2006). Both vitamin D and RA exert their cellular effects via nuclear receptors, which bind to the promoters of their response genes to facilitate transcription. Once vitamin D is converted to its active metabolite, 1, 25 dihydroxyvitamin D (1, 25(OH) D3), it will form a complex with VDR. Binding of 1, 25(OH) D3 leads to a conformational change in VDR and enables binding to the retinoic X receptor (RXR) (Mora et al., 2008, Pike and Meyer, 2010).

After heterodimer formation, VDR/RXR OR RAR/RXR is translocated to the nucleus, where it can exert three different effects: it can bind to a vitamin D3 response element (VDRE) in the promoter region of target genes and turn on genes; it can bind to what is termed a 'negative' VDRE and prevent gene transcription; or it can bind to transcription factors present in the nucleus and prevent them from binding to target genes (Nagpal et al., 2005). RXR is a shared nuclear hormone receptor as it can also bind as a homodimer or as a heterodimer with retinoic A receptor (RAR) (Blomhoff and Blomhoff, 2006). The binding of the RAR/ RXR heterodimer to the retinoic acid response element (RARE) sequence in the promoter region of the target genes results in the transcription of target genes (McGrane, 2007).

1.4.2.1 Role of vitamin D in the immune system

Vitamin D is a pleiotropic regulator of immune functions (as well as calcium homeostasis and bone metabolism), with many possible modes of action in auto-immunity (Pludowski et al., 2013). Vitamin D plays an important role in both innate and adaptive immune response.

Calcitriol plays an important role in innate immunity, in particular in inducing antimicrobial peptides, such as Cathelicidin, an essential innate component for combating *Mycobacterium*

tuberculosis (Liu et al., 2006). Bioactive vitamin D has also been shown to upregulate the pattern recognition receptor Nucleotide-binding oligomerization domain containing 2 (NOD2) which, when activated in the presence of bacteria, leads to release of the antimicrobial peptide defensin β2 (Wang et al., 2010)**.** Calcitriol may act on the innate immune system in several other ways, with the general result of enhancing innate immunity.

The effects of vitamin D on the adaptive immune system are also numerous. Calcitriol inhibits T cell proliferation (Rigby et al., 1990). Calcitriol has also been reported to promote tolerance and regulation by inhibiting the maturation of DCs and promoting T regulatory cell (Treg) populations (Penna et al., 2005). Thus, calcitriol renders the DCs more immature and hence more tolerogenic, and also upregulates molecules on the cell surface of DC resulting in the inhibition of effector T cells whilst promoting induction and recruitment of Tregs. In B cells, calcitriol has been found *invitro* to decrease cell proliferation, antibody production and plasma cell proliferation (Chen et al., 2007). However, it is still not clear whether this also occurs *in vivo* (Rolf et al., 2014). Calcitriol has also been found to affect DCs; it influences their cytokine production (Barragan et al., 2015). Calcitriol has been reported to prevent the maturation of DCs, resulting in reduced expression of the costimulatory molecules CD80, CD86, and HLA-DR and the maturation marker CD83 (Canning et al., 2001, Sochorova et al., 2009). However in Epstein-Barr virus (EBV) transformed B cells, where there is vitamin D response element (VDRE), calcitriol is able to increase the expression of HLA-DR (explained further in section 1.4.6) (Ramagopalan et al., 2009). There may be different effects of calcitriol on APCs depending on the presence of the VDRE. The effects of bioactive

vitamin D on the immune system have been summarized in Figure 1.7.

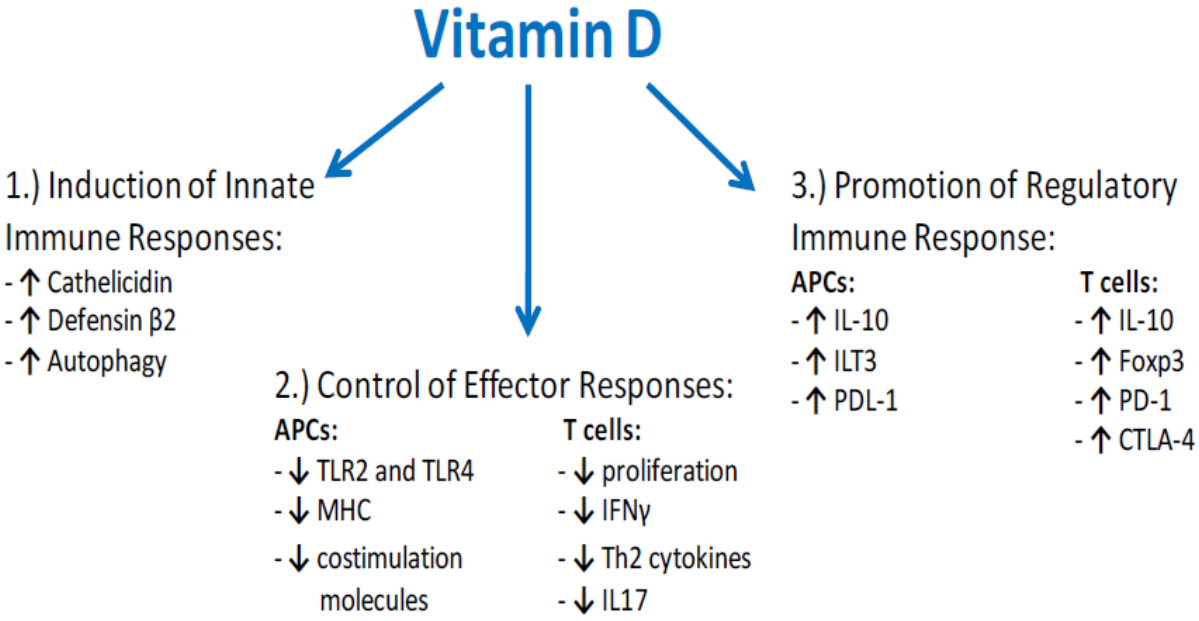

Figure 1.7 Roles of vitamin D in the immune system. Vitamin D has wide ranging immunomodulatory properties. Vitamin D effects on the innate immune system include induction of antimicrobial peptides, such as cathelicidn and defensin β2 and induction of autophagy. Vitamin D controls the effector CD4+ T cell response through decreasing expression of TLR molecules and costimulatory molecules on the antigen presenting cells. Additionally Vitamin D enhances regulatory T cell populations by enhancing IL-10 production and inhibitory molecule expression on antigen presenting cells. Figure adapted from Chambers and Hawrylowicz (2011).

1.4.2.1 Role of RA in the immune system

RA, a derivative of vitamin A (Harrison, 2005), is important for the immune system (Pino-Lagos et al., 2008, Hall et al., 2011, Erkelens and Mebius, 2017). The general effects of RA on immune system are summarised in Figure 1.8. RA is also central for the differentiation of myeloid cells and affects the maturation and survival of macrophages (Kim, 2011). RA can inhibit B cell proliferation (Blomhoff et al., 1992, Ballow et al., 1996), although it has also been found to enhance B-cell activation under some conditions (Saurer et al., 2007). RA can

also modulate antigen presentation by exerting direct effects on DC function (Darmanin et al., 2007). In addition, in the presence of inflammatory stimuli, RA enhances DC maturation and antigen-presenting capacity (Geissmann et al., 2003).

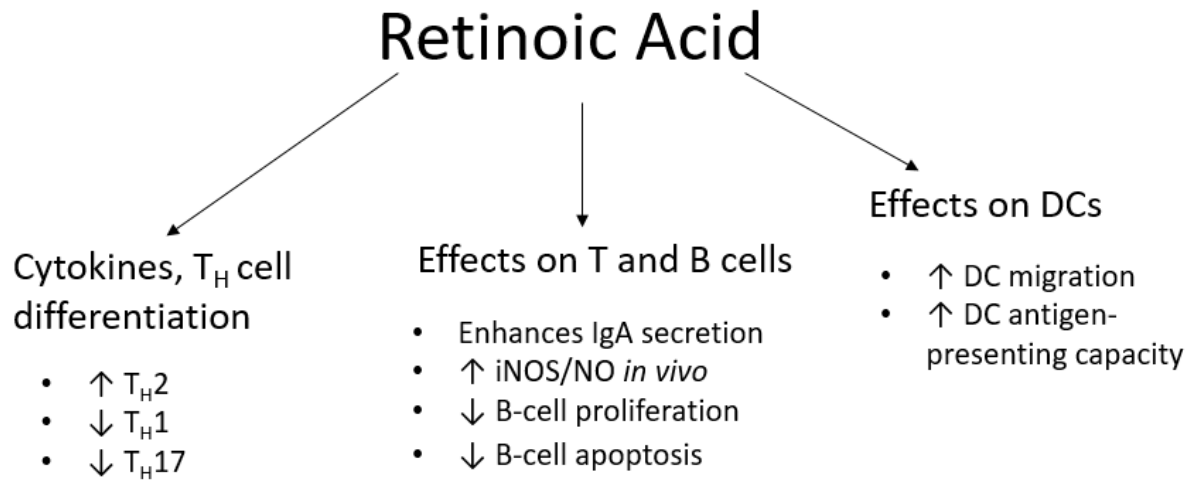

Figure 1.8 Roles of RA in the immune system. RA exerts its effects on several immune cell types, including macrophages, DCs, T and B cells. Figure adapted from Mora et al., (2008)

Thus, considering the wide range of immunomodulatory effects of vitamin D, it is not surprising to find a lack of vitamin D being associated with several diseases. Multiple sclerosis (MS) is the perfect example of an autoimmune disease known for its association with both MHC II polymorphism and vitamin D deficiency in the development of disease.

1.5 Multiple Sclerosis

MS is a chronic complex autoimmune disorder of the central nervous system (CNS). MS patients develop multiple lesions in their CNS, where the axons of neurons have been demyelinated (Lucchinetti et al., 2000, Kornek and Lassmann, 2003). These lesions may develop in virtually any region of the CNS and may lead to a wide range of motor, sensory

and/or cognitive deficits. Clinically, MS presents in a variety of ways; some of the most common initial symptoms are optic neuritis, sensory disturbances and diplopia (Soderstrom et al., 1998). During the course of the disease, fatigue, cognitive dysfunction, bladder disturbances, weakness, and a wide variety of other neurological dysfunctions commonly occur (DasGupta and Fowler, 2003, Opara et al., 2010). The usual clinical definition of the disease is "dissemination in time and space" of lesions of inflammatory demyelinating origin, i.e. recurrence of symptoms from different locations (multiple) of the nervous system (and where other causes have been ruled out).This definition is the basis for the diagnostic criteria, the McDonald criteria (McDonald et al., 2001), that have been used clinically and in research for the last two decades with some modifications (Polman et al., 2005, Polman et al., 2011, Thompson et al., 2018). Moreover, MS is also classified into four different types based on the progression of the disease. This classification are relapsing remitting MS, primary progressive MS**,** secondary progressive MS, and progressive relapsing MS (Rovaris et al., 2009). This classification along with common characteristics can be found in Table 1.2. There is no cure for MS and the disease can lead to disability and sometimes death (Roxburgh et al., 2005, Pachner and Steiner, 2009). Although the age of onset for MS varies greatly, most patients receive their diagnosis of definite MS between 20 and 45 years of age (Hammond et al., 2000), but recent advances in magnetic resonance imaging (MRI) technology have led to earlier diagnosis (Rovaris et al., 2009).

Table 1.2 Various types of MS.

Types of MS	Characteristics
Relapsing-Remitting Multiple Sclerosis (RRMS)	Symptom flare-ups followed by recovery; stable between attacks
Secondary Progressive Multiple Sclerosis (SPMS)	progressive worsening of symptoms with or without superimposed relapses
Primary-Progressive Multiple Sclerosis (PPMS)	Gradual but steady accumulation of neurological problems from onset
Progressive-Relapsing Multiple Sclerosis (PRMS)	Progressive course from the onset, sometimes combined with occasional acute symptom flare-ups
Benign MS	Few attacks and little or no disability after 15 or more years

Table adapted from Miller et al.(2005)

1.5.1 Pathophysiology of MS

The most widely accepted view of the pathophysiology underlying MS is that it is an autoimmune disease of the CNS (Holmøy, 2007). Several lines of evidence support the view of MS as an autoimmune disease: animal models of MS, the characteristics of MS lesions, and the efficacy of immunotherapy in MS. Here, a short overview of the immunological dysfunction that may be important for the development of MS is given.

Virtually all our mechanistic concepts of adult MS are derived from an animal model, experimental autoimmune encephalomyelitis (EAE) (Ben-Nun et al., 2014, Baker and Amor, 2014). EAE is induced by immunizing animals with myelin-derived proteins or peptides such as myelin basic protein (MBP), hydrophobic proteolipid proteins (PLPs), and myelin oligodendrocyte glycoprotein (MOG) or by transfer of immune T-helper cells that have been sensitized to such myelin peptides (Emerson et al., 2009, Ben-Nun et al., 2014). Overall, the lesions and clinical signs induced in EAE by these myelin-associated antigens bear resemblance to the inflammatory demyelinating processes observed in MS.

The prevailing view of MS immunopathogenesis is that autoreactive immune cells are activated peripherally and gain access to the CNS (Dendrou et al., 2015). T cells are activated against a CNS autoantigen and are transported to the CNS, where they pass across the blood brain barrier (BBB), which has become permeable, and then initiate an inflammatory process by recognizing the antigen presented by APCs (Broux et al., 2013, Hemmer et al., 2015). The macrophages and or microglia have the capacity to secrete cytokines, may thus modulate immune responses, and may attract specific activated immune cells (Imitola et al., 2005). Recently, the role of the B cell, the other cell type of the adaptive immune system, in MS has attracted attention (Hauser et al., 2008, Disanto et al., 2012). The functions of B cells range from antibody production to antigen presentation and immune system regulation through cytokine production (Hoffman et al., 2016). In MS, it has been postulated that B cells produce antibodies which attack the neurons causing demyelination (Dendrou et al., 2015, Dolati et al., 2017). The immune-pathogenesis in MS is depicted schematically in Figure 1.9. Furthermore, higher circulating levels of immune cells and immunoglobulins specific to the CNS are found in the cerebrospinal fluid (CSF), and immune cells are found in MS lesions.

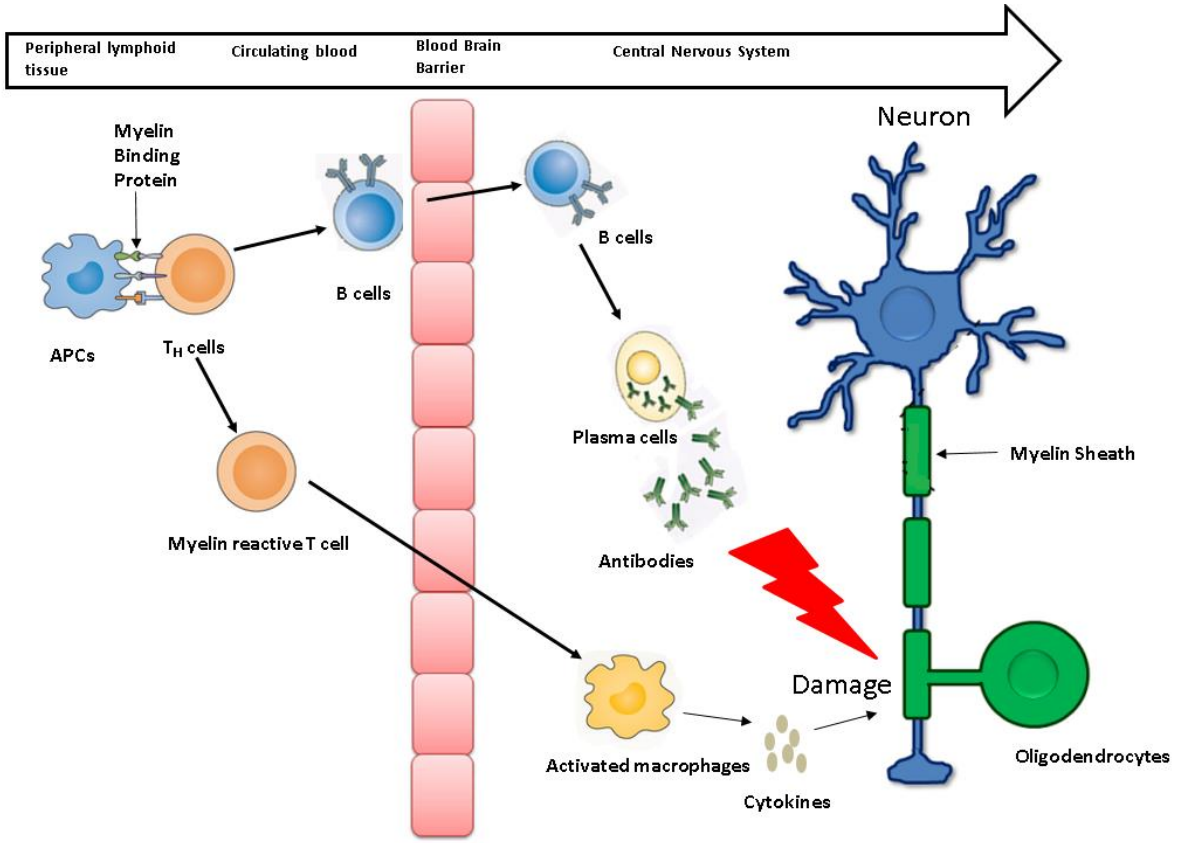

Figure 1.9 Postulated immune cascades in multiple sclerosis. Myeloid cells and B cells are competent antigen-presenting cells that are thought to present a molecular mimic of a myelin peptide to generate myelin-reactive T_H cells, which can further activate the myeloid cells into the central nervous system (CNS). Activated immune cells produces pro-inflammatory cytokines, which direct phagocytic attacks on the myelin sheath. After clonal expansion, B cells mature to plasma and release large amounts of antibodies, which can cause damage to the myelin sheaths. Figure adapted from Dolati (2017).

In addition to the inflammation described above, there is also a neurodegenerative component to MS that results in axonal damage and neuronal loss (Trapp and Nave, 2008). While the increase of new demyelinating lesions can be associated with acute clinical relapse, it is the progressive increase of both clinical and subclinical pathological disease (focal areas of inflammation as well as widespread neuronal cell loss and axonal) that is thought to trigger progression to irreversible disability. The risk of irreversible disability depends on the phenotype of MS and increases with disease duration; however, pathological features of

tissue injury are also detectable from clinical disease onset (Trapp and Nave, 2008). Effective strategies for neuroprotection against MS have not yet been established.

1.5.2 MS risk determinants

Our understanding of the factors involved in the etiology and progression of MS remains incomplete. Epidemiological studies have shed light on ethnic, seasonal and geographical variations in MS incidence, leading to the various hypotheses regarding the genetic, hormonal and environmental risk factors, and their potential interactions (Ascherio, 2013). While the present thesis is largely concerned with the role of vitamin D and genetics in MS, other candidate risk factors for MS, such as sex hormones, viral infection (particularly EBV) and cigarette smoke exposure are also important (Ascherio et al., 2001, Compston and Coles, 2002).

1.5.3 Geographical pattern

It became clear during the first half of the 20th century that there are geographical differences in MS prevalence. The prevalence of MS is higher in areas with temperate rather than tropical climates. It generally increases with distance from the equator, and is inversely associated with average sunlight exposure (McMichael and Hall, 1997). There are several comprehensive reviews on this topic discussing the relationship between sunlight exposure and the prevalence of MS (Holmøy, 2007, Giovannoni and Ebers, 2007, Pugliatti et al., 2008, Handel et al., 2009, Correale and Farez, 2013). One thing to consider here is that the healthcare system in equatorial countries and polar countries are very different and there is a north-south gradient in the quality of healthcare surveillance at least historically. But within the same country, when work-related sun exposure was evaluated in the USA, based on death certificates, increasing sun exposure was negatively associated with death due to MS (Freedman et al., 2000). Also, in Sweden,

using register data, a decreased risk of MS with increasing occupational sun exposure was found (Westberg et al., 2009). The striking correlation between MS prevalence and latitude has suggested sunlight and resultant vitamin D status as a determinant of MS risk (Kampman and Brustad, 2008, Pierrot-Deseilligny, 2009).

1.5.4 Serum 25-OH-D concentration among MS patients

A number of studies have reported lower serum levels of 25-OH-D, the precursor of active vitamin D, in MS patients than in healthy controls (Munger et al., 2006, van der Mei et al., 2007, Kampman and Brustad, 2008, Kragt et al., 2009, Simpson et al., 2010, Salzer et al., 2012, Runia et al., 2012, Duan et al., 2014). In most of these studies, there was a control group in addition to the patient group, but there was not always a significant difference in the serum levels of 25-OH-D between the two groups and therefore clinical significance remains unclear. Lacking to date are studies of vitamin D status in regions where MS is rare. Lastly, serum 25-OH-D levels are rarely evaluated in apparently healthy individuals prior to the onset of disease; one study did demonstrate that vitamin D status in early adulthood was inversely related to subsequent MS risk (Munger et al., 2006), but more such studies are needed.

There are several other factors which can affect the serum 25-OH-D serum concentration in the blood. Clothing and time in the sun also determine the serum level of 25-OH-D. Even in areas of high sunlight, vitamin D synthesis can vary markedly between individuals (Holick, 2014). Application of sunscreen can impair endogenous vitamin D synthesis. There is also evidence that the amount of 7-dehydrocholesterol in the skin decreases with age such that the elderly may have reduced capacity to synthesize vitamin D (MacLaughlin and Holick, 1985).

In addition, people who have more melanin pigment in their skin also typically require longer sun exposure to achieve adequate vitamin D synthesis (Clemens et al., 1982).

An important unanswered question here is: does vitamin D affect MS or does MS affect vitamin D metabolism? While the contribution of vitamin D deficiency to the development of MS and other immune-mediated diseases has been suggested for decades, it has not been discussed whether the disease process itself and physiological effects of the disease could modify vitamin D metabolism.

It also has to be considered that vitamin D insufficiency is common in temperate climates, yet most individuals with low serum 25-OH-D concentrations do not develop MS. However, the absence of MS in these individuals does not negate the potential importance of vitamin D insufficiency as a risk factor for MS. Rather this does suggest that other factors potentially can lead to MS progression apart from vitamin D deficiency. One such factor is the genetics.

1.5.5 MS and Genetics

MS risk increases with increasing degree of relatedness or similarity of DNA. The concordance rate of MS among monozygotic twins, who share virtually 100% of their DNA, is generally between 25-31% (Dyment et al., 2004). In contrast, the prevalence rate for MS in dizygotic twins and full siblings, who share approximately 50% of their DNA, is only 4-5% (Willer et al., 2003, Fagnani et al., 2015). The risk of MS is increased in close relatives of MS patients, varying proportionally to the fraction of shared genes. Thus, genetic factors add to the disease predisposition.

The genes with the strongest and most consistent association with MS risk are found on chromosome 6 and cluster within regions of DNA that encode the HLA system (Lincoln et al., 2005, Ramagopalan and Ebers, 2009). In almost all the studied MS populations in Europe there is an association to the HLA DRB1*1501 allele (Masterman et al., 2000, Weatherby et

al., 2001, Hensiek et al., 2002, Ballerini et al., 2004, Schmidt et al., 2007, Ramagopalan et al., 2008, Alcina et al., 2012). This allele is in strong linkage disequilibrium with DRB5*0101 and DQB1*0602 and therefore no primary susceptibility allele has been resolved (Fogdell et al., 1995, Lincoln et al., 2009). This haplotype increases the risk of MS about 2-4 fold in both sporadic and familial MS. However the DRB1*1501 allele is not linked with the Asian type of MS, which is also characterised by a different pathology than the Western type of MS (Asians have fewer brain lesions and more spinal-cord lesions when compared to Western) (Kira et al., 1996, Yoshimura et al., 2012). In addition, Sardinians who have a relatively low frequency of the MS associated DRB1*1501 haplotypes in both patients and the normal population, have the DRB1*13:03-DQB1*03:01 haplotype as a susceptibility factor in MS (Marrosu et al., 2001). These observations suggest that MS may be immunogenetically different in different populations. Why the risk of MS varies between certain alleles remains to be determined, but is likely related to the physiological function of HLA molecules in antigen presentation. The effect of vitamin D on the most common alleles is examined in Chapter 5.

1.5.6 Biological Plausibility of Vitamin D and HLA-DR interactions

Investigation of the major candidate genes, HLA-DRB1, HLA-DQA1 and HLA-DQB1, led to discovery of a conserved, functional vitamin D response element (VDRE) in the promoter region of the HLA-DRB1*1501 allele (Ramagopalan et al., 2009). Furthermore, the authors demonstrated that addition of calcitriol to DRB1*15 homozygous B-cells *in vitro* resulted in increased expression of HLA-DR (Ramagopalan et al., 2009). Therefore, it is plausible that the association between the HLA-DRB1 allele and risk of MS may be modified by vitamin D status, which determines the availability of the activated metabolite of vitamin D. This observation suggests that vitamin D might protect from MS in part by differentially

influencing the expression and function of HLA-DR protein variants associated with MS risk. It could be that vitamin D deficiency or impaired vitamin D metabolism may lead to lower expression of the MHC II molecule (Handunnetthi et al., 2010a). Reduced expression of MHC II molecules could impair presentation of self-antigens during negative selection, resulting in a lack of tolerance being established against those self-antigens. If the immune system fails to establish and maintain immune tolerance to molecules derived from the BBB or CNS myelin, this could result in the type of demyelinating immune attacks observed in MS. This does form a conceptual basis for a nutrient-gene interaction, thus connecting the genetic and environmental evidence implicating sunlight and vitamin D in the determination of MS risk or other autoimmune diseases in which MHC and vitamin D plays a pivotal role in the pathogenesis.

Since vitamin D is pleiotropic, and other factors do complicate the above explanation. Vitamin D responsiveness is shared by a subset of DRB1 alleles, not all of which are associated with MS (Cocco et al., 2012), and why the risk of MS varies between certain alleles remains to be determined. One possibility is that vitamin D could modulate the relative expression levels of DR allelic variants encoded by maternal vs. paternal haplotypes, if the co-expressed alleles differ in their vitamin D responsiveness. Moreover, vitamin D could influence the relative levels of DR molecules containing DRB1 vs. alternate DRB gene products, including DRB5 in the MS-associated DRB1*15 haplotype. These changes could help vitamin D to maintain immune tolerance to myelin autoantigens. Therefore, the regulation by vitamin D of HLA-DR expression and fate, and the effects of structural and promoter polymorphisms need to be investigated at the protein level, before implications for MS can be evaluated. The method development for measuring changes in the allelic composition, in the presence of vitamin D in heterozygous APCs, constitutes Chapter 6 of this thesis.

Antibody-based approaches for quantifying allelic composition are potentially biased by the antibodies conformational preferences (Woolley et al., 2015), hence mass spectrometry based approach will be used to quantify DRB allelic composition in heterozygous APCs. Mass spectrometry is an analytical technique that measures the mass/charge ratio of charged particles in vacuum. Mass spectrometry can determine masse/charge ratio with high accuracy. Molecules in a test sample are converted to gaseous ions that are subsequently separated according to mass/charge ratio (Eliuk and Makarov, 2015). A mass spectrometry experiment typically consists of five steps: sample introduction, analyte ionization, mass analysis, ion detection, and data processing and interpretation of the results (Yates et al., 2009). A simplified scheme on how mass spectrometry works is shown in Figure 2.0

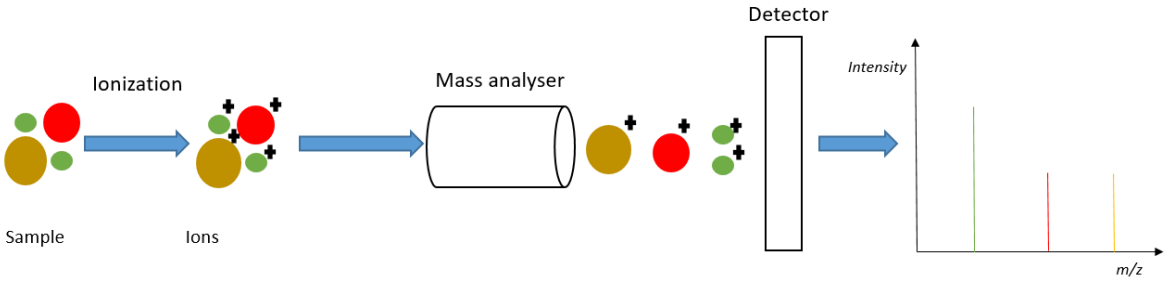

Figure 2.0 A simplify scheme of Mass spectrometry.

Mass spectrometry is a powerful tool in qualitative and quantitative analysis of compounds with biological relevance. Owing to its high-resolution mass spectrometry, based approach will be used to detect the effect of vitamin D and or RA on the allelic variants of the HLA-DR in Chapter 6

Aims and Objectives

This thesis pursues two objectives as discussed in the general introduction. The first objective is to elucidate the regulation of the MHC II molecules particularly its degradation. There has been speculation that faster turnover of MHC II molecules is not good for maintaining immune tolerance. The first broad aim is **to characterise the role of specific lysosomal proteases in the turnover of HLA-DR glycoproteins in model APCs**. Work described in Chapter 3 identified a specific lysosomal protease playing a role in the degradation of MHC II (HLA-DR) molecules. The particular form of DR degraded by the lysosomal protease was evaluated in studies described in Chapter 4 of the thesis.

The second objective of this dissertation is to study the interaction of micronutrients like vitamin D and RA on the expression of the MHC II by developing new tool to study the allele specific effects on the cell lines that are heterozygous for MHC II allele. The second aim is **to understand how the expression of MHC II alleles and gene variantgene variants is regulated by vitamin D and retinoic acid**. Chapter 5 describes the combined effects of bioactive vitamin D and retinoic acid on common DRB1 alleles in homozygous typing cell lines and in a myeloid APC. Chapter 6 describes the development of new methods using stable isotope labelling for quantifying the allelic composition of the HLA-DR β chains in heterozygous APCs. This chapter also describes the effects of vitamin D and retinoic acid on the allelic composition of HLA-DR β chain. The conclusions are discussed in Chapter 7 of the thesis.

Chapter 2 Materials and methods

This chapter describes the methods and instruments used in the different experiments performed in this thesis.

2.1 Materials

2.1.1 Cell lines

The cell lines used in the thesis are listed in Table 2.1. MANN, BOLETH, COX, HOM-2, PGF and WDV are homozygous typing cells (HTCs) covering the six most prevalent HLA-DRB1 alleles found in one or both haplotypes of 90% of the White British/ White Irish/ Caucasian individuals. KG-1 cells are an acute myeloid leukaemia cell line. The L243 hybridoma produces monoclonal antibody L243, which is capable of binding the α domain of HLA-DR molecules (Lampson and Levy, 1980). EK and JBUSH are HTCs matched for the DRB1 alleles found in KG-1 cells.

Table 2.1 List of cell lines

Cell line	**Type**	**DR**	**Reference**
KG-1	Human acute myeloid leukaemia (AML) cell line	DRB1*11, DRB1* 14 DRB3*29	(Koeffler and Golde, 1978, Ning et al., 2011)
Priess	Homozygous typing cell line	DRB1*04:01	(Brodsky et al., 1979)
L243 Hybridomas	Hybridoma cells capable of producing L243 antibodies	-	(Nagy et al., 2002)
MANN	Homozygous typing cell line	DRB1*07:01 DRB4*01:01	

BOLETH	Homozygous typing cell line	DRB1*04:01 DRB4*01:03	(Marsh et al., 2010)
COX	Homozygous typing cell line	DRB1*03:01 DRB3*01:01	
HOM-2	Homozygous typing cell line	DRB1*01:01	
PGF	Homozygous typing cell line	DRB1*15:01 DRB5*01:01	
WDV	Homozygous typing cell line	DRB1*13:01 DRB3*01:01	
EK	Homozygous typing cell line	DRB1*11:01	
JBUSH	Homozygous typing cell line	DRB1*14:01	

2.1.2 Kits and reagents

The reagents used in the study were of the highest grade commercially available. Kits and chemicals used in the study are listed in Table 2.2 along with their catalogue number and supplier.

Table 2.2 List of kits and reagents

Items	**Supplier**
Kits	
Fixation/Permeabilization Solution Kit	BD life sciences (554714)
SYBR Green Cells-to-Ct Kit	Life technologies (4402954)
GenElute DNA Miniprep Kit	Sigma-Aldrich, G1N 70
8 peak and 6 peak validation beads	BD life sciences (653145)

Bicinchoninic acid assay (BCA) kit	Thermofisher (23225)
Chemicals	
rH Cathepsin D	R&D Systems (1014-AS)
rH cathepsin E	R&D Systems (1294-AS)
Complete protease inhibitor	Roche (11697498001)
Gentamycin	Sigma-Aldrich (G1272)
RT-PCR grade water	Ambion (AM 9935)
Fixation solution	BD life sciences (554655)
Protein A sepharose	GE life science (193256)
Instablue	Expedeon (SKU: ISB1L)
40% Acrylamide	Bio-Rad (161044)
Western ECL reagent	Clarity western ECL substrate (Biorad 1705060)
Pepstatin A	Sigma-Aldrich (P5318)
RA	Sigma-Aldrich (R2625)
Vitamin D3	Sigma-Aldrich (D1530)
IMDM	Gibco (12440053)
RPMI 1640	Gibco (11875093)
IMDM GlutaMAX	Gibco (31980030)
SILAC labelled RPMI (R6K6)	DC Biosciences (LM018)
L-glutamine	Sigma (G7513)
Fetal bovine serum	Sigma (F3145)
Penicillin/streptomycin	Sigma (P4333)
Dialysed serum (MWCO 10 kDa)	DC Biosciences (DS 1002)
Phosphate buffer saline tablets	Sigma (P4417)

2.1.3 Culture media

Cell lines were grown in either complete RPMI media or complete IMDM media with L-glutamine or Glutamax as described in Table 2.3.

Table 2.3 List of cell culture media

Media	**Cells**	**Description**
Complete IMDM	KG-1	IMDM , 20% (v/v) heat-inactivated foetal bovine serum (HIFBS), 2mM L-glutamine and 1% (v/v) penicillin/streptomycin
Complete IMDM Glutamax	KG-1	IMDM, 20% (v/v) HIFBS and 1% (v/v) penicillin/streptomycin
Complete RPMI	MANN, BOLETH, COX, HOM-2, WDV, PGF, PRIESS, EK, JBUSH	RPMI, 10% (v/v) HIFBS, 2mM L-glutamine and 1% (v/v) penicillin/streptomycin
Hybridoma media	L243 Hybridoma	RPMI , 10% (v/v) HIFBS, 2mM L-glutamine and 1% (v/v) penicillin/streptomycin
SILAC media	KG-1, MANN, BOLETH, COX, HOM-2, WDV, PGF	RPMI , 10% dialysed FBS and 1% (v/v) penicillin/streptomycin
Freezing media	various	90% HIFBS and 10% DMSO (sigma D2650)

2.1.4 Buffers and Solutions

All dilutions were made volume/ volume (v/v) for liquids and weight/volume (w/v) for solids unless otherwise stated. Table 2.4 states various buffers and solutions used in the study.

Table 2.4 List of buffers and solutions

Buffer/ Solutions	**Recipe/ Manufacturer**
Cell culture	
5 mM Pepstatin A stock	3.5 mg of Pepstatin A in 1 ml of DMSO
10 mM RA	3mg of RA in 1 ml of DMSO
10 µM Vitamin D3	4.16 mg of Vitamin D3 in 1 ml DMSO
1 mM $CuSO_4$	160 mg of $CuSO_4$ in 1 litre ddH_2O
Western Blot	
Phosphate buffer saline (PBS)	10x PBS tablets dissolved in ddH_2O
PBS-T	PBS + 5% Tween 20
RIPA buffer	50 mM Tris-Base, 150 mM NaCl, 1% Triton-X-100 and 0.1% SDS + Protease inhibitor cocktail (1 in 10ml)
SDS resolving buffer	1.5 M Tris-HCl pH 8.8; 0.4% SDS
SDS stacking buffer	0.5 M Tris-HCl pH 6.8, 0.4% SDS
SDS PAGE running buffer	25 mM Tris, 192 mM glycine, 0.1 % SDS
LaemmIisample buffer	0.5 M Tris-HCl pH 6.8, 10% glycerol, 2% SDS and bromo-phenol blue + – β-mercaptoethanol
Western Transfer buffer	25 mM Tris, 192 mM glycine and 20% v/v methanol
Western Blocking buffer	PBS-T + 5% skimmed milk powder
Stripping Buffer	0.1 M glycine, 20 mM magnesium acetate, 50 mM HCl, pH 2.2
Flow cytometry	
FACS buffer	PBS + 5% Bovine Serum Albumin +0.01% Sodium Azide

Perm-Wash buffer	Diluted from 10x stock of wash buffer BD
Antibody diluent	5% BSA in PBS
Immunoprecipitation	
Lysis buffer I	150 mM NaCl, 5 mM EDTA (pH 8), 50 mM Tris-HCl (pH 7.4), 1% CHAPS + complete protease inhibitor
Lysis buffer II	150 mM NaCl, 5 mM EDTA (pH 8), 50 mM Tris-HCl (pH 7.4), 0.1% CHAPS
Protein purification (L243 antibody)	
Wash buffer	200 mM sodium phosphate buffer, pH 7.0
Elution buffer	1 M glycine-HCl, pH 2.7
Neutralizing buffer	1 M Tris ,pH 9.0
Protein purification (sDR0401)	
Elution buffer	1 M Tris base pH 11.0
Neutralizing buffer	1 M glycine, pH 2.0
Molecular biology	
Loading buffer	0.25% bromophenol blue, 30% glycerol
Tris acetate EDTA (TEA) buffer	40 mM Tris, 20 mM acetic acid ,1 mM EDTA
Primer dilution (TE buffer)	10 mM Tris, 0.1mM EDTA, pH 8.0

2.1.5 Antibodies

A list of all the antibodies used in this study is provided in Table 2.5, together with their use and working dilution. For flow cytometry, antibody dilutions are commonly described as µl

of antibody added per test of 50 µl cell suspension. Cell numbers can range from 10^5 to 10^6 cells/test.

Table 2.5 List of Antibodies

Antibody	**Specificity**	**Supplier**	**Dilution**
Western Blot			
Anti HLA-DRα (DA6.147) mouse IgG	Binds to the DR α of the mature αβ heterodimer of the HLA-DR	Santa Cruz Biotechnologies	1:1000
Anti HLA-DRβ (DA2) mouse IgG	Binds to the DR β of the mature αβ heterodimer of the HLA-DR	Santa Cruz Biotechnologies	1:1000
CD74 (PIN.1) mouse IgG	Binds against amino acids 12-28 of CD74 (invariant chain).	Santa Cruz Biotechnologies	1:1000
CLIP (cerCLIP.1) mouse IgG	Epitope corresponding to class II invariant chain peptide (CLIP) amino acids 103-117	Santa Cruz Biotechnologies	1:1000
Human Cathepsin D (185111)	Mouse myeloma cell line NS0-derived recombinant human Cathepsin D	R&D Systems	1µg/ml
Human Cathepsin E (212211)	Mouse myeloma cell line NS0-derived recombinant human Cathepsin E	R&D Systems	1µg/ml
Human Cathepsin E (polyclonal) Goat IgG	Mouse myeloma cell line NS0-derived recombinant human Cathepsin E	R&D Systems	0.1µg/ml
Vitamin D receptor (D-6) mouse IgG	Monoclonal antibody raised against amino acids 344-424 of VDR of human origin.	Santa Cruz Biotechnologies	1:100
GAPDH mouse IgG	Monoclonal antibody raised against recombinant GAPDH of human origin.	Santa Cruz Biotechnologies	1:1000
β-Actin mouse IgG	Monoclonal antibody raised against recombinant β-Actin of human origin	Santa Cruz Biotechnologies	1:1000
HRP-conjugate anti mouse IgG	Polyclonal antibody which detects heavy and light chains of mouse IgG, raised in goat.	Dako	1:1000

HRP conjugate anti Goat IgG	Polyclonal antibody which detects heavy and light chains of goat IgG, raised in donkey.	R&D Systems	1:1000
Flow cytometry and Fluorescence microscopy			
Human HLA-DR – FITC (L243)	Murine IgG2a monoclonal antibody specific for the α-chain of correctly assembled HLA-DRαβ complex.	Biolegend or eBiosciences	5 µl/ test
CD 74 (BU45) FITC	Monoclonal antibody raised against various isoforms of CD 74	Novus biotech	5 µl/ test
CD74 (PIN.1) FITC	Monoclonal antibody raised against amino acids 12-28 of CD74.	Santa Cruz Biotechnologies	5 µl/ test
Mouse IgG2a k isotype control-FITC	NA	Biolegend	5 µl/ test
Anti HLA-DR Rabbit monoclonal	Monoclonal antibody corresponding to Human HLA-DR amino acids 150-250.	Abcam	1:50
Cathepsin D Rabbit polyclonal	Synthetic peptide corresponding to residues with the heavy chain subunit of human Cathepsin D	Invitrogen	1:200
Goat anti-Rabbit IgG- APC	Polyclonal antibody which detects heavy and light chains of rabbit IgG, raised in goat.	Invitrogen	1:500
DAPI	A probe which selectively binds to the minor groove of the double stranded DNA in the nucleus	Invitrogen	1:100
Mouse IgG1 isotype control - APC	NA	R&D Systems	2.5 µl/ test

2.1.6. Lab instruments

A list of all the instruments used for this work is provided in Table 2.6

Table 2.5 List of general laboratory instruments

Instrument	**Manufacturer**
Agarose gel electrophoresis system	Bio-Rad
Bench-top centrifuge	Eppendorf
Biochemical fridge	Loviband
Bio-safety class II cabinet	Envair
End over-end rotor	Stuart rotator
Flow cytometer Accuri C6	B.D
Fluorescent microscope	Nikon
Fridge and freezer	Various
Gel imager	Bio-Rad
Gel imager	Licor
Humidified incubator	Hera cell 240
Light microscope	Olympus
Pipettes	Sartorius
Mass spectrometer	Thermofisher (outsourced to CCP)
Nanodrop	G.E
Plate centrifuge	Eppendorf
Plate reader	Thermoscientific
Plate Shaker	VWR
Power pack	Bio-Rad
Real time PCR	Applied Bio-systems
SDS gel system	Bio-Rad
Thermocycler	Bio-Rad
Water bath	Techne

2.2 Methods

2.2.1 Cell culture

All cell culture work was performed in a laminar flow hood under appropriate aseptic conditions and as described in Freshney (1987).

2.2.1.1 Maintenance of cell lines

Cells were maintained in suspension culture in a humidified CO_2 incubator at 37 ˚C. They were diluted thrice a week to maintain approximately 10^5-10^6 cells/ml. Cell dilution was performed after counting by haemocytometer. The average of two counts was used to calculate cell numbers in the culture flask. Media used for the cell dilution were incubated at 37 ˚C for at-least 20 minutes before usage.

2.2.1.2 Cell freezing

Cells were centrifuged at 300 x *g* for 5 minutes and the supernatant discarded. The cell pellet was re-suspended in ice-cold freezing media at a concentration of 1 x 10^7 cells/ ml in a cryovial. The DMSO in the freezing media acts as a cryoprotective agent (Lovelock and Bishop, 1959). The cryovial was then placed into a "Mr Frosty" (Thermo Scientific 5100-0001) container for slow freezing and stored at -80°C for 24 hours. The cryovials were transferred to liquid nitrogen (-196°C) for long term storage.

2.2.1.3 Cell thawing

A vial containing a frozen aliquot of the cells was taken from liquid nitrogen and thawed rapidly by gently agitating the vial in a water bath set to 37°C. Using a plastic Pasteur pipette, the contents of the vial were quickly transferred to a centrifuge tube. To this, 9 mL of pre-warmed complete medium was added gradually and centrifuged at 300 x *g* for 10 minutes.

The cell pellet was then re-suspended in 10 mL of pre-warmed complete medium and added to a tissue culture flask. Cells were monitored for recovery and growth, and split after 2-3 days.

2.2.1.4 Cell treatment with protease inhibitor or vitamin D or Retinoic acid

KG-1 cells were incubated in medium supplemented with 20μM Pep A or 10μM Pepstatin A –penetratin (Pep A-P) for up to 72 hours, along with untreated cells as a control. 0.4% DMSO and PBS were used as vehicle controls for Pep A and Pep A-P, respectively. Cells were harvested after 24, 48 or 72 hours and were analysed by flow cytometry and Western blot.

In order to assess the effect of vitamin D and retinoic acid (RA), cells were grown in complete medium supplemented with 10nM active vitamin D (calcitriol) and or 1μM *all-trans* RA for up to 96 hours. As vehicle control KG-1 cells were treated with 0.5% DMSO. Cells were harvested after 24, 48 or 72 hours and were analysed by flow cytometry.

2.2.1.5 Protein production

L243 hybridoma cells were cultured as described in section 2.1.2 and expanded to large cultures (in T-125 flasks). At a cell density around 10^6 cells/ ml, cells were left for protein recovery (Iiet al., 2010). After 5 days, media were collected and centrifuged at 300 x *g* for 10 minutes at 4°C to remove the cells and debris. The supernatant was then transferred to fresh tubes. For long term storage 0.1% sodium azide was added to supernatants which were stored at -20°C.

2.2.1.6 Stable Isotope labelling

Stable Isotope labelling of Amino acids in Culture (SILAC) was performed using the protocol described by Ong and Mann (2007a). The cells were diluted in complete SILAC

media containing labelled Lysine and Arginine. Cell growth was monitored by regular haemocytometer count. Cells were labelled to completion by culturing the cells in SILAC media for at least 5 doublings.

2.2.2 Biochemical Techniques

2.2.2.1 Cell lysis

To extract proteins from cultured cells, samples containing at least 1 x 10^6 cells were taken, and the cells were pelleted by centrifugation at 400 x *g* for 5 minutes. The supernatant was discarded, and the cells were washed twice with cold PBS and centrifuged again at 400 x *g* for 5 minutes. Ice-cold RIPA buffer containing protease inhibitor cocktail was added to the cell pellet, using 0.5 ml of buffer per 1 x10^6 cells, as described by Harlow and Lane (2006). The samples were placed on an end-over-end rotator for at least 1 hour at 4 °C and were then centrifuged at 10000 x *g* for 30 minutes at 4 °C to pellet the cell debris. The supernatants were transferred to a new tube for analysis or kept at -20°C for longer term storage.

2.2.2.2 Bicinchoninic acid assay (BCA) protein quantification assay

Protein concentration of RIPA extract was estimated using the Pierce BCA Protein Assay Kit (Smith et al., 1985). The BCA assay was performed in a 96-well microplate and the procedure was conducted as per the manufacturer's instructions. Bovine Serum Albumin (BSA) was used as a standard. Briefly, 200 µL of working reagent was used. To this 10 µL of RIPA extract was added per well. Samples were run in triplicate and compared to a standard curve (20µg/ml to 2mg/ml BSA in water). The plate was then placed in an incubator at 37°C for 30 minutes before the sample concentrations were determined using a microplate reader, reading at 570 nm.

2.2.2.3 Sodium Dodecyl Sulphate Polyacrylamide Gel Electrophoresis (SDS-PAGE)

As described (Laemmli, 1970), proteins can be separated on the basis of their mass by electrophoresis in a SDS polyacrylamide gel under denaturing conditions. To prepare the SDS polyacrylamide gel, vertical gels were set between two glass plates within a casting chamber and two spacers, giving an internal thickness of 1.0 mm between the two plates. The gels were composed of two layers: a 12% acrylamide/bisacrylamide separating gel that separates the proteins according to size and a lower percentage (4%) stacking gel that ensures simultaneous entry of the proteins into the separating gel. The gel compositions are listed in Table 2.7. Protein samples were mixed in SDS LaemmIisample buffer with or without reducing agent, 2-mercaptoethanol (5%v/v), and denatured by heating at 95°C for 5 minutes. Electrophoresis was carried out using BioRad mini-Protean II electrophoresis equipment in SDS PAGE running buffer for 20 minutes at 80 V, followed by approximately 45 minutes at 120 V or until the dye front reached the bottom of the gel.

Table 2.7 Solutions for SDS PAGE gels

Component	**12% Resolving gel**	**4% Stacking gel**
ddH_2O	11.15 ml	6.4 ml
Acrylamide (40%)	7.5 ml	1.0 ml
1.5M Tris HCl buffer pH 8.8	6.25 ml	-
0.5M Tris HCl buffer pH 6.8	-	2.5 ml
10% Ammonium Per-Sulphate (APS)(fresh)	125 µl	50 µl
Tetramethylethylenediamine (TEMED)	13 µl	10 µl

The above recipes are for four gels.

2.2.2.4 Western Blot

Protein samples resolved by SDS PAGE were transferred onto PVDF membrane (Bio-Rad). The PVDF transfer membrane was soaked in 100% methanol for one minute, then with water, and equilibrated in western blot transfer buffer for a few minutes. The gel was placed on top of the PVDF membrane. Care was taken to avoid trapping of air bubbles (Mahmood and Yang, 2012). The transfer was performed for 90 minutes at 90 V. A pre-stained molecular weight protein ladder (Bio-Rad 1610394) served as an indication of successful transfer. Membranes were briefly washed in PBS-T before being blocked in blocking buffer overnight. Primary antibody was diluted into blocking buffer at dilution listed in Table 2.4 and incubated with the membrane for 3 hours at room temperature, unless specified, with gentle agitation. The membrane was washed five times for 5 minutes each with 10 mL of PBS-T wash buffer. The membrane was then incubated with the species-appropriate horseradish peroxidase (HRP) -conjugated secondary antibody at the dilutions given in Table 2.4 in 10 mL of blocking buffer for 1 hour at room temperature. Again, the membrane was washed five times for 5 minutes each with 10 mL of PBS-T.

In order to visualise the blot using chemiluminescent detection, the membrane was incubated in 10 mL of ECL Clarity Western blotting substrate. To prepare the HRP substrate, equal volumes of Luminol Reagent and Peroxide Solution were mixed to give a final volume of 10 mL. The membrane was placed protein side up in a clean container and the HRP substrate was carefully applied to the membrane and left to incubate for 5 minutes at room temperature. After 5 minutes, excess substrate was drained off and the membrane was imaged either by exposure to film or by using the Li-COR Odyssey gel imager Fc. Li-COR's proprietary imaging software, Image studio (version 5.2), was used to quantify bands of interest.

If necessary, the blot was stripped again and re-probed with another antibody. This was mainly done for loading controls (GAPDH or β-actin). The blots were incubated with stripping buffer for 30 minutes and later washed with PBS for 10 minutes. The blot was then re-blocked for 1 hour and re-probed with primary antibody of the loading controls.

2.2.2.5 Immunoprecipitation

A 50% slurry (i.e., 50% settled beads by volume) of protein A sepharose beads was prepared as per the manufacturer's instructions. Briefly, lyophilized powder of protein A-sepharose beads was allowed to rehydrate by incubating 100 mg of beads in 1 ml PBS at 4°C for 1 hour for swelling. The rehydrated beads were then washed three times with 10 volumes of PBS by centrifuging at 400 x *g* for 10 minutes each in a refrigerated benchtop centrifuge, and carefully aspirating the supernatant. Lastly the final volume was adjusted with PBS to obtain the 50% slurry. In order to preserve the slurr,y sodium azide was added at final concentration of 0.2% (Bonifacino and Dell'Angelica, 2001).

A total of 5 x 10^6 cells were harvested and lysed at 4°C in 500µl of lysis buffer I, which was freshly supplemented with complete protease inhibitor mixture. Nuclei were removed by centrifuging at 10,000 x *g* for 30 minutes. Soluble cell lysates were precleared for 1 hour using 40 µl of 50% protein A sepharose beads. After removing the sepharose beads by centrifugation (5 minutes at full speed in an Eppendorf microcentrifuge), the lysate were incubated overnight with 10 µg L243 and 40 µl of 50% sepharose beads at 4°C. Unbound material was removed by washing four times with lysis buffer II. Immunoprecipitated material was eluted in non-reducing SDS sample buffer for 5 min at 100°C and separated by SDS-PAGE. Gels were then either fixed and stained using InstantBlue^{TM,} with relevant bands excised after scanning them using Licor or Bio-Rad gel Doc system and stored at -20˚C or below for later LC-MS/MS analysis.

2.2.2.6 Protein purification

Unless specified, the entire process of protein purification was performed at 4°C. L243 was purified from the hybridoma supernatant by protein A- sepharose affinity chromatography. Debris was removed by centrifuging the supernatant at 3500 x *g* and filtered through a 0.45 µm filter. The supernatant was adjusted to pH 8.0 using 1M NaOH and passed over a protein A sepharose column. The column was washed with binding buffer until a baseline (monitored by absorption at 280 nm using a Nano-drop) was re-established, and eluted with elution buffer. Fractions were immediately neutralized with neutralizing buffer. Eluate fractions absorbing at 280 nm were pooled and concentration was established using Nano-drop. The specificity of the antibody was checked by flow cytometry and immunoprecipitation.

The activity of the purified L243 monoclonal antibody was detected by competitive inhibition of HLA-DR using flow cytometry in KG-1 cells. The method and results are described in Appendix 2.1.

2.2.3 Fluorescence staining

2.2.3.1 Preparation of samples for flow cytometry

In order to quantify surface expression of mature HLA-DR molecules, live cells were suspended in FACS buffer. FcR and other free IgG binding sites were blocked by incubation with 10% (v/v) normal mouse serum (NMS) for 15 min at 4˚C prior to addition of anti-HLA-DR (L243) FITC conjugated antibody (5µl) or isotype control (IgG2a-FITC), which was incubated for 1 hour at 4 ˚C. Cells were washed twice and re-suspended in FACS buffer or post-fixed with BD cytofix buffer and analysed using an Accuri C6 flow cytometer.

To detect combined surface and intracellular MHC class II molecules, cells were fixed and permeabilised using Cytofix/Cytoperm™ solution as per manufacturer's instructions. Cells were suspended in Cytofix/Cytoperm™ solution (45µl per test) for 20 minutes and washed with Perm/Wash buffer. FcR and any other free IgG binding sites were blocked by incubation with 10% (v/v) NMS for at least 15 min at 4˚C prior to addition of anti-HLA-DR (L243) FITC- conjugated antibody, as described above. Cells were washed twice, re-suspended in Perm/Wash buffer, and analysed using Accuri C6 after fixing with BD cytofix buffer.

For the detection of Cathepsin D, KG-1 cells were fixed, permeabilized and blocked as described above. Then cells were incubated with 50 µl (1:200) rabbit polyclonal unconjugated anti-cathepsin D at 4˚C for 60 minutes. Cells were then washed with wash buffer and incubated with 50µl (1:500) goat anti-Rabbit IgG-APC conjugate 4˚C for 30 minutes. Cells were washed twice, re-suspended in Perm/Wash buffer, and analysed using Accuri C6 after fixing with fixation buffer.

2.2.3.2 Flow cytometry setup and analysis

Flow cytometry analysis was performed on BD Accuri C6. Fluorescence excitation was generated using a 488 nm or 640 nm laser while the fluorescence emission was detected by either FL1 for FITC conjugates or FL4 for APC conjugates. All samples were run for 20,000 events in medium flow and all samples were at least run in duplicate. Results were analysed using the BD Accuri C6 software (BD Biosciences) and visualized in histogram plot (counts versus fluorescence). The median (mean in some experiments) fluorescence intensity (MFI) value for each sample run was used for the measurement after gating for single intact cells based on light scatter.

2.2.3.3 Fluorescence microscope sample preparation

Cells were stained as explained in section 2.2.3.1. In addition, nuclei was visualised by counter staining using DAPI. Cells were then washed with wash buffer and fixed with fixation solution for 20 min on ice. After washing cells were allowed to adhere on polylysine coated slides. Slides were allowed to dry overnight in the dark and once dried, slides were mounted with Vectashield and analysed on the microscope (Nikon).

2.2.4 Molecular Biology Techniques

2.2.4.1 Total RNA preparation

RNA was isolated from cells using the power SYBR® Green Cells-to-Ct^{TM} Kit (Life Technologies, 4402954) as per manufacturer's instructions. Briefly, 1.0 x10^5 KG-1 or Priess cells were incubated with 50 µl lysis solution containing DNase I (1:100 dilutions) for 5 minutes. After incubation, stop solution was added to the lysis reaction and incubated at room temperature for 2 minutes. The lysate containing RNA were generally used immediately for cDNA synthesis. If required, overnight storage was at -20 °C.

2.2.4.2 c-DNA synthesis

Complementary (c) DNA must be synthesised from mRNA to provide a template for PCR amplification. Complementary DNA was synthesised from mRNA by reverse transcriptase (RT), transcribing single- stranded DNA from an RNA template. Buffers containing dNTPs (25 µl), NF (nuclease free) H_2O (12.5 µl), 20x RT enzyme mix (2.5 µl) and RNA (10 µl) were mixed. The total volume for each reaction was 50 µl. Using a thermocycler samples were incubated at 37°C for 1 h followed by 95°C for 5 min to inactivate the enzyme. The resulting cDNA was used for PCR analysis.

2.2.4.3 PCR

PCR (polymerase chain reaction) was carried out using the power SYBR® Green Cells-to-Ct™ Kit as per manufacturer's instructions. SYBR Green is a reporter cyanine dye that intercalates with double strand (ds) DNA emitting green fluorescence (Ponchel et al., 2003). During the denaturing step of the PCR reaction, ds DNA becomes single stranded DNA and the fluorescence is lost. When the primers anneal to their target and extension occurs, SYBR Green binds the newly synthesised ds DNA strand, and the amount of fluorescence emitted is proportional to the quantity of product present in that cycle. The amount of transcript is determined by the cycle threshold (Ct) value. The Ct is the cycle at which the fluorescence reaches a certain threshold, above that of background fluorescence, during the exponential phase of the reaction. To confirm the presence of a specific amplification product, a dissociation (melting) curve (Tm) was included (Bustin, 2002). The PCR was set up for qualitative analysis, and hence the results were reported as an amplification curve and the melting temperature.

RT-PCR was performed in a 96 well plate format (Applied Biosystems). A 20µl final volume was prepared containing 10µl Power SYBR Green Master Mix, 2µl primer pairs (0.5µM), 4µl NF H_2O and 4µl cDNA generated from the above step. The plates were briefly spun to remove liquid from the side of the well, and the plate loaded into the Step one plus qPCR instrument (Applied Biosystems). The qRT-PCR cycling programme is detailed in Table 2.8. Each set of samples was run for the gene of interest in parallel with GAPDH as an internal control. The list of primers used in the study is shown in Table 2.9.

Table 2.8 PCR thermo-cycling conditions.

Step		**Temperature (°C)**	**Duration (min:sec)**
Enzyme activation		95	10:00
c-DNA denaturation	**X 30 cycles**	95	00:15
Primer annealing		55-60*	01:00
Primer extension		72	00:15
Dissociation		95	1°C per minute

* The annealing temperature was optimized.

Table 2.9 List of primers used in the study. All primers are shown from 5'to 3'

Gene		**Sequence**	**Molecular weight* (bp)**	**Reference**
Cat D	Forward	CATTGTGGACACAGGCACTTC	296	(Hausmann et al., 2004)
	Reverse	GACACCTTGAGCGTGTAGTCC		
Cat E	Forward	CTGCTGGTCGGACTCACAAT	500	(Puizdar et al., 2012)
	Reverse	CCACCTGGTAGGAGAAAGCA		
GAPDH	Forward	AGGGCTGCTTTTAACTCTGGT	206	(Hausmann et al., 2004)
	Reverse	CCCCACTTGATTTTGGAGGA		

*Molecular weight of the amplified PCR product

2.2.4.4 Agarose gel Electrophoresis (AGE)

The PCR product was run on an agarose gel. Agarose (350 mg) was dissolved in Tris EDTA buffer (50 ml; TBE) by heating in a microwave until boiling this solution was allowed to cool and DNA Sybr safe dye (Invitrogen) was added (5 µl/ 50 ml). Gels were then cast in a 10 x 20 cm gel tank, which was set in a mould containing a toothed comb. The 10µl PCR product was pipetted into wells alongside a well containing 5µl 100 kb ladder combined with 1µl 6X

loading dye (Promega UK Ltd.). Electrophoresis was performed at 70V for 90 min. Gels were imaged using the LI-COR Odyssey Fc.

2.2.4.5 DNA extraction

DNA was extracted from the cell lysates using the GenElute DNA Miniprep Kit (Sigma-Aldrich, G1N 70) according to the protocol provided by the manufacturer. Briefly, cells were incubated with lysis solution containing RNase for 2 minutes, followed by incubating with Proteinase K solution (20mg/ml) at 70 C for 10 minutes. After several centrifugation steps using DNA- columns, the trapped DNA was eluted in a Tris–EDTA buffer (pH 8–8.5). The quality and concentration of the DNA was determined using Nano-drop.

2.2.4.6 HLA Genotyping

HLA genotyping was performed at the Anthony Nolan Research Institute, Royal Free Hospital, Pond Street, Hampstead, NW3 2QG in collaboration with Professor Steven Marsh and Dr. Neema Mayor. This was done by using Sequence Specific Primers (PCR-SSP) and PCR Sequence Based Typing (PCR-SBT) methods as described by Dunckley (2012). HLA-DRB1 and any additional DRB3/4/5 genotypes were reported.

2.2.4.7 Knockdown

2.2.4.7.1 Lentiviral vector and mechanism of transduction

Lentiviruses are a subset of retroviruses, which are naturally occurring single stranded RNA containing viruses (Baltimore, 1970). Upon entry into the cell cytoplasm, the viral RNA is reverse-transcribed into double stranded DNA by the viral enzyme reverse transcriptase, encoded by the pol gene. The viral DNA is then translocated into the cell nucleus, where it is incorporated permanently and indiscriminately into the host cell genome due to the presence of long terminal repeats (LTRs) (Joyner and Bernstein, 1983). As a result, all cells descended

from an infected cell carry the viral genome (Walsh and Cepko, 1988). During cellular transcription and translation, the viral genomic RNA and viral structural proteins such as *gag* and *env*, coding for viral capsid and envelope proteins respectively, are produced and assembled to generate viral progeny (Kaye et al., 1995). This unique feature of the lentiviruses albeit with some modifications is exploited for research purposes (Zhao and Lever, 2007, Singer and Verma, 2008, Manjunath et al., 2009).

The modifications are performed to convert natural viruses into useful tools for genetic modification for research and for biosafety. Alterations include the removal of viral genes responsible for virulence and pathogenesis (Delenda, 2004). The entire lentiviral vector system is usually separated in three or four plasmids in the interest of improving biosafety: the packaging plasmid (may be split into 2 plasmids), the gene transfer plasmid and an envelope (env) plasmid. Hence, viral packaging can be achieved by using triple (2^{nd} generation) or quadruple (3^{rd} generation) co-transfection (Lever et al., 2004) to generate lentiviruses that express the desired foreign genetic element. Further modifications include the removal of the env gene from the lentiviral genome and replacement with a heterologous glycoprotein, vesicular stomatitis virus glycoprotein (VSVG). The presence of this protein confers the virus particle with the ability to transduce a wide range of cell types including primary cells, stem cells and early embryos (Naldini et al., 1996, Lois et al., 2002, Pfeifer et al., 2002).

In this study, lentiviral cloned into pLKO.1-puro vector were used (Sigma MISSION® shRNA Human Gene Family Set, Lentiviral Particles). In order to obtain sustained knockdown of the cathepsin D gene, short hairpin RNA (shRNA) was cloned in the pLKO.1-puro vector. The vector also carried $puro^R$ i.e. the puromycin resistance gene for the selection of successfully transduced cells. In order to assess any off-target phenotypical or biochemical effects of transduction and/ or selection, an empty vector containing only $puro^R$ was used as a

control in the experiment. The lentiviral construct is shown in Figure 2.1. The resulting recombinant viral genome thus converts the infection process to an efficient transduction one, allowing for non-replicative entrance of a virus into the host cell, followed by expression of the desired genetic information it carries in its genome. In the interest of biosafety, the resultant viruses produced are replication-incompetent, hence unable to produce viral progeny.

2.2.4.7.2 Method of infection.

KG-1 cells ($0.5x10^5$) were re-suspended in 200 µl of fresh media in 96 well plate and treated with a final concentration of 8µg/ml polybrene, in order to facilitate the fusion of the virus particle to the cell membrane, hence increasing the infection efficiency. This was done 15-16 hours prior to the commencement of the transfection. On the day of infection, the lentiviral supernatants were added to the cells at the desired multiplicity of infection (MOI) and the plates were centrifuged for 30 minutes at 500 x *g* at RT.

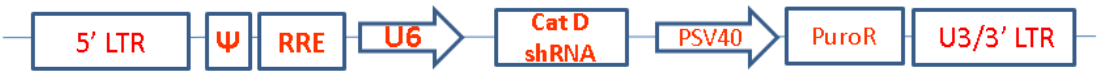

5' LTR➔ 5' HIV long terminal repeats
Ψ➔ HIV PSI packing signal
RRE➔ HIV-1 Rev response element
U6➔ U6 promoter
Cat D shRNA➔ short hairpin RNA targeting cathepsin D
PSV 40➔ SV 40 promoter
PuroR➔ Puromycin resistance gene
U3/3' LTR ➔ U3/HIV-1 truncated 3' LTR

Figure 2.1 Lentiviral construct of the PLKO.1 vector. The above diagram is the schematic representation of the lentiviral construct used for the knockdown of the cathepsin D gene in the KG-1 cells.

Note: MOI is the number of transducing lentiviral particles per cell. It was calculated as per manufacturers' instruction. To calculate: (total number of cells per well) x (desired MOI) = Total transducing units needed (TU)

Total ml of lentiviral particles to add to each well = (Total TU needed) / (TU/ml reported on certificate of analysis provided).

Cells were monitored for 48 hours and then expanded to 24 well plates with a total volume of 500 µl in each well. Cells were monitored regularly, and selection was initiated by adding 1 µg/ml of puromycin into the media. Puromycin resistant cells were identified and expanded further into 6-well plates and later to T-25 culture flasks by adding fresh media supplemented with puromycin.

2.2.5 Mass spectrometry

This section describes the general approach for generating isotopically labelled standards and mass spectrometry.

2.2.5.1 LC-MS sample preparation

Excised DR α/β bands from SDS gels (section 2.2.2.5) were analysed by liquid chromatography-tandem mass spectrometry (LC-MS/MS) following tryptic digestion at the Cambridge Centre for Proteomics (De Riva et al., 2010, Prevosto et al., 2016). SDS–PAGE gel pieces were thawed and transferred into 96-well PCR plates for automated sample preparation in a Mass Prep Station (Waters). Briefly, the gel bands were destained, reduced (dithiothreitol [DTT]), alkylated (iodoacetamide), and digested with trypsin overnight at 37 °C. Thereafter, 20 µl of supernatant was pipetted into a sample vial and loaded onto an autosampler for LC-MS/MS analysis.

2.2.5.2 Liquid chromatography-tandem mass spectrometry (LC-MS/MS)

Tandem mass spectrometry analysis was carried out on an Orbitrap Q-Exactive mass spectrometer (ThermoFisher). The Q Exactive instrument includes an atmospheric pressure ion source (API), a stacked-ring ion guide (S-lens) in the source region, a quadrupole mass filter, a C-trap, an HCD cell, and an Orbitrap mass analyzer. Ions are formed at atmospheric pressure, pass through a transfer tube to an S-lens and then via an injection multipole into a bent flatapole (Michalski et al., 2011). The data acquisition was carried out at lower resolution (17,000) and higher resolution (70,000). The mass spectrometric raw data were analysed further with Proteome Discover (PD) and Maxquant (MQ) (Cox and Mann, 2008) software packages. Parameters set for quantitative analysis included up to two missed cleavages and variability of mass i.e. due to phosphorylation (S, T, and Y), ubiquitination, oxidation (Met, *in vitro* processing) and carbamido-methylation (iodoacetamide alkylation prior to trypsin digestion). The parameters defined are important, as they can increase the stringency of the search, increase confidence in protein identification, and simplify analysis.

2.2.5.3 Peptide identification and assignment to MHC II alleles

The data generated from the software packages gives the list of all identifiable peptides from the proteins in the mass spectrometry analysis with the corresponding normalised Heavy/Light SILAC ratios. The list also included some of the common contaminants like human keratin (comes from handling) and bovine serum proteins, which were omitted from further analysis. In addition, neither software programmes are not sufficient for the task of peptide assignment for the alleles. It can generate false positive matches to MHC II alleles which are not present in the HLA genotype of the cells being analysed. This was due to matches of the identified peptides, in novel combinations, to irrelevant MHC II alleles in the sequence databases.

In order to assign the peptides to the MHC II alleles, the cDNA sequences of the alleles (obtained from HLA genotyping section 2.2.4.6) were obtained from IMGT/HLA database (http://www.ebi.ac.uk/ipd/imgt/hla/). These sequences were then subjected to *in-silico* tryptic digestion with Peptide Mass on the Expasy server (http://web.expasy.org/peptidemass/). Incomplete cleavages were allowed in order to keep the parameters similar for both the tryptic digestion. Virtual digests were used to identify the subset of peptides that are specific for a particular MHC II allele, or shared between the alleles. Such peptides were then selected from the amongst the MHC II peptides in LC-MS/MS and analysed further for SILAC labelling by calculating % light or % heavy values.

2.2.6 Statistical analysis

Statistical analysis was performed either using R software (Knezevic et al., 2007) or SPSS statistics 24 software (IBM Corp, 2012). For all tests, a p value ≤ 0.05 was taken as statistically significant. For all bar graphs, the mean ± SD was plotted in MS Excel. Mean and median fluorescence values were extracted using the native C6 softwar.

Chapter 3: Non-redundant role of Cathepsin D in the degradation of HLA-DR molecules in KG-1 cells.

3.1 Abstract

The expression of major histocompatibility complex class II (MHC II) molecules is post-translationally regulated by endocytic protein turnover, but the mechanisms remain poorly understood. In this study, cathepsin D was implicated in the degradation of HLA-DR. Using flow cytometry, pepstatin A (Pep A), an inhibitor of the lysosomal aspartyl proteases, cathepsin D and E (Cat D/E), was shown to rescue human leukocyte antigen (HLA)-DR molecules from degradation. This was observed in the myeloid cell line, KG-1 but not in the B-lymphoblastoid cell line, Priess, correlating with expression of Cat D in these cells, which was assessed by Western Blot and qRT-PCR. Fluorescence microscopy of KG-1 cells also showed the co-localisation of HLA-DR and Cat D in the vesicular compartment. Lastly, lentiviral knockdown of Cat D protein expression in KG-1 cells caused elimination of the Pep A effect on HLA-DR expression. Thus, Cat D has a vital role in the degradation of HLA-DR molecules in KG-1 cells. In addition, in cell lines in which Cat D activity was inhibited for prolonged periods there was evidence of adaptation, based on steady- state levels of HLA-DR, raising the possibility that other enzymes might substitute.

3.2 Introduction

As explained in section 1.3, MHC II molecules are expressed mainly on professional APCs and display antigenic peptides to CD4+ T cells. (Rigby et al., 1990, Chaplin, 2006, Zhu and Paul, 2010). MHC II maturation is a complex process involving the assembly of MHC II αβ dimer with invariant chain (Ii) (Busch et al., 1996), transport of the MHC II/Ii complexes and their sorting to endocytic compartments (Busch and Mellins, 1996, Brachet et al., 1997), degradation of peptides and their HLA-DM catalysed binding to MHC II (Blum et al., 2013), and transport of MHC II/peptide complexes to the plasma membrane (Mak and Saunders, 2006). After presentation of antigen, MHC II are degraded in lysosomes (ten Broeke et al., 2013).

The cellular factors that regulate MHC II maturation have been studied extensively, but their degradation, to date, has not been understood completely. Most cell surface proteins undergo ubiquitination and sorting into late endosomal compartments (Wright et al., 2011), and MHC II molecules follow this pathway (Hor et al., 2009). Lapaque et al. have shown that α and β chains of MHC II can be ubiquitylated by membrane associated RING-CH 1 (MARCH 1) protein, which is a RING- family ubiquitin E3 ligase (Lapaque et al., 2009). Internalisation and turnover of MHC II molecules are regulated by ubiquitination of the β-chain (Shin et al., 2006, van Niel et al., 2006). Moreover, the fact that MARCH 1 knockout mice display increased levels of MHC II at the plasma membrane also highlights the importance of internalization of MHC II for its degradation. Thus, ubiquitination promotes MHC II endocytosis and lysosomal sorting, which results in degradation of MHC II (Furuta et al., 2013), as shown in Figure 3.1.

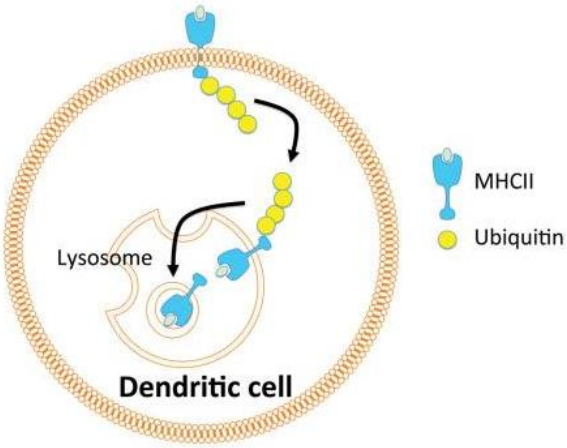

Figure 3.1 Degradation of MHC II molecules. MHC-II is ubiquitinated at a conserved lysine in the cytoplasmic tail of the β chain, which promotes its internalisation into lysosomes, where it may be degraded by lysosomal proteolysis. Adapted from Oh and Shin (2015) .

3.2.1 Lysosomes

Lysosomes are single membrane-bound intracellular organelles containing various acid hydrolyases in their acidic lumen (Mindell, 2012, Luzio et al., 2007). They serve as the final destination of molecules targeted for destruction by numerous peptidases, called cathepsins. The term “cathepsin” stands for “lysosomal proteolytic enzyme”, regardless of the enzyme class. Cathepsins include cysteine proteases, aspartic proteases and serine proteases (Turk et al., 2012). They are so named because because the active sites of cathepsins utilises, respectively a cysteine thiol, an aspartic acid, or a serine residue to attack the peptide bond at the catalytic site (Turk et al., 2000, Turk et al., 2001). They are involved in a number of important biological processes, such as intracellular protein turnover, antigen processing, hormone activation, remodelling of the extracellular matrix, and apoptosis (Im and Kazlauskas, 2007, Nomura and Katunuma, 2005, Friedrichs et al., 2003).

3.2.2 Role of cathepsins in antigen presentation.

Lysosomal proteases have several different roles in antigen processing, presentation and MHC II maturation. They process antigen and process Iichain. There is certainly a level of redundancy to this system (Reich et al., 2011). Even the otherwise non-redundant cysteine proteases, cathepsins L and S (Cat L/S), can play the same role in the degradation of Ii, with Cat L being copiously expressed in thymic epithelial cells, whereas B cells and DCs express Cat S (Hsing and Rudensky, 2005, Reich et al., 2011). In addition, Cat G, a serine protease, plays a vital role in the degradation of some antigens for presentation (Stoeckle et al., 2009). Various lysosmal proteases involved in MHC II maturation along with their broad spectrum inhibitors, are listed in Table 3.1.

Table 3.1 Proteases found in the Lysosomes along with their Inhibitors.

Catalytic type	**Protease**	**Role in Antigen presentation**	**Reference**	**Inhibitor**
Cysteine Proteases	Cathepsin B	Intracellular proteolysis	(Gondi and Rao, 2013)	E-64, E-64d, leupeptin.
	Cathepsin C	Antigen processing	(Kummer et al., 1996)	
	Cathepsin F	Degradation of antigenic peptides	(Wang et al., 1998)	
	Cathepsin L	Processing of Iiin Thymic epithelial cells	(Hsieh et al., 2002)	
	Cathepsin S	Processing of Iiin B cells and DCs	(Riese et al., 1996)	
	Cathepsin W	Degradation of antigenic peptides.	(Riese and Chapman, 2000)	
	asparaginyl endopeptidase (AEP)	Degradation of antigenic peptides	(Manoury et al., 1998)	
Serine Proteases	Cathepsin A			phenylmethylsulfonyl fluoride (PMSF), 4-(2-aminoethyl)benzenesulfonyl fluoride hydrochloride (AEBSF)
	Cathepsin G	Destruction of auto-antigen myelin basic protein Destruction and generation of specific T cell epitopes	(Stoeckle et al., 2009). (Burster et al., 2004)	

Aspartyl Proteases	Cathepsin D	Thought to play a role in Iidegradation but some studies do contradict it. Antigen processing	(Marić et al., 1994) (Deussing et al., 1998)	Pepstatin A, Pepstatin A-penetratin
	Cathepsin E	Antigen processing in APCs like Langerhans	(Hewitt et al., 1997, Chain et al., 2005)	

3.2.3 Lysosomal degradation of MHC II

Early biochemical studies showed that MHC II molecules are resistant to many proteases *in vitro*, but can be cleaved off the plasma membrane by papain (Gorga et al., 1991). The proteases that degrade MHC II molecules *in vivo* remain unknown. One study showed that MHC II molecules accumulate in immature DCs treated with E64, an inhibitor of cysteine proteases (Herrmann et al., 2007), but that effect was small, and a number of these enzymes failed to cleave purified DR molecules in vitro (Burster et al., 2010). Conversely, the serine protease, cathepsin G (Cat G), was able to cleave many HLA-DR alleles *in vitro* but did not cause degradation of membrane bound HLA-DR *in vivo*, nor did its inhibition cause accumulation of HLA-DR, suggesting that *in vivo*, the Cat G site is sterically inaccessible or masked by other associated molecules (Burster et al., 2010).

The degradation of MHC II is an important un-elucidated process. MHC II molecules are extraordinarily stable but still display cell type-specific half-lives (Busch and De Riva, 2013). It is most likely that MHC-II molecules are degraded in similar a way to other lysosomal proteins. The mechanism/s involved are interesting because MHC II molecules resist proteolysis during normal peptide loading in lysosome-like compartment (MIIC) and yet are degraded there ultimately. APCs regulate the process actively; therefore, it seems to have some functional significance.

It is surprising that the enzymes involved in the degradation of MHC II have not been previously identified. Paul et al. (2011) carried out a genome wide screen to identify various factors affecting the MHC II pathway. They looked for mutant cells that had abnormally low or high MHC II expression and looked for genes that were altered in the mutant cells. Some interesting interacting proteins were identified, which play important roles in the MHC II pathway, but the study did not identify any enzymes involved in the degradation of MHC II.

In mice, many cathepsin genes have been knocked out (Potts et al., 2004, Reinheckel et al., 2012) but no effects on MHC II levels were noted.

Previously work from Dr Busch's group implicated lysosomal aspartyl proteases in the degradation of MHC II proteins in physiological APCs. Treatment of immature MoDCs and acute myeloid cells (AML) like KG-1 with lysosomal aspartyl protease inhibitor, pepstatin A, rescued intracellular HLA-DR protein degradation, suggesting that Cat D, Cat E or both mediated HLA-DR degradation. Moreover, recombinant Cat D cleaved purified recombinant HLA-DR proteins *in vitro* (Busch 2016, personal communication, 10 October). Building on those observations, the aim of this chapter was to identify and characterise specific proteases involved in HLA-DR degradation in KG-1 cells. KG-1 cells were selected because they express HLA-DR protein constitutively and exhibit a phenotype similar to that of immature DC (Ackerman and Cresswell, 2003, Berges et al., 2005) making this cell line a useful model system to study. The experiments here point to a role of cathepsin D and the possible additional process that regulate the MHC II levels.

3.3 Results

3.3.1 Pepstatin A (Pep A) mediated rescue of HLA-DR from degradation

Pepstatin A is an inhibitor of the lysosomal aspartyl proteases, cathepsin D and cathepsin E (Cat D/E) (Umezawa, 1976). Previous work by Dr. Busch's group had indicated that Pep A causes accumulation of HLA-DR in intracellular compartments of monocyte-derived dendritic cells (MoDCs) and in the myeloid tumour line, KG-1 (Busch 2016, personal communication, 10 October). To confirm this, KG-1 cells were cultured for up to 72 hours with Pep A (20µM) or DMSO (vehicle control). To quantify total (surface plus intracellular) DR, cells from each culture were fixed and permeabilized before blocking of FcR, immunofluorescent staining, and flow cytometric analysis. In order to assess the DR level only on intact single cells, doublets were gated out, and intact KG-1 cells were distinguished based on forward and side scatter as shown in Figure 3.2 (A and B).

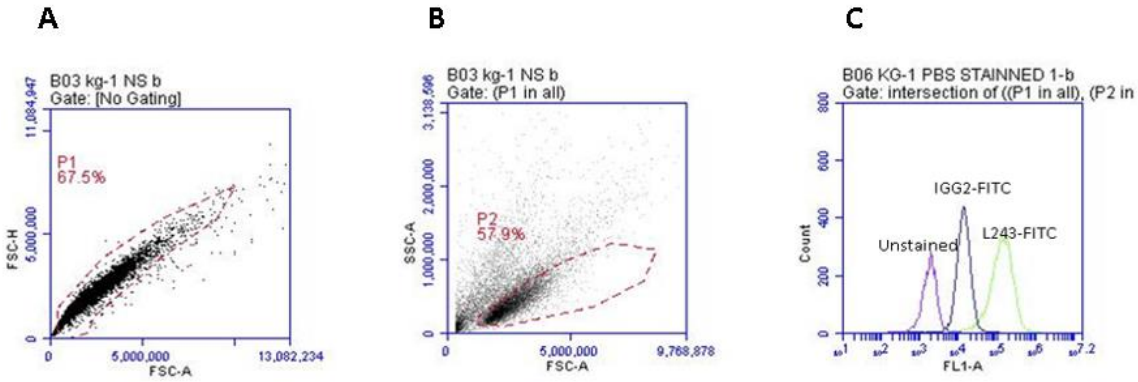

Figure 3.2 Gating strategy for immunofluorescence analysis for fixed and permeabilized KG-1 cells. The figures show the gating strategy for exclusion of doublets and scatter gating for fixed and permed KG-1 cells. Doublets were excluded using forward side scatter height vs. area (FSC-A vs. FSC-H). Intact single cells were selected using forward side scatter area (FSC-A) versus side scatter (SSC-A). In the figure, gate P1 represents the doublet exclusion gate (A), whereas P2 identifies the intact KG-1 cells (B). The staining of fixed and permeabilized KG1 cells is represented through histograms (C). The staining for IGG2 shown above is the worst-case scenario. In a majority of the studies, less background staining was seen.

In order to quantify the levels of DR, immunofluorescence staining was quantified by flow cytometry. Figure 3.1 (C) shows examples of staining of fixed and permeabilized KG-1 cells with L243-FITC (anti-HLA-DR) or IgG2a-FITC along with unstained cells. The IgG2a-FITC is an isotype- matched negative control antibody to assess background fluorescence. The histograms in this figure show that there was only a small shift in mean fluorescence intensity when stained with IgG2-FITC when compared to the unstained cells. By comparison, there was a larger shift in the population of cells stained with L243-FITC.

As shown in Figure 3.3, cell treatment with the aspartyl protease inhibitor, Pep A showed higher staining for DR when compared with vehicle controls. Moreover, there was no effect of Pep A on autofluorescence or nonspecific staining with isotype control. The maximum accumulation of DR was around 50% and observed at 48 hours post treatment. Thus, this result indicated that inhibition of aspartyl proteases causes accumulation of HLA-DR in KG-1 cells. Since the accumulation did not continue past 48 hours, it also raises the possibility that cells later adapt to this inhibition of aspartyl proteases.

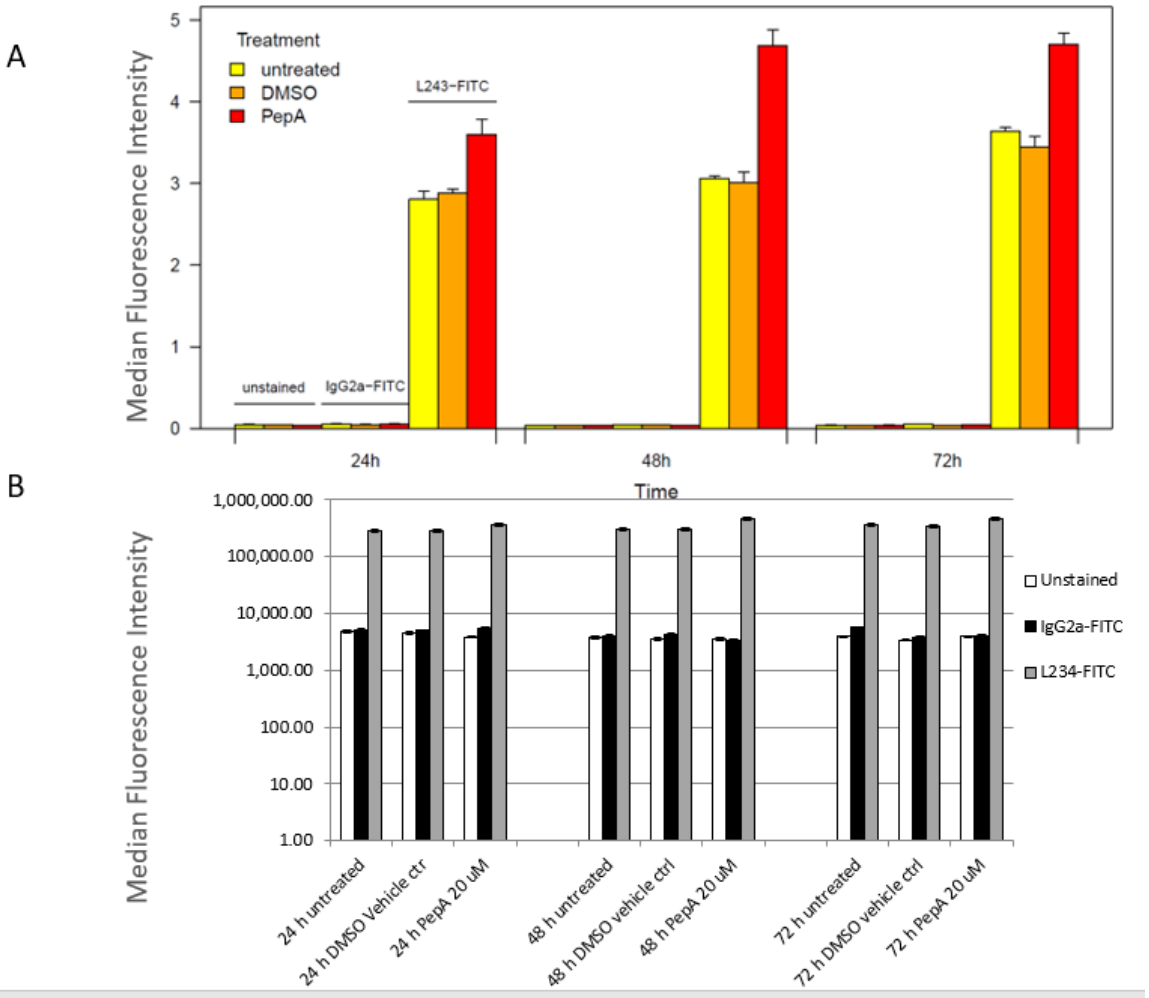

Figure: 3.3 Effect of pepstatin A on HLA-DR in fixed and permeabilized KG-1 cells. KG-1 cells were cultured for the indicated periods of time in the presence or absence of 20 μM pepstatin A in DMSO. Cells were harvested, fixed and permeabilized, stained with FITC-conjugated anti-DR antibody to reveal total HLA-DR molecules and analyzed by flow cytometry. Each bar represents the median fluorescence intensities. (MFI; mean +- S.D. of triplicate analysis).(A) Y axis in normal scale (B) Y axis is in log scale.

Two-way ANOVA indicated a significant effect of the treatment on HLA-DR levels, F (2, 18) = 150.306, $p<0.001$ (Appendix 3.1). Post-hoc Tukey's HSD tests showed that KG-1cells treated with pepstatin A had significantly higher HLA-DR expression than the other groups (Appendix 3.1, Post-hoc test). It also indicated that the increase in the DR level was dependent on time, F (2, 18) =27.527, $p<0.001$ (Appendix 3.1). The effect of time was statistically significant, but this was not necessarily biologically meaningful because of

confounding technical variables, as the cells were stained separately on each day of analysis. On each occasion, the incubation conditions are not quite the same, and therefore staining intensities vary.

The effect shown in Figure 3.3 was reproducible in nine independent repeats performed on KG-1 cells (shown in Figure 3.4). A single sample t-test was conducted to determine if a statistically significant difference existed in DR accumulation in KG-1 cells treated with and without Pep A. There was significant accumulation of DR in KG-1 cells treated with Pep A, $t(8) = 5$, $P<0.01$ (Appendix 3.2). This result confirms that Pep A reproducibly prevents DR degradation in KG-1 cells.

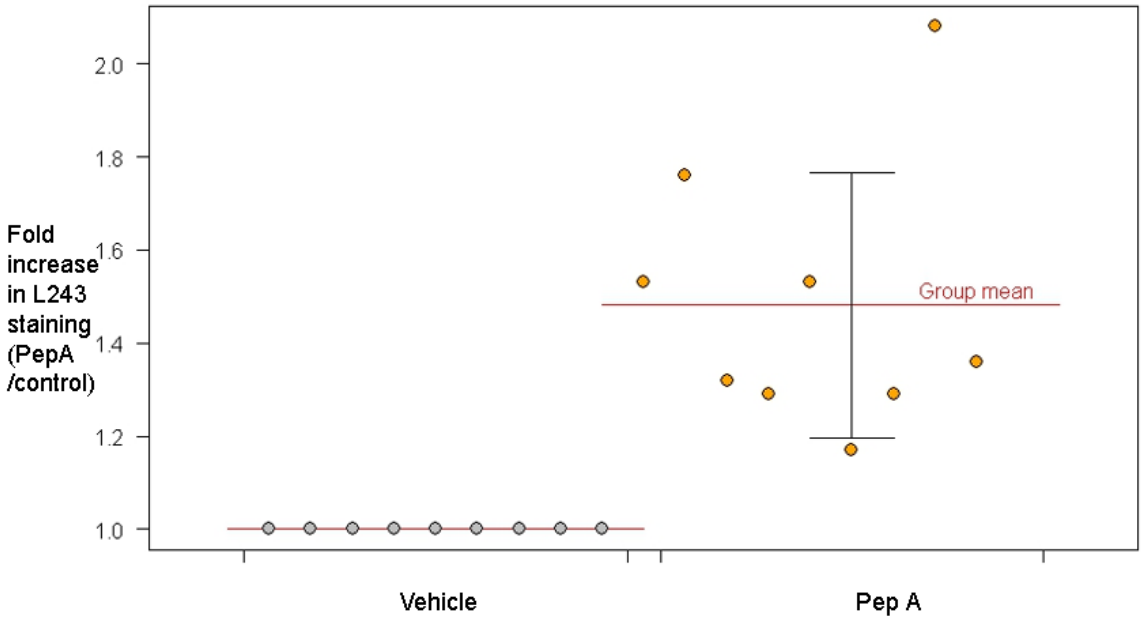

Figure 3.4 Summary of nine independent experiments of pepstatin A treated KG-1 cells at 48 hours. The increase in HLA-DR staining on pepstatin A treatment was reproducible in KG-1 cells at 48 hours.

The ~50% mean increase in total HLA-DR observed after 48 hours in Pep A-treated KG-1 cells may not be the maximal effect. Previous unpublished work in Dr Busch's group has shown that the effects of Pep A was dose-dependent up to 20 μM and at higher concentration toxic effects of the treatment were observed. Therefore, in order to increase the

bioavailability of the enzyme without increasing toxicity, Pepstatin-A-Penetratin (Pep A-pen) was used.

A number of natural and synthetic peptides, soluble in water, are able to translocate across cell membranes non-endocytically. One such peptide, Penetratin, has a sequence corresponding to the 16 residues of the third α-helix (residues 43 to 58: RQIKIWFQNRRMKWKK) of the Antennapedia homeodomain of *Drosophila* (Derossi et al., 1994, Prochiantz, 1999). This helix is able to translocate the entire homeodomain across cell membranes (Derossi et al., 1996) and therefore has been used as an intercellular delivery vector. Accordingly, Pepstatin-A-Penetratin (Pep A-pen), which is Pep A conjugated with the cell penetrating peptide, enhancing its cell permeability (Zaidi et al., 2007), was used to rescue DR.

Pep A-pen, used at 10 μM, was able to cause the accumulation of DR in KG-1 cells (Figure 3.5). The effect size was similar to that observed with 20 μM of Pep A (around 50%). Perhaps, therefore, the 50% accumulation is the maximum DR accumulation possible using this inhibitor. Two-way ANOVA indicated that the increase in the DR level on the treatment with Pep A-pen was statically significant, $F(2, 18) = 133.6$, $p < 0.001$ (Appendix 3.3). Post-hoc Tukey's HSD tests showed that KG-1cells treated with Pep A-pen had significantly higher HLA-DR expression than the other groups (Appendix 3.3, post-hoc test)

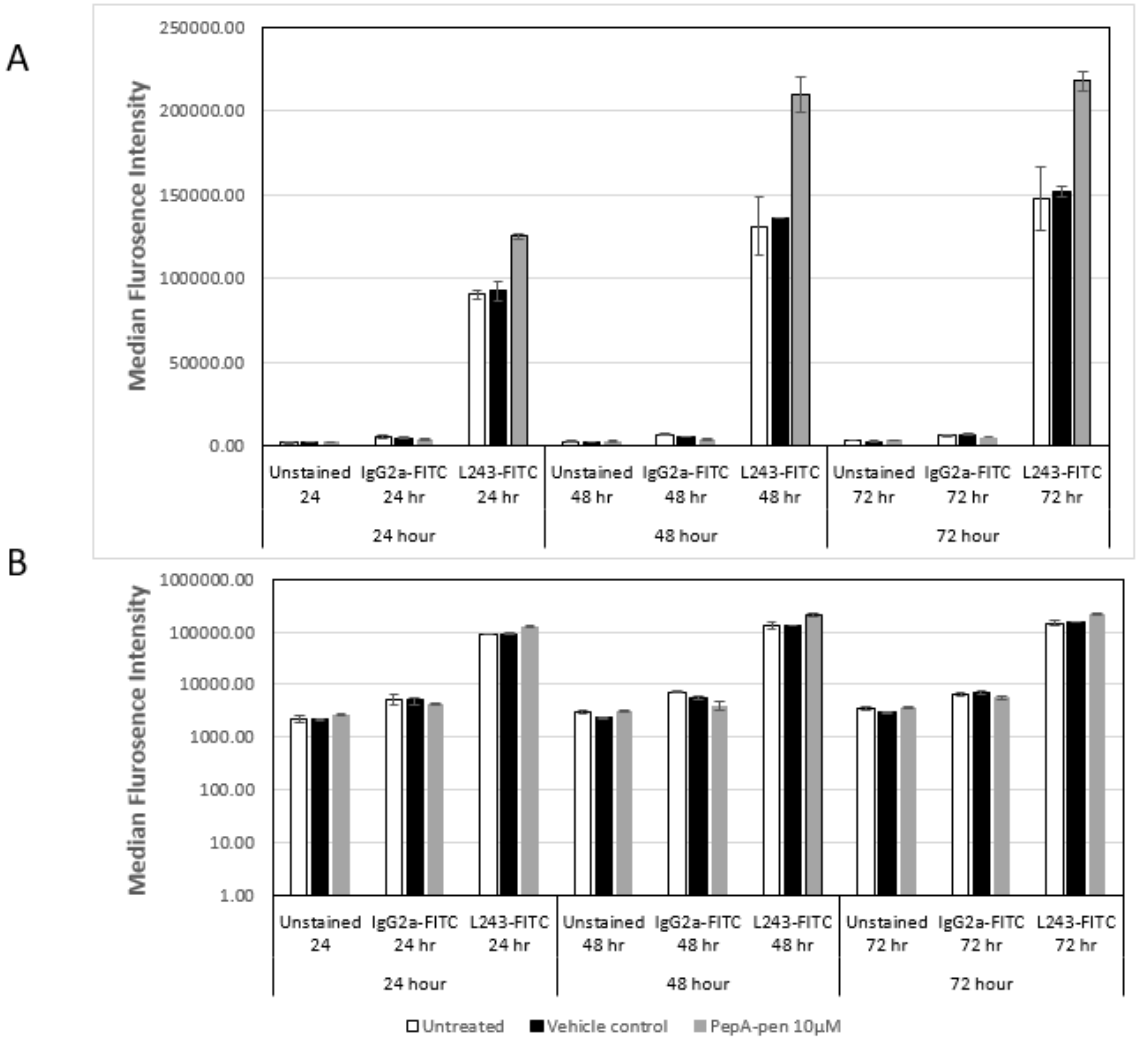

Figure 3.5 Accumulation of HLA-DR in fixed and permeabilized KG-1 cells with Pepstatin-A-penetratin.
There was accumulation of DR molecules in Pep A-pen treated KG1 cells as compared to the controls. L243-FITC antibody was used to stain the DR molecules. Cells were analysed after fixation and permeabilization. Staining was quantified by flow cytometry. Each bar represents the median fluorescence intensities (MFI; mean +- S.D. of triplicate analysis). This experiment was performed once. (A) Y axis in normal scale (B) Y axis is in log scale.In the EBV-transformed B-cell line, Priess, previous work had shown that DR molecules exhibit very slow turnover rates (unpublished work from RB). Priess cells were treated with Pep A or vehicle for 72 hours, and DR was quantified by flow cytometry after fixation and permeabilization. The accumulation of the DR was not as evident as in KG-1 cells but there was a small effect (between 5-7%) observed as shown in Figure 3.6. This increase in the HLA-DR level on treatment with Pep A was statistically significant $F(2, 18) = 30.817$, $p<0.001$ as analysed by two-way ANOVA (Appendix 3.4), consistent with slow turnover observed in this cell line. It

may take longer to accumulate DR molecules, resulting in the smaller effect of Pep A observed in Priess cells than in KG-1 cells.

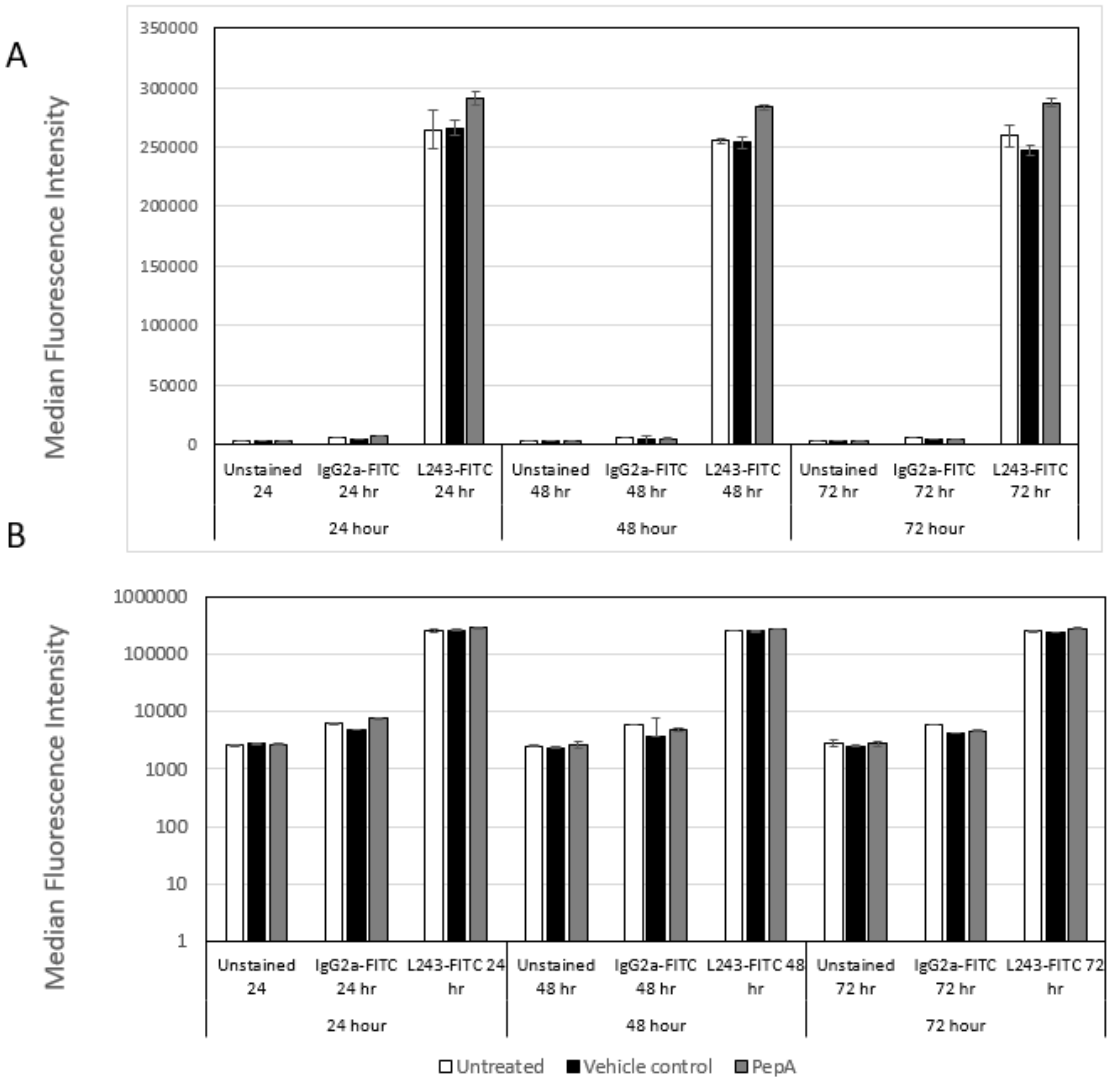

Figure 3.6 Small effect of Pepstatin-A on fixed and permeabilized Priess cells. There was little accumulation of DR molecules in Pep A treated Priess cells. L243-FITC antibody was used to stain the DR molecules. Cells were analysed after fixation and permeabilization. Staining was quantified by flow cytometry. Each bar represents the median fluorescence intensities (MFI; mean +- S.D. of triplicate analysis). This experiment was performed three times with similar results. (A) Y axis is in normal scale (B) Y axis is in log scale.

3.3.2 Effect of Glutamine hydrolysis

Glutamine in the culture media is capable of raising the endocytic pH due to its decomposition into pyrrolidone-carboxylic acid and the weak base ammonia (NH_3) (Ozturk and Palsson, 1990, Slivac et al., 2010). Ammonia can be protonated to NH_4^+ and can neutralize the endocytic pH, which may affect the activity of the lysosomal enzymes. In order to examine whether this altered the effect of Pep A on HLA-DR accumulation cells were cultured in media containing GlutaMAX.

As shown in Figure 3.7 (A), Pep A treated KG-1 cells cultured in GlutaMAX media had an effect of similar magnitude as Pep A treatment of KG-1 cells cultured with glutamine. Two-way ANOVA indicated a noteworthy increase in the DR level on treatment was significant, $F(1, 20) = 71.449$, $p<0.001$ (Appendix 3.5). Since there were only two groups post-hoc test was not performed. The maximum rescue of HLA-DR by Pep A was of 50%, similar magnitude, as observed in the cells cultured with glutamine (Figure 3.3). The maximal effect was observed earlier, however, which is consistent with the idea that in GlutaMAX media there is faster lysosomal turnover. Lastly, despite the continuous presence of inhibitor, the effect waved over time.

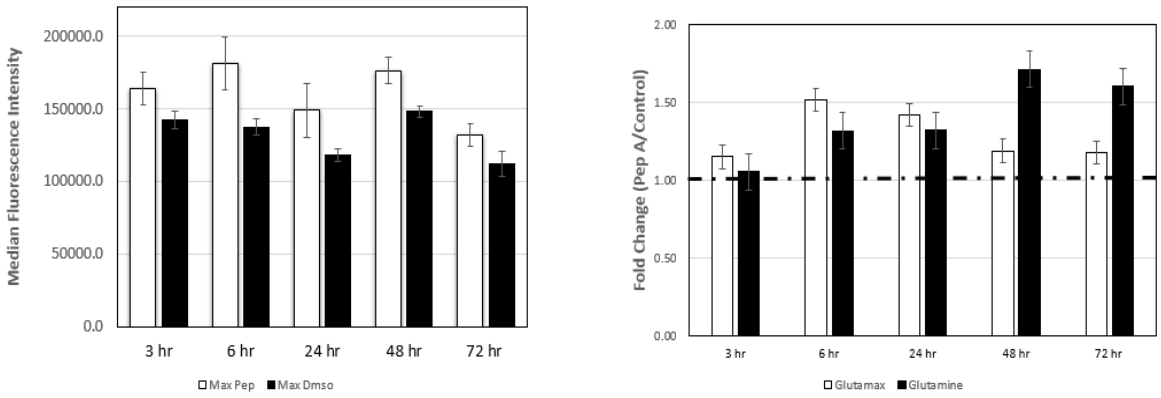

Figure 3.7 The peak effect of pepstatin A treatment in KG-1 cells seems to be independent of glutamine hydrolysis. KG-1 cells were cultured for the indicated periods of time in the presence or absence of 20 μM pepstatin A in DMSO. Cells were harvested, fixed and permeabilized and stained with ant-DR FITC conjugated to reveal total HLA-DR molecules and were analyzed by flow cytometry. (A) Each bar represents the median fluorescence intensities (MFI; mean +- S.D. of triplicate analysis). (B)

shows the comparative fold change (Pep A treatment/ control) in KG-1 cells cultured in glutamine and GlutaMAX media at different time points.

Taken together, the results showed that Pep A and Pep A-pen are able to rescue HLA-DR molecules in KG-1 and to a lesser extent in Priess cells, correlating with their known difference in DR turnover. The effect of pepstatin A on accumulation of DR was also seen in immature monocyte-derived dendritic cells (MoDCs) (Appendix 7.1).

3.3.3 Differential expression of aspartyl proteases in Priess and KG-1 cells

Cat D and Cat E are the only aspartyl proteases present in the lysosomes of human APCs (Tang and Wong, 1987, Szecsi, 1992, Eder et al., 2007). In order to examine the expression of aspartyl proteases, Priess and KG1 cell extracts were separated by SDS-PAGE under non-reducing conditions (in order to preserve Cat E as a disulphide-bonded homodimer (Finley and Kornfeld, 1994)), and Western Blots were probed with antibodies to Cat D and Cat E. Cat D was clearly detected in KG-1 but not Priess cells, as shown in Figure 3.8. Two Cat D bands were observed at molecular weights around 48 kDa and 33 kDa, corresponding to the previously-reported molecular weights of pro Cat D (48 kDa) and mature Cat D (33 kDa) (Horikoshi et al., 1998). On longer exposure, faint bands were observed in Priess cells and an additional band at 25kDa (Figure 3.8). Thus, a small amount of Cat D was present in Priess cells. Recombinant human Cat D was used as a quantitative standard, and recombinant human Cat E was used as a control for any cross-reactivity of the antibody. As visible from the figure, no cross-reactivity with recombinant Cat E was observed.

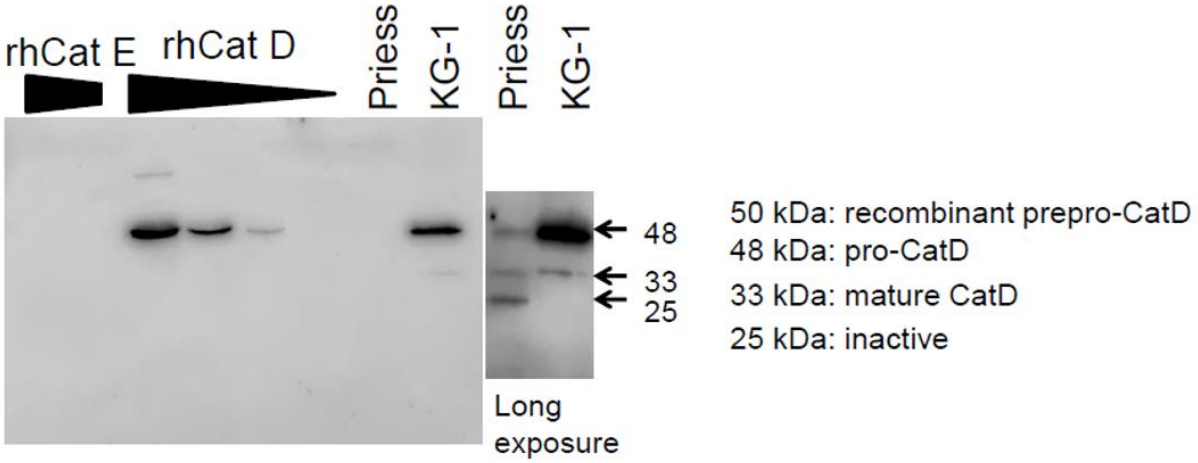

Figure 3.8: KG-1 and Priess cells express Cat D. Protein extracts from equal cell equivalents of KG-1 and Priess were resolved by 12% non-reducing SDSPAGE and immunoblotted for Cat D. Recombinant human Cat D (rh Cat D) was used as a standard while, rh Cat E served as a control for any crossreactivity. The amounts of rh Cat D used was 250 ng, 50 ng, 10 ng and 2 ng while the amount of rh Cat E used was 50 ng and 250 ng. This is image is representative of 4 independent informative repeats.

Similarly, Western blots were probed with a goat polyclonal anti-Cat E antibody to detect the presence of any Cat E in the extracts. Cat E is a homodimer consisting of two monomers linked by an inter molecular di-sulphide bond (Fowler et al., 1995). As shown in Figure 3.8, rh Cat E resolved at molecular weight 80 kDa (homo-dimer) and 44 kDa (monomer), whereas no bands were detected in KG1 or Priess extracts. Hence, there was no detectable Cat E present in these cells. Recombinant human Cat E and Cat D were used as standards and also as a control to detect any cross-reactivity of the antibody. As visible from the figure, there was no cross-reactivity observed with recombinant Cat D.

The product literature for the commercial monoclonal anti-cat D and polyclonal anti-cat E antibodies left open the possibility that the antibodies were crossreactive. In the blots shown, this was not observed. Cross reactivity was observed, however, when a monoclonal anti-cat E antibody was used (Appendix 3.6). In that case, immuno-reactivity with recombinant Cat D

and with the KG-1 cell extract were observed. However, there was no dimer observed in the KG-1 cell extract, and hence it was concluded that there was no evidence of Cat E being present. The polyclonal anti-Cat E antibody showed no crossreactivity (Figure 3.9), so this experiment was more definitive.

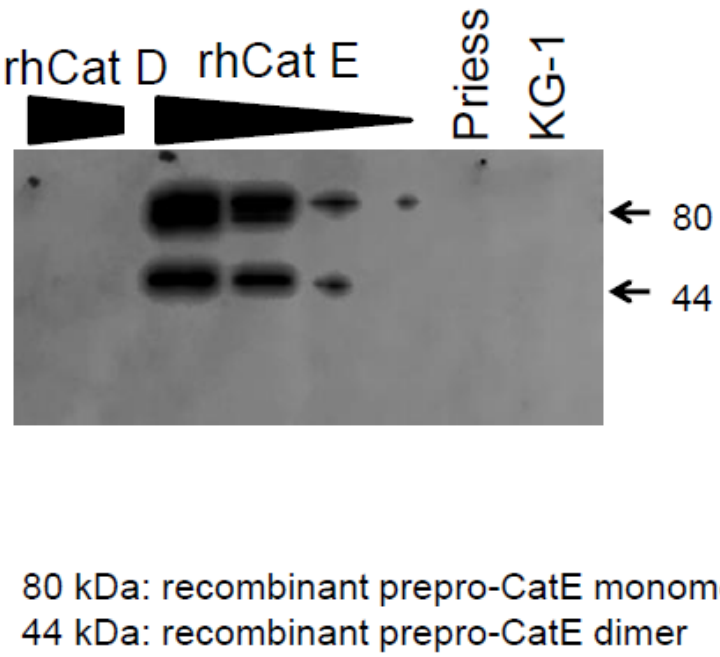

Figure 3.9 No detectable cathepsin E present in KG-1 and Priess cells. Protein extracts from equal cell equivalents of KG-1 and Priess cells were resolved by 12% non-reducing SDS PAGE and immunoblotted for Cat E. rh Cat E migrated partly as a homo-dimer, which is observed at 80 kDa (homo-dimer) and as a 44 kDa (monomer). The quantities of rh Cat E used ranged from 2 ng to 250 ng while for rh Cat D they were 50 ng and 250 ng. This is image is representative of two independent informative repeats.

The blots were quantified, using Image Studio 5.2 software. The band intensity was quantified after subtracting the local background. In five different attempts, the amount of pro-Cat D ranged from 17 femtogram (fg) to 26 fg per KG-1 cell. But in no experiment it was possible to detect Cat E, even though 2ng of r-Cat E per lane was readily detected. Based on this it was estimated that the amount of Cat E could not be more than 7 fg per cell. These

calculations are based on the assumption that the antibody binds equally to native and recombinant forms of the enzyme.

The Western blot results showed the presence of Cat D in KG-1 cells as well as low level expression in Priess cells. Absence of evidence for Cat E expression does not rule out low level expression, below the sensitivity of these Western Blots. Enzymes are able to act catalytically on their substrates even in minute quantities. Thus, the levels of Cat D encoded by CTSD and Cat E encoded by CTSE mRNA were assessed by real time PCR using SYBR green chemistry. The RNA from both KG-1 and Priess was extracted, reverse transcribed for c-DNA synthesis, and amplified using primers specific for CTSD and CTSE. As explained in section 2.2.4.3, SYBR green dye binds to all double stranded products including nonspecific PCR product or primer dimer. Thus, the proper amplicons or the PCR products were identified using melt curve analysis after qRT-PCR and confirmed by agarose gel electrophoresis (AGE).

The RNA from both KG-1 and Priess was amplified with primers for Cat D or Cat E encoding transcripts. As expected from the Western blots, KG-1 cells showed the presence of CTSD mRNA but not CTSE mRNA, shown in Figure 3.10 (A). Melt curve analysis of Cat D showed the presence of a single peak, which assured the amplification of genuine PCR product. On the other hand, melt curve analysis of Cat E revealed that the slight amplification observed towards the end of the PCR cycle was a primer dimer (Figure 3.10 B). For the Priess cells, as shown in Figure 3.11, CTSD was amplified and also through melt curve analysis a single peak was observed, suggesting the presence of CTSD mRNA. As observed with KG-1 there was no detectable amount of CTSE present in the Priess cells (Figure 3.11). GAPDH was used as a housekeeping control gene in all sets of PCR.

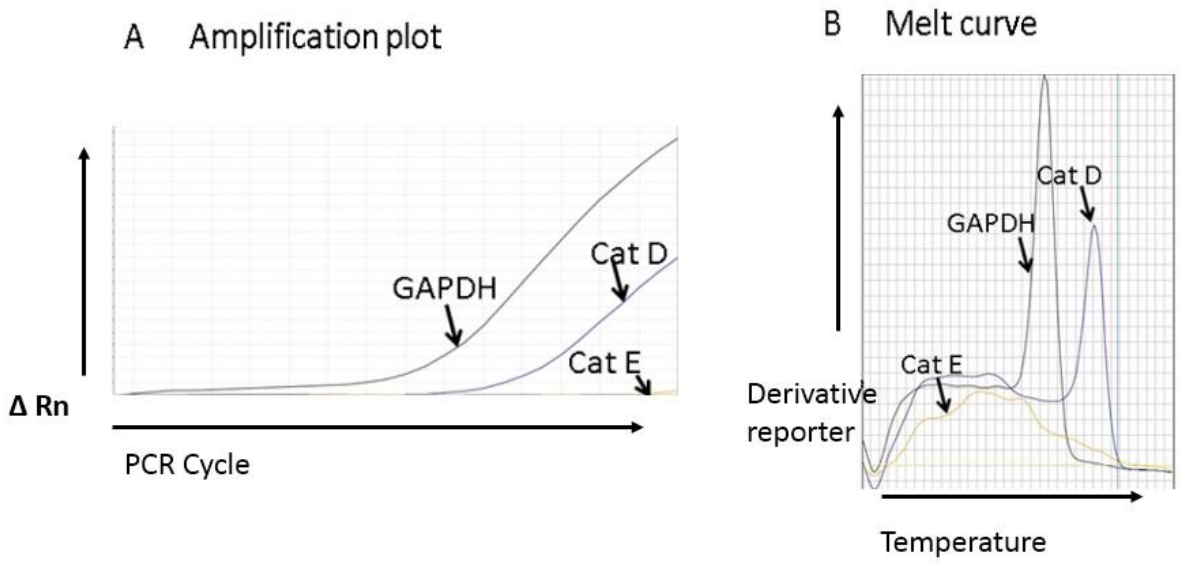

Figure 3.10 Expression of CTSD mRNA in KG1 cells. CTSD and CTSE mRNA expression in KG1 was detected by real time RT-PCR using SYBR green chemistry. The presence of CTSD mRNA appeared on the amplification plot (A), which was also confirmed through melt curve analysis (B). There was no detectable level of CTSE mRNA in KG-1 cells. GAPDH was used as a positive control. This image is representative of three independent repeats.

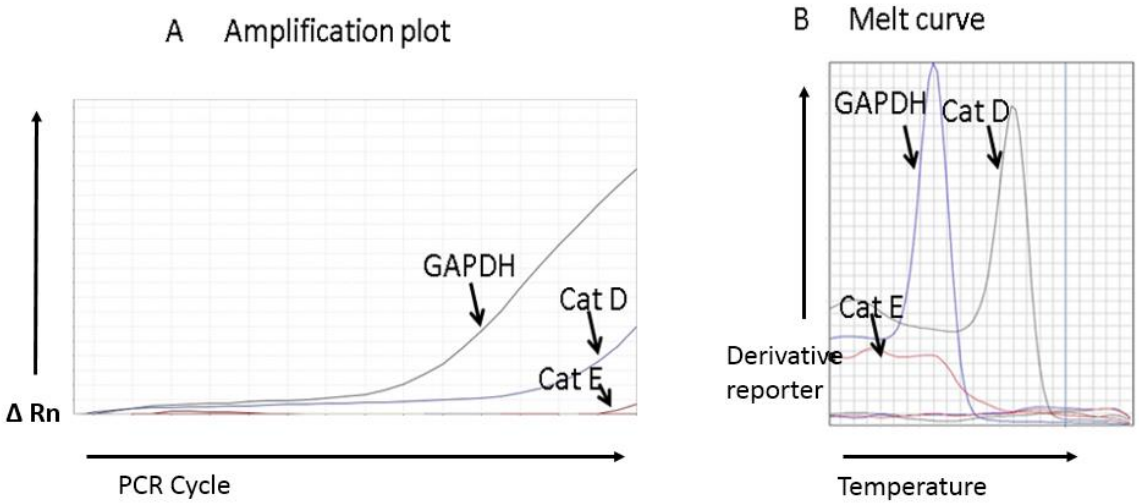

Figure 3.11 Expression of CTSD mRNA in Priess cells: CTSD and CTSE mRNA expression in Priess was detected by real time RT-PCR using SYBR green chemistry. The presence of CTSD mRNA was detected through amplification plot (A), which was also confirmed through melt curve analysis (B). There was no detectable level of CTSE in Priess cells. GAPDH gene was used as a house keeping gene. This image is representative of three independent repeats.

The PCR products were also analysed by agarose gel electrophoresis to detect the presence of the gene. The results as shown in Figure 3.12 confirm the presence of CTSD and not CTSE mRNA in both KG-1 and Priess. The band intensities of GAPDH and CTSD in case of Priess cells were very low when compared to KG-1 cells, even though equal numbers of cells were used. The reason for this can either be low RNA yield per cell in Priess cells, or there may some difference in the expression levels of the housekeeping gene between the two cell lines.

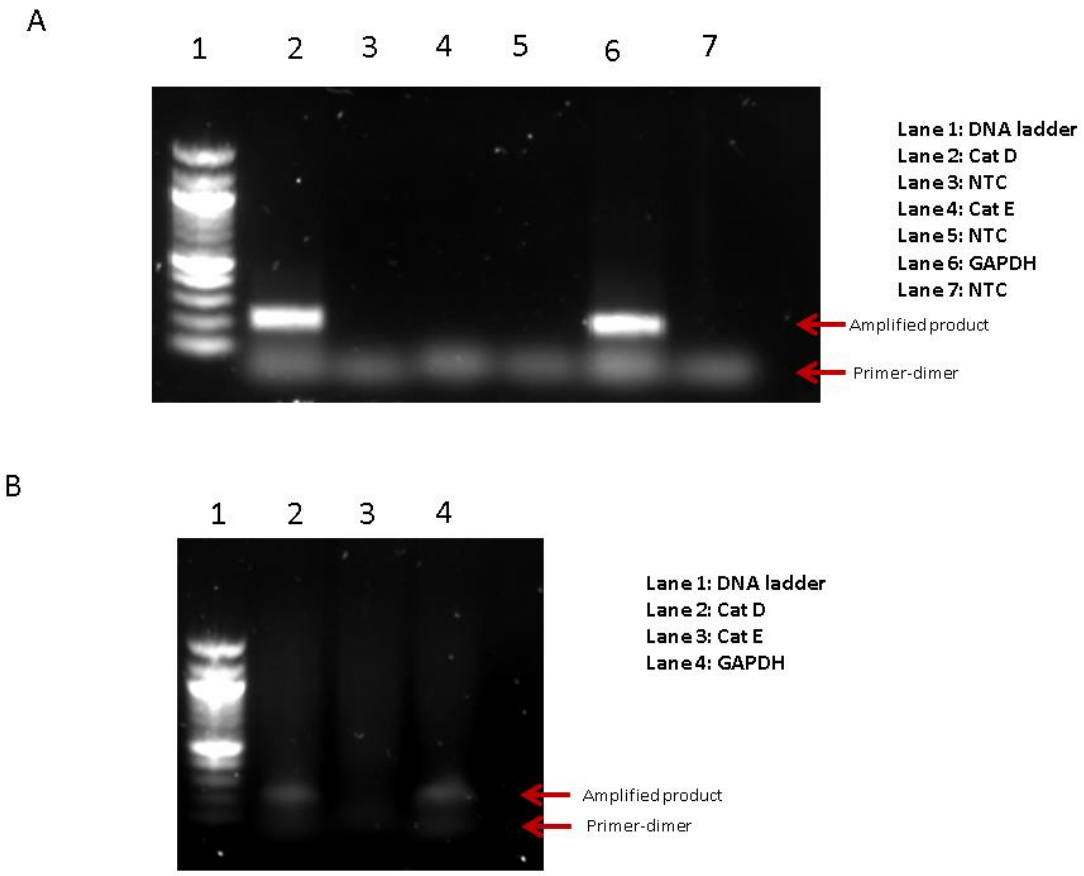

Figure 3.12 Presence of CTSD and not CTSE in KG-1 (A) and Priess cells (B). The RNA from both KG-1 and Priess were extracted, reverse transcribed for c-DNA synthesis and later were amplified. After amplification they were run through 0.7% agarose gel. There is band visible corresponding to amplification product of CSTD in both KG-1 and Priess. GAPDH was used as positive control. The band intensities of CSTD and GAPDH in Priess cells were faint.

Cat D was also detected when fixed and permeabilized KG-1 cells were stained with unconjugated anti-cathepsin D polyclonal rabbit antibody. Anti-rabbit IgG conjugated with allophycocyanin (APC) [2(Ab)-APC] was used as a secondary antibody to detect anti-cathepsin D. Appropriate controls were used to quantify auto-fluorescence and any non-specific background from the APC conjugated secondary antibody. This staining of the Cat-D is shown in Figure 3.13.

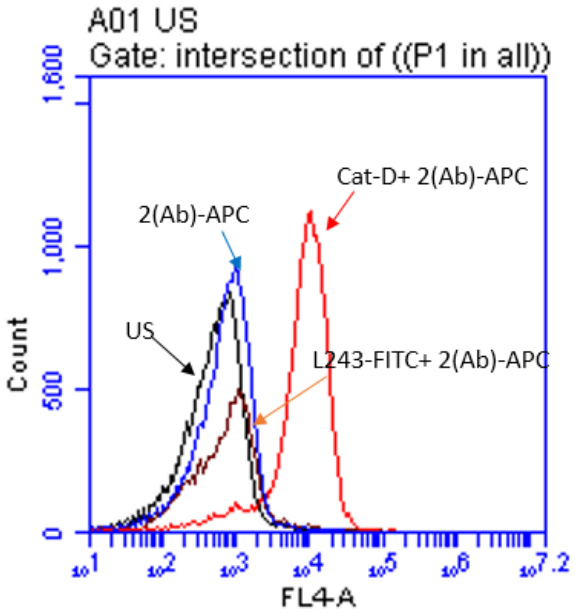

Figure 3.13 Staining of Cat D in KG-1 cells by flow cytometry. The figure shows the presence of Cat-D in the KG-1 cells. Fixed and permeabilized KG-1 cells were stained with L243-FITC and unconjugated anti-Cat D rabbit polyclonal. Anti-rabbit IgG conjugated with APC [2(Ab)-APC] was used as a secondary antibody control. Unlabelled sample (US, unstained) was used as another control. The figure shows the overlay of the histograms in FL-4 when stained with 2(Ab)-APC under different conditions.

3.3.4 Co-localisation of Cat-D and HLA-DR.

In order to investigate whether Cat-D and HLA-DR are co-localized, KG-1 cells were fixed, permeabilized, and stained for HLA-DR (green) and Cat-D (red), and then were attached to polylysine coated slides at 4 C to visualise by fluorescence microscopy. Individual cells were identified by their fluorescent blue nucleus through DAPI staining. HLA-DR staining was observed in green on the cell surface and also in intracellular vesicular compartments, whereas Cat D staining was observed in red in the vesicular compartment, shown in Figure 3.14. The intracellular compartments that can be stained by L243-FITC are the MHC II compartment (MIIC) and related compartments. Cat D is a known lysosomal marker. So from this, it can be inferred that some DR molecules end up in cathepsin D positive lysosomes, where degradation of HLA-DR is hypothesised to be taking place.

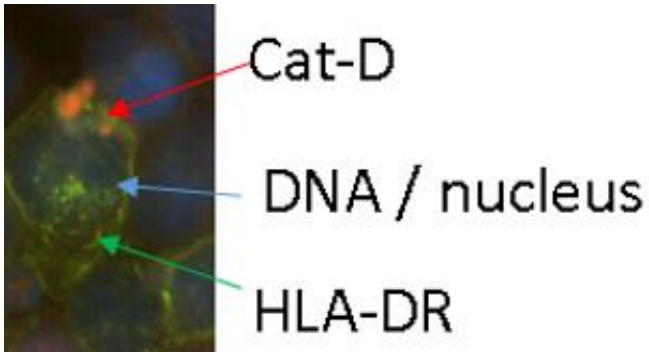

Figure 3.14 Co-localization of HLA-DR and Cat D with fluorescence microscopy in KG-1 cells. Co-localization of DR molecules and Cat D in KG-1 cells. KG-1 cells were fixed and permeabilized and blocked with normal mouse serum. DR molecules are stained green with L243-FITC antibody and Cat D in Red. Cat-D was stained with anti-Cat D rabbit polyclonal IgG and Alexa-Fluor 568 conjugated anti-rabbit IgG second-step reagent. Cells were counterstained with DAPI to highlight the nuclei. Arrows indicate protein localization.

In summary, Cat D was the only aspartyl protease that was detected in KG-1 by Western Blot and qRT-PCR. In Priess cells, it was possible to detect the presence of CTSD mRNA by qRT-PCR, and Cat D bands were observed on overexposing Western blots, albeit with a

different band pattern. There might be some differences in the transcriptional activity of the CTSD and post-translational fate of enzyme in both cell lines. Co-staining of KG-1 cells for Cat-D and HLA-DR and their co-localization by fluorescence microscopy were consistent with expectations.

3.3.5 Lentiviral knockdown of Cat D.

In order to provide formal proof that degradation by Cat D is responsible for the Pep A effect on HLA-DR levels in KG-1 cell lines, the CTSD gene was knocked down using a commercially available lentiviral vector at a multiplicity of infection (MOI) of 5 and above. Cat D sh-RNA transduced cells were selected by culturing cells in complete IMDM media containing 1μg/ml puromycin (the viral constructs had a puromycin resistance gene for selection). Non-targeting sh RNA vector was used as a negative control in order to observe cellular effects, if any, of the transfection process. This control vector will activate RISC and the RNAi pathway, but does not target any human genes, thus offering a useful reference for interpretation of the knockdown experiment (Moore et al., 2010)

To examine knockdown efficiency, cell extracts from Cat D and control knockdown transduced KG-1 cells and non-transduced KG-1 cells were immuno-blotted with Cat D antibody after separation by SDS-PAGE under non-reducing conditions. Recombinant human Cat D at 10ng was used as a positive control. Two Cat D bands were observed, as seen previously, at molecular weights around 48 kDa (pro Cat D) and 33 kDa (mature Cat D). In contrast, there was a 96% decrease when the band intensity of Cat D knockdown KG-1 cells was compared with the control knockdown and non-transduced KG-1 cells (Figure 3.15 (A)). The cell extracts from all the samples contained comparable amount of protein extract, as judged by re-probing for GAPDH after stripping the blot (Figure 3.15 (B)). The band

intensity was quantified with image studio version 5.2 and the quantification results confirms the successful knockdown of the Cat D (Figure 3.15 (C)).

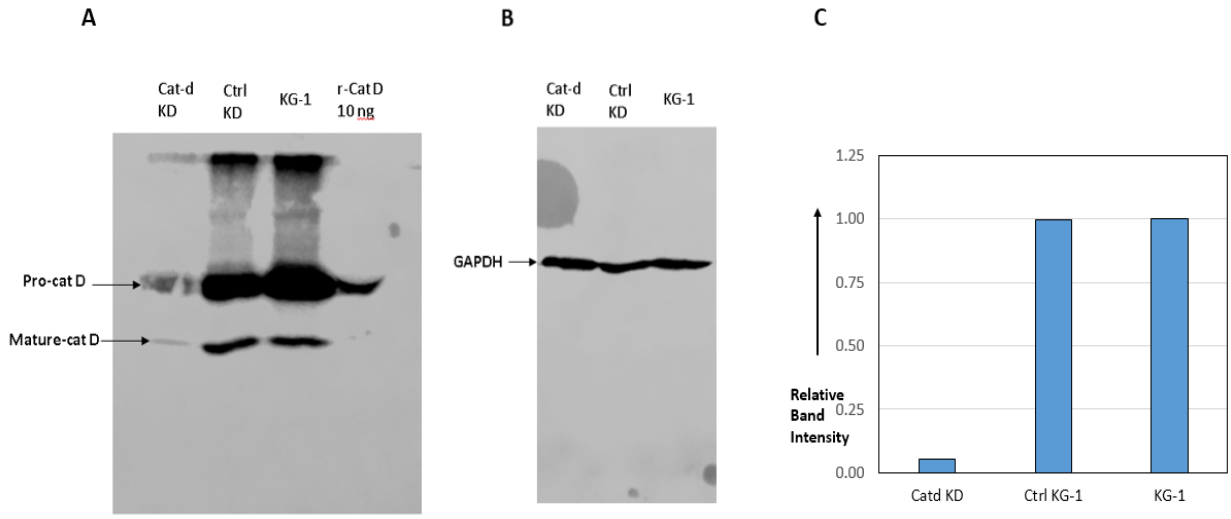

Figure 3.15 Knockdown of Cat D protein expression in KG-1 cells. The CTSD gene was knocked down (KD) in KG-1 cells to validate its role in DR degradation. Control knockdown and non-transduced KG-1 cells were used as controls in the experiment. (A) Whole cell lysates, prepared in RIPA buffer, were resolved by 12% SDS-PAGE, and Western Blots were probed using anti-Cat D antibody. (B) The blot was stripped and re-blotted with anti-GAPDH antibody as a loading control. (C) Bar graph showing ratio of intensities of Cat-D and GAPDH. This experiment was performed once.

3.3.6 Loss of DR accumulation in Cat D knockdown KG-1 cells through Pep A.

As shown in Figure 3.3, the maximum accumulation of DR caused by Pep A was seen after 48 hours of treatment, and thereafter there was no further accumulation. It took weeks to expand the knockdown KG-1 cells for analysis, so it was technically impossible to detect DR accumulation within 48-72 hours after successful knockdown. However, if Cat D is indeed responsible for DR degradation, then there should be no accumulation of DR when Cat D knockdown cells are treated with Pep A.

Hence, Cat D knockdown KG-1 cells were treated with 20 μM Pep A or vehicle control for 72 hours. Control knockdown KG-1 cells were used to control for any effect of transfection on DR levels. The total DR was then quantified, as described earlier, by L243-FITC antibody daily for up to 72 hours following treatment. As shown in Figure 3.16, the control knockdown in KG-1 cells showed accumulation of DR when treated with Pep A. Two-way ANOVA showed that accumulation of HLA-DR at 24 hours in control knocked down KG-1 cells was statistically significant, $F(1, 6) = 81.159$, $p < 0.001$ (Appendix 3.7). Similarly, in control knocked down KG-1 cells, accumulation of HLA-DR was statistically significant at 48 and 72 hours $F(1, 6) = 200.851$, $p < 0.001$ (Appendix 3.8) and $F(1, 6) = 81.03$, $p < 0.001$ (Appendix 3.9). Cat D knock down cells had no persistent accumulation of DR when analysed several of weeks after selection. The statistical analysis showed that the effect of Pep A in Cat D knocked down KG-1 cells was statistically significant but magnitude was very small (Appendix 3.7, 3.8, and 3.9). Their HLA-DR levels seemed to have returned to the wild type. However, in these cells Pep A mediated accumulation of HLA-DR molecules was no longer effective, which suggests that the Pep A effect is due to Cat D. There may be some adaptation in cells, similar to that seen in KG-1 cells in which Cat D was inhibited for longer times (72 hours in Figure 3.3 and 3.7).

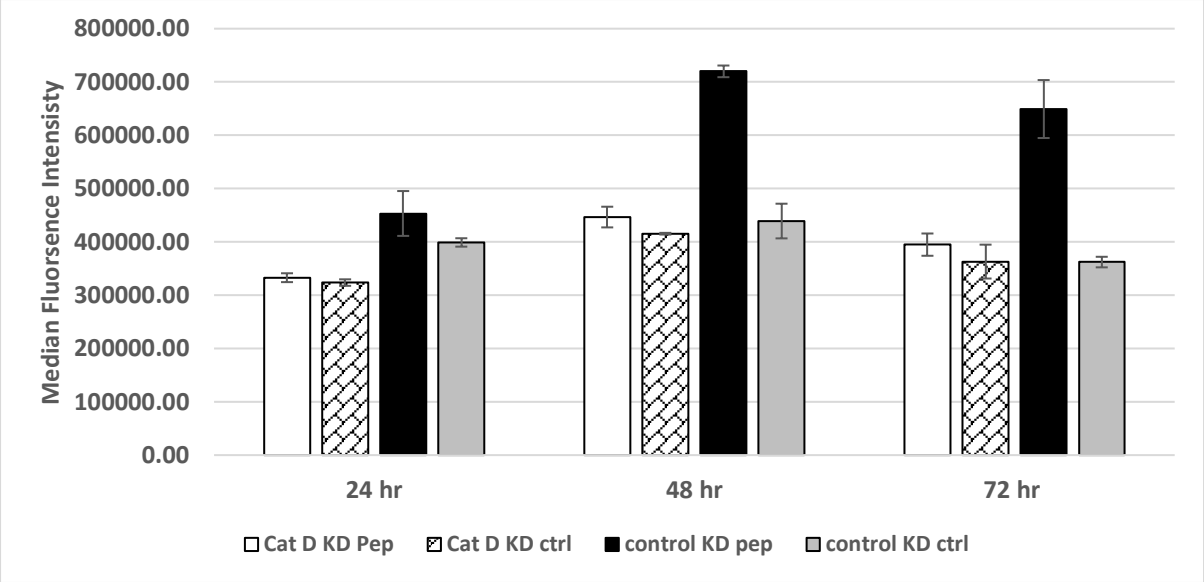

Figure: 3.16 Loss of Pepstatin A-mediated accumulation of HLA-DR in cathepsin D knockdown KG-1 cells. Staining of DR molecules was quantified by flow cytometry and is reported as median fluorescence intensities (MFI; mean +/- S.D. of triplicate analysis). There was a significant accumulation of the DR molecules in the pepstatin A treated control knockdown (KD) KG-1 cells but not in Cat Dknockdown KG-1 cells, when compared to the controls. Cells were analyzed after fixation and permeabilization. L243-FITC antibody was used to stain the HLA-DR molecules

To summarize, Cat D was the only aspartyl protease that was detected in KG-1 by Western Blot and qRT-PCR. In Priess cells, it was possible to detect the presence of CTSD mRNA by qRT-PCR, and Cat D bands were observed on overexposing Western blots, albeit with a different band pattern. There might be some differences in the transcriptional activity of CTSD and the post translational fate of the enzyme between both cell lines. Nevertheless, the Cat D may well be responsible to initiate the DR degradation. This assumption is also supported through the co-localization of Cat D and HLA-DR in KG-1 cells. The loss of the Pepstatin effect in Cat D knockdown KG-1 cells demonstrates the involvement of Cat D in DR degradation.

3.4 Discussion

The inhibitor, gene expression and knockdown studies reported here support the idea that HLA-DR protein turnover in KG-1 cells is critically dependent on Cathepsin D. Cat D is the only target enzyme of Pep A that seems to be expressed in KG-1 cells. The Pep A effect is ablated in KG-1 cells in which Cat D gene expression is knocked down. The proposed hypothesis for HLA-DR degradation is shown in Figure 3.17.

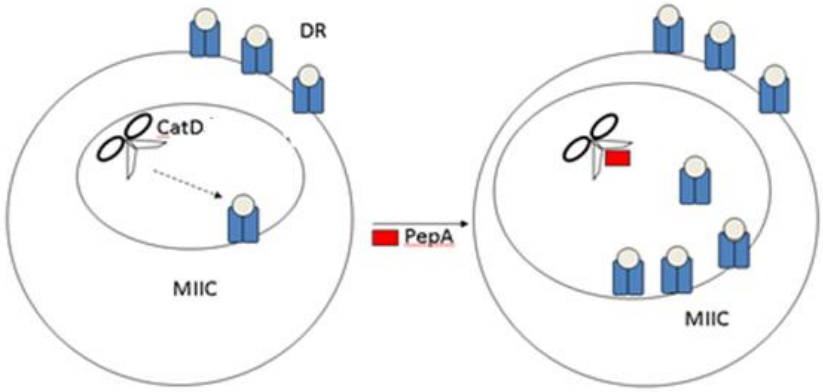

Figure 3.17 Proposed hypotheses for HLA-DR degradation. Rescue of the HLA-DR molecule by Pepstatin A and other evidence (see text) suggests a role of Cathepsin D in HLA-DR degradation.

The Pep A effect occurs in a variety of cell types, including immature MoDCs (Appendix 7.1). Pep A also rescues HLA-DP molecules in KG-1 cells from degradation, and the effects of Pep A on mouse class II molecules vary. Moreover, the result also suggest a correlation between the expression of Cat D and the turnover of HLA-DR molecules. This is based on the similarity in the effect of Pep A in MoDCs (Appendix 7.1) and KG-1 cells and thus it is indirect. However, Priess cells have slow turnover ($t_{1/2}$ > 60 h), and in this cells Pep A had at most a very small effect and the abundance of Cat D was much lower (Figure 3.7), suggesting that cells that are low in Cat D have slower turnover of HLA-DR proteins. The different

effects of Pep A on different cell lines suggest that different rates of turnover correlate with differential expression of aspartyl proteases. Independent of this, differences in ubiquitin-mediated internalisation into lysosomes could contribute to differences in DR turnover between cell types. In any case, the ability of Pep A to rescue DR in KG-1and MoDCs (and to a small extent in Priess cells) indicates the involvement of aspartyl proteases in DR degradation. The accumulation of DR was observed intracellularly on fixed and permeabilized KG-1 cells, but was not observed when only cell surface HLA-DR was stained (Appendix 7.1). In conclusion, this data suggest this is more broadly relevant phenomenon.

When KG-1 cells were cultured in the GlutaMAX media, which favours lysosomal activity (Heeneman et al., 1993, Ten Broeke et al., 2010), the Pep A effect was of similar magnitude as in regular media but peaked earlier. Thus, the Pep A effect (and therefore the role of Cat D in DR degradation) is not an artefact of having worked in culture conditions that inherently slow down lysosomal degradation.

Previous work by Dr Busch's group has mapped the initial cleavage site of Cat D on HLA-DR. The observed initial cleavage site after residue Phe 54 in the α-chain maps to an extended strand shared between MHC II molecules, which flanks the N terminus of the bound peptide. The α-chain is highly conserved in the HLA-DR molecules (Trowsdale, 1993). Thus, based on the cleavage preference of Cat D, the mechanism of degradation observed in KG-1 cells will apply to all variants of HLA-DR, including gene variantgene variants.

Prior attempts to identify MHC II regulatory factors have used genetic manipulation, and that may be the reason why Cat D was not identified. The cells seem to adapt, as can be seen in KG-1 cells cultured with GlutaMAX media where, after the initial peak effect of Pep A, the effect wears off. Even in cells grown in regular media, in which lysosomal activity is lower,

further DR accumulation ceased on the third day of treatment. Moreover, when Cat D was knocked down in KG-1 cells, the cells were expanded for 2-3 weeks before analysis, by which time HLA-DR levels were no longer elevated above baseline.

Together, these lines of evidences indicate that cells eventually adapt to maintain the levels of HLA-DR. There can be two possibilities: either there is feedback down- regulation of HLA-DR protein synthesis or there is adaptation of the lysosomal compartment to the lack of Cat D by up-regulating other enzymes, possibly with similar cleavage specificities, so that overall lysosomal function is restored. Further studies on this interesting issue are needed.

Since various cathepsins play different roles in the MHC II maturation, it is also possible that Cat D might be involved in maturation of HLA-DR and thus the Pep A rescue, which is observed, is merely an accumulation of immature HLA-DR molecules. The L243 antibody used in this chapter does not recognize immature HLA-DR molecules (Roche and Cresswell, 2011), but there was no control used to detect immature HLA-DR in this study. Therefore, Chapter 4 examines the form of HLA-DR rescued by the Cat D. Nevertheless, all the results so far indicate that Cat D has a vital role to play in the degradation of HLA-DR molecules.

Chapter 4: Characterizing the molecular form of HLA DR molecules degraded by cathepsin D

4.1 Abstract

Several key stages of HLA-DR maturation take place in lysosomes. Different molecules may be found ssociated with HLA-DR in lysosomes: invariant chain (li), Class II associated invariant chain peptide (CLIP), other peptides. Cathepsin D (Cat D) could act on any of these forms or it could be more selective in its action. Work described in this chapter characterised the form of the HLA-DR degraded by Cat D. Biochemical and immunological tools were used to investigate which of the different forms of HLA-DR accumulate in KG-1 cells when Cat D action is blocked with pepstatin A. Resistance to SDS-induced denaturation at room temperature was used as a known proxy for peptide binding to HLA-DR. Results showed no rescue of SDS stable HLA-DR molecules. Of the known SDS unstable species, Iiassociated molecules seemed not to be rescued, because quantification of Iiby flow cytometry or Western Blot did not show any change after pepstatin A treatment. There was no detectable accumulation of ubiquitinated DR β chain which would have been seen as multiple higher molecular weight bands on a Western blot. Of the different association states of MHC II molecules, the results are consistent MHC II molecules which either never acquired a peptide or lost peptide following antigen presentation to be degraded by Cat D. This study supports a working model for HLA-DR degradation in which peptide loading and the associated molecular machinery protect HLA-DR from Cat D attack, whereas MHC II are degraded selectively upon loss of bound peptide by Cat D.

4.2 Introduction

Lysosomal proteases carry out several steps in the maturation and peptide loading pathway of MHC II molecules (van Kasteren and Overkleeft, 2014). They generate peptides that are loaded into the peptide binding groove (Hsing and Rudensky, 2005). They also participate in the way in which Iiregulates access to peptide binding groove by mediating the degradation of the Iichain (van Kasteren and Overkleeft, 2014). Results from Chapter 3 provided evidence that one lysosomal protease, Cat D, plays a specific role in the disposal of HLA-DR molecules. Cat D might act not just by degrading the HLA-DR molecules themselves but also at other points where proteases influence the maturation of HLA-DR molecules. The objective of this chapter was to examine which forms of HLA-DR are susceptible to attack by Cat D.

The antibody used in Chapter 3 to quantify DR levels was the well-characterised L243 antibody (Lampson and Levy, 1980), which reacts well with the DR α chain of mature DR αβ dimers, but reacts poorly with immature, Ii-associated DR during pulse/chase analyses (Roche and Cresswell, 2011). PIN.1 is an antibody which binds to the N terminus of Ii(Roche et al., 1991) whereas the CerCLIP.1 antibody binds to CLIP (van Luijn et al., 2011). The invariant chain degradation and antibody binding specificities are shown in Figure 4.1.

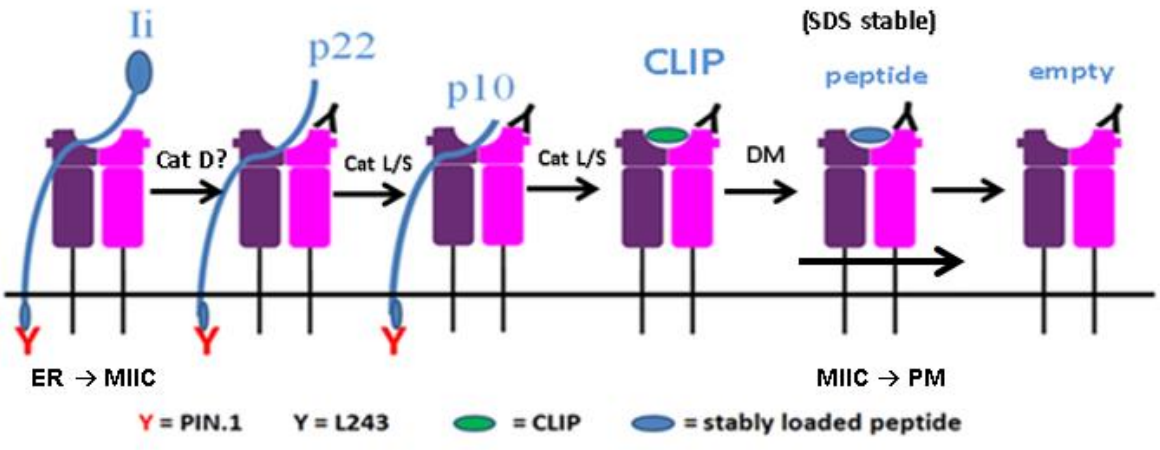

Figure 4.1 HLA-DR protein maturation, fate, and antibody binding specificity. Full length invariant chain creates steric interference, preventing L243 binding. PIN.1 binds the N-terminus of Ii. Ii and its degradation intermediates are indicated. Initiation of Ii degradation (generating p22) may involve aspartyl proteases; subsequent steps (generating p10 and CLIP) are mediated by cysteine proteases. L243 binds to DR α chain of mature DR $\alpha\beta$ dimers, either loaded with peptide or empty. DR molecules loaded with peptide are SDS stable, while empty DR molecules are SDS unstable.

In order to address whether peptide loaded HLA-DR, immature forms of HLA-DR, or both, were rescued by Pep A, SDS stability assays were performed. The peptide loaded DR is highly stable, and cannot be dissociated by SDS (without boiling) at room temperature. However empty DR or DR bound to Iiis generally less stable and dissociated by SDS at room temperature (Busch et al., 1998, Natarajan et al., 1999b, Sadegh-Nasseri et al., 2010). In cells that lack HLA-DM catalysed peptide editing and/or where CLIP dissociates spontaneously, the resulting MHC II molecules, which are either empty or not loaded with stable peptides, exhibit faster turnover (Busch et al., 2012, De Riva et al., 2013). Ubiquitination is a known regulator of degradation, in which ubiquitin, a 76 residue protein (Callis, 2014), is covalently attached to the β chain of the HLA-DR and initiates its internalization (Shin et al., 2006, van Niel et al., 2006).

These different forms of HLA-DR can be distinguished in cells according to their biochemical phenotype, based on SDS stability, reactivity with different antibodies and molecular weight of associated Iichain fragments.

4.2.1 Potential role of cathepsin D in MHC II pathway

Cat D is a major aspartyl protease of the lysosomal compartment, thanks to its localization in multi-vesicular endosomes (MIIC) (Benes et al., 2008). Considering the entire life span of MHC II molecules, Cat D has the potential to act at several steps in antigen presentation and MHC II maturation, with distinct biochemical consequences as set out below.

4.2.1.1 Potential role of Cat D in the degradation of antigens.

Antigen processing is the process by which antigens are prepared for presentation by MHC molecules (Mellman et al., 1998). The general steps in antigen processing are unfolding of native proteins, reduction of disulphide bonds and proteolytic fragmentation (Watts, 2012). MHC II binding can occur at any stage after the unfolding step (Santambrogio et al., 1999). Some studies have shown Cat D to have a role in antigen degradation (Mizuochi et al., 1994, Villadangos et al., 1999). In contrast, DCs derived from Cat D deficient mice were capable of antigen processing as well as antigen presentation. Microglia isolated from such mice also retained ability for antigen presentation (Nishioku et al., 2002). In knockout mice, cells might adapts and even if there is a role of Cat D in antigen processing perhaps a remodelling of other lysosomal enzymes could compensate to some extent. There might be a role of Cat D in processing of antigens but it is not one that is quantitatively important. There is no evidence that lysosomes that are deficient in Cat D are inefficient at processing antigens in general or result in an overall peptide loading defect.

If Cat D were primarily important for antigen supply, its inhibition would reduce SDS stability and accelerate HLA-DR degradation by other proteases due to the under supply of stabilizing peptides (Busch et al., 2012, De Riva et al., 2013). This is not in accordance with the rescue of HLA-DR from degradation by Cat D inhibition seen in Chapter 3.

4.2.1.2 Potential role of Cat D in degradation of invariant chain

MHC II αβ heterodimers assemble in the endoplasmic reticulum (ER), where they associate with invariant chain (Ii) (Neumann and Koch, 2005). The peptide binding groove of the MHC II molecule is blocked by a disordered region of Ii, thus preventing ER polypeptides from associating with the groove (Busch et al., 1996). MHC II/Ii complexes accumulate transiently in late endosomal compartments under the direction of the cytoplasmic tail of Ii (Busch and Mellins, 1996). MHC II/Ii complexes are then transported to endocytic compartments, where Ii chain is sequentially degraded by cysteine proteases to give the p22 or p10 degradation intermediates and then finally, CLIP. The process of Iidegradation is depicted in Figure 4.1. The terminal Ii degradation fragments (Mak and Saunders, 2006), CLIP, continue to block the peptide binding groove and must dissociate to allow presentation of antigen. The enzymes involved in the initial steps of degradation have been in debate.

The enzyme that initiates degradation of Iihas been proposed to be an aspartyl protease (Marić et al., 1994), but this has not been reproduced by others (Villadangos et al., 1997, Deussing et al., 1998). Riese et al (1996) reported that cathepsin S, but not cathepsin B or D, is necessary for the digestion of Ii from MHC II molecules. The progressive degradation of p22 to p10 and then to CLIP is performed by the cysteine proteases, cathepsin L and S (Hsing and Rudensky, 2005). Costantino et al. (2008) reported that there is considerable variation in

lysosomal activity between different cell lines. Thus, results reported earlier may not be mutually contradictory and the activity of lysosomal enzymes depends on the cell system used.

If Cat D were important in initiating Iiprocessing in KG-1 cells, as reported by Marić et al., (1994), one would predict accumulation of Iiand li/DR complexes. Data in Chapter 3 had shown accumulation of HLA-DR molecules using an antibody, L243, which poorly reacts with Iiassociated HLA-DR molecules (Lampson and Levy, 1980, Roche and Cresswell, 2011). However, this did not fully rule out the possibility that Cat D acts to prevent the degradation of li/DR complexes. If Cat D has a role in the degradation of Iithen there would be accumulation of PIN.1 reactive DR/Ii complex on Pep A treatment.

4.2.1.3 Potential role of Cat D in degradation of empty MHC II molecule

Unpublished work by the group of Dr Busch has shown that cathepsin D is able to degrade HLA-DR molecules *in vitro* (Appendix 7.1). This observation suggests the vulnerability of HLA-DR towards direct attack by the cathepsin D. Moreover, Cat D fragments of DR chain were identified by Orbitrap LC-MS/MS analysis of tryptic digests, and compared with cleavage preferences predicted from the MEROPS database to identify the cleavage site. Initial Cat D cleavage *in vitro* was mapped to α54 a site in DR α that interacts with bound peptide and changes conformation when peptides bind (Ferrante, 2013). Thus, it is possible that peptide binding regulates Cat D attack so that empty molecules are degraded.

If empty HLA-DR molecules are selectively targeted for Cat D attack in KG-1 cells, then Pep A treatment will result in the accumulation of SDS-unstable DR molecules but not of Iior its fragments.

4.2.1.4 Potential role of Cathepsin D in the activation of other proteases

Many of the proteases, including Cat D, are synthesised as pre-pro or immature forms. The activation of such forms is achieved by cleaving the pre-pro form by other proteases. So it is possible that cathepsin D might act on the pre-pro form of another enzyme that then attacks HLA-DR molecules. However to our best knowledge, there has been no previous evidence of this role of cathepsin D in the literature (Brix, 2005, Colbert Jeff et al., 2009). So this function of cathepsin D seems to be less likely. Also there isevidence, as reported in section 4.2.1.3, that Cat D is capable of attacking HLA-DR molecules directly.

As the preceding sections have shown the rescue of specific forms of HLA-DR will produce distinct phenotypes. The objective of this chapter was to compare the biochemical phenotypes of HLA-DR molecules rescued by Pep A with these expectations and thereby infer which forms of HLA-DR is being rescued.

4.3 Results

The objective of this chapter was to findout which forms of HLA-DR are susceptible to attack by Cat D.

4.3.1 No evidence that Iiis rescued by Pep A

Marić et al. (1994) observed that an inhibitor of aspartyl proteases accounted for Iidegradation. If this observation was true then in the KG-1 cells blocking Cat D should rescue li. In order to address this, KG-1 cells were treated with pepstatin A for up to 48 hours, fixed and permeabilized, and analysed for Iiusing PIN.1-FITC antibody. PIN.1 binds to the N terminus of the Iichain (Roche et al., 1991).

Flow cytometry showed immunoflurorescence staining with anti-Iiantibody (PIN.1) in KG-1 cells at baseline, over and above unstained control and isotype control IgG2, as shown in Figure 4.2 (A). In Pep A, treated KG-1 cells, there was no effect on the invariant chain, as a positive control we reproduced the finding of Pep A mediated rescue of HLA-DR molecules as it had done in previous experiments in Chapter 3 (Figure 3.6), as shown in Figure 4.2 (B). There was no detectable accumulation of Iiin Pep A treated KG-1 cells compared, to the KG-1 cells that were left untreated or treated with DMSO as a vehicle control. One-way ANOVA indicated no significant effect of Pep A on Iiaccumulation $F(2, 15) = 1.388$, $p = 0.280$ (Appendix 4.1). However, the increase in DR level on treatment with pepstatin A in KG-1 cells was significant, $F(2, 15) = 18.17$, $p < 0.001$, as analysed by one-way ANOVA (Appendix 4.2). Hence there is no evidence that cathepsin D degrades li.

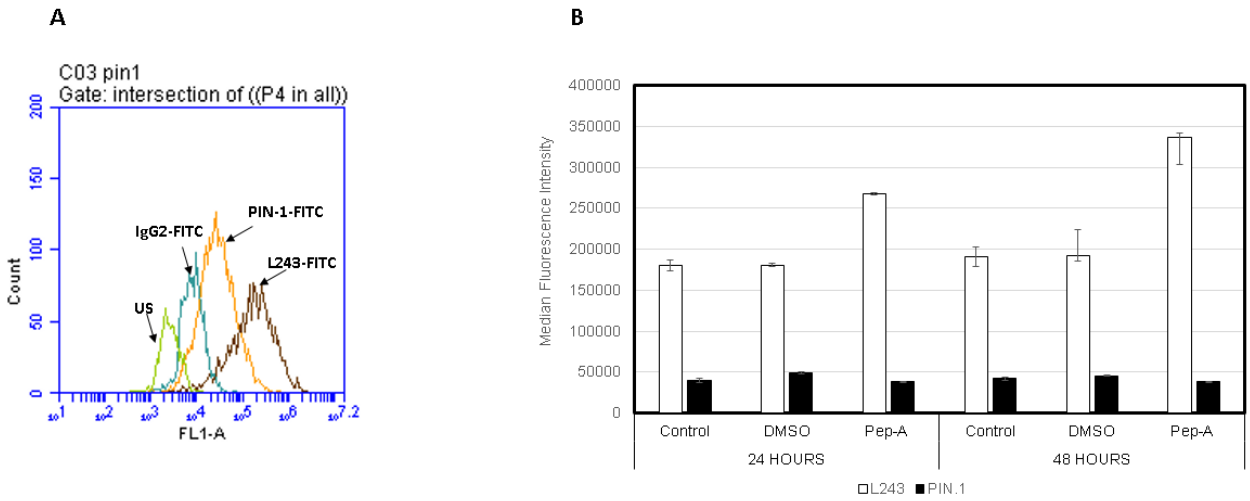

Figure 4.2 No evidence for rescue of invariant chain by Pepstatin A in KG-1 cells. KG-1 cells were treated with 20 µM Pepstatin A, DMSO (vehicle) or left untreated (control) for 48 hours. Cells were fixed and permeabilized and analysed for Iiand HLA DR with PIN.1-FITC and L243-FITC respectively, by flow cytometry. (A) Shows the overlay of histograms in FL-1 when stained with L243-FITC, IgG2-FITC, PIN.1-FITC or nothing. (B) Shows staining of Iiand DR molecules quantified by flow cytometry and reported as median fluorescence intensities (MFI; mean +/- S.D. of triplicate analysis). The results show no evidence for the rescue of IiI KG-1 cells when the action of cathepsin D was blocked by Pepstatin A. This experiment was repeated three times.

Thus, PIN.1 staining showed no evidence that Iichain is degraded by Cat D. In contrast, HLA-DR molecules that are preferentially recognised by L243 were rescued in the same experiment (Figure 4.2). The li-DR complexes are reactive to PIN.1 antibody and poorly reactive to L243 antibody. Thus li-DR complexes are unlikely to be the potential targets for the DR degradation.

To confirm Pep A does not rescue Iichain complexes, extracts from Pep A- treated and control KG-1 cells were resolved by 12% reducing SDS PAGE, and Western blots were probed with PIN.1 antibody. The quantification results from the Western blot, shown in Figure 4.3, also showed that there is no accumulation of Ii or its degradation intermediates by Pep A in KG-1 cells. Thus, cathepsin D does not detectably act on the degradation of Ii chain

in the KG-1 cells. Not only is there no measurable change in the total Ii chain but also there is no indirect effect on the degradation of Ii at the later stages.

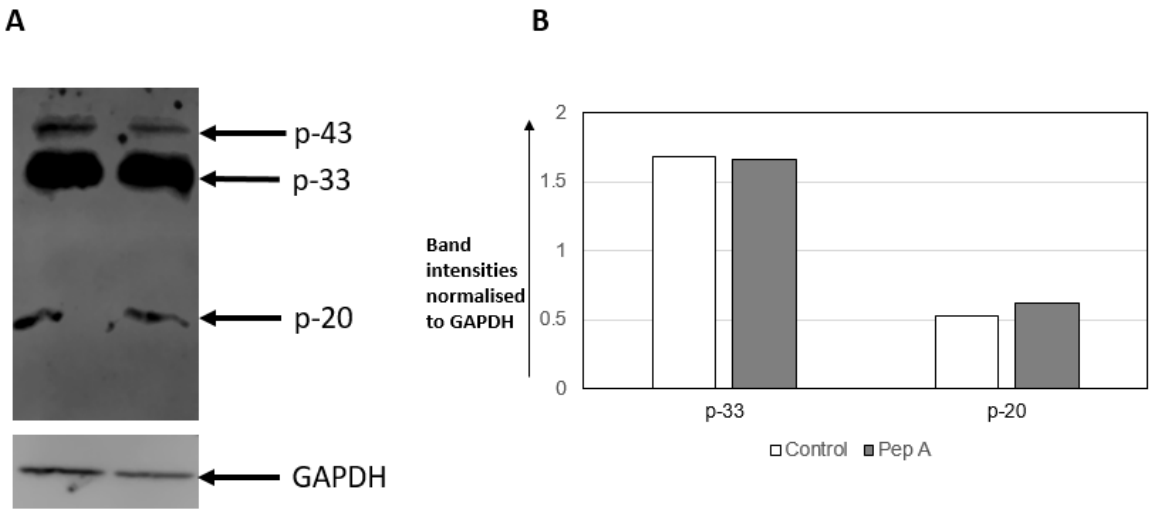

Figure 4.3 No accumulation of invariant chain when KG-1 cells are treated with pepstatin A: KG-1 cells were treated with 20 µM Pepstatin A, DMSO (vehicle control) for 48 hours. (A) KG-1 cell extracts were resolved by 12% reducing SDS PAGE and immuno-blotted for invariant chain (Ii) using PIN.1 antibody. Ii and its degradation intermediates were observed at (molecular weights of) 43kDa, 33 kDa and 20 kDa. There was no visible difference between the band intensities of the Iidegradation intermediates between pepstatin A treated KG-1 cells and untreated cells. This was confirmed by quantification of p-33 and the p-20 bands by Image studio version 5.2 software. (B) Bar graph showing to the band intensities of p-33 and p-20 intermediate of Ii. This confirmed that there is no measurable change in Iiprocessing in Pep A treated KG-1 cells.

These experiments were done in regular media supplemented with glutamine. In Chapter 3 it had been shown that the peak pep A effect on mature HLA-DR levels occurred earlier (section 3.3.2) in media containing GlutaMAX. This is likely to be related to release of ammonia on hydrolysis of glutamine. So the KG-1 cells were cultured in media containing GlutaMAX. Once adapted to the new media, KG-1 cells were treated with pepstatin A for up to 48 hours, fixed and permeabilized, and analysed at various time points for Iiusing PIN.1-FITC antibody. The staining intensity was indistinguishable between the controls and Pep A-

treated cell for the Iias shown in Figure 4.4 (A). Figure 4.4 (B) compares the Pep A effect on levels of Ii, as detected with PIN.1-FITC, between KG-1 cells grown with L-glutamine and GlutaMAX. Two-way ANOVA revealed no significant change in the Ii levels on treatment with Pep A in KG-1 cells cultured in GlutaMAX media, F (1,20) =0.124, p=0.729 (Appendix 4.3). As before, cells were stained separately at each time point, so that effect of time in culture was statistically significant but not necessarily biologically meaningful, due to possible confounding technical variations.

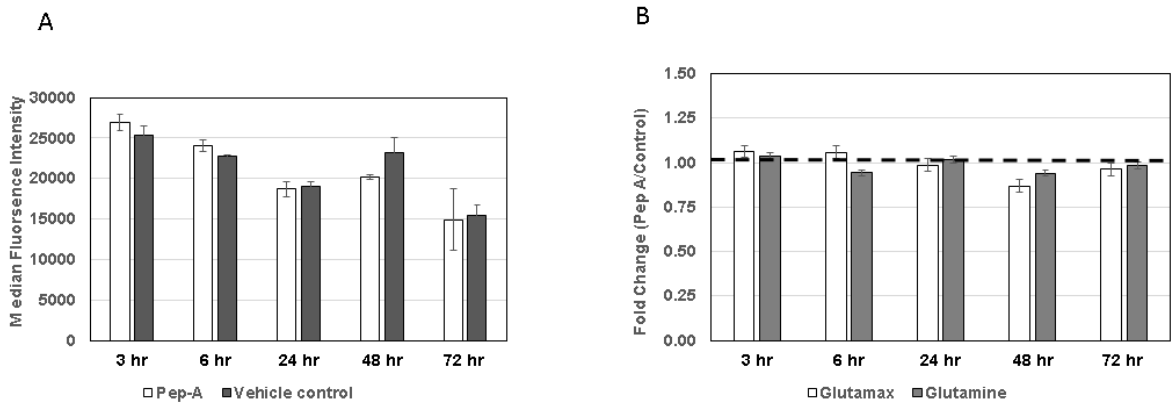

Figure 4.4 No accumulation of Iichain in KG-1 cells treated with Pep-A using GlutaMAX media.. KG-1 cells were cultured in IMDM media containing GlutaMAX instead of traditional glutamine containing medium, and the effect of Pep A was analyzed. (A)There was no accumulation invariant chain (Ii) when stained with PIN.1 antibody in KG-1 cells treated with Pep A in GlutaMAX media. Cells were analysed after fixation and permeabilization. Staining was quantified by flow cytometry and is reported as median fluorescence intensities (MFI; mean +/- S.D. of triplicate analysis). (B) There was no effect of Pep-A on the Ii regardless of whether cells were grown in glutamine or GlutaMAX containing media. Each bar represents the fold change, i.e., Pep-A treatment divided by the control. This experiment was repeated twice.

4.3.2 Rescue of SDS-unstable DR molecules by pepstatin A

In order to examine whether peptide loading influences the susceptibility of the HLA-DR molecules to cathepsin D, the SDS stability (as proxy of stable peptide loading) of HLA-DR molecules from Pep A-treated and control KG-1 cells was compared. The resistance to SDS-induced denaturation was investigated by comparing the migration on polyacrylamide gels of identical boiled and non-boiled protein samples containing SDS.

Accordingly, KG-1 cells were treated with 20 μM Pep A or vehicle control for 48 hours, and the rescue of DR molecules was confirmed by flow cytometry with similar results as shown before in Figure 3.3. Proteins were extracted from both sets of samples and quantified using BCA assay. Protein quantities were matched between the extracts. The samples were then resolved by 12% SDS PAGE in either boiled or non-boiled conditions, and Western blots were probed with anti- DRα and DRβ antibodies. On boiling the sample, the native structure is denatured and the observed single band (35 kDa for α and 29 kDa for β) would consist of total DR (including both SDS stable and unstable DR molecules). In non-boiled samples, the SDS-stable form will retain its native structure, whereas SDS unstable molecules will be denatured in SDS. Thus, SDS-stable DR will be observed at around 55 kDa (for both α and β since structure is intact) whereas the unstable DR should be observed around 35 kDa for α and 29 kDa for β.

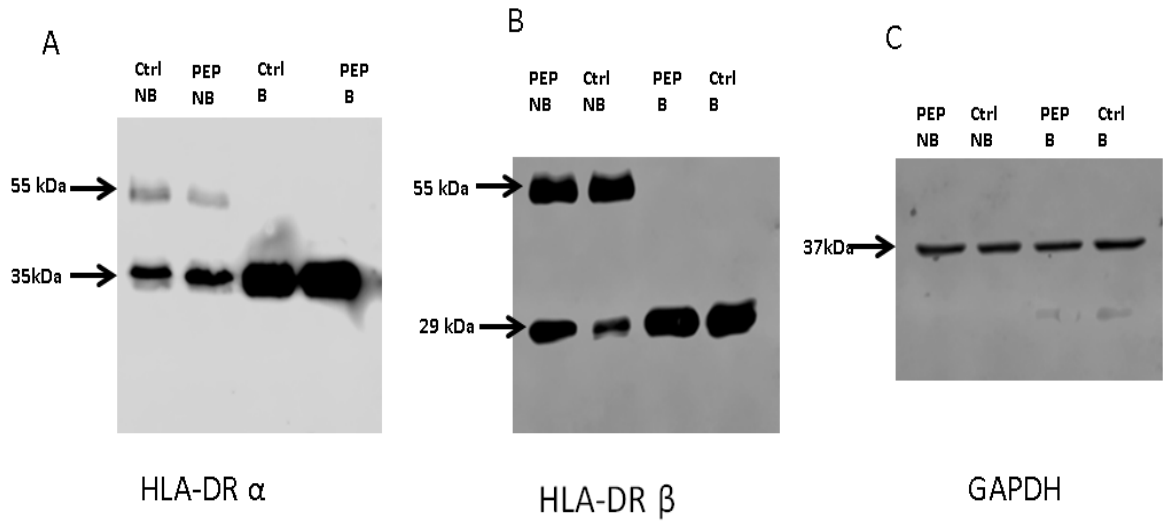

Figure 4.5 Accumulation of SDS unstable DR molecules in Pep A treated KG-1 cells. Whole cell lysates, prepared with RIPA buffer, were resolved by 12% SDS-PAGE with or without boiling (lanes labelled B and NB respectively); Western Blots were probed using anti-DRα (A) and anti-DRβ antibodies (B). The position of monomeric DRα (35 kDa), DRβ (29 kDa) and SDS stable DR α/β dimers (55 kDa) are indicated in the figure.(C) The HLA DRβ membrane was stripped and re-probed with anti-GAPDH antibody as a loading control. Please note that the order of pepstatin A and control was reversed in panel B. This experiment was repeated twice.

The blots shown in Figure 4.5 revealed similar amounts of SDS stable DR (αβ dimer at 55 kDa) in KG-1 cells treated with and without pepstatin A. On the other hand, the SDS unstable DR was rescued by pepstatin A. Both cell extracts contained comparable amounts of protein extract, as judged by re-probing for GAPDH. The molecular weight of GAPDH 37 kDa, is similar to HLA-DR α (35 kDa), and stripping of anti-DR α from blots was inefficient, so only the HLA-DRβ blot was re-probed with the GAPDH antibody. The band intensities were quantified with Image studio version 5.2. The quantification results confirm the selective rescue of SDS unstable DR molecules (Figure 4.6).

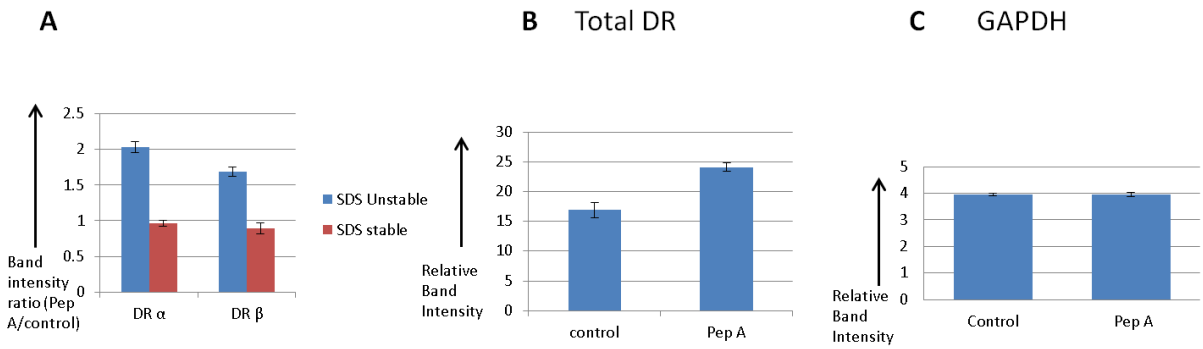

Figure 4.6 Quantification of Western Blots shown in Figure 4.5. (A) Bar graph representing the fold change in Pep-A treated KG-1 cell extracts. Bands were quantified by Image Studio version 5.2 software. The SDS stable DR complexes remained unaffected, while there was an increase in the SDS unstable DR molecules after Pep A treatment. (B) Bar graph showing intensities of total DR (C) Bar graph comparing intensities between both the extracts of the loading control GAPDH, based on the re-plot of the DRβ blot. The graph shows mean +/- SD of the band intensities in experiments such as the one showed in Figure 4.5. The values are from two independent repeats.

Together, these experiments showed that pepstatin A rescues SDS unstable DR molecules which are not associated with li. In most allelic variants of DR, CLIP-DR complexes form SDS-unstable complexes. To check whether pepstatin A rescues CLIP-DR, KG-1 cells treated with pepstatin A were analysed by flow cytometry using the Cer-CLIP.1 antibody, which binds to CLIP. As shown in Figure 4.7, there was no detection of the CLIP using the Cer-CLIP antibody. This may be due to low levels of CLIP-DR molecules present in the KG-1 cells. A caveat is the lack of a positive control showing that Cer-CLIP antibody was actually working.

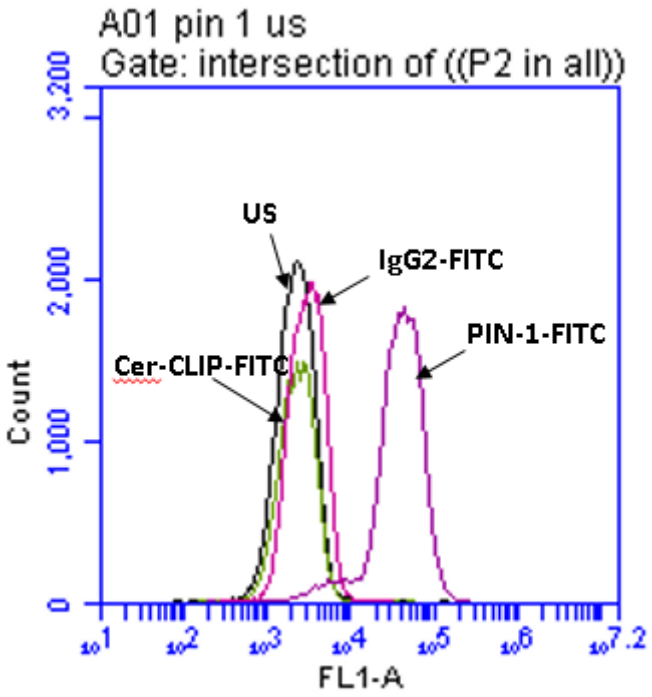

Figure 4.7 Inability to detect CLIP on KG-1 cells with Cer-CLIP antibody. Fixed and permeabilized KG-1 cells, treated with pepstatin A, were stained with Cer-CLIP-FITC and PIN1-FITC. Unlabelled and IgG2-FITC samples were also used as controls. The figure shows the overlay of gated histograms in FL-1 when stained with Cer-CLIP-FITC and PIN.1-FITC. Unlabelled sample and irrelevant antibody (IgG2-FITC) were used as a control. There was no shift in the histogram when KG-1 cells treated with Pep A were stained with Cer-CLIP- FITC antibody, suggesting a failure to detect CLIP. This experiment was repeated twice.

In conclusion, SDS unstable DR molecules that are not associated with the Iiare selectively rescued by pepstatin A in KG-1 cells.

4.4 Discussion

Cat D, as discussed in Introduction section 4.1, could conceivably target several molecular forms of MHC II. The molecular form of DR accumulated in KG-1 cells treated with Pep A was characterised here. In KG-1 cells treated with Pep A, there was no evidence for the accumulation of Iichain and the rescued DR molecules were SDS unstable, implying that cathepsin D targets empty mature HLA-DR molecules. Table 4.1 shows the expected features of different forms of HLA-DR and compares them with the form that the data shows being rescued.

Table 4.1 Various forms of DR

Biochemical property	DR-Ii	DR-p20 Ii	DR-CLIP	DR-Peptide	Ubiquitin-DR	Empty DR	Observed
PIN.1 reactive	+	+	-	-		-	**-**
L243 reactive	low	high	High	High	High	High	**+**
Cer-CLIP reactive	-	-	+	-	-	-	**Not detected**
β chain MW	29kDa	29kDa	29kDa	29kDa	> 37 kDa	29kDa	**29kDa**
SDS stable	-	-	-	+	-	-	**-**

Flow cytometry and Western blot data showed that PIN.1 immuno-reactive molecules were not rescued by Pep A, suggesting that Ii chain, and its degradation intermediates were not targets of the cathepsin D degradation. This finding contradicts Marić et al (1994) who had found that a proprietary aspartyl protease inhibitor blocked the first step of Iidegradation, but consistent with negative findings by other groups in this regards (Deussing et al., 1998, Villadangos et al., 1997). Accordingly, in KG-1 cells, cathepsin D does not target the early forms of the DR, which are PIN.1 reactive. Similarly, there was no accumulation of Ii when

KG-1 cells cultured in GlutaMAX media were treated with pepstatin A. Thus, Ii is not targeted by cathepsin D regardless of whether lysosomes are highly active or less active. Considering that there is variation in lysosomal activity between different cell lines as reported by Costantino et al., (2008). This finding indicates that in KG-1 cells, Cat D is dispensable for Ii chain processing, and the interference with early maturation steps does not explain the accumulation of HLA-DR molecules follow Pep A treatment.

Having been unable to detect CLIP in untreated KG-1 cells, we did not pursue the possibility that Cat D inhibition could affect the exchange of CLIP for antigenic peptides. This is less plausible because it would involve changing a non-covalent interaction, rather than blocking a degradation step (Kropshofer et al., 1996). Thus, there is no reason to expect CLIP exchange for antigenic peptide to be affected by Cat D inhibition. CLIP generation involves cysteine proteases, which are not affected by Pep A (Riese et al., 1996).

Ubiquitination takes place at the DR β chain of mature DR αβ dimers (Moffat et al., 2013). Ubiquitination is the covalent attachment of ubiquitin to target proteins (here DR). Ubiquitin is a small, 76-residue, protein (8.5 kDa) which attaches to the DR β chain (De Gassart et al., 2013). Hence the ubiquitin associated DR would produce a ladder like pattern above the β chain when observed on Western blot. The Western Blot shown in Figure 4.5 does not show this. It is not clear whether KG-1 cells use ubiquitin-dependent or alternative internalisation pathways to target HLA-DR molecules for degradation. Thus, degradation happens either to molecules that were never ubiquitinated or to the DR molecules that have been de-ubiquitinated before being degraded.

The biochemical and immunological profile of the rescued molecules fits best, having excluded the other possibilities, with that of empty DR molecules. Thus, I propose that Cat D in KG-1 cells selectively degrades empty HLA-DR.

4.4.1 Working model

The working model that emerges from these observations is that the lysosomal degradation of HLA-DR follows a multi-step processes as shown schematically in Figure 4.8.

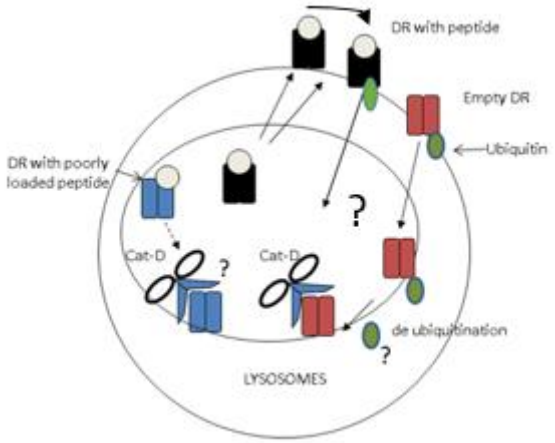

Figure 4.8 Working hypothesis of DR degradation. This study shows that the aspartyl protease Cathepsin D is responsible for the selective degradation of empty DR molecules in KG-1 cells. Once the peptide is presented by mature DR (black), empty DR (red) is internalized, which may depend on ubiquitination (green) based on he studies in other cells. In lysosomes, Cat D initiates the degradation by cleavage at the Phe 54 site on the α chain. The DR molecules that are poorly loaded with peptide during endosomal maturation (blue).

Even though a role of MARCH 1- dependent ubiquitination has not been documented in KG-1 cells, studies in other cell systems suggest that in primary APCs, the first step in the lysosomal disposal of MHC II molecule is the ubiquitin-mediated internalization (Shin et al., 2006, Moffat et al., 2013, ten Broeke et al., 2013), followed by the loss of ubiquitin to restore the HLA-DR, which is then degraded by Cat D. It is not clear where de-ubiquitination of MHC II molecules takes place or which enzymes mediate the process. It is also unclear whether empty DR molecules can selectively ubiquitinated and then internalised, or selectively attacked by Cat D or both.

Mapping of the initial Cat D cleavage site of DR by Dr Busch's group onto the crystal structure of HLA-DR (Appendix 7.1) strongly suggests a model for the initiation of DR breakdown. The observed initial cleavage site after residue Phe 54 in the α-chain maps to an extended strand, which flanks the N terminus of the bound peptide (Figure 4.9). It is potentially accessible to proteolytic attack in the native structure but not when it is hydrogen-bonded to the peptide. Thus, cleavage after αPhe54 may only be possible following release of peptide. Moreover, the known interactions with Ii, DM, and bound peptide may protect maturing MHC II molecules from proteolysis throughout the process of peptide loading (Pos et al., 2012). This region of the molecule is conformationally flexible in mutant DR molecules that undergo rapid peptide exchange without DM (Painter et al., 2011). This model explains how stable peptide occupancy would render DR molecules highly resistant to initial cleavage at this site. Cathepsin D may serve as an initiator in the degradation of HLA-DR, after the loss of peptide. This causes a partial loss of conformation in DR potentially revealing otherwise sterically inaccessible cleavage sites for further degradation by Cat D and other lysosomal proteases.

Figure 4.9 Crystal structure of HLA-DR bound to CLIP. α Phe 54 is the predicted Cat D cleavage sites Image from Protein Data Bank (PDB).

In conclusion, the results in this study suggest that the accumulation of DR molecules induced by Pep A in myeloid APCs is due to inhibition of direct cleavage of empty DR molecules by Cat D. Initial cleavage occurs at the peptide bond between Phe54 and Glu55, a conserved site on the monomorphic DR α chain. The known interactions of MHC II molecules with Ii, DM, and bound peptide may protect maturing MHC II molecules from proteolysis throughout peptide loading, but release of bound peptide without participation of these molecules may render them susceptible to cleavage by cathepsin D. The working model proposed in Figure 4.9 provides a mechanism by which MHC II molecules survive during maturation, yet are degraded at the end of their useful lifespan. Thus, this fills a key gap in our understanding of the molecular pathways by which MHC II proteins are degraded in APCs.

Chapter 5: Interacting effects of vitamin D and retinoic acid on HLA-DR expression in cell lines

5.1 Abstract

Vitamin D plays a major role in immune regulation. Thus, it is associated with protection from autoimmune diseases, including multiple sclerosis (MS). Retinoic Acid (RA) has been ascribed crucial roles in immunological fitness. These micronutrients play a vital role in immune homeostasis. Moreover, MS risk is influenced by polymorphisms in HLA-DRB1, which encodes the β chain of HLA-DR antigen-presenting molecules, and by polymorphisms affecting vitamin D metabolism. Vitamin D regulates antigen-presenting cell function, including the transcription and expression of some DRB alleles, such as the DRB1*15 MS risk variant. Vitamin D might protect from MS in part by differentially influencing the expression of HLA-DR protein variants associated with MS risk. Here, the effect of vitamin D (10nM) and or RA (1μM), at pharmacologically active doses, on HLA-DR expression was investigated in lymphoblastoid cell lines (LCL) homozygous for eight common DRB1 alleles and in KG-1 cells. In most LCL, neither vitamin D nor RA consistently altered HLA-DR expression. However, vitamin D enhanced HLA-DR expression in LCL homozygous for DRB1*15 PGF cells, and DRB1*13 WDV cells, whereas RA increased HLA-DR levels in the DRB1*07 homozygous LCL, MANN. Vitamin D effects were reversed by RA, and vice-versa consistent with mutual competition for the shared RXR transcription factor. In contrast, the combined treatment of KG-1 cells with vitamin D and RA resulted in decreased HLA-DR expression. The result confirms previous findings that vitamin D has allele dependent and independent effects of HLA-DR protein expression, which are modest in size, involve several different mechanisms and are further modulated by RA. The finding highlights the need for studying how these effects are integrated in primary APCs.

5.2 Introduction

This chapter investigates the interaction between vitamin D and RA signalling in the regulation of MHC II protein expression in model APCs. As discussed in Chapter 1, section 1.4.2., vitamin D metabolites are involved in the regulation and expression of several hundred genes implicated in innate and adaptive immune defence (Hewison et al., 2003, Liu et al., 2009, Smolders and Damoiseaux, 2011, Tiosano et al., 2013). Similarly, retinoic acid (RA) is pleotropic in terms of its effect on the immune system.

5.2.1 Interaction of vitamin D and retinoic acid

As discussed earlier in the Chapter 1, (1.4.1)RXR is a shared nuclear hormone receptor as it can also bind as a homodimer or as a heterodimer with retinoic A receptor (RAR) (Blomhoff and Blomhoff, 2006). The binding of the RAR/ RXR heterodimer to the retinoic acid response element (RARE) sequence in the promoter region of the target genes results in the transcription of target genes (McGrane, 2007). Figure 5.1 shows how vitamin D and RA regulate the transcription of target genes.

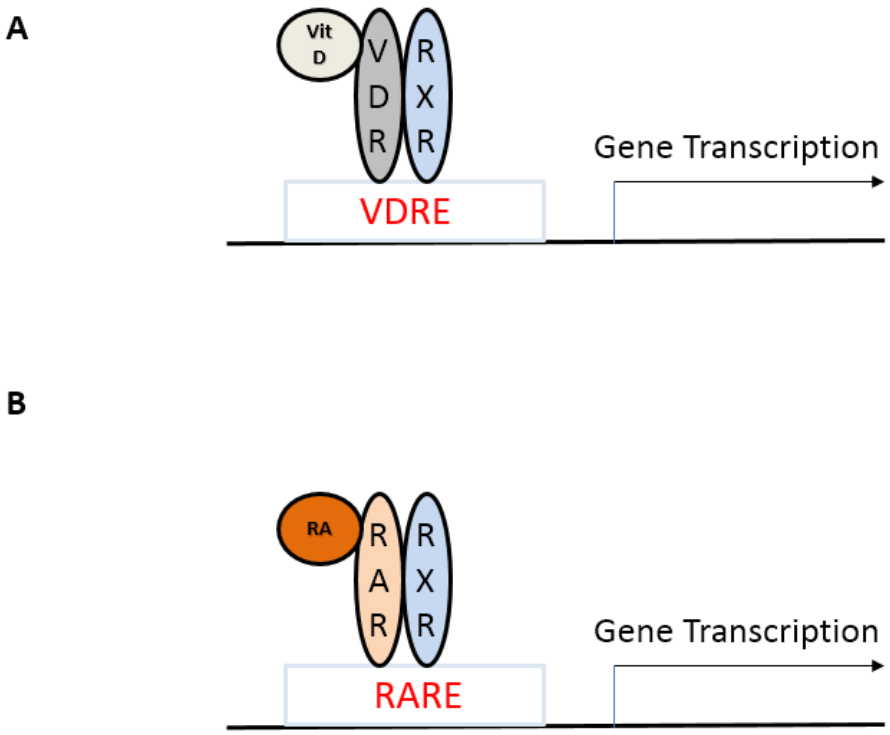

Figure 5.2 Regulation of nuclear receptor mediated gene transcription: The figure provides a schematic representation of the pathway via which vitamin D and RA mediate the transcriptional effects on target genes. In panel (A) the binding of active vitamin D to VDR results in activation of VDR. Active VDR than heterodimerizes with RXR and binds to VDRE within target gene promoters and modulates their transcription. Similarly, RA can also mediate gene transcription via RAR/RXR binding to RARE, as shown in (B).

This common ability for RXR to bind to both VDR and RAR can lead to the possibility of cross-talk within their response elements (Tavera-Mendoza et al., 2006) that may lead to a synergistic (Anand et al., 2008) or antagonistic effect (Bastie et al., 2004) depending on the response element being evaluated. Previous research has found RA and vitamin D to have a synergistic effect in inducing tumour cell differentiation in the hematopoietic system (Muto et al., 1999). Researchers have also reported the synergistic differentiation of myeloid leukemia cells by RA and vitamin D, which was probably mediated through their cognate nuclear receptors (Defacque et al., 1994, MasciulIiet al., 1995, Nakajima et al., 1996).

5.2.2 Vitamin D and HLA-DR protein

As discussed in section 1.5.6 of Chapter 1, VDREs exist in the promoter region of certain DRB1 alleles, which can enhance the expression of HLA-DR molecules. A study performed by Ramagopalan et al. (2009) showed that bioactive vitamin D enhances the expression of the particular HLA-DRB1 allele most strongly associated with increased risk of MS, DRB1*15:01. However, other studies have failed to find similar effects of bioactive vitamin D on other DRB1 (DRB1*13:03 and DRB1*04:05) alleles, which are associated with MS in a Sardinian population (Cocco et al., 2012). The authors found VDREs in close proximity of the examined HLA haplotypes, but they did not find a consistent HLA expression increase when adding vitamin D, and some of the VDREs were not functional. Thus, there may be a gene environment interaction at the level of regulating expression of one MS risk allele but not of other risk alleles that are prevalent in other populations. Cocco et al. (2012) examined gene promoter activity in response to bioactive vitamin D in the particular allele. It is also possible that some of the effects of vitamin D on HLA-DR protein expression are not transcriptional but post-translational. There might be redistribution of HLA-DR taking place in the APC that could have different rate of turnover and so potential of an indirect effect of vitamin D on the expression of HLA-DR cannot be ruled out.

The main objective of this chapter was to examine the effect of vitamin D and / or RA on HLA-DR expression in model cell lines. The earlier studies (Ramagopalan et al., 2009, Cocco et al., 2012) only examined the effect of vitamin D on some HLA-DR alleles in homozygous typing cells (HTCs), by either measuring the activity of the DRB1 promoter or by measuring surface expression of the protein. The current study investigates the combined effect of vitamin D and RA on the total (surface + intracellular) HLA-DR expression in a

similar cell system, but expanding the panel of cell lines in a systematic way to include alleles most prevalent in majority of the UK population.

KG-1 cells were also selected because they have more active turnover of HLA-DR molecules as compared to HTCs (Chapter 3) and they are heterozygous in the expression of HLA-DR. Considering the aim of looking at the effect on the alleles, HTCs representing the alleles found in KG-1 cells were also selected to investigate whether there is any similarity between the behaviour of alleles found in haplotypes and HTCs.

5.3 Results

In order to examine the responsiveness of HLA-DR expression in HTCs to vitamin D and RA, cells were treated with either of these reagents, or both, and the HLA-DR levels were quantified by flow cytometry.

Pharmacological bioactive doses of 10 nM vitamin D and 1 µM RA were selected, based on those previously reported for cell cultures (Adamson, 1996, Ryan et al., 2013). These doses were deemed to be non-toxic for cell culture and are considered to be comparable with doses of vitamin D (25-OH-D) and RA found in the serum of adults (Bischoff-Ferrari et al., 2012, Johnson and Redner, 2015).

The group of Professor Steven G E Marsh at the Anthony Nolan Research Institute identified the top six most frequent HLA-DRB1 alleles in the UK cohort (White British / White Irish / Caucasian). The frequencies of these were calculated both as predicted proportions by Hardy-Weinberg (Chen et al., 1999) and based on actual counts from a cohort of adult donors from the UK. This information was also crosschecked with the allele frequency database (http://www.allelefrequencies.net/default.asp). Thus, these six alleles represents a 90% of the population in the UK (White/Irish/ Caucasian) cohort having one of the allele and 50% for the two allele. The list of the cell lines along with their alleles is provided in Chapter 2 Table 2.1.

5.3.1 Effect of vitamin D and RA on total HLA-DR expression in HTCs

HTCs representing the six commonest HLA-DRB1 alleles in the Caucasian British/ Irish population and the two DRB1 alleles present in the KG-1 cells were selected for the study. The HTCs were treated with calcitriol, RA, or both. The maximum treatment was for 72 hours, and DMSO matched to the volume used in the combination treatment (0.02% v/v) was

used as a vehicle control. Earlier studies examining at the effect of vitamin D on specific alleles of HLA-DR have not considered any possible interaction with RA (Ramagopalan et al., 2009, Cocco et al., 2012). The cells were cultured with vitamin D and or RA, fixed and permeabilized, stained for HLA-DR using L243-FITC antibody, and analysed by flow cytometry at 48 hours and 72 hours post treatment. Representative FACS plots are shown in Figure 5.3, which show total HLA-DR staining for the HTCs.

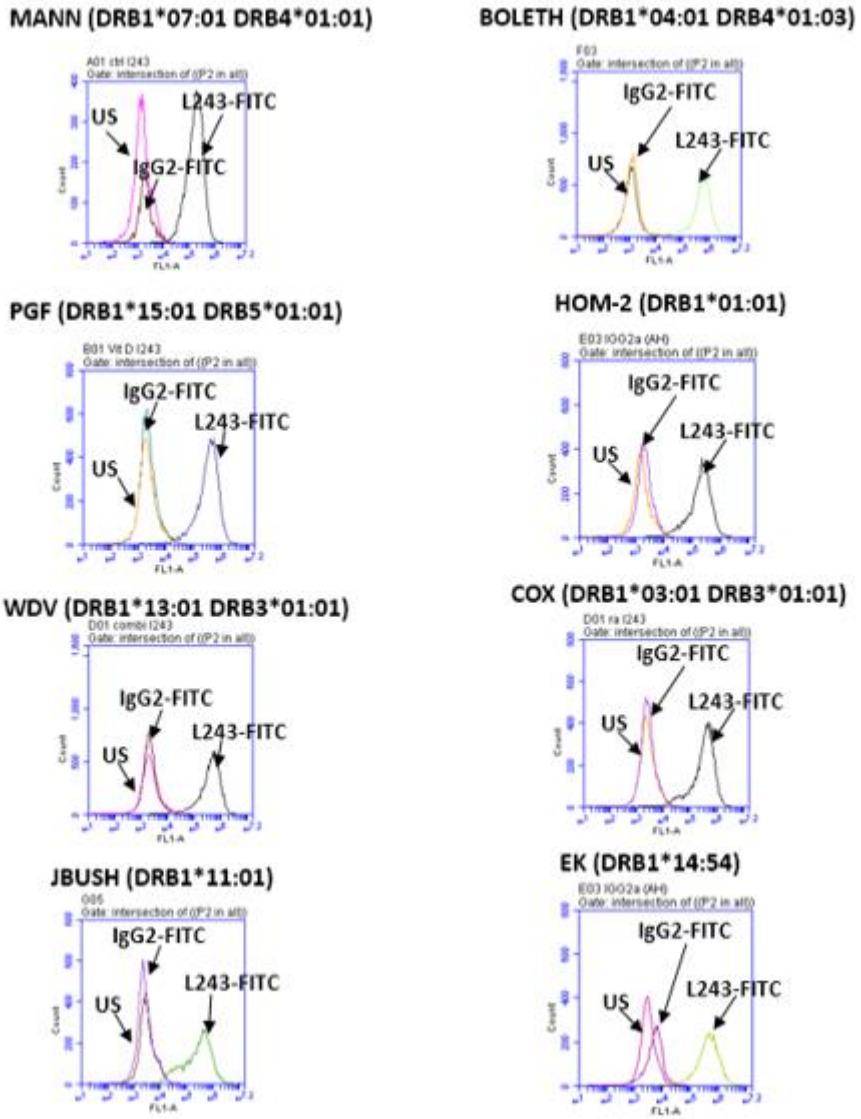

Figure 5.3 Representative FACS plots for total HLA-DR staining of HTCs. The figure shows representative FACS plots for total HLA-DR staining of HTCs representing eight common DRB1 alleles. Cells were fixed and permeabilized and stained with anti-DR (L243-FITC) antibody. Unstained

(US) and isotype control (IgG2-FITC) staining were used as controls in the experiment. The analysis was performed by flow cytometry.

Unstained cells (US) and IgG2a-FITC, an isotype matched negative control, were used as controls to assess autofluorescence and background fluorescence. The histograms show that there is little if any increase in fluorescence intensity when stained with IgG2-FITC compared to the unstained cells. By comparison, there was a substantial increase in fluorescence when HTCs were stained with L243-FITC.

In such flow cytometry experiments, fluorescence intensities vary for technical reasons between staining experiments performed on different days. Moreover, different batches of the antibody were used between experiments, which can also have impact on the staining intensities. So because of the way the experiments were set up, day-to day variations were not considered biologically meaningful. Internal comparisons, however, with the control on the same day, are more valid. The raw data showing day-to-day fluctuations are shown in the Appendices (5.1 and 5.2), and Figure 5.4 shows the effects of vitamin D and/ or RA, normalised to vehicle control (DMSO) =100% on the same day. Figure 5.4 summarizes two independent experiments for eight HTCs. The cell lines responded differently to individual or combination treatment with vitamin D and RA. The effects observed on HLA-DR expression was reproducible in most cases. Based on the experience from Chapter 3 in quantifying modest changes in HLA-DR levels, effect sizes of more than 20% were considered meaningful if they were reproduced in both experiments. Most cell lines showed no or small effects of vitamin D or RA, except PGF, WDV and MANN.

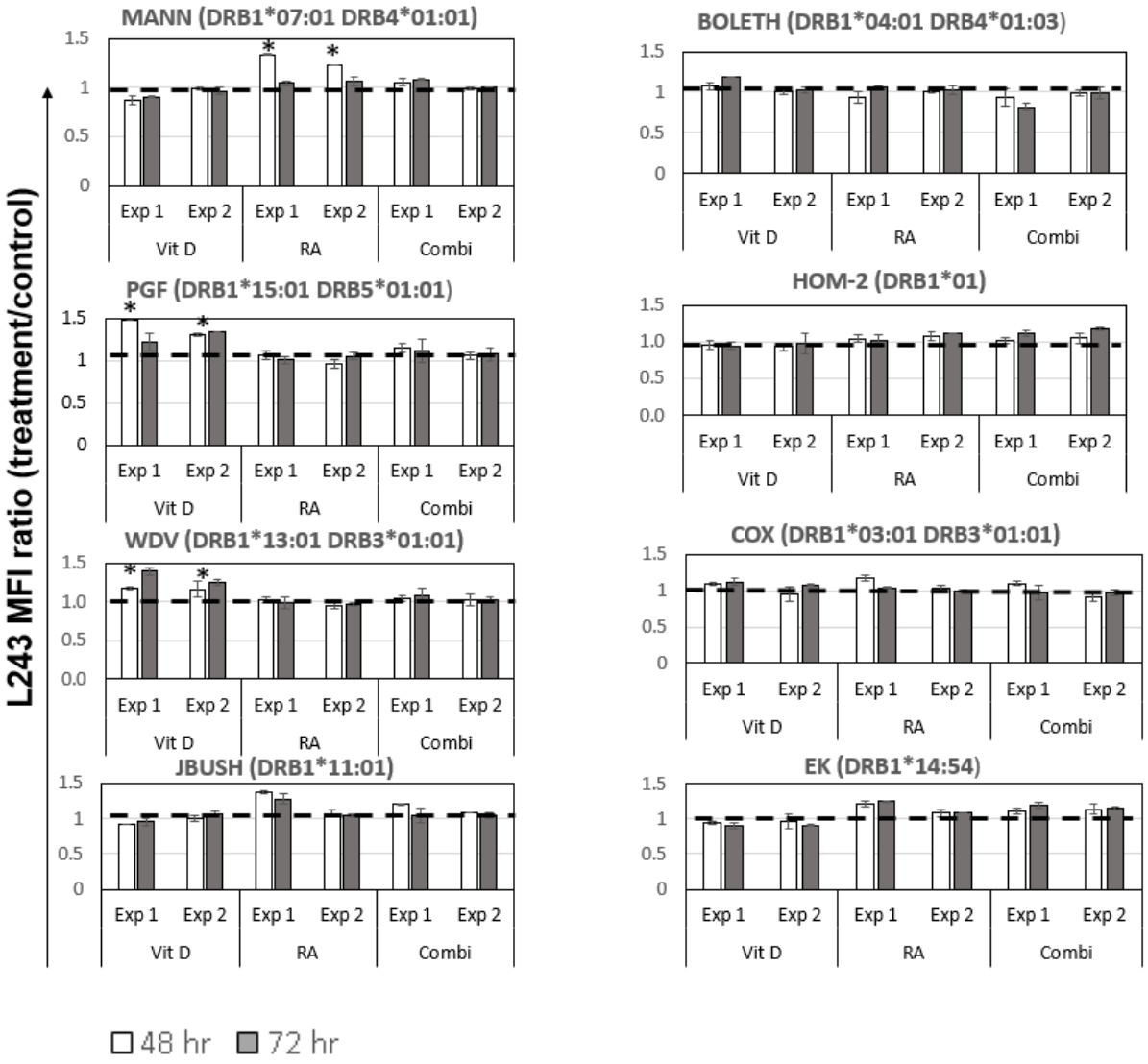

Legend

Figure 5.4 Fold changes of HLA-DR in HTCs covering eight common DRB1 alleles on treatment with vitamin D and RA. A panel of eight HTCs, covering the six common DRB1 haplotypes present in over 90% of white British/Irish/Caucasian people and the two alleles present in KG-1 cells, were treated with 10 nM Vit D, 1μM RA, or both (Combi) for up to 72 hours. Total HLA-DR expression was quantified using flow cytometry on fixed and permeabilized cells using FITC-conjugated anti-DR mAb (L243). Each bar represents the fold change, i.e. treatment divided by vehicle control (DMSO). Some HTCs responded to individual treatment with vitamin D or RA. The figure shows two independent repeats denoted by Exp 1 and Exp 2.

Bioactive vitamin D (calcitriol) alone increased HLA-DR expression levels in PGF and WDV cell lines, which are homozygous for the DRB1*15 and DRB1*13 alleles, respectively. The increase in HLA-DR expression level was dependent on time. For the other HTCs, the effect

of vitamin D was not detectable. There was a modest increase in HLA-DR expression in MANN cells, homozygous for DRB1*07. In each of the above-mentioned HTCs, the effect were reproduced in both experiments. There were some effects of RA (increase in the HLA-DR level), in EK and JBUSH cells, in one of the experiment but were not reproduced in the other experiment.

In PGF and WDV cells, the effect of combination treatment of vitamin D and RA is not the sum of the individual effects. The effect of vitamin D alone was not reproduced by combination treatment in both the cell lines. Conversely, the effect of RA on HLA-DR expression in MANN cells was lost when vitamin D was added in the combination treatment. So in HTCs the effect of each individual was neutralized in the presence of the other agent.

5.3.2 Unresponsiveness of KG-1 cells to pharmacological doses of bioactive vitamin D

Myeloid cells may behave differently when compared to the EBV- transformed lymphoblastoid cells (HTCs), and hence the effect of vitamin D and RA on HLA-DR expression was studied in KG-1 cells. KG-1 cells were treated with 10 nM calcitriol (recommended pharmacological dose) or DMSO (vehicle control) for up to 72 hours. DR levels were quantified either on live or fixed and permeabilized cells using L243-FITC conjugated antibody by flow cytometery. Total DR (i.e. surface HLA-DR and intracellular HLA-DR) was detected by staining of fixed and permeabilized cells, whereas only surface HLA-DR was detected by staining of with live cells (Figure 5.5 (A)). Vitamin D alone had no detectable effect on surface HLA-DR levels in live KG-1 cells. Similarly, there was only a very slight increase in the expression of HLA-DR in fixed and permeabilized KG-1 cells treated with vitamin D over control. The result is shown in Figure 5.4 (A) for surface DR and in Figure 5.5 (B) for total DR. Two-way ANOVA indicated a significant difference between treatment for surface HLA-DR, $F(2,18) = 3.859$, $p = 0.040$ (Appendix 5.3) and for total

HLA-DR F (2, 18) = 17.956, p = 0.010 (Appendix 5.4). However, in both cases the magnitude of the effect is very small, less than 5 %, reproduced in both the attempts.

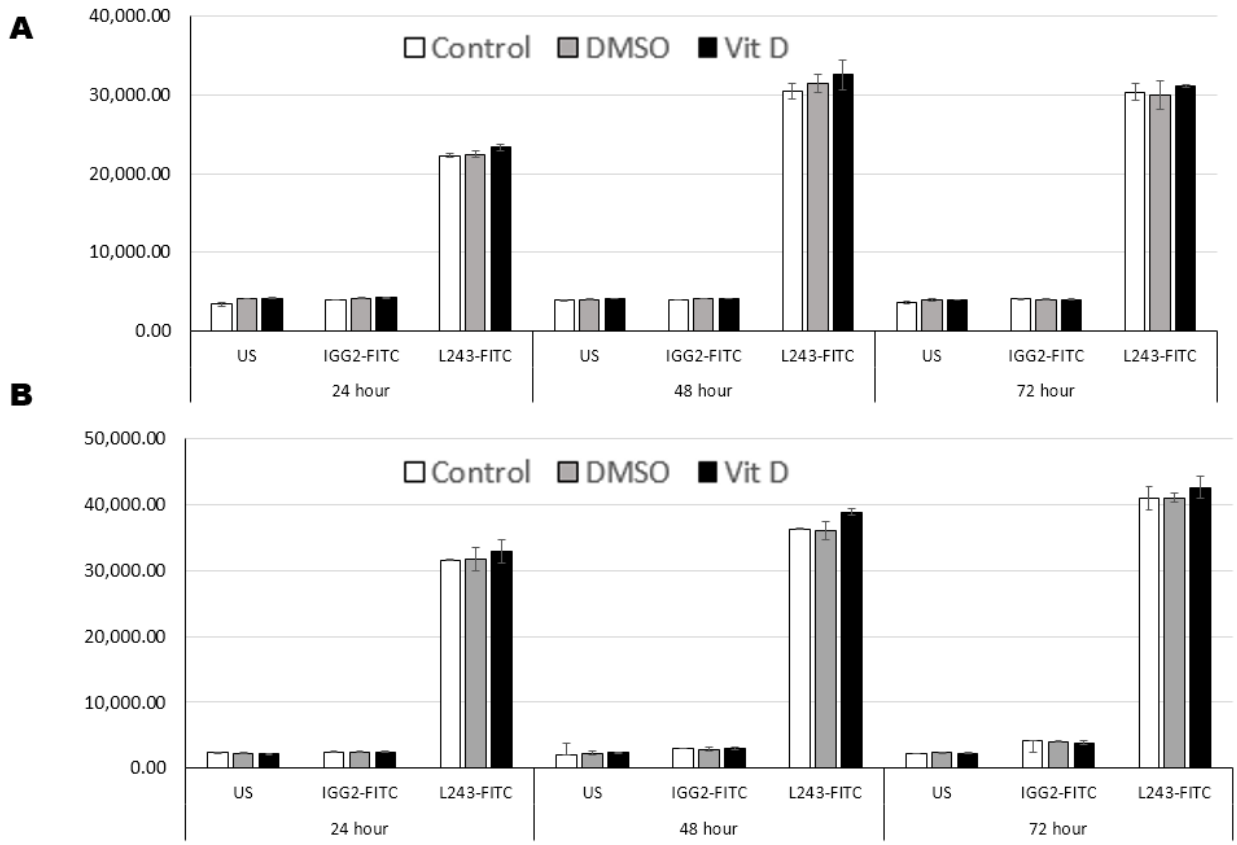

Figure 5.5 Minimal effect of vitamin D alone on HLA DR protein expression in KG-1 cells. KG-1 cells were treated with 10 nM bio-active vitamin D (1 α, 25-dihydroxyvitamin D3) or DMSO (vehicle control) or nothing (control) for up to 72 hours. The HLA DR levels were assessed on either live KG-1 cells (A) or fixed and permeabilized KG-1 cells (B). L243-FITC antibody was used to stain the DR molecules while IgG2a- FITC was used as an isotype control. Unstained cells (US) were also used as a control for auto-fluorescence. Staining of DR molecules and isotype control was quantified by flow cytometry and is reported as median fluorescence intensities (MFI; mean +/- S.D. of triplicate cultures). The graphs show no biologically meaningful difference on the HLA-DR levels on treatment with pharmacological doses of bioactive vitamin D. This graph is representative of two independent repeats.

5.3.2 Reduction of HLA-DR expression in KG-1 cells treated with vitamin D and RA

KG-1 cells were treated as described earlier in order to assess the effect of vitamin D and RA on HLA-DR expression. Total DR was detected on fixed and permeabilized KG-1 cells using flow cytometry. The individual treatments had no effect on HLA-DR levels, but the combination treatment of RA and vitamin D was able to reduce HLA-DR expression by around 20-36%. As before, there was day-to-day variability in the staining intensities in the control on any given day due to technical reasons, and therefore the informative analysis is shown in Figure 5.6, where the effect is expressed relative to control equal to 100% on the same day.

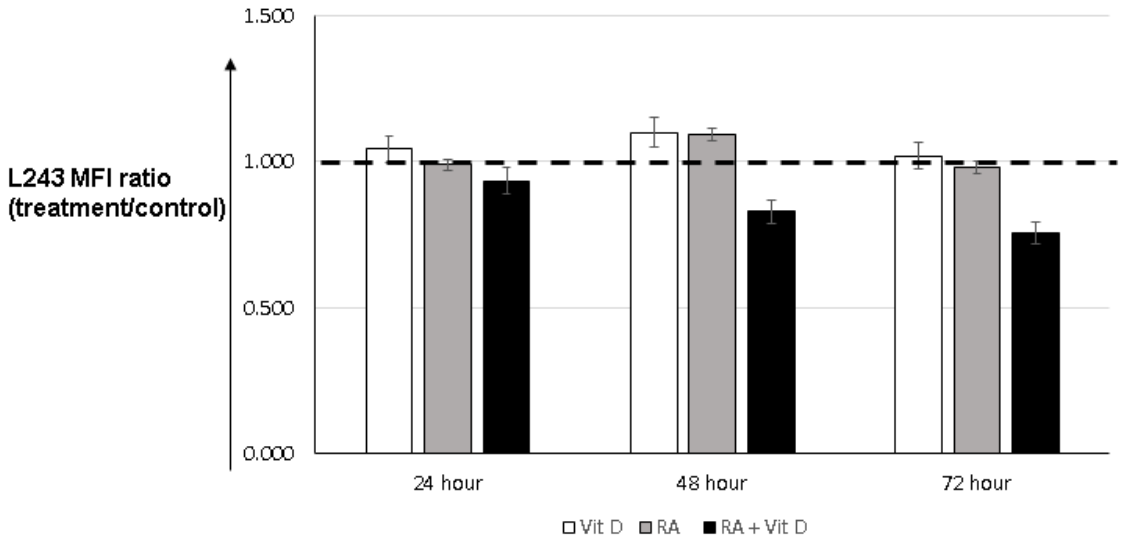

Figure 5.6 Fold changes of HLA-DR observed when KG-1 cells treated with VitD and or RA. Each bar represents the fold change i.e. treatment divided by control. When treated with either Vit D or RA alone, there was very little effect on HLA DR, but on combination treatment there was a decrease in total HLA DR over time. This graph is representative of four independent repeats.

Two-way ANOVA revealed that neither vitamin D nor RA individually had a statistically significant effect on HLA-DR expression ($F(1, 8) = 6.22$, $p = 0.166$ and $F(1, 8) = 10.531$, $p = 0.084$ respectively (Appendix 5.5)), at 24 hours after treatment. However, there was a significant interaction between vitamin D and RA, $F(1, 8) = 37.885$, $p < 0.001$ (Appendix 5.5) at 24 hours on the expression of HLA-DR. Similarly, there was a statistically significant interaction observed at 48 and 72 hours after treatment $F(1, 8) = 36.873$, $p < 0.001$ (Appendix 5.6) and $F(1, 8) = 32.647$, $p < 0.001$ (Appendix 5.7) respectively as determined by two-way ANOVA. At 48 and 72 hours post treatment, vitamin D and RA individually showed statistically significant effects on the HLA-DR expression (Appendix 5.6 and 5.7 respectively), but the effect sizes are not impressive relative to the error in the system.

In the overall data set, vitamin D and RA individually have very little effect but there is a reduction in HLA-DR expression when combined with each other. Therefore, the effect of two reagents (vitamin D and RA) shows up statistically significant (though effect is unimpressive) but their interaction shows impressive and statistically significant effects, as the effect is not additive. Thus, a synergistic effect leads to the reduction of the HLA-DR expression when vitamin D and RA are combined. In the four independent repeats the % decrease of the HLA-DR at 2-3 days after treatment varied between 20-36%.

5.4 Discussion

The objective of this Chapter was to investigate how HLA-DR levels in cell lines respond to the combined or separate treatment with vitamin D and RA. To our knowledge, this is the first examination of this interaction with any cell line. In HTCs, the effects of vitamin D and RA on the expression of HLA-DR varied between the cell lines and over time and competed with each other. In contrast, in the myeloid cell line, KG-1, combined treatment with vitamin D and RA synergistically lowered HLA-DR expression.

5.4.1 Increase in HLA-DR expression on vitamin D treatment of HTCs is limited to DRB1*15 and DRB1*13 alleles

Of the six most common HLA-DRB1 alleles in the White British/ White Irish/ Caucasian cohort, and the alleles found in KG-1 cells, calcitriol treatment increased total HLA-DR for HTCs expressing the DRB1*15 allele (PGF cell, Figure 5.4). There also was an increase in the total HLA-DR also observed in case of HTC expressing the DRB1*13 allele (WDV cell, Figure 5.4). Ramagopalan et al. (2009), had reported increased DRB1*15 gene transcription in PGF cells after treatment with vitamin D and increased protein expression of the same magnitude as observed here. They also reported no such effect on HTCs expressing the DRB1*07 allele, which was also reproduced in this work, although the cell lines used were different (DBB vs. MANN in this chapter). It was reassuring to reproduce similar effects as reported earlier. In the other HTCs, no effect of biologically active vitamin D was detectable (Figure 5.4).

The magnitude of increase in the HLA-DR expression observed in PGF and WDV cells was between 25-50 %, and its biological significance might be questionable. The PGF cells, homozygous for HLA-DRB1*15, however, express an alternate β-chain gene, DRB5 (Andersson et al., Horton et al., 2008) at a higher level, whereas the DRB1*15 gene product

is in the minority, at the mRNA and protein level. As reported earlier by Ramagopalan et al. (2009), vitamin D interacts on a VDRE in the HLA-DRB1*1501 promoter to enhance its transcription. That the total HLA-DR expression increases by upto 50 % (in PGF cells) may all be attributed to DRB1,whereas the expression of the DRB5 could remain constant. In this case, the increase could be much bigger than 50 % for the DRB1 gene product. The increase in the expression of HLA-DR after vitamin D treatment could be important in the particular genetic variant DRB1*15:01. Further examination of gene variant is described in Chapter 6.

In addition, RA increased total HLA-DR in MANN cells which is homozygous for the DRB1*07 allele (Figure 5.4). The increase may be due to transactivation of RARE, as observed in the PGF cells, but more work is required before definite conclusions can be drawn.

No effects of either vitamin D or RA on the remaining cell lines were observed in this study. This highlighted the need for further controls to test whether these cell lines are vitamin D responsive using other criteria, such as CD38 expression (Ramagopalan et al., 2010). Preliminary findings (RB et al., unpublished) show an increase in CD38 expression after 48 hours of vitamin D treatment in HOM-2 and JBUSH HTCs, in which HLA-DR expression was unresponsive. PGF cells included as a positive control also showed increased CD38 expression under these conditions. Although these controls need to be extended to the full HTC panel, so far no HTCs have been found to be unresponsive to vitamin D.

5.4.2 Competition for the binding of RXR receptor

The effect of vitamin D on the expression of HLA-DR depended on the interaction with RA. In those HTCs in which vitamin D increased the expression of HLA-DR (PGF, WDV), that effect was abolished by the addition of RA. Conversely, in MANN cells the modest effect of RA on HLA-DR expression was lost with the addition of vitamin D. One reason for this non-

additive effect may be because VDR and RAR compete for their shared binding partner, RXR (Bastie et al., 2004). The common ability for RXR to bind to both VDR and RAR can lead to the possibility of cross-talk within their response elements (Tavera-Mendoza et al., 2006). This would explain why the combination treatment did not show the effects of individual treatment, suggesting that there is mutual interaction between the two pathways, such that activation of one pathway stops the other pathway from up-regulating HLA-DR expression in some way.

5.4.3 Protective effect of vitamin D in auto-immunity

The presence of a functional VDRE in the promoter region of HLA-DRB1*15 has been reported (Ramagopalan et al., 2009). In addition, the expression of HLA-DRB1*15 increased on adding the biologically active vitamin D both in this study and the study by Ramagopalan et al. (2009), confirming a functional link between this important genetic risk factor and the environmental factor, vitamin D. This suggests that vitamin D deficiency could lead to lower HLA-DRB1*15 expression and subsequently lack of deletion of autoreactive T cells, which could increase the risk of autoimmune disease. However, HLA DRB1*15 is not the only allele associated with MS. In Sardinia, where the MS prevalence is also high and HLA DRB1*15 is a rare allele, the HLA alleles associated with MS are DRB1*04:05 and DRB1*16:01 (Lampis et al., 2000, Cocco et al., 2013). VDREs were found in close proximity to several examined HLA-DRB1 haplotypes, but there was no consistent HLA-DR expression increase when adding biologically active vitamin D (Cocco et al., 2012). So even if the sequence motif that defines VDREs is conserved, in a highly polymorphic gene like MHC (HLA), there is individual variation such that some alleles may have functional VDREs and others have mutant VDREs. Nonetheless, in individuals harbouring the DRB1*15, allele the regulation of vitamin D could be an important mechanism that contributes to the balance

between tolerance and auto-immunity. Thus, vitamin D might play a protective role against autoimmune disease like MS in populations expressing a particular allele. It is difficult to rule it out, even though the effects are not impressive (35-50% increase). However, it also has to be considered that vitamin D can protect from auto-immunity independent from this gene environment interactions.

Interestingly, a study found a functional VDREs in the promoter region of the HLA-DRB1*03:01 allele in a population of patients from North India (Israni et al., 2009). The patients were screened for Type 1 diabetes, an autoimmune disease. The authors reported an increase in HLA DR levels, around 1.2 fold, on treatment with vitamin D in the homozygous B-lymphoblastoid cells. They also speculate that in conditions of low vitamin D levels, the expression of HLA DRB1*03:01 is insufficient to reach the threshold of thymic deletion, similarly to that hypothesized in MS. When COX cells containing HLA DRB1*03:01 were used in the present study, no such increase was observed when treated with calcitriol. Israni et al. (2009) used VAVY and DUCAF B-lymphoblastoid cells, which are different from the ones used in the present study. Sometimes promoter polymorphism does not track closely with structural polymorphism, and so the choice of cell line does matter. A significant difference between both studies was the concentration of calcitriol used. Israni et al. (2009) used 100 nM calcitriol, whereas this study was performed using 10 nM calcitriol. The higher concentration may be un-physiological and cause off-target effects, including apoptosis. Hence, a careful dose response needs to be performed before considering the cells un-responsive towards vitamin D and RA.

5.4.4 Suppressive effect of RA and vitamin D co-treatment on HLA DR in KG-1 cells.

Unlike the EBV transformed B cell lines, KG-1 cells have more active turnover of the HLA-DR molecules, suggesting post-translational effects of vitamin D and RA might be observed. Indeed, there was a reduction in the expression of total HLA-DR on combination treatment of vitamin D and RA. On the other hand, the individual agents had no effect on the expression of HLA-DR. In EK and JBUSH cells, which are haplotype matched to the DRB1 alleles in KG-1, there was no effect of vitamin D and a variable effect of RA on the expression of HLA-DR molecules.

Calcitriol is a ligand for VDR, which in its active state forms heterodimers with RXRs (Haussler et al., 1997). After ligation, VDR and RXRs undergo conformational changes that induce binding to specific sequences in the promoter regions of target genes (Aranda and Pascual, 2001, Janik et al., 2017). Interaction with the general transcription machinery is essential to initiate target gene transcription. In KG-1 cells this plays out differently than in HTCs, and one possible reason could be because cell line specific differences in the handling of the HLA-DR molecules post transcriptionally or post translationally. There are examples of genes, such as interleukin 2 (IL 2), which are repressed by vitamin D via direct transcriptional repression (Alroy et al., 1995, Issa et al., 1998) but there is no evidence of such thing happening to VDRE genes.

However, the most probable possibility is that the combination of vitamin D and RA for some unknown reason changes the differentiation of KG-1 cells. KG-1 cells may degrade HLA-DR molecules faster under the influence of treatment with vitamin D and RA, or co-treatment may lowers the gene transcription of HLA-DR proteins in KG-1 cells. Thus, the reduction in the expression of HLA-DR in KG-1 cells on treatment with vitamin D and RA could also be

either transcriptional or post-translational. These possibilities are not mutually exclusive, and hence further studies are required.

A technical limitation of the study is that a low level of vitamin D may be present at baseline. The two media preparations used in the experiments contained no vitamin D. Fetal bovine serum (FBS) may contain some vitamin D, but at pharmacological dose it was possible to see effects on HLA-DR expression, consistent with previous literature (Ramagopalan et al., 2009, Israni et al., 2009). In some cell lines, a small effect of vitamin D might be observed by the background stimulation from residual vitamin D. This might be important for the cells where no effect has been observed. In future, charcoal-stripped FBS could be used to see any minor effects (Dembinski et al., 1985, Dang and Lowik, 2005).

This study does reproduce the effects of vitamin D on the phenotypic expression of HLA-DR, which another group has attributed to transcription (Ramagopalan et al., 2009) and the work extends to other HTCs corresponding to the common alleles found across the UK (White British/ Irish) population. This is the only study to have looked at the combined effects of vitamin D and RA. In the myeloid KG-1 cells, vitamin D alone had no effect on the expression of HLA-DR but the combination with RA reduced the expression of HLA-DR. There was no consistent increase in the HLA-DR expression in HTCs, other than PGF and WDV, on treatment with vitamin D, suggesting that there is allele specificity most probably via VDRE. In contrast, in DRB1*07 HTC, MANN, RA alone increases the expression of HLA-DR molecules. Lastly, the effect of vitamin D is abolished on addition of RA and vice versa probably because of the competition between activated VDR and RAR for the shared RXR subunit.

If more than one gene variant is present, then it is not clear whether any effect is specific to either variant or shared. Therefore, there is a need to be able to track them separately. This

may be especially important for the DRB1*15:01 haplotype (MS risk allele), given that the abundance of the DRB5 gene product is known, at least in B lymphoblastoid cells, to be higher than DRB1 gene product (Horton et al., 2008). Thus, the DRB3/4/5 gene loci have to be considered and evaluated separately, and an approach to this will be provided in the Chapter 6.

Chapter 6: Quantifying changes in HLA-DR allelic composition using stable isotopes and mass spectrometry

6.1 Abstract

Of the MHC II genes, HLA-DRB1, which encodes the β chain of the HLA-DR molecule, is the most polymorphic. HLA genes exhibit codominant expression of the maternally and paternally inherited alleles and gene variation. The codominant expression of these alleles is functionally important, but how it is regulated by external factors is not fully understood because of difficulties in its measurement. Here, a stable isotope and mass spectrometry approach was used to quantify changes in the relative amounts of co-expressed HLA-DR allelic and gene variants in response to vitamin D and RA. As a model system, KG-1 cells were treated for up to 72 hours with bio-active vitamin D3 (10 nM), RA (1 μM), both, or vehicle control (DMSO). As a quantitative standard, KG-1 cells were labelled with all-[^{13}C]-Arg/Lys SILAC media, and were mixed 1:1 with cell pellets from each culture condition. DRβ was isolated by immunoprecipitation and SDS-PAGE and SILAC ratios determined by Orbitrap LC-MS after tryptic digestion. This approach reliably detected subtle effects of different culture media and RA on the contribution of the DRB3 gene product to the total DR β chain pool. This highlights the sensitivity of the SILAC approach. However, neither vitamin D nor RA changed the mix of DRB1 alleles. Alternatively, SILAC standards were prepared from HTCs expressing only one of the two DRB1 alleles expressed in KG-1 cells, expecting to obtain information about the DRB1 allelic composition from differences in SILAC ratios between shared and allele specific peptides. However, these differences were too small to allow reliable estimates of allelic composition. Mathematical analysis indicated that for optimal quantification of allelic composition, the SILAC standard must be matched to

the unknown for total DR content. The results provide proof of principle that this approach can quantify changes in DR β allelic composition and informs the design of experimental strategies for future studies in primary antigen presenting cells.

6.2 Introduction

The overall objective of this chapter is to quantify the effects of vitamin D and RA (alone or combined) on the co-dominant expression of HLA-DR proteins, using stable isotopes and mass spectrometry. This chapter also aimed to devise strategies for measuring the effect of vitamin D and/or RA in primary APCs from healthy donors and patients with DRB1-linked autoimmune diseases like MS.

6.2.1 Variations in HLA-DRB genes

As explained in Chapter 1, section 1.3.4, DRB genes, which encode the HLA-DR β, chain are highly polymorphic, existing in hundreds of variants in the human population (Reche and Reinherz, 2003). All haplotypes have one major DRB locus, DRB1. In addition, many haplotypes have an additional, closely linked locus, which encodes an alternate DR β chain polypeptide, DRB3/4/5 (Andersson et al., 1998). Thus, any one individual human can produce between two and four different variant DR molecules, due to the genetic variation. These variants are difficult to distinguish in the experiments normally used to quantify the amounts of HLA-DR molecules, but this is important because HLA-DR variants may respond differently to vitamin D, as seen from the results from Chapter 5. It is still unknown how environmental factors such as vitamin D and RA influence the allelic composition of HLA-DR, as well as the relative expression of gene products of HLA-DRB1 and any gene variants (DRB3/4/5). Antibody-based approaches for quantifying allelic composition are potentially biased by the antibodies, conformational preferences (Woolley et al., 2015), so there was a need to develop unbiased methods for quantifying DRB allelic composition in heterozygous APCs and their responsiveness to environmental factors.

6.2.2 Proteomics

The term proteome refers to the complete set of proteins expressed in cells or tissue of an organism at a given time (Wilkins et al., 1996, Garrels, 2001). Accordingly, proteomics is used to describe the methods used to study proteomes (Clark and Pazdernik, 2013). These methods include chromatographic and electrophoretic techniques for protein or peptide fractionation, mass spectrometry for their identification, and the use of computational methods to assist the complicated data analysis (Godovac-Zimmermann and Brown, 2001).

In order to interpret the biological phenomena a quantitative analysis is required. In proteomics, quantification can be absolute or relative (Bantscheff et al., 2007). Within quantitative proteomics, relative quantification is much more commonly used to compare protein levels between two or more different biological conditions. Relative quantification methods used in proteomics studies can be divided in two main categories, namely gel based quantification and mass spectrometry based quantification (Ong and Mann, 2005). Different relative quantification approaches are depicted in Figure 6.1.

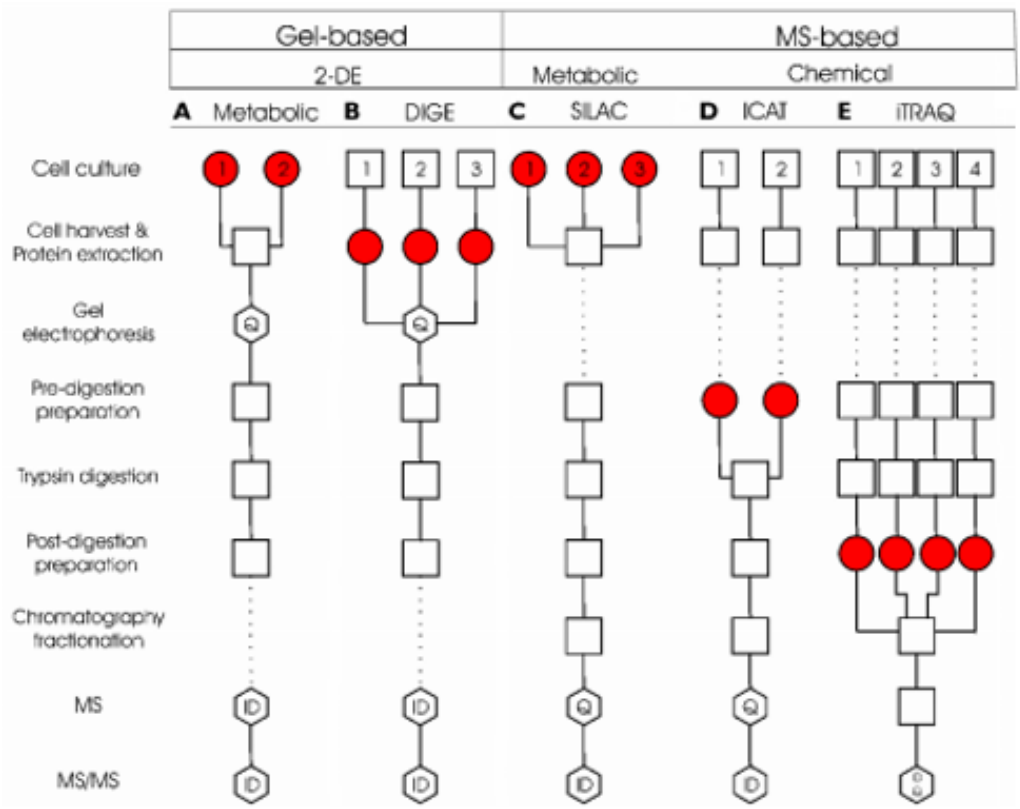

Figure 6.1 A flow-chart of different stages in quantitative proteomics experiments: A) Metabolic labeling, B) DIGE- Difference Gel Electrophoresis, C) SILAC Stable Isotope Labelling of Amino-acid in Cultures, D) ICAT Isotope-Coded Affinity Tags and E) iTRAQ Isobaric Tags for Relative and Absolute Quantification Methods. A and B present gel-based methods, while C, D and E present mass spectrometry based methods. Stable isotopes are incorporated in the mass spectrometry based methods metabolically (C), or chemically (D, E). Different symbols and solid lines in the figure indicate the stages performed in the method, while the stages marked with dashed lines are not necessary in the method. Red circles describe the labelling stage, and hexagons with id and/or q indicate the identification and quantification stages, respectively. Figure adapted from Bantscheff et al., (2007).

From the variety of options available, as set out in Figure 6.1, the SILAC approach seemed well suited to our problem. Even though LCMS is capable of quantifying peptides of interest with accuracy and precision, its dose response to different tryptic peptides from the same protein varies, for two main reasons: first, the efficiency of tryptic digestion may vary between samples; secondly, different peptides vary in their ionisation efficiency (Mann, 2006). In the SILAC approach for quantification, the addition of an internal standard to the

experimental data ensures any variation that is technical can be corrected for, because it will affect both the internal standard and the unknown. SILAC does not require any changes to the routine tissue culture method in practice, the heavy amino acids have no influence on cellular metabolism and the labelling strategy is universal throughout the protein; therefore, several peptides can be used for quantification (Ong and Mann, 2007b, Chokkathukalam et al., 2014). This takes out the problem of variability and downstream processing that some of the other methods suffer. Additionally, the advantage of labelling lysine and arginine is that all tryptic cleavage products are labelled (Gan et al., 2007). Hence metabolic labelling, which allows protein labelling at the time of protein synthesis, presents a valuable strategy for quantitative proteomics.

6.2.3 SILAC experiment

SILAC is a relative quantification method used for the proteomic analysis of cell lines to compare the expression levels of proteins between two or more samples (Harsha et al., 2008). This method was developed to analyse complex proteomes in cell culture by Mann and Ong (Ong et al., 2002, Ong and Mann, 2007b). In SILAC, cells are cultured either in a normal medium (light) or in a medium containing ^{13}C-labelled arginine and lysine (heavy). Generally, cells grown in heavy media are supplemented with dialysed foetal bovine serum (FBS) instead of normal FBS to ensure there is no contamination from free amino acids or peptides present in normal FBS (Ong and Mann, 2006). Samples are prepared from cells cultured in both light and heavy media and mixed in a 1:1 ratio at a very early stage of the experiment, such that both samples are treated identically in subsequent steps, ensuring that the abundance ratios are maintained throughout and are not affected by any experimental errors. The sample is then prepared for mass spectrometry analysis (Ong and Mann, 2006). The light and heavy labelled peptides ions are chemically identical but exhibit distinctively

different mass spectra (Hoedt et al., 2014). The basic workflow of a proteomic experiment using SILAC is depicted in Figure 6.2.

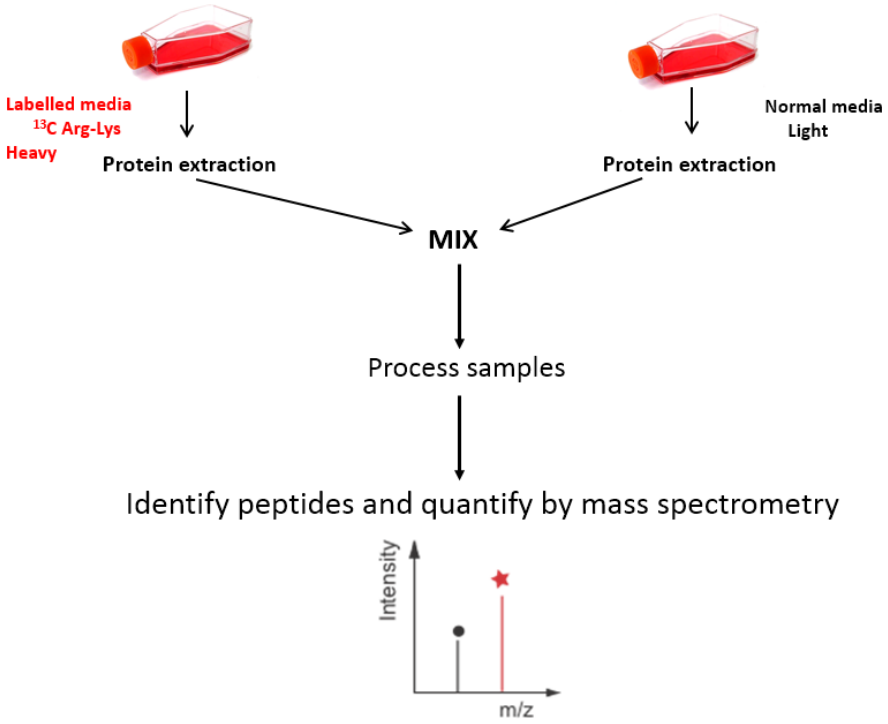

Figure 6.2 General workflow for SILAC experiment. The workflow illustrates the overview of SILAC for relative quantification in cell culture system.

6.2.4 SILAC approach and experimental strategies

KG-1 cells were chosen as a model cell line because is heterozygous for HLA-DR, having the DRB1*11, *14, DRB3*02 alleles (Ning et al., 2011) and has turnover of the HLA-DR comparable to physiological APCs (As discussed in Chapter 3 from the comparable Pep A effects on MoDCs). There will be three different strategies used for the quantification of the HLA-DR admixture.

6.2.4.1 SILAC analytics in KG-1 cell

The first experimental aim was to develop analytics and establish proof of feasibility. A SILAC approach was used as depicted in Figure 6.2, where SILAC labelled KG-1 cells were

mixed with unlabelled KG-1 cells following protein extraction. Mixed samples were immuno-precipitated with the L243 monoclonal antibody, which binds the conserved α chain of assembled DR αβ dimers. Following SDS-PAGE separation, the mixed β chains were excised, digested with trypsin, and resolved by mass spectrometry. If light and heavy samples are cultured identically, all peptides present are expected to exhibit the same L: H ratio. This strategy helped in establishing the protocols for the other experiments.

6.2.4.2 Relative quantification with SILAC

The standard SILAC approach, as depicted in Figure 6.2, measures changes with respect to controls when quantified by use of SILAC labelled control samples as an internal standard. This approach was used to determine the effect of vitamin D, RA, or both on the individual alleles present in the KG-1 cells. SILAC labelled KG-1 cells were used as control samples whereas un-labelled KG-1 cells were treated either with vitamin D, RA, or both and used as unknowns. The workflow for this experiment is depicted in Figure 6.3. This experiment quantifies changes from baseline in the relative expression of allelic or gene variants in the KG-1 cell line. This helped to determine whether the reduction of total DR on treatment with vitamin D and RA (as observed in Chapter 5, Figure 5.6) is general or selective for a particular allele.

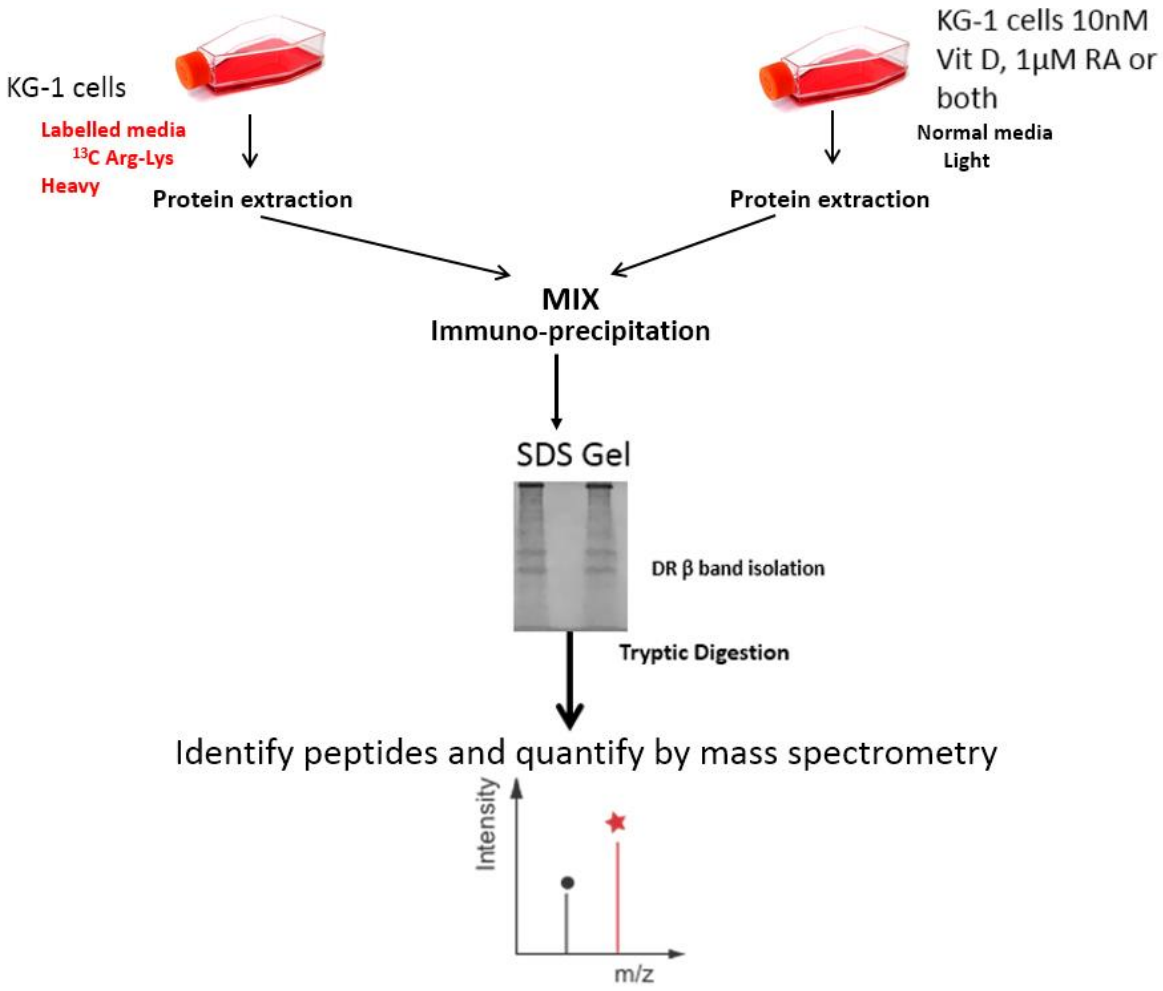

Figure 6.3 SILAC workflow for relative quantification from baseline. For relative quantification, SILAC labelled KG-1 cells were used as standards, and unlabelled KG-1 cells treated with vitamin D, RA, or both were used as unknowns and mixed in 1:1 ratio following protein extraction. Mixed samples were immuno-precipitated and following SDS-PAGE separation, the mixed β chains were excised, digested with trypsin, and resolved by mass spectrometry.

6.2.4.3 Quantification of HLA-DRB1 alleles using SILAC

In order to quantify the relative admixture of different HLA-DR allelic variants, the general SILAC approach was modified. HLA-DR variants share some tryptic fragments but differ in other tryptic fragments as a result of allelic polymorphism. The key way of quantifying the allelic mix involves the use of a labelled reference preparation containing only one of the two allelic forms present in a heterozygous sample. If this is done, allele-specific and shared

peptides will differ in their admixtures of heavy reference peptides, depending on the abundance of the second allele in the test sample.Hence homozygous typing cells (HTCs) which are monoalleleic for the DR expression were used as a reference cell line. . The SILAC strategy is depicted in Figure 6.4

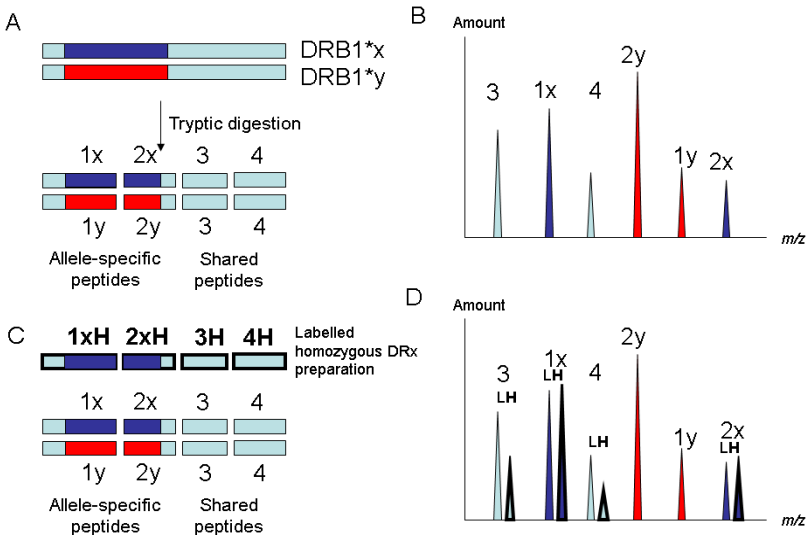

Figure 6.4 Experimental design for quantitative measurements of co-dominant DR protein expression. (A) Tryptic digestion of a mixture of two co-expressed allelic variants yields shared as well as allele-specific peptides. (B) The corresponding peptide mass spectrum does not, in practice, reflect the relative amounts of the two alleles, because of variation in the efficiency with which different peptides are released by trypsin and ionised in the mass spectrometer. (C) If an isotopically labelled (Heavy) variant of ONE of the alleles is added, the relative admixture of the two alleles can be determined by the relative amounts of heavy and light species in the mass spectrum (D). In the example, the heavy reference allele and the two unlabelled alleles are present in equimolar amounts, so that the measured L/H ratio is 1:1 for allele-specific and 2:1 for shared peptides (figure obtained from MS society project proposal by Dr Busch).

In order to quantify the DRB1 allelic composition of KG-1 cells, protein extracts from un-labelled KG-1 cells (treated with vitamin D, RA, or both) were mixed with labelled extracts of EK and JBUSH (HTCs for DRB1*14 and 11 respectively). Mixed samples were immuno-precipitated with anti-DR antibody (L243) and resolved by SDS-PAGE. Following SDS-PAGE, the mixed β chains were excised, digested with trypsin, and resolved by mass

spectrometry. HLA-DR peptide ions were identified by tandem mass spectrometry, and the relative proportions of labelled reference and unlabelled test peaks were quantified to estimate the mixture of DR alloforms present in the unlabelled test sample, as depicted schematically in Figure 6.4. Usually, more than one allele-specific and more than one shared peptide were detected, which allowed measurement error to be estimated. This approach, if successful, could also be used to study primary APCs without the use for bespoke autologous SILAC standards. So in order to inform the design of experiment with primary cells, it was necessary to evaluate the different ways of quantifying either changes in allelic composition from base line or direct quantification of allelic composition itself.

6.3 Method

The procedure for generating labelled standards and performing mass spectrometry is described in Chapter 2, section 2.2.5. This section focuses on calculations to determine the allelic mix within heterozygous cells for the strategy described in section 6.1.4.3. SILAC ratios should be an accurate reflection of the molar ratios between heavy and light peptides and assuming that the molar amounts need to add up in theory and on that basis the following formula has been derived. The objective here was to derive from the experimental data about measured SILAC ratios an estimate of the contribution of an allele that is shared with a homozygous typing cell line mixed to the total DRB1 pool.

Consider a SILAC experiment in which the heavy labelled standard expresses one of two DRB1 alleles, which we will call A and B. DRB1 alleles will have shared peptides derived from their conserved domains and allele specific peptides coming mostly from their peptide binding grooves. Let the suffix sh represent shared peptide and the subscript A, refer to the allele that is shared between HTCs and unknown heterozygous (here, KG-1). Allele B is the non-shared allele, which is only present in the unknown heterozygote, and for which no direct calculations be made from the SILAC ratios.

$$H\ sh = H_A$$

$$L\ sh = L_A + L_B \qquad (1)$$

Where H stands for the amount in moles of the heavy protein and L stands for light.

The molarity of A specific peptides is aL sh while for B specific peptides it is (1-a) L sh, in order to add up to 100%. So,

$$L_A = a\ L_{sh} \quad \& \quad L_B = (1\text{-}a)\ L_{sh}$$

Where a, is the mole fraction of allele A in the light sample

Thus replacing those value in equation 1

$$L_{sh} = a\ L_{sh} + (1\text{-}a)\ L_{sh}$$

The % light value for shared peptides, expressed in terms of the molar abundance of their source proteins. is defined as follows.

$$\%L_{SH} = \frac{L_{sh}}{(H_{sh} + L_{sh})}$$

Or equivalently,

$$\frac{1}{\%L_{SH}} = \frac{Lsh+Hsh}{Lsh}$$

$$\frac{1}{\%L_{SH}} = 1 + \frac{Hsh}{Lsh}$$

And then

$$\frac{1}{\%L_{SH}} - 1 = \frac{Hsh}{Lsh} \qquad (2)$$

Similarly % Light for allele-specific peptides (L_A) will be

$$\%L_A = \frac{L_A}{(H_A+L_A)}$$

And, expressing it in terms of a, the allelic contribution of A in the heterozygote,

$$\%L\mathrm{A} = \frac{a\mathrm{L}sh}{(\mathrm{H}sh + a\mathrm{L}sh)}$$

$$\frac{1}{\%L\mathrm{A}} = \frac{aLsh + Hsh}{aLsh}$$

$$\frac{1}{\%L\mathrm{A}} = 1 + \frac{Hsh}{aLsh}$$

$$\frac{1}{\%L\mathrm{A}} - 1 = \frac{Hsh}{aLsh}$$

$$a\left(\frac{1}{\%LA} - 1\right) = \frac{Hsh}{Lsh} \qquad (3)$$

The right hand side of equation (2) and (3) is identical hence,

$$a\left(\frac{1}{\%LA} - 1\right) = \frac{1}{\%L\mathrm{SH}} - 1$$

Hence

$$a = \frac{\left(\frac{1}{\%L\mathrm{SH}}\right) - 1}{\left(\frac{1}{\%LA}\right) - 1} \qquad (4)$$

Thus, based on this equation the allelic contribution for each allele in the heterozygous cells can be calculated from the % light values for shared and allele specific peptides obtained from mass spectrometry data.

6.4 Results

The overall objective of this chapter was to quantify changes in HLA-DR allelic composition in response to external stimuIilike vitamin D and or RA using stable isotope and mass spectrometry.

6.4.1 Characterisation of KG-1 cells, preparations of SILAC standards and method optimization

KG-1 cells were used as a model cell line since it is heterozygous for HLA-DR (Ning et al., 2011) and based on Pep A effects, has turnover of the HLA-DR comparable to physiological APCs (Appendix 7.1 and Chapter 3). SILAC labelling was performed in order to generate labelled standards.

6.4.1.1 KG-1 genotyping and qualitative analysis of peptide

HLA typing of KG-1 cells has previously been reported to only two digits as having DRB1*11, *14, DRB3*02 alleles (Ning et al., 2011), hence higher resolution HLA typing was done at the Anthony Nolan Research Institute. The higher resolution was helpful in picking the most appropriate homozygous typing cell lines (mono-allelic) as reference cells. The higher resolution HLA typing gave the following results: HLA-DRB1*11:01, 14:01/54, DRB3*02:02/12/28/29N/34/42/46/54.

Owing to the ambiguous results of genotyping, it was necessary to perform qualitative peptide analysis to compare the observed peptides to those expected from the HLA genotype of KG-1 cells. To address this, translated protein sequences of all the possible results for HLA-DRB1*14 (01/ 54) and DRB3*02 (02/12/28/34/42/46/54) were obtained from the IMGT/HLA database. DRB3*02:29N was not considered because it is a null allele. IMGT/HLA database (http://www.ebi.ac.uk/ipd/imgt/hla/) is a public database for the storage of sequences of the HLA system including the official nomenclature for genes and alleles

(Robinson et al., 2016). The predicted protein sequences were then subjected to *in-silico* tryptic digestion with Peptide Mass (http://web.expasy.org/peptidemass/) (Wilkins et al., 1997). The work flow has been depicted in Figure 6.5.

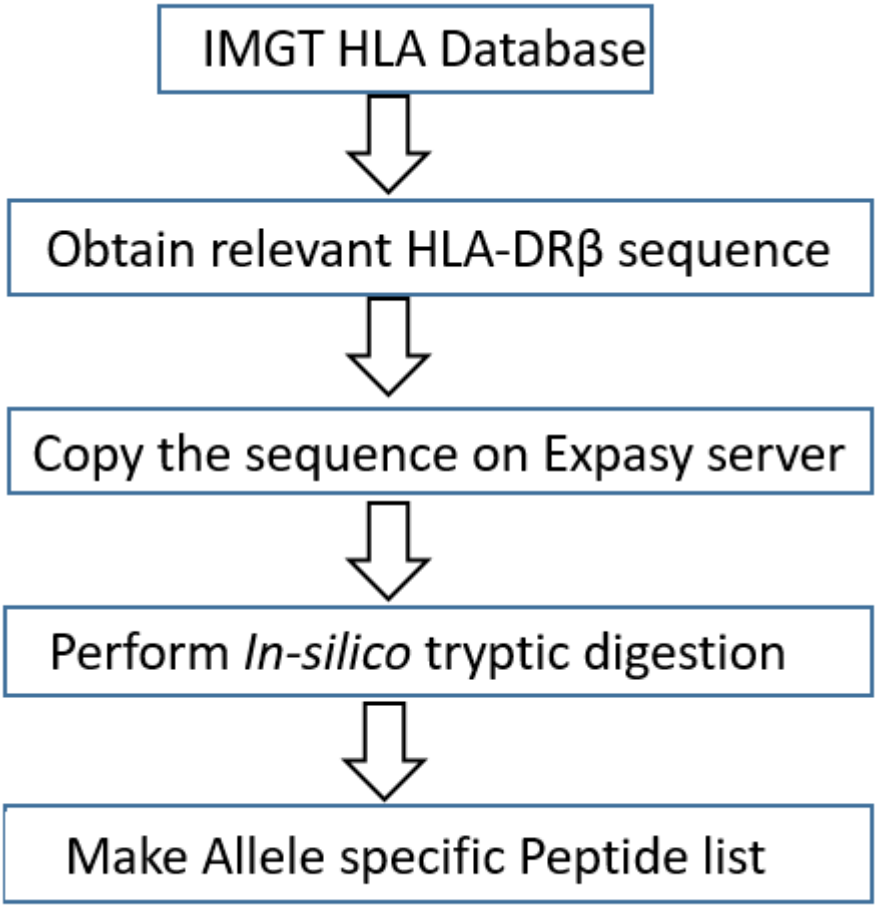

Figure 6.5 Flow chart for *in silico* tryptic digestion. The peptide sequences of the relevant HLA-DRβ) allele were obtained from the IMGT/HLA database (http://www.ebi.ac.uk/cgi-bin/ipd/imgt/hla), and were subjected to *in silico* tryptic digestion with Peptide_Mass (http://web.expasy.org/peptide_mass). A virtual digest was obtained. These virtual digests were used to identify the group of peptides that are specific for a particular allele or shared between the allele

With the help of the virtual digest, peptide list , representing each of the alleles obtained through genotyping, was made. This list was than matched with the peptides obtained after tryptic digestion of the KG-1 cells during the actual mass spectrometry to identify HLA typing of the KG-1 cells. The peptide list and the virtual digest gave the following: HLA-DRB1*11:01, HLA-DRB1*14:54 and HLA-DRB3*02:02 as the best matched HLA typing of the KG-1 cells. This is depicted schematically in Figure 6.6.

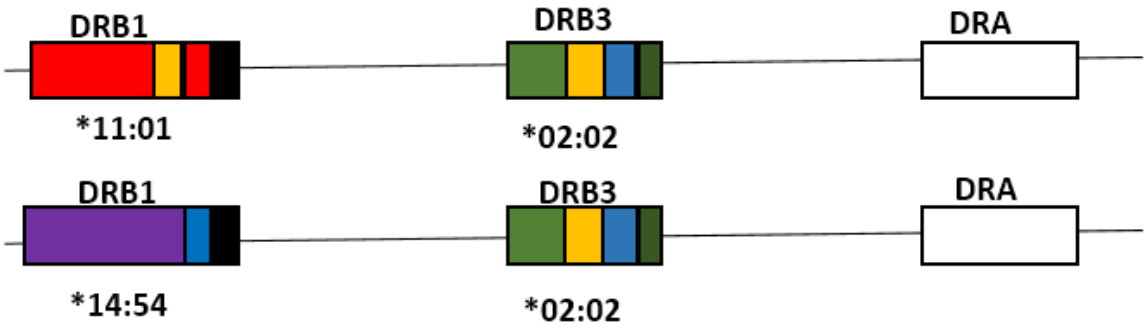

Figure 6.6 Mapping of shared and allele specific peptide sequence to the DRB genes in KG-1 cells. This is a schematic representation and do not show accurate distances between the loci. N.B one of the DRB3 allele could be null.

The virtual digests were also used to identify the subset of peptides that are specific for a particular HLA-DRB allele or shared between two or all three alleles. Such peptides were then selected from amongst the observed HLA-DR derived peptides and used for analysis. In total, 29 peptides were identified which are shown in Table 6.1. The list is colour-coded based on the schematic representation shown in Figure 6.7. Of the 29 peptides, eight peptides were unique to DRB1*11:01 (red), six peptides unique to DRB1*14:01 (purple) and seven peptides unique to DRB3*02:02 (green). There were five peptides that were shared between the two DRB1 alleles (DRB1*11:01 and DRB1*14:54) depicted in **black**. One peptide each was shared between DRB1*11:01 and DRB3*02:02 (yellow) and between DRB1*14:01 and

DRB3*02:02 (blue). There was one peptide which, according to virtual digests was shared between all three alleles, shown in maroon, but it was not detected in the actual experiment.

Table 6.1 List of allele specific and shared peptides in KG-1 cells

Peptide no.	Sequence	DRB1*11:01:01	DRB1*14:54	DRB3*02:02
1	WFRNGQEEK	x	x	x
2	FLEYSTSECHFFNGTER	x	x	
3	GHSGLQPR	x	x	
4	SGEVYTCQVEHPSVTSPLTVEWR	x	x	
5	VHPKVTVYPSK	x	x	
6	VTVYPSK	x	x	
7	HNYGVGESFTVQR	x		x
8	AAVDTYCR	x		
9	AVTELGRPDEEYWNSQK	x		
10	AVTELGRPDEEYWNSQKDFLEDR	x		
11	DFLEDRR	x		
12	FDSDVGEFR	x		
13	FLDRYFYNQEEYVR	x		
14	RAAVDTYCR	x		
15	YFYNQEEYVR	x		
16	FDSDVGEYR		x	x
17	AEVDTYCR		x	
18	AVTELGRPAAEHWNSQK		x	
19	FLDRYFHNQEEFVR		x	
20	HNYGVVESFTVQR		x	
21	RAEVDTYCR		x	
22	YFHNQEEFVR		x	
23	DLLEQKR			x
24	ELGRPDAEYWNSQK			x
25	ELGRPDAEYWNSQKDLLEQK			x
26	GQVDNYCR			x
27	HFHNQEEYAR			x
28	RVHPQVTVYPAK			x
29	VHPQVTVYPAK			x

6.4.1.2 Qualitative peptide analysis of HTCs

The mono-allelic standards, JBUSH (DRB1*11:01) and EK (DRB1*14:54) were selected based on the higher resolution genotyping and qualitative analysis of peptides in KG-1 cells. HLA-DR preparation for JBUSH and EK cells were also subjected to tryptic digestion, and the peptides obtained were matched with the translated cDNA sequences of the particular alleles present in the HTCs in order to facilitate the SILAC analysis. In both HTCs, a DRB3 gene was also present, but it was not considered for the SILAC analysis to quantify the allelic composition in the heterozygous KG-1 cells, since only the peptides coming from the shared allele are useful for this analysis. The list of informative peptides is shown in Table 6.2. Moreover, for of the HTCs, MASCOT search identified some peptides which were genetically not plausible. There was one example in JBUSH cells where two peptides (* marked, they are length variants) belonging to the DRB1*14 gene were identified, which should not be present. The reason for this mismatching is still not clear since analysis of the peptide peak did not indicate a false positive result. In this experiment, not all the peptides were found and blanks are shown where applicable.

Table 6.2 comparison of the peptides found across KG-1, JBUSH and EK cells.

Peptide no.	Sequence	KG-1 (DRB1*11:01, DRB1*14:54, DRB3*02:02)	JBUSH (DRB1*11:01, DRB3*02:01)	EK (DRB1*14:54, DRB3*02:02)
1	WFRNGQEEK			
2	FLEYSTSECHFFNGTER	x	x	x
3	GHSGLQPR	x	x	
4	SGEVYTCQVEHPSVTSPLTVEWR	x	x	x
5	VHPKVTVYPSK	x		
6	VTVYPSK	x	x	x
7	HNYGVGESFTVQR	x	x	x
8	AAVDTYCR	x	x	
9	AVTELGRPDEEYWNSQK	x	x	
10	AVTELGRPDEEYWNSQKDFLEDR	x		
11	DFLEDRR	x		
12	FDSDVGEFR	x	x	
13	FLDRYFYNQEEYVR	x		
14	RAAVDTYCR	x		
15	YFYNQEEYVR	x	x	
16	FDSDVGEYR	x	x	x
17	AEVDTYCR	x	*	x
18	AVTELGRPAAEHWNSQK			
19	FLDRYFHNQEEFVR	x		
20	HNYGVVESFTVQR	x		x
21	RAEVDTYCR	x	*	x
22	YFHNQEEFVR	x		x
23	DLLEQKR	x	x	
24	ELGRPDAEYWNSQK	x	x	x
25	ELGRPDAEYWNSQKDLLEQK			
26	GQVDNYCR	x	x	x
27	HFHNQEEYAR	x	x	x
28	RVHPQVTVYPAK			
29	VHPQVTVYPAK			

6.4.1.3 SILAC labelling of KG-1 cells

Since SILAC labelled IMDM media are not commonly used, bulk purchase of custom media would have been required, which was expensive. There are some published papers in which KG-1 cells have been grown in the RPMI media (Furley et al., 1986, Kojima et al., 1999, Gadeock et al., 2012). Hence, KG-1 cells were adapted to RPMI media before initiating SILAC labelling. Adaptation was monitored by regular cell counting and there was no obvious difference noticed in the growth rate. HLA-DR levels were compared in KG-1 cells grown in both IMDM and RPMI media and there was no substantial difference in HLA-DR expression between the cells grown in the two media, as shown in Figure 6.7.

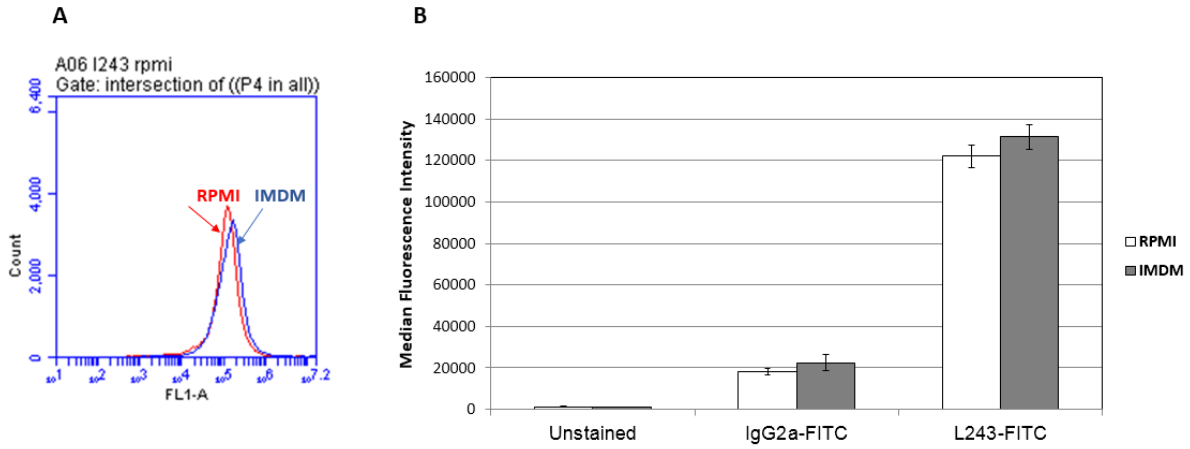

Figure 6.7 Effect of RPMI1640 media on HLA-DR expression in KG-1 cells. HLA-DR levels were compared between the KG-1 cells cultured in IMDM and adapted to RPMI media. Cells were fixed and permeabilized, stained with L243-FITC antibody, and analysed by flow cytometry. (A) Fluorescence histograms after staining with L243-FITC. (B) Staining, quantified by flow cytometry, was reported as median fluorescence intensities (MFI; mean +- SD of triplicate analysis). The result shows no effect on the DR levels when the KG-1 cells were switched from IMDM to RPMI media.

After successful adaptation to RPMI media, SILAC labelling of KG-1 cells was initiated. KG-1 cells were cultured in SILAC RPMI media containing all-[^{13}C] - Arginine and Lysine

supplemented with 20% dialysed FBS. Cells were cultured for a minimum of 5 doublings in order to allow complete labelling. During the course of the labelling, cell growth was monitored. SILAC labelled cells were growing more slowly than cells grown in unlabelled IMDM media, as shown in Figure 6.8. The slower growth kinetics can be attributed to the use of dialysed serum (MW < 10,000 kDa), which may be devoid of some growth factors.

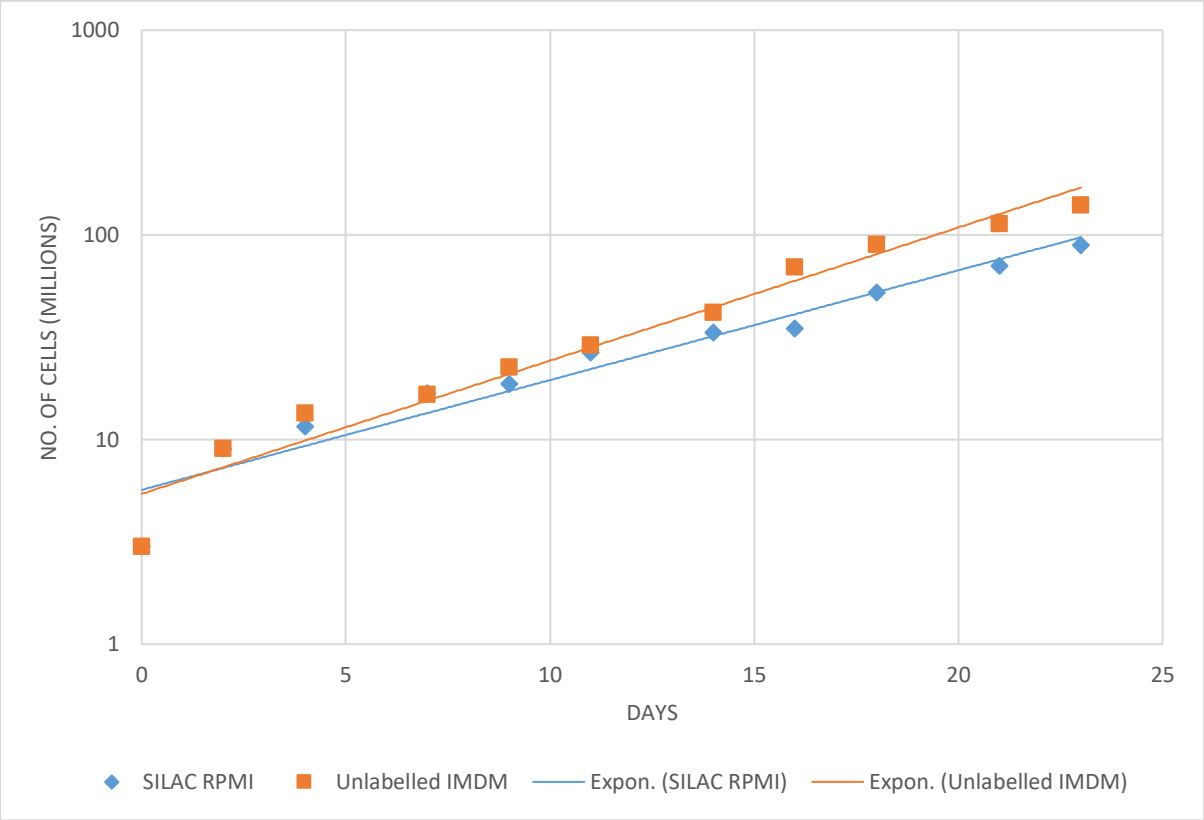

Figure 6.8 Growth Kinetics of KG-1 cells in SILAC labelled and IMDM unlabelled media. KG-1 cells were grown all-[^{13}C]-Arg/Lys media (SILAC RPMI media) containing dialysed (MW <10KDa) foetal bovine serum in order to label them. SILAC labelled cells grew more slowly than cells grown in unlabelled IMDM media. The dots in the graph represents count of cells on a particular day as if no cells had been discarded. The Y-axis is on a log scale.

The HLA-DR levels of KG-1 cells cultured in SILAC labelled RPMI media and unlabelled IMDM media were assessed by flow cytometry on fixed and permeabilised cells using FITC conjugated L243 antibody. As shown in Figure 6.9, the SILAC labelled KG-1 cells showed a

reduction in total HLA-DR levels by around 20-25% when compared with KG-1 cells cultured in unlabelled IMDM. This plus the slower growth rate may be due to the difference in growth factor supply between the two culture media. A *t* test, confirmed that the reduction in HLA-DR expression was statistically significant F (1, 1) = 484.83, p <0.001 (Appendix 6.1).

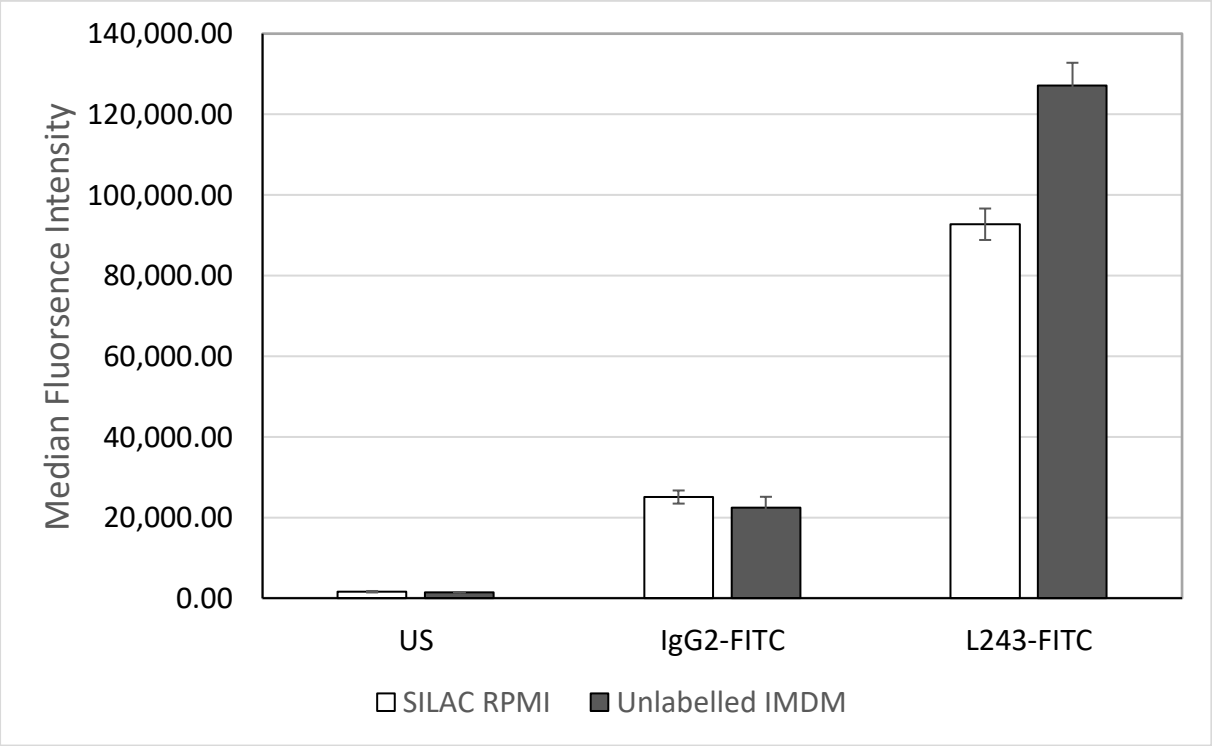

Figure 6.9 Reduction in total HLA-DR in SILAC labelled KG-1 cells. HLA-DR levels were compared between KG-1 cells grown in SILAC labelled RPMI media and unlabelled IMDM media by flow cytometry. Briefly cells were fixed and permeabilised stained with L243-FITC or isotype control IgG2-FITC or kept unstained (US) and analysed by flow cytometry. The graph shows the median fluorescence intensity (MFI; mean +- SD of triplicate analysis). Cells grown in SILAC RPMI expressed less HLA-DR than cells grown in IMDM. The reduction in total DR expression was seen in two independent repeats.

6.4.1.4 SILAC labelling of HTCs

Unlike KG-1 cells, HTCs (EK and JBUSH) were normally cultured in RPMI media containing 10% FBS for regular cell culture. So their SILAC labelling was straightforward and cells maintained healthy growth in the SILAC media containing 10% dialysed FBS with no detectable difference in the growth rate. Cells were cultured for a minimum of 5 doublings in order to allow nearly-complete labelling.

6.4.1.5 HLA-DRβ isolation and mass spectrometry

SILAC labelled standards (KG-1 cells and HTCs) and unlabelled test samples (KG-1 cells treated with vitamin D and/or RA, or left untreated, depending on the experimental strategy) were subjected to detergent extraction. Labelled and unlabelled samples were mixed mixtures were immuno-precipitated using L243 antibody and resolved by SDS-PAGE. The DR-β bands were then excised and sent to the Cambridge Centre for Proteomics for further analysis by mass spectrometry. Figure 6.10 (A) is a representative SDS-PAGE image showing DR-α and DR-β bands while (B) is the same gel following excision of α and β chain bands.

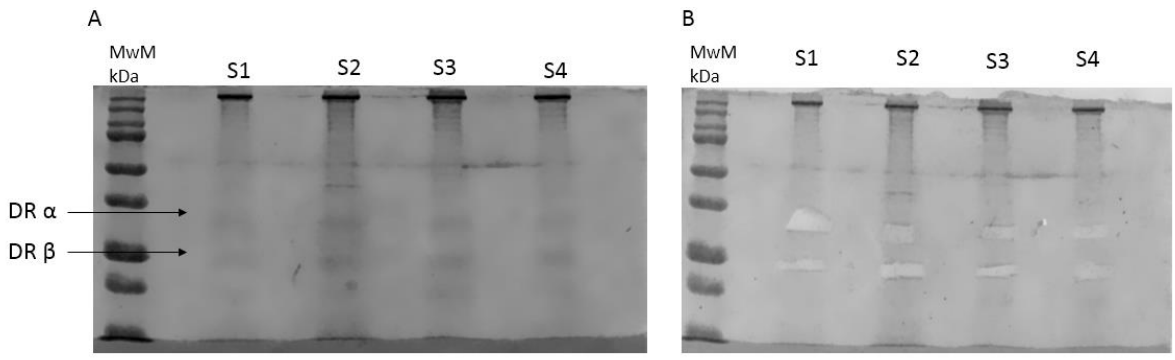

Figure 6.10 Isolation of DR α and β molecules from KG-1 cells. KG-1 cell extracts were immuno-precipitated with in-house prepared L243 mAb and protein A-sepharose. Samples were resolved on 12% acrylamide SDS-PAGE gels under non-reducing conditions and stained with Instant Blue. HLA-DR-α and β chains are indicated (A). The samples S1 and S2 were the fully labelled and unlabelled samples, respectively. In contrast, S3 and S4 were 1:1 mixtures of labelled and unlabelled samples. (B) Shows the excision of HLA DR α and β, which were stored at -80C until further analysis.

At Cambridge Centre for Proteomics, the excised DR β bands were analysed using Q Exactive™ Hybrid Quadrupole-Orbitrap (Thermo Fisher). Figure 6.11 shows representative mass spectra for the unlabelled, labelled and mixture of peptides specific for the three alleles present in the KG-1 cells.

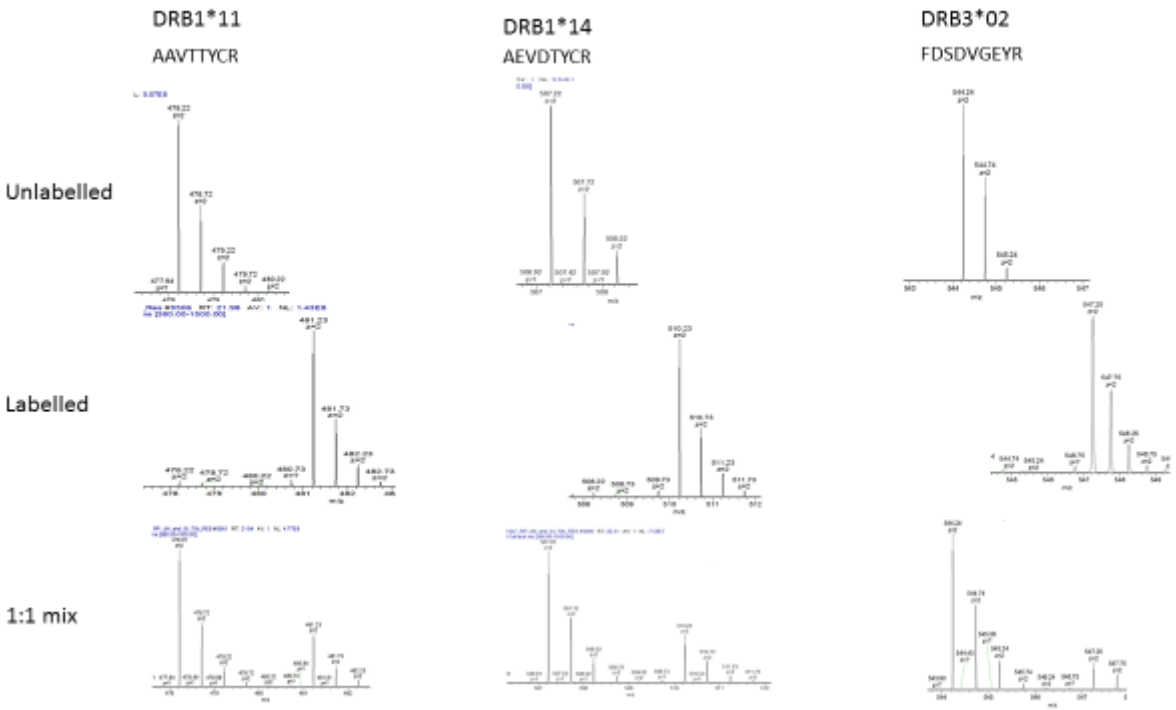

Figure 6.11 Representative mass spectra. The figure shows representative mass spectra for peptides from each of the alleles for labelled, unlabelled and 1:1 mix. There was a 6 Dalton mass shift for the peptides derived from the cells cultured in the SILAC media when compared to the unlabelled samples. These spectra samples were provided by Mike Deery from Cambridge Centre for Proteomics under collaborative arrangements.

6.4.1.6 Method optimization

For method optimization, the excised DR-β bands were analysed at two different *m/z* resolutions, 17K and 70K, using Q Exactive™ Hybrid Quadrupole-Orbitrap at the Cambridge Centre for Proteomics. Data analysis was performed using the output from two different software packages: MaxQuant (MQ) (Cox and Mann, 2008) and Proteome Discover (PD) (Välikangas et al., 2017). Next, I investigated which of the resolution settings and software packages provided the most robust quantification of the proportion of labelled peptides in the mixed samples. These comparisons are shown in Figure 6.12.

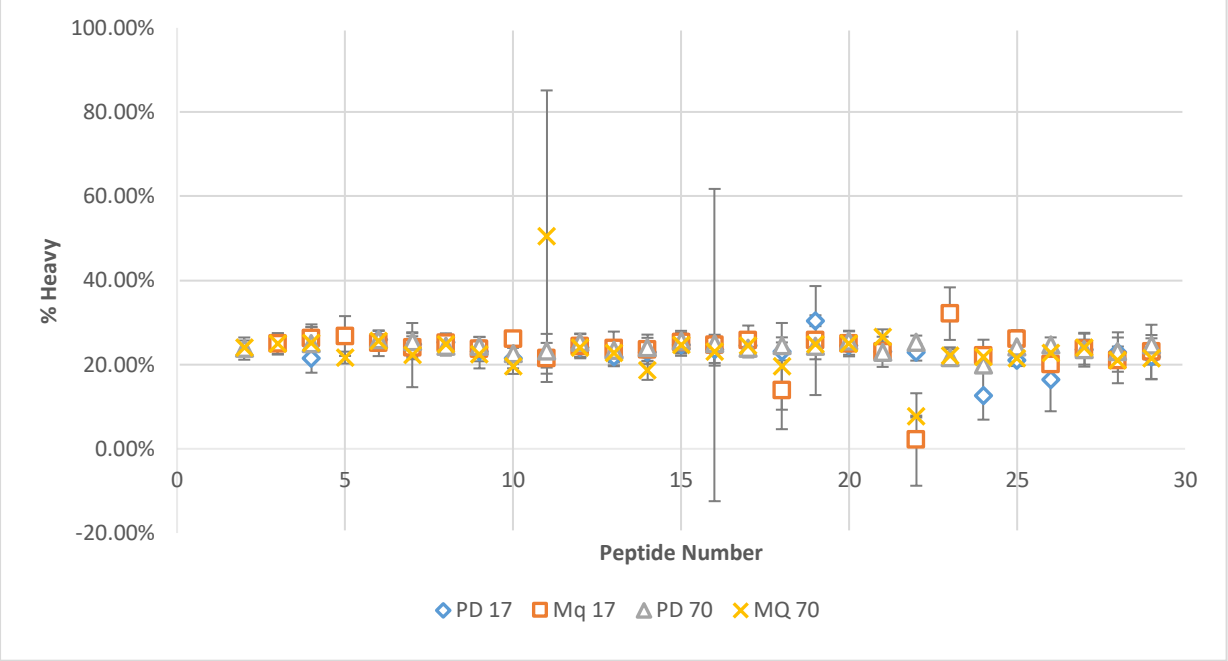

Figure 6.12 Comparison between 17K and 70K resolution and Proteome Discover and MaxQuant software. For method development SILAC, labelled and unlabelled KG-1 cells were mixed 1:1 by cell number. Protein extraction was carried out and DR β was isolated by IP with L243. The excised DR β band, after tryptic digestion, was analysed at two different *m/z* resolutions (17K and 70K) using Q Exactive™ Hybrid Quadrupole-Orbitrap. Post run, data analysis was performed using two different software packages, MaxQuant (MQ) and Proteome Discover (PD). In this figure, the X-axis represents the individual peptides obtained through LCMS post tryptic digest (numbered as in Table 6.1). Each dot represents the percentage of labelled peptides measured at the indicated m/z resolution, and analysed by the indicated software. The values represented here are means +- SD of quadruplicate analyses.

There was a difference in the number of peptides identified between the two *m/z* resolution settings. The higher-resolution (70K) analysis was able to identify 28 peptides, while at lower-resolution (17K) analysis, 20-22 peptides were identified. Both software packages were able to identify more peptides at higher resolution. But as seen from the graph the variability both between peptides and between samples analysed by PD was less than that for MQ. So, all the further samples were run at 70K *m/z* resolution and were analysed by PD. The 1:1 mixture (by cell count) between heavy and light samples failed to yield a % heavy ratio of 50%, as expected theoretically. This may be because of inaccuracy in the haemocytometer cell counts, differences in the protein content per cell in light and heavy media, or the lower HLA-DR expression in SILAC RPMI.

In order to assess the completion of labelling of the SILAC standards, % Heavy values were determined for all the SILAC labelled standards (KG-1, EK and JBUSH), using Proteome Discover software, as shown in Figure 6.13. The analysis showed that all the SILAC standards were labelled more than 99%.

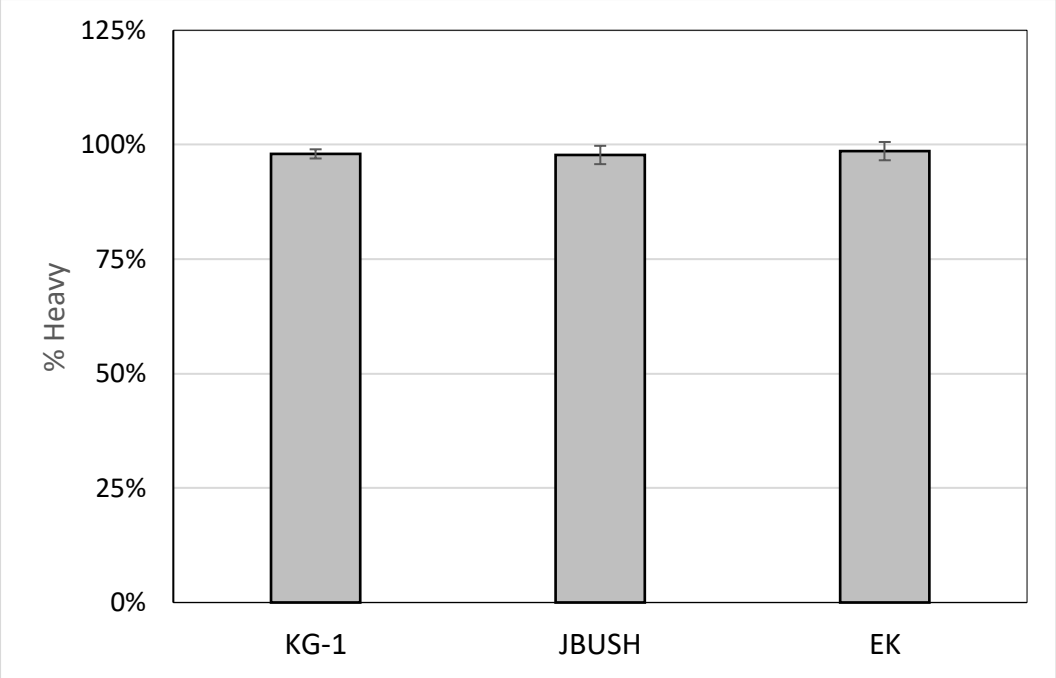

Figure 6.13 SILAC standards were labelled to nearby 100%. Bar graph of % heavy calculated based on the output of Proteome Discover after samples were run at 70K resolution in mass spectrometry. Each bar represents mean +- SD across all informative peptides observed following tryptic digestion by mass spectrometry. There were at least two SILAC standards for each cell line (KG-1 cells had four).

6.4.2 Effect of switching media in KG-1 cells.

In order to determine the effect of switching media on the DRB1 alleles, SILAC labelled KG-1 cells were mixed with unlabelled KG-1 cells grown in either RPMI or IMDM in 1:1 ratio by cell counts. Total protein extraction was performed using lysis buffer and were immunoprecipitated with monoclonal L-243 antibody and resolved by SDS-PAGE. DR β was excised and after tryptic digestion was run at 70K on the Q Exactive™ Hybrid Quadrupole-Orbitrap. Data analysis was performed using Proteome Discover software . Ideally, both culture media produce a similar co-dominant expression of the HLA-DR variants. The results shown in Figure 6.14 (A) represent KG-1 cells cultured in RPMI media mixed with SILAC

standard, whereas Figure 6.14 (B) represents KG-1 cells cultured in IMDM media mixed with SILAC standard.

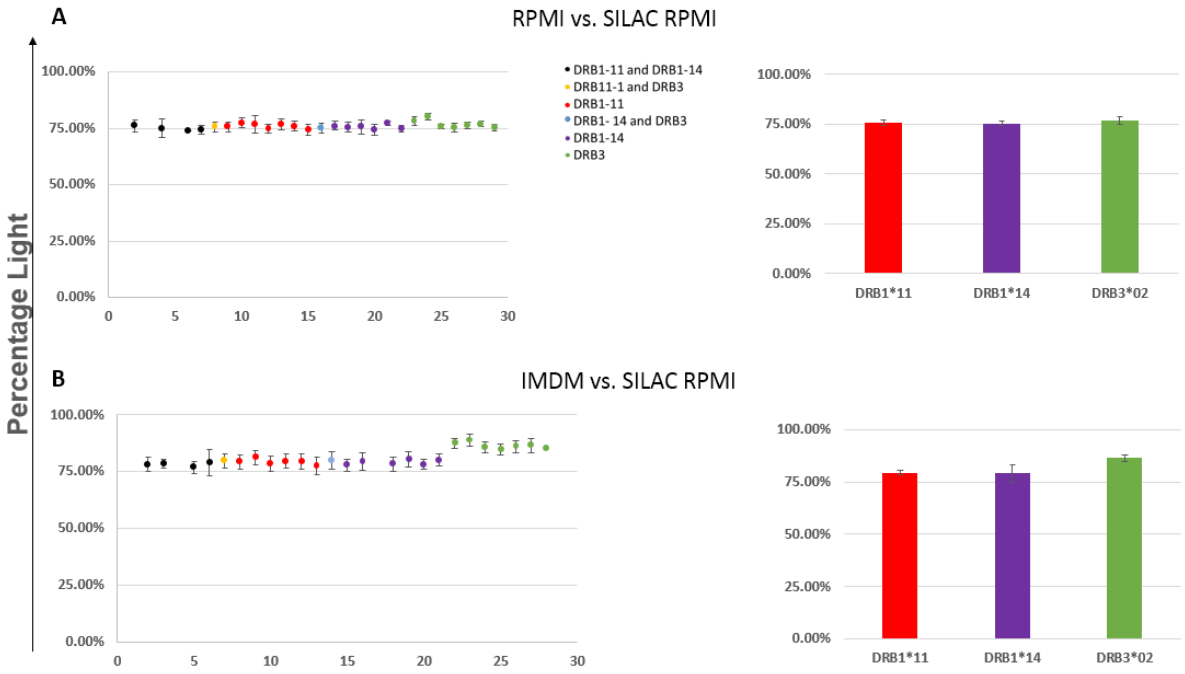

Figure 6.14 SILAC analytics in KG-1 cells. KG-1 cells were cultured in unlabelled RPMI (A) or IMDM (B) media with 20% FBS; extracts were mixed 1:1 (by cell count) with extracts from > 99% labelled KG-1 cells grown in ^{13}C-Arg/Lys RPMI with 20% dialysed FBS. DRβ was isolated by IP and SDS-PAGE, trypsinised, and heavy and light peptide mass clusters were quantified by mass spectrometry. Scatter plots show the mean % light values +/- SD (n=4) for individual DRβ peptides; the column graphs show the means +- SD for groups of peptides from the indicated individual alleles. The colour coding is as per Figure 6.7 and Table 6.1

As observed in Figure 6.14 (A), the SILAC ratios for all DR β chain peptides was the same when the SILAC labelled KG-1 cells were mixed in 1:1 ratio (by cell count) with unlabelled KG-1 cells adapted to RPMI media. All the peptides gave indistinguishable SILAC % light values. Surprisingly when KG-1 cells were grown in IMDM media, co-dominant expression was also altered. As observed in Figure 6.14 (B), there was a difference in the SILAC ratios

between DR-β1 and DR-β3 peptides when the SILAC labelled KG-1 cells were mixed in 1:1 ratio with unlabelled KG-1 cells cultured in IMDM media. The % light values differed systematically between DR-β1 and DR-β3 derived peptides, showing that the expression of the DRB3 gene product was selectively altered in IMDM. Two-way ANOVA revealed that there was a statistically significant difference in the HLA-DR expression between the two media conditions $F(1, 18) = 243.203$, $p < 0.001$ (Appendix 6.2). The Tukey's post-hoc test revealed that allele DRB3 is significantly different from both the DRB1 alleles in the IMDM condition (Appendix 6.2). Moreover, SILAC % light values for DRB1/DRB3 shared peptides were much closer to those for DRB1 than for DRB3 specific peptides. This suggests that, as expected, DRB1 gene products comprise the great majority of the total DR-β chain, though with only two B1/B3 shared peptides, quantification of this ratio was not reliable. Nevertheless, these results highlight the feasibility of using this SILAC approach (i.e., using autologous standards) to quantify subtle changes in DR beta chain composition depending on the nutrient status of the cells.

Another observation from these experiments was that the measured SILAC % light values were higher than the 50% expected value, similar to the low % H values in Figure 6.12. One contributing factor may be the reduction in total HLA-DR expression when cells were cultured in the SILAC labelled media (Figure 6.10), although this alone does not fully explain the increase in the % light ratio. There may also be a small contribution from the residual unlabelled material in the SILAC standard as a reason of how they were generated. Another possible explanation could be the technical issue of creating 1:1 mix due to inaccurate haemocytometer counts. As noticed earlier in Figure 6.8 and 6.9 there was a difference in the growth rate which may be associated with a difference in the total protein content per cell resulting in more % light DR molecules in the mix. In this experiment, the 1:1 mixture was based only on cell counts, but it seemed better to use protein concentration when normalising

the mixture, rather than cell counts. Hence, all the subsequent mixing was performed based on protein concentration.

6.4.3 Allele independent effect of Vitamin D and RA in KG-1 cells.

In order to determine the effect of vitamin D and/or RA on the DRβ chain composition, KG-1 cells were treated with vitamin D, RA, or both for up to 72 hours. As a vehicle control, DMSO matched to the total volume of treatment was used. After 72 hours of treatment, protein extraction was carried out from the KG-1 cells for each of the four conditions (i.e. DMSO, Vitamin D, RA, and RA + Vitamin D). SILAC labelled KG-1 cells were used as a labelled standard. Protein were extracted from the labelled standard, which was mixed in 1:1 ratio with protein extracted from unlabelled KG-1 cells under the four different conditions. In this experiment, normalisation (1:1 mixture) was based on protein content, which was determined by BCA assay. The 1:1 mixed protein extracts were then immuno-precipitated using L243 antibody and resolved by 12% non-reducing SDS PAGE. DR-β bands were then excised and sent to the Cambridge Centre for Proteomics for tryptic digestion and mass spectrometry analysis. SILAC ratios were calculated as % light with the help of Proteome Discover software . Combined treatment with vitamin D and RA synergistically lowered HLA-DR expression, as shown by both flow cytometry and SILAC in Figure 6.15 (A) (also in Chapter 5, section 5.2.2). Since the protein content was normalised, the overall SILAC ratios were closer to 50% in vehicle controls, and there was little change on treatment with either vitamin D or RA alone.

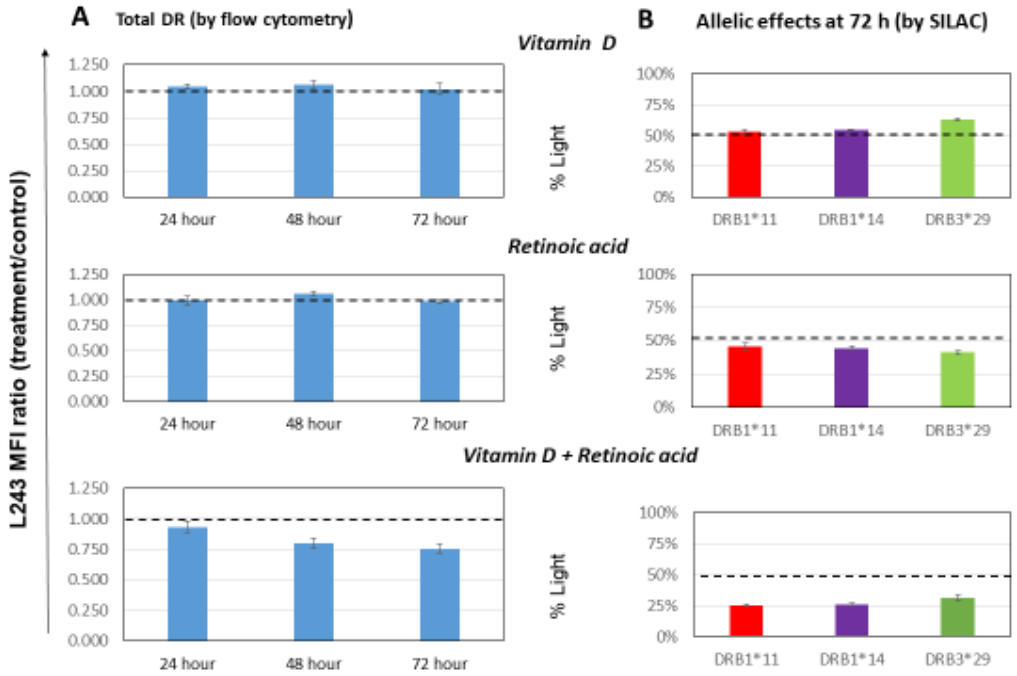

Figure 6.15 Allele independent effect of Vitamin D and RA on KG-1 cells. (A) shows the change in total HLA DR levels in KG-1 cells treated with Vitamin D and /or RA for up to 3 days, quantified by flow cytometry. Each bar represents the mean fold change in MFI, i.e. treatment divided by DMSO control (n=3). (B) KG-1 cultures (n=4) were treated with Vit-D and or RA for 72 hours in light media. Extracts were mixed 1:1 (by protein content) with SILAC labelled KG-1cells. Mean % light ratios of the allele-specific DR β peptide sets were quantified from the SILAC ratios obtained after LC-MS. The result indicates that the reduction of the total DR levels is irrespective of the DRB1 allele. The % light ratio has been calculated in this instance to emphasise the reduction in the DR levels. The colour coding is as per the Figure 6.6 and Table 6.1.

At baseline, as before (Figure 6.15 (B)), DRB3 specific peptides had a slightly higher % light value than that of the DRB1 derived peptides (Appendix 6.3). There was no systematic difference observed between the DRB1 allele specific peptides. The representation of DRB1*11 vs. DRB1*14 gene products was unaffected upon any of the combination treatments. In contrast, RA slightly diminished the contribution of DRB3 gene to total HLA-DR, but this was reversed when the cells were treated with both RA and vitamin D. This indicates that the relative expression of the DRB3 gene variants may be differentially affected by vitamin D and RA. Two-way ANOVA revealed that there is a statistically

significant effect of treatment, F (3, 36) = 873.473, p <0.001 (Appendix 6.4). Turkey's post-hoc test revealed that there is a reduction in the expression of HLA-DR on combined treatment of vitamin D and RA. Moreover there was statistically significant interaction between the alleles and culture conditions, F (6, 36) = 41.744, p <0.001 (Appendix 6.4). Tukey's post-hoc test revealed that the DRB3 values were significantly different from both the DRB1 alleles. The estimated marginal means plot showed that with RA, there was a selective reduction in the expression of DRB3 allele (Appendix 6.4). The effect of vitamin D and RA co-treatment on HLA-DR expression was more pronounced when measured by SILAC than in the flow cytometry experiment.

6.4.4 Quantification of HLA-DRB1 allelic contributions in KG-1 cells using mono-allelic SILAC standards

In order to quantify the HLA-DRB1 alleles in KG-1 cells, EK and JBUSH cells were used as SILAC labelled standards. EK and JBUSH cells are homozygous for the DRB1*14 and DRB1*11 alleles respectively, which are expressed in KG-1 cells. Both EK and JBUSH were cultured in in all-[^{13}C] - Arginine/ Lysine SILAC media for labelling. KG-1 cells were treated for 72 hours with 1 µM RA and /or 10 nm vitamin D. As a vehicle control, DMSO matched to the total volume of treatment was used. After 72 hours of treatment, protein extraction was carried out from the KG-1 cells for each of the four conditions (i.e. DMSO, Vitamin D, RA and RA + Vitamin D), and extracts were mixed in a 1:1 ratio (based on protein content) with the protein extracts from the SILAC labelled cells (JBUSH or EK). The 1:1 mixed protein extracts were then immuno-precipitated using L243 antibody and resolved by 12% non-reducing SDS PAGE. DR β bands were excised and sent to Cambridge Centre for Proteomics for tryptic digestion and mass spectrometry analysis. SILAC ratios were calculated as % light with the help of Proteome Discover software. Total HLA-DR expression in the two HTCs was not well matched to KG-1 cells, and therefore SILAC %

light values for DRB1 shared peptides were either much less than 50 % for the JBUSH/KG-1 and much more than 50 % EK/KG-1 mixtures, respectively. Figures 6.16 and 6.17 show the result representing % light values of EK and JBUSH cells respectively.

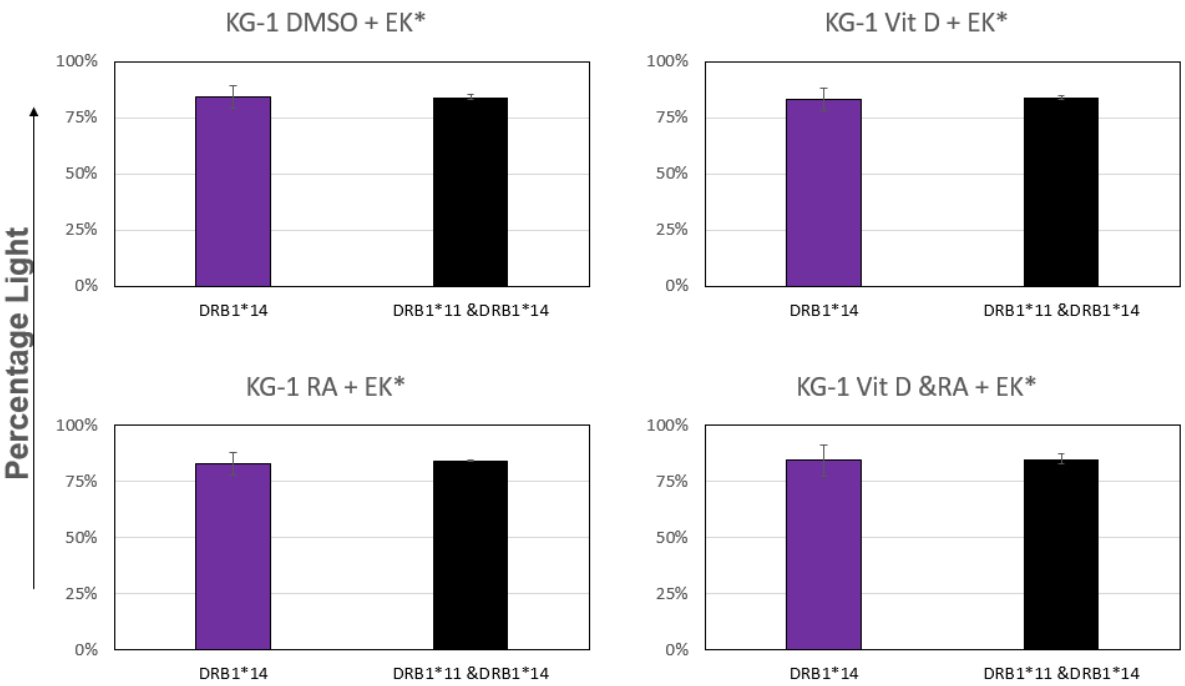

Figure 6.16 % light values of the alleles in KG-1 vs EK cells. KG-1 cultures (n=4) were treated with Vit-D and or RA for 72 hours in light media. Extracts were mixed 1:1 (by protein content) with SILAC labelled EK cells. Mean % light ratios of the allele-specific DR β peptide sets were quantified from the SILAC ratios obtained after LC-MS. The column graphs show the means +- SD for groups of peptides from the indicated individual alleles. The colour coding is as per Figure 6.6 and Table 6.1.

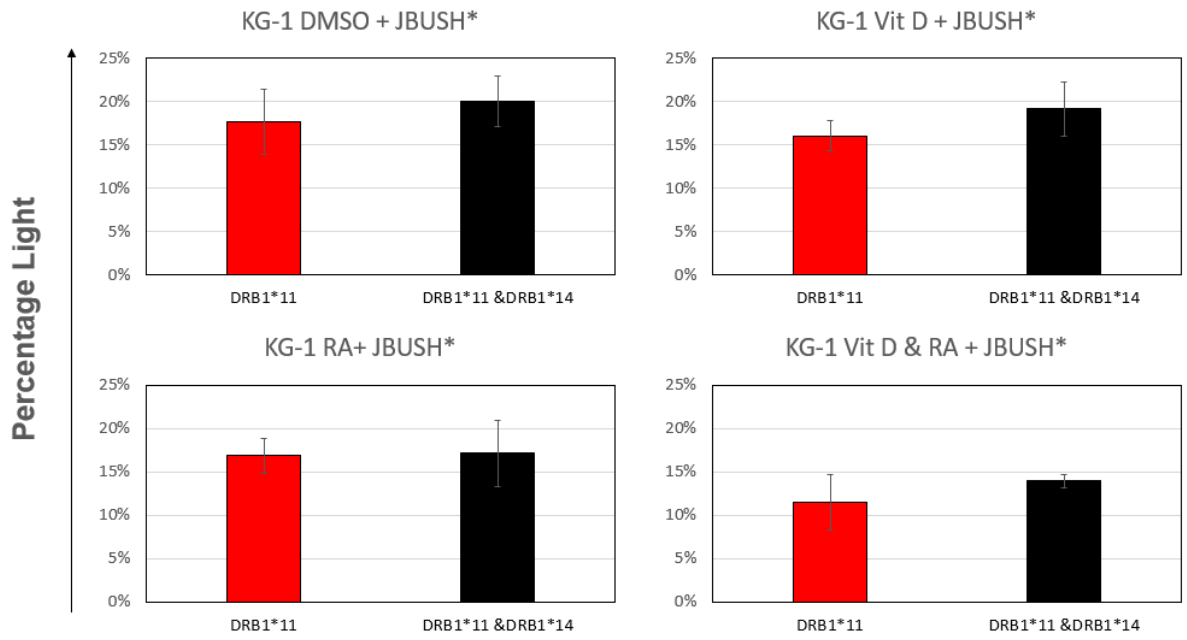

Figure 6.17 % light values of the alleles in KG-1 vs JBUSH cells. KG-1 cultures (n=4) were treated with Vit-D and or RA for 72 hours in light media. Extracts were mixed 1:1 (by protein content) with SILAC labelled JBUSH cells. Mean % light ratios of the allele-specific DR β peptide sets were quantified from the SILAC ratios obtained after LC-MS. The column graphs show the means +- SD for groups of peptides from the indicated individual alleles. The colour coding is as per the Figure 6.6 and Table 6.1.

The low % light values indicated that the HLA-DR amounts were mismatched between KG-1 and HTCs standard cells, after matching for protein contents. On this basis, the HLA-DR level was highest in JBUSH cells, followed by KG-1 with the lowest levels in EK cells.

Quantification of allelic composition was attempted, based on the difference in the SILAC % light values for DRB1 shared and DRB1 specific peptide, as described in Section 6.2. Because of difficulties in error propagation with this formula, all permutations of values for shared and allele specific peptides were generated to estimatethe variance in the values of 'a' (the % contribution to the total DRβ pool from the allele which is shared between heterozygous sample and SILAC standards). This is shown in Figure 6.18 (A) for the

DRB1*14 allele and in (B) for the DRB1*11 allele. The data are represented as the mean of the quadruplicate analysis.

A

KG-1 DMSO + EK*

DRB1 Shared	Peptide No	DRB1*14 Specific Allele		
		85%	85%	86%
		18	21	23
84%	3	108%	108%	93%
84%	5	108%	108%	93%

KG-1 Vit D + EK*

DRB1 Shared	Peptide No	DRB1*14 Specific Allele		
		85%	85%	86%
		18	21	23
86%	3	89%	92%	100%
85%	5	100%	100%	112%

KG-1 RA + EK*

DRB1 Shared	Peptide No	DRB1*14 Specific Allele		
		85%	85%	83%
		18	21	23
86%	3	89%	92%	82%
84%	5	108%	108%	94%

KG-1 Vit D & RA + EK*

DRB1 Shared	Peptide No	DRB1*14 Specific Allele			
		85%	82%	81%	83%
		18	19	21	23
85%	3	100%	85%	80%	82%
84%	5	108%	89%	83%	94%

B

KG-1 DMSO + JBUSH*

DRB1 Shared	Peptide No	DRB1*11 Specific Allele			
		18%	19%	14%	19%
		9	13	15	16
17%	5	108%	115%	79%	115%
20%	7	90%	94%	58%	94%

KG-1 Vit D + JBUSH*

DRB1 Shared	Peptide No	DRB1*11 Specific Allele			
		16%	12%	18%	18%
		9	10	13	16
21%	5	71%	60%	88%	88%
20%	7	81%	57%	91%	91%

KG-1 RA+ JBUSH*

DRB1 Shared	Peptide No	DRB1*11 Specific Allele			
		17%	13%	17%	17%
		9	10	13	16
20%	5	79%	56%	81%	81%
19%	7	87%	62%	89%	89%

KG-1 Vit D & RA+ JBUSH*

DRB1 Shared	Peptide No	DRB1*11 Specific Allele			
		13%	7%	13%	13%
		9	10	13	16
14%	5	89%	44%	90%	90%
14%	7	92%	46%	92%	92%

Figure 6.18 Estimation of the DRB1allelic mix in KG-1 cells. The table shows the percentage of the allele present in the KG-1 cells, calculated based on equation (4) derived in section 6.2. The figure represents data for the DRB1*14 allele (A) and DRB1*11 (B) allele. The peptide number is based on Table 6.1. The results shown are means of the quadruplicate analysis. In this figure * indicates labelled cells, % values in the shaded region are the % light values obtained from the SILAC experiment shown in Figure 6.16 (for A) and Figure 6.17 (for B)

As seen from the result, the difference in the SILAC ratio between shared and allele specific peptides were small whereas the error on the resulting estimate of the allelic mix was large.

For both the alleles, this approach yielded best estimates of allelic contributions of more than 50%, which is not plausible because the allelic contributions should add up to 100%. It was concluded that the approach needed further optimization to yield reliable, internally consistent estimates of allelic composition.

6.5 Discussion

The aim of this chapter was to develop methods for tracking, in heterozygote APCs, any potential difference in the responses of allelic and gene variant of HLA-DR to environmental agents, such as vitamin D or RA. The results suggest that HLA-DR β-chain targeted SILAC can reliably quantify small effects of media composition or other environmental agents, such as vitamin D and RA, on the allelic composition of HLA-DR. In addition, the findings will also help to improve the design of future experiments with primary antigen presenting cells.

6.5.1 SILAC analytics with KG-1 cells

Experiments with KG-1 cells established proof of feasibility of quantifying changes in allelic composition based on the SILAC approach. Pilot studies also showed that there is good analytical precision of SILAC values (% heavy or % light) between samples and between sets of peptides specific for the same allele. They also helped in choosing the analytical parameters; specifically, 70k resolution was better than 17k resolution, and Proteome Discover, an analysis software package, yielded more precise estimates of SILAC ratios than MaxQuant.Another practical conclusion from the pilot studies was that mixing of SILAC standards with unlabelled samples is best done based on protein content rather than cell equivalents.

6.5.2 Relative quantification of the effects of vitamin D and/or RA on HLA-DR alleles in KG-1 cells

SILAC labelled KG-1 cells were mixed with KG-1 cells treated with vitamin D and/ or RA, in order to quantify changes from baseline in the relative expression of allelic or gene variants.

As observed by flow cytometry in Chapter 5, and mass spectrometry combined treatment with vitamin D and RA synergistically lowered HLA-DR expression in KG-1. At baseline, DRB3 specific peptides had a slightly higher % light value than that of DRB1 derived peptides. There was no systematic difference observed between DRB1 allele specific peptides. Thus, in this cell line, neither vitamin D nor RA had any substantial effect on the relative contributions of DRB1*11 and *14. However, RA seemed to affect the relative representation of the minor gene variant, DRB3, but this was reversed when the cells were treated with both RA and vitamin D. This observation suggests that the relative expression of DRB3 gene variants may be differentially affected by vitamin D and or RA.

The magnitude of the vitamin D effects on the DRB1 vs. DRB3 contribution in this instance was small and would be unlikely to yield biologically meaningful differences in antigen presentation or tolerance induction. However, larger effects might be expected, based on results in Chapter 5 and previously published literature of PGF cells homozygous for the HLA-DR1*15, a major MS risk allele. The PGF cells expresses an alternate β-chain gene, DRB5, at a higher level, whereas the DRB1*15 gene product is in the minority, at the mRNA level (Andersson et al., Horton et al., 2008). This remains an important focus for future work, both in primary cells and in cell lines.

6.5.3 SILAC based allelic composition quantification in KG-1 cells

In principle, mixing of heterozygous APCs with a mono-allelic standard should enable quantification of the contributions of the co-expressed DRB1 alleles to the total DR β1 chain pool. The contributions of the two alleles should add up to 100%. However, attempts to measure this for KG-1 cells using DRB1 haplotype matched HTCs (JBUSH and EK) have so far proved unsuccessful: the estimated allelic contributions obtained from mixing experiments with SILAC-labelled HTCs expressing either DRB1*11 (JBUSH) or DRB1*14

(EK) were both well above 50% and thus mutually inconsistent, as well as being subject to large errors. The actual magnitude of SILAC ratios is not influenced by the mixing ratio but also by the amount of HLA-DR present in the standard and the unknown. Therefore, model calculations were performed (based on equation 4 in section 6.2) to explore how the measured % light difference between the shared and the allele specific peptides is affected by the contribution of the allele that is shared with the HTC standard, as well as by the relative abundance of total DR in the homozygous standard and the heterozygous unknown sample. This is shown in Figure 6.19.

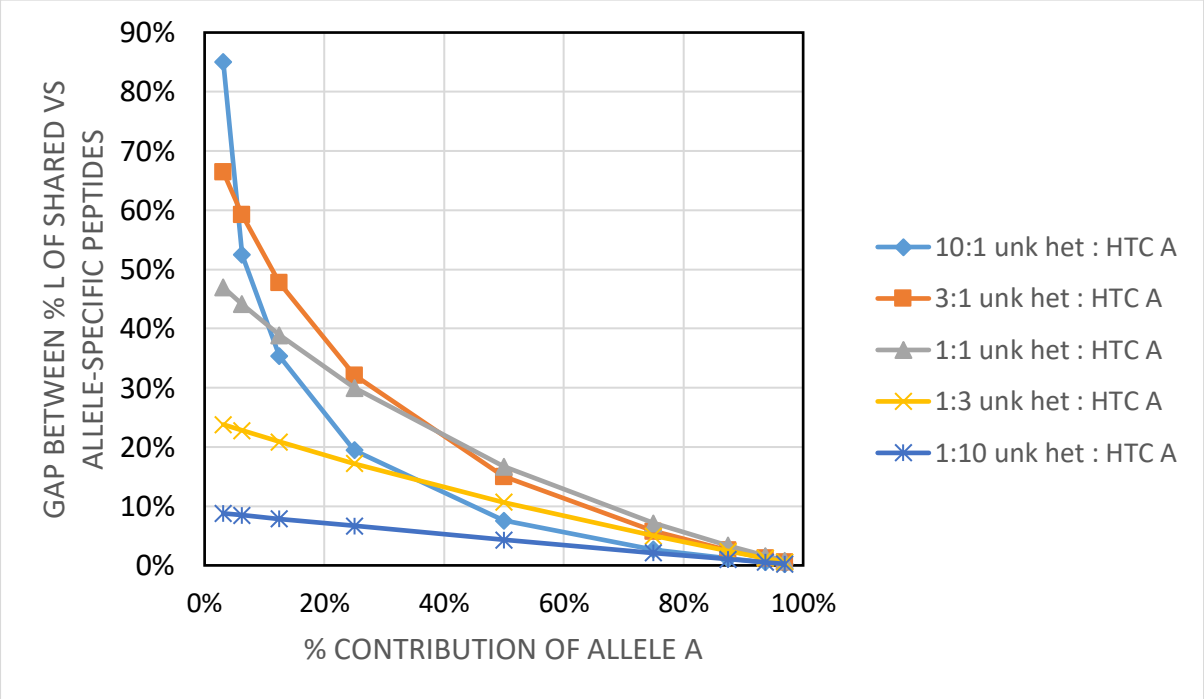

Figure 6.19 Model calculations to estimate optimum mixing ratio. The graph shows how the measured % light difference between shared and allele specific peptide depends on the contribution of the allele that is shared with the HTC standard at different DR abundance ratios between known and standard. This model is ideal when any heterozygous unlabelled unknown cells, such as KG-1, are mixed with labelled HTCs mono-allelic for one of the allele from heterozygous. In the above figure, unk and het stands for unknown and heterozygous respectively. This graph is based on equation 4 derived in section 6.2

The model calculations in Figure 6.21 show how the measured output (i.e. the gap between % light values of shared and allele specific peptides) varies as the function of contribution of the matched allele at different mixing ratios of HLA-DR protein from SILAC standards in unknown. It turns out that the mix between standard and unknown is optimal at around 1:1 molar ratio, or with the standard in slight excess. This is because the dose response observed, with such mixing ratios is nearly linear over the entire range of possible allelic contributions. When the unknown is in large excess, it turns out that the relationship is non-linear, so that the dose response is very small for greater than 50% of allelic contribution. Conversely, when the SILAC labelled standard is in large excess, there is no % allele contribution that creates a large difference.

In the actual experiments in which KG-1 cells were mixed with SILAC labelled HTCs, in 1:1 ratio based on total protein, HLA-DR was in large excess in KG-1 cells when mixed with EK (Figure 6.16). In contrast, the SILAC labelled standard was in large excess in the mix between KG-1 cells and SILAC labelled JBUSH (Figure 6.17). The predicted responsiveness of the experimental measurements to the allelic contribution at HLA-DR abundance ratio obtained when KG-1 cells was mixed with SILAC labelled EK or JBUSH cells is shown in Figure 6.20.

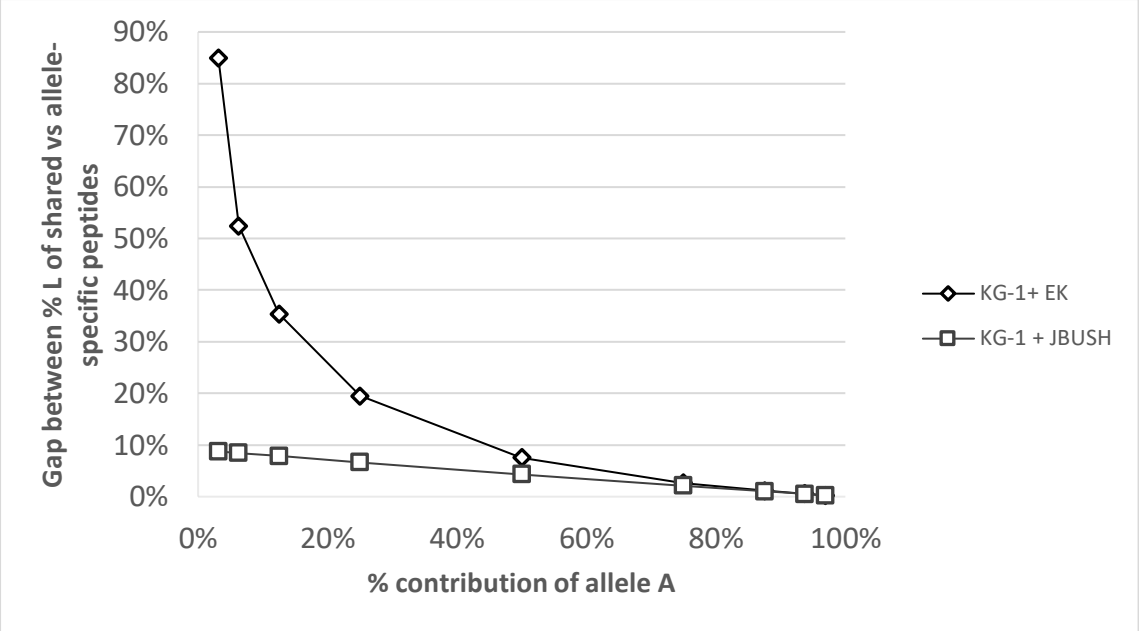

Figure 6.20 Predicted contribution of DRB1 alleles in KG-1 cells based on model calculations.. Due to unequal HLA-DR expression there was an unfavourable mixing ratio between the KG-1 cells and HTCs which led to a nonlinear relationship, leading to a poor constraint in determining the allelic contribution.

Since the HLA-DR expression varied between the three cell lines, the DR β-chain SILAC ratios observed in both experiments were far from 1:1, the optimal ratio for quantifying the allelic contributions based on mathematical modelling. Instead, when the unlabelled KG-1 extracts were mixed at 1:1 total protein ratio, with SILAC labelled JBUSH extracts, DR molecules derived from JBUSH were in large excess. On the other hand, when the unlabelled KG-1 cells were mixed at 1:1 total protein ratio, with SILAC labelled EK cells, the DR molecules derived from unlabelled KG-1 cells were in large excess. Under either condition, there were small differences in SILAC ratios between DRB1-shared and allele-specific peptides, which provided a poor constraint on the allelic composition. Lastly, there was also a small amount of residual un-labelled material (< 5%) in the SILAC standards, which could exaggerate the problem further.

In order to obtain reliable estimates of the DRB1 allelic contributions, it is apparently critical to get the mixing ratio correct. The mixing ratio for SILAC standards and the unknown samples must be individualised, so that the extracts contain approximately equal amounts of total HLA-DR from the labelled HTCs and the unlabelled unknown sample. In this particular instance, the protein content of SILAC labelled EK would have to be increased to give an approximate ratio of 1:1 for HLA-DR. In contrast, the protein content of KG-1 cells would need to be increased in mixtures with the JBUSH cells to get the optimal mixing ratio. Time constraints did not permit further optimisation of mixing ratios prior to thesis submission, but such experiments are planned after submission.

The results from this chapter suggest that HLA-DR β-chain targeted SILAC can reliably quantify small effects of media composition or other environmental agents, such as vitamin D and RA, on the allelic composition of HLA-DR. To our knowledge, this is the first study which attempts to determine the effect of vitamin D and RA on the allelic composition in the heterozygous cells using SILAC approach. However, in this instance, the allelic contribution could not be determined because of differences in the total HLA-DR expression between the cell lines. Model calculations performed in this study also establish the foundation for performing such studies with precision in order to obtain reliable estimate of the allelic contributions of maternal and paternal DRB1 alleles in any particular cell population.

These studies prompt the re-design of experimental strategies for exploring vitamin D effects on DR β chain composition in primary APCs, as follows:

One option is, following relative quantification (as explained in section 6.1.4.2), to focus on changes from baseline of DR β chain composition caused by vitamin D, RA or both. This approach requires autologous SILAC standards from each donor. These could be obtained by EBV transformation of primary B cells from each donor, but this is subject to regulatory

constraints, since this university does not have a Human Tissue Act licence. Alternatively, there may be sufficient protein turnover and new synthesis to allow acceptable SILAC standards to be produced from short-term primary cell cultures, e.g., from monocytes, immature DCs, or LPS/IL4-stimulated B-cell blasts. Either way, a disadvantage is that some of the primary samples would be sacrificed for preparation of SILAC standards, and that the % contributions of each DRB1 allele to the total β chain pool would not be quantifiable by this approach.

A second option is, following the quantification strategy as explained in section 6.1.4.3, to use DRB1-homozygous typing cells as heterologous standards. These can be prepared in advance, with a small number of cell lines able to cover one or both alleles in most donors, if the study is restricted to a defined ethnicity with a limited number of prevalent alleles (as explained in chapter 5). However, in order to extract reliable estimates of DRB1 allelic contributions, the results (Figure 6.16, 6.17, and 6.19) show that the mixing ratio for SILAC standards and primary APC samples must be individualised, so that the extracts contain approximately equal amounts of total DR from the HTC and the primary APC sample. Based on the overall experience from these studies, this could be based on flow cytometric analysis of HLA-DR levels from primary APCs and standards, as well as on exploratory titrations of standard vs unknown, which complicates the logistics of studies with human subjects using this approach.

Thus, this study is an excellent starting point through which much has been learnt about the further steps required, and the results from this chapter and Chapter 5 suggest that the goal remains achievable.

Chapter 7: General conclusions and future perspectives

The overall objective of this PhD thesis was to study mechanisms by which the expression of tissue antigens, specifically, HLA-DR MHC II proteins, are regulated. This study identified Cathepsin D (Cat D) as a lysosomal enzyme playing a vital role in the degradation of HLA-DR molecules in the myeloid cell line, KG-1. This study also provided evidence that empty HLA-DR molecules are especially susceptible to degradation by Cat D. Moreover, this study showed that vitamin D interacts with retinoic acid (RA) in regulating the expression of HLA-DR in B lymphoblastoid cell lines representing some common DRB1 alleles in White British, Irish or Caucasian individuals but not others. Lastly, methods were developed to quantify changes in HLA-DR allelic composition in response to various interventions, in DRB1 heterozygous cells, using stable isotopes and mass spectrometry. This provides an approach for exploring the consequences of MHC gene/ environment interactions in auto-immune diseases, including multiple sclerosis (MS).

In this final chapter, the limitations of the findings presented herein will be placed in the context of the present literature, and potential avenues for further studies will be discussed.

7.1 Characterisation of lysosomal proteases involved in HLA-DR protein breakdown

The results in Chapter 3 showed, for the first time, that the protease, Cat D, plays a non-redundant role in the degradation of HLA-DR molecules. The identification was based on pharmacologically inhibiting Cat D KG-1 cells or using targeted genetic knockdown and observing the accumulation of HLA-DR molecules. Based on the limited data available, there were no examples of APCs with a high HLA-DR turnover but no pepstatin A effect or Cat D expression. This suggests that the mechanism is not limited to the KG-1 cell culture system.

Another important conclusion from Chapter 3 was that KG-1 cells by some means adapt to the lack of Cat D. One possibility is that the cells have some way of sensing HLA-DR levels and down-regulate the synthesis of new HLA-DR molecules through the master regulator of MHC II transcription, CIITA (LeibundGut-Landmann et al., 2004). Another possibility is that Cat D can be functionally replaced. It is plausible that cells recognise lysosomal overload and there is some compensating change in the composition of lysosomal enzymes. Another enzyme that otherwise makes a minor contribution to HLA-DR degradation could take over to restore a steady state. Both explanations are compatible with the data. However, the adaptation works, this is worth further study, because not much is known about the mechanisms by which lysosomal composition responds to demand and there is very little understanding on feedback mechanisms regulating MHC II expression.

Data in Chapter 4 support a model whereby empty HLA-DR molecules are selectively degraded by Cat D. The HLA-DR molecules that accumulated when Cat D was inhibited were SDS unstable and were neither associated with invariant chain (Ii) nor conjugated to ubiquitin. Their biochemical properties are consistent with empty molecules, and this is structurally plausible, based on the results from the initial cleavage site identified *in vitro* (Appendix 7.1). Cleavage occurs at αPhe54 in the peptide binding groove which is "locked" in by hydrogen bonds when peptides binds to the HLA-DR complex (Jardetzky et al., 1990), while during maturation, the CLIP region of Iistabilizes this region (Cresswell, 1996). Moreover, the trimerization domain of intact Iisterically masks the same region (Busch et al., 1996, Busch and Mellins, 1996). HLA-DM also binds selectively to empty HLA-DR molecules, but in the process, it changes the conformation of that binding region and makes it sterically inaccessible (Pos et al., 2012). The initial cleavage site at αPhe54 is conformationally flexible in mutant DR molecules that undergo rapid peptide exchange

without DM (Painter et al., 2011). A working model for Cat D cleavage of empty DR was proposed in Chapter 4 (Figure 4.7).

Together, these findings suggest that Cat D mediates quality control by selectively degrading HLA-DR molecules that lack stably bound peptides and that are not associated with Iichain or HLA-DM. This is an important insight into normal immune function, but it also has implications for autoimmunity. Importantly, this mechanism for lysosomal quality control acts to limit the availability of empty molecules that could aberrantly bind peptides outside of the conventional peptide-loading pathway. Previous work has failed to provide evidence that fast turnover is a factor in MHC II-linked risk of autoimmunity (Busch et al., 2005). In fact, it seems that the selective destruction of empty molecules could limit the risk of triggering autoimmunity by ectopic antigen presentation.

7.2 Effects of vitamin D and RA on the co-dominant expression of HLA-DR allelic and gene variants

Chapter 5 showed that HLA-DR levels in cell lines respond in several distinct ways to the combined or separate treatment with vitamin D and RA. To our knowledge this is the first examination of this interaction. In HTCs, the effects of vitamin D and RA on the expression of total HLA-DR (i.e. regardless of copy number variation) varied between the cell lines and over time and competed with each other. In contrast, in the myeloid cell line, KG-1, combined treatment with vitamin D and RA synergistically lowered HLA-DR expression.

The present work reproduced previously observed differences between HTCs in the effects of vitamin D on expression of HLA-DR protein, which another group has attributed to VDRE-mediated upregulation of DRB1*15:01 but not of other DRB1 alleles (Ramagopalan et al., 2009). This study extended these findings to other HTCs homozygous for common DRB1

alleles found in White British/ Irish population. Vitamin D only increased HLA-DR expression in two HTCs, PGF and WDV, homozygous for DRB1*15:01 and DRB1*13:01, respectively. In other HTCs, no such induction effect by vitamin D was detected. This suggests that there is allele specificity in regard to how vitamin D affects antigen presentation. When some of the HTCs were tested for vitamin D responsiveness (by CD38 induction), all were vitamin D responsive ((Busch 2018, personal communication, 2 February). This reflects allelic differences in the VDR mediated transactivation of some DR alleles and not others, rather than some differences in cellular background that enables cells to respond to vitamin D.

Conversely, observations also suggested that DRB1*07 allele, possibly by same criterion, is inducible by RA in MANN cells. It opens an interesting aspect in future to find whether there is retinoic acid response element (RARE) present in that allele. Moreover, complexity of VDR-RXR or RAR-RXR mediated regulation is highlighted by the data in this study. The combined treatment of HTCs with vitamin D and RA reversed any effects of the individual treatments, suggesting that there is mutual competition between the two pathways, such that activation of one pathway stops the other pathway from up-regulating HLA-DR expression in these cells. The common ability for RXR to bind to both VDR and RAR is one possible explanation of cross talk between vitamin D and RA signalling pathway (Tavera-Mendoza et al., 2006). Competition between the nuclear receptors may not be the only possible mechanism. This study examined the phenotypic change only and not the genetic mechanism, which would be an interesting future aspect.

Unlike EBV transformed B cell lines (HTCs), in the myeloid KG-1 cells, neither vitamin D nor RA alone had any effect on the expression of HLA-DR, but combined treatment reduced the expression of HLA-DR. Vitamin D by itself has shown to reduce the MHC II levels in primary APCs by reprograming differentiation (Bscheider and Butcher, 2016). In HTCs (EK

and JBUSH), having the same alleles as KG-1, there was no effect of vitamin D and no reproducible effect of RA on the expression of HLA-DR, which suggests that the effect is dependent on the cell type and not only on the type of allele.

Any one individual human can produce between two and four different variants of DR molecules, due to the genetic variation. These variants are difficult to distinguish in the experiments normally used to quantify the amounts of DR molecules, but this is important because DR variants may respond differently to vitamin D. Therefore, a new analytical approach was developed that allowed us to detect such differences.

Using this approach, the effect of vitamin D and RA on the co-dominant expression of HLA-DR allelic and gene variants were quantified in KG-1 cells, which express DRB1*11 and DRB1*14 alleles and the and DRB3*02 gene variant (Ning et al., 2011) (also Chapters 2,5 and 6 of this thesis). In this cell line, neither vitamin D nor RA had any substantial effect on the relative contributions of DRB1*11 and *14. However, RA seemed to affect the relative representation of the minor gene variant, DRB3, and this was reversed when the cells were treated with both RA and vitamin D. This observation suggests that vitamin D and or RA may differentially affect the relative expression of DRB3 gene variants. The combination of vitamin D and RA did not detectably change the allelic mix for DRB1 but there is a possibility that the behaviour of gene variants is not perfectly synchronised with the behaviour of DRB1 gene products. This could extend to the DRB1*15 haplotype, where DRB1 is a less expressed molecule (Horton et al., 2008). It could be that total HLA-DR measurement underestimates the extent to which DRB1*15 changes its expression. This remains an important focus for future work in the PGF cell line.

In addition, JBUSH and EK, two HTCs haplotype matched for the DRB1*11 and DRB1*14 alleles, respectively, were used as internal SILAC standards to estimate DRB1 allelic

contributions to the total DR pool. This experiment was not able to quantify the DRB1 allelic contribution, because there were only small differences in SILAC ratios between DRB1-shared and allele-specific peptides, which provided a poor constraint on the allelic composition. These studies were successful in developing a novel stable isotope approach to quantify the effect of micronutrients on the HLA-DR molecules.

Vitamin D in general seems to diminish the total HLA-DR expression in dendritic cells (Bscheider and Butcher, 2016), and in KG-1 cells (Chapter 5), whereas in HTCs with a VDRE in the promoter of HLA-DRB1, vitamin D is able to increase the expression of HLA-DR, as shown in Chapter 5 and also by Ramagopalan et al (2009). Thus, it remains an important objective to quantify the effects of vitamin D and RA on DR allelic variants in primary antigen presenting cells.

The work here developed a novel approach to investigate how environmental factors such as vitamin D and RA effect the allelic composition of the HLA-DR molecules in heterozygous cells. This approach can be extended to studies of other autoimmune diseases, in which MHC polymorphism plays an important role along with environmental factors, including those associated with MHC I alleles. This study provides evidence that allele dependent effects of vitamin D or RA on HLA-DR expression could influence MHC associations with auto immunity. Lastly, vitamin D and RA could also influence other aspects of MHC II antigen presentation by influencing other aspects of MHC protein maturation, peptide loading, trafficking and degradation. Future studies, using the tools developed and applied in this thesis, can explore these possibilities. It will be also interesting to assess whether there are allelic differences in the turnover of the HLA-DR molecules.

This study will help MS researchers to understand the mechanisms that link MHC II molecules to the disease process, and to understand how environmental factors, such as

vitamin D, influence disease risk. The methods that will be applied here to MS-related tissue antigens will have wider applications in understanding how other genetic and environmental factors determine outcomes in MS and other autoimmune diseases. Thus, the findings of this project may ultimately contribute to better prevention and/or treatment of MS.

Appendices

Appendix 2.1 L243 antibody activity assay

L243 monoclonal antibody was produced from the hybridoma cells by affinity chromatography as described in section 2.2.1.5. Before the purification, the presence of active L243 mAb was detected by competitive inhibition of HLA-DR using flow cytometry. Fixed and permeabilized KG-1 cells were incubated with the supernatant from the hybridoma producing L243mAb prior to incubation with L243-FITC, creating a competition between both antibodies for the binding site (i.e. DR molecules) on KG-1 cells. The general staining protocol described in section 2.2.3.1, except that volume of primary antibody was reduced to 2.5 µl per test. Thus as shown in Figure 2.1, the low median fluorescence intensity (MFI) of samples containing L243 supernatant indicated that L243 present in the supernatant binds to the DR and thus inhibits the binding of L243-FITC. The decrease in the MFI values provides a clear indication for the presence of the L243 Ab in the supernatant

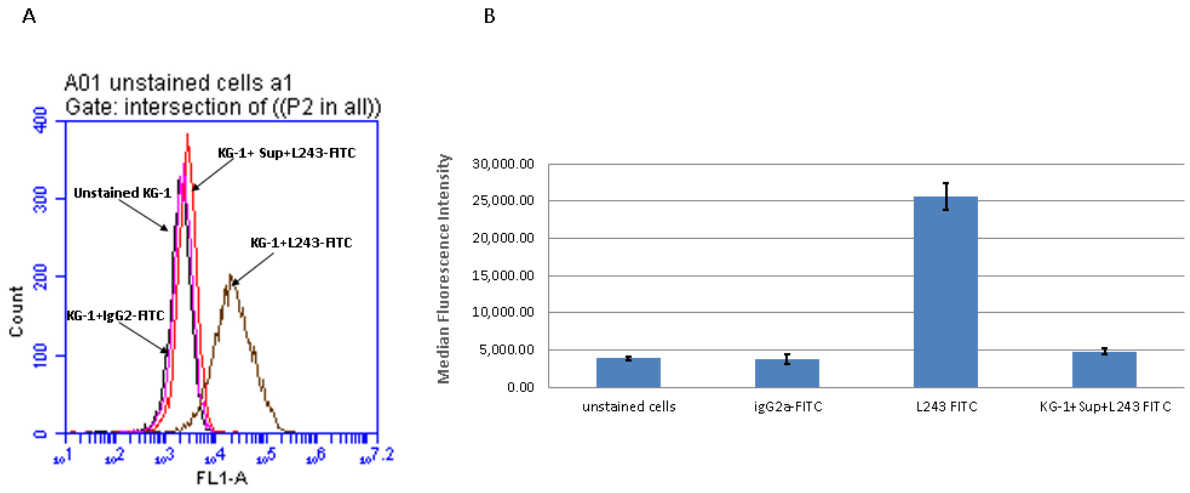

Figure Method for detecting active L243 mAb in hybridoma supernatants by competition for L243-FITC binding to HLA-DR+ cells: KG-1 cells were incubated with the supernatant containing L243, released from the hybridoma cells, prior to incubation with L243-FITC and analysis by flow cytometry. (A) Shows the overlay of the representative FACS plots. (B) Staining was quantified by flow cytometry and each bar represents the median fluorescence intensities. (MFI; mean +- S.D. of triplicate analysis).

Thus, this result showed the presence of active L243 mAb in the supernatant of the hybridoma cells, which was then purified by affinity chromatography. Purified antibody was stored at -20 C in aliquots at concentration of 1mg/ml for future use.

Appendix 3.1 Effect of pep A on KG-1 cells

Between-Subjects Factors

		Value Label	N
Type	1	untreated	9
	2	vehicle control	9
	3	PepA	9
Hour	24	24 hours	9
	48	48 hours	9
	72	72 hours	9

Tests of Between-Subjects Effects

Dependent Variable: MFI

Source	Type III Sum of Squares	df	Mean Square	F	Sig.
Corrected Model	164054681232.836[a]	8	20506835154.104	46.586	.000
Intercept	3635959589381.588	1	3635959589381.588	8259.958	.000
Type	132326718958.445	2	66163359479.223	150.306	.000
Hour	24234261413.591	2	12117130706.796	27.527	.000
Type * Hour	7493700860.800	4	1873425215.200	4.256	.013
Error	7923439366.185	18	440191075.899		
Total	3807937709980.599	27			
Corrected Total	171978120599.021	26			

a. R Squared = .954 (Adjusted R Squared = .933)

Post Hoc Tests

Multiple Comparisons

Dependent Variable: MFI

Tukey HSD

(I) Type	(J) Type	Mean Difference (I-J)	Std. Error	Sig.	95% Confidence Interval Lower Bound	95% Confidence Interval Upper Bound
untreated	vehicle control	7846.8633	9890.41147	.712	-17395.0810	33088.8077
	PepA	-144428.4244*	9890.41147	.000	-169670.3688	-119186.4801
vehicle control	untreated	-7846.8633	9890.41147	.712	-33088.8077	17395.0810
	PepA	-152275.2878*	9890.41147	.000	-177517.2321	-127033.3435
PepA	untreated	144428.4244*	9890.41147	.000	119186.4801	169670.3688
	vehicle control	152275.2878*	9890.41147	.000	127033.3435	177517.2321

Based on observed means.

The error term is Mean Square(Error) = 440191075.899.

*. The mean difference is significant at the 0.05 level.

Homogeneous Subsets

MFI

Tukey HSD[a,b]

Type	N	Subset 1	Subset 2
vehicle control	9	313593.4822	
untreated	9	321440.3456	
PepA	9		465868.7700
Sig.		.712	1.000

Means for groups in homogeneous subsets are displayed.

Based on observed means.

The error term is Mean Square(Error) = 440191075.899.

a. Uses Harmonic Mean Sample Size = 9.000.

b. Alpha = 0.05.

Appendix 3.2 One sample t-test of % increase in HLA-DR levels 48 hours after Pep A treatment of KG-1 cells in 9 independent experiments on nine independent repeats.

mean	1.48
sd	0.287663
n	9
SE	0.095888
df	8
hypoth mean	1
t stat	5.005858
p	0.001045
t crit	0.064701

Appendix 3.3 Effect of pepstatin- penetratin A on KG-1 cells

Between-Subjects Factors

		Value Label	N
Type	1	untreated	9
	2	vehicle control	9
	3	Pep-Pen	9
Hour	24	24 hours	9
	48	48 hours	9
	72	72 hours	9

Tests of Between-Subjects Effects

Dependent Variable: MFI

Source	Type III Sum of Squares	df	Mean Square	F	Sig.
Corrected Model	46442249855.078[a]	8	5805281231.885	59.591	.000
Intercept	583113766459.260	1	583113766459.260	5985.642	.000
Type	26030377120.046	2	13015188560.023	133.600	.000
Hour	19890626707.845	2	9945313353.923	102.088	.000
Type * Hour	521246027.187	4	130311506.797	1.338	.294
Error	1753537641.695	18	97418757.872		
Total	631309553956.032	27			
Corrected Total	48195787496.773	26			

a. R Squared = .964 (Adjusted R Squared = .947)

Post Hoc Tests

Dependent Variable: MFI

Tukey HSD

(I) Type	(J) Type	Mean Difference (I-J)	Std. Error	Sig.	95% Confidence Interval	
					Lower Bound	Upper Bound
untreated	vehicle control	-3849.0956	4652.80699	.691	-15723.8184	8025.6273
	Pep-Pen	-67706.6467*	4652.80699	.000	-79581.3695	-55831.9238
vehicle control	untreated	3849.0956	4652.80699	.691	-8025.6273	15723.8184
	Pep-Pen	-63857.5511*	4652.80699	.000	-75732.2739	-51982.8283
Pep-Pen	untreated	67706.6467*	4652.80699	.000	55831.9238	79581.3695
	vehicle control	63857.5511*	4652.80699	.000	51982.8283	75732.2739

Based on observed means.

The error term is Mean Square(Error) = 97418757.872.

*. The mean difference is significant at the

Homogeneous Subsets

MFI

Tukey HSD[a,b]

Type	N	Subset 1	Subset 2
untreated	9	123106.6044	
vehicle control	9	126955.7000	
Pep-Pen	9		190813.2511
Sig.		.691	1.000

Means for groups in homogeneous subsets are displayed.

Based on observed means.

The error term is Mean Square(Error) = 97418757.872.

a. Uses Harmonic Mean Sample Size = 9.000.

b. Alpha =

Appendix 3.4 Effect of Pepstatin A on Priess cells

Between-Subjects Factors

		Value Label	N
Type	1	untreated	9
	2	vehicle control	9
	3	PepA	9
Hour	24	24 hours	9
	48	48 hours	9
	72	72 hours	9

Tests of Between-Subjects Effects

Dependent Variable: MFI

Source	Type II Sum of Squares	df	Mean Square	F	Sig.
Corrected Model	6468669705.964[a]	8	808583713.246	9.645	.000
Intercept	1995395686267.870	1	1995395686267.870	23802.043	.000
Type	5166931064.564	2	2583465532.282	30.817	.000
Hour	1245662223.719	2	622831111.859	7.429	.004
Type * Hour	56076417.682	4	14019104.420	.167	.952
Error	1508993253.116	18	83832958.506		
Total	2003373349226.947	27			
Corrected Total	7977662959.081	26			

a. R Squared = .811 (Adjusted R Squared = .727)

Appendix 3.5 Pep A effects on HLA-DR levels in KG-1 cells grown with GlutaMAX media

Between-Subjects Factors

		Value Label	N
Type	1	vehicle control	15
	2	Pep A	15
Hour	3	3 hour	6
	6	6 hour	6
	24	24 hours	6
	48	48 hours	6
	72	72 hours	6

Tests of Between-Subjects Effects

Dependent Variable: MFI

Source	Type III Sum of Squares	df	Mean Square	F	Sig.
Corrected Model	13192005940.719[a]	9	1465778437.858	16.692	.000
Intercept	652133934873.868	1	652133934873.868	7426.382	.000
Type	6274192058.700	1	6274192058.700	71.449	.000
Hour	6013072328.363	4	1503268082.091	17.119	.000
Type * Hour	904741553.655	4	226185388.414	2.576	.069
Error	1756262903.494	20	87813145.175		
Total	667082203718.082	30			
Corrected Total	14948268844.213	29			

a. R Squared = .883 (Adjusted R Squared = .830)

Appendix 3.6 Cross reactivity of commercial monoclonal anti-cat E antibody with Cat D

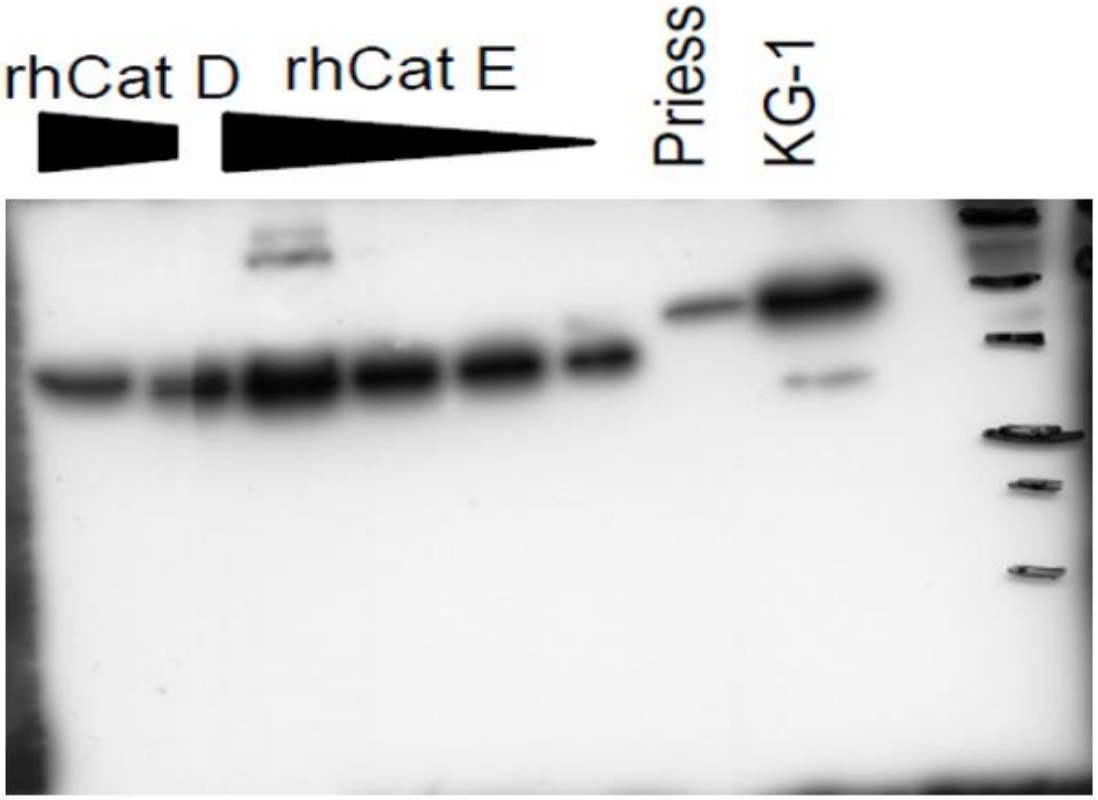

Protein extracts from equal cell equivalents of KG-1 and Priess cells were resolved by 12% non-reducing SDS PAGE and immunoblotted for Cat E. rh Cat E migrated partly as a homo-dimer, which is observed at 80 kDa and as a 44 kDa (monomer). The quantities of rh Cat E used ranged from 2 ng to 250 ng while for rh Cat D they were 50 ng and 250 ng. As observed in the figure, rh Cat D was detected with anti-Cat E antibody, demonstrated cross-reactivity. In addition, specific bands were detected in KG-1 and Priess cell extracts, but they migrated as a monomer which is typical of Cat D rather than as a homodimer seen for Cat E. Hence the result provided by this monoclonal anti- Cat E reflected Cat D cross reactivity.

Appendix 3.7 Effect of Pepstatin A on cat D knocked down cells at 24 hours.

Between-Subjects Factors

CatD KD			Value Label	N
Presence	PepA	1	Presence	3
		2	Absent	3
Absent	PepA	1	Presence	3
		2	Absent	3

Tests of Between-Subjects Effects

Dependent Variable: MFI

CatD KD	Source	Type III Sum of Squares	df	Mean Square	F	Sig.
Presence	Corrected Model	11297909963.344[a]	1	11297909963.344	81.159	.001
	Intercept	196511794237.510	1	196511794237.510	1411.645	.000
	PepA	11297909963.344	1	11297909963.344	9.628	.086
	Error	556830541.458	4	139207635.365		
	Total	208366534742.313	6			
	Corrected Total	11854740504.802	5			
Absent	Corrected Model	67946887.809[b]	1	67946887.809	9.628	.036
	Intercept	101209021208.102	1	101209021208.102	14341.776	.000
	PepA	67946887.809	1	67946887.809	81.159	.001
	Error	28227751.423	4	7056937.856		
	Total	101305195847.334	6			
	Corrected Total	96174639.232	5			

a. R Squared = .953 (Adjusted R Squared = .941)

b. R Squared = .706 (Adjusted R Squared = .633)

Appendix 3.8 Effect of Pepstatin A on cat D knocked down cells at 48 hours.

Between-Subjects Factors

CatD KD			Value Label	N
Presence	PepA	1	Presence	3
		2	Absent	3
Absent	PepA	1	Presence	3
		2	Absent	3

Tests of Between-Subjects Effects

Dependent Variable: MFI

CatD KD	Source	Type III Sum of Squares	df	Mean Square	F	Sig.
Presence	Corrected Model	1460862084.375[a]	1	1460862084.375	7.714	.050
	Intercept	1114475060855.042	1	1114475060855.042	5885.149	.000
	PepA	1460862084.375	1	1460862084.375	5.714	.050
	Error	757483039.833	4	189370759.958		
	Total	1116693405979.250	6			
	Corrected Total	2218345124.208	5			
Absent	Corrected Model	118252670262.251[b]	1	118252670262.251	200.851	.000
	Intercept	2015124631459.344	1	2015124631459.344	3422.662	.000
	PepA	118252670262.251	1	118252670262.251	200.851	.000
	Error	2355038047.673	4	588759511.918		
	Total	2135732339769.269	6			
	Corrected Total	120607708309.924	5			

a. R Squared = .659 (Adjusted R Squared = .573)

b. R Squared = .980 (Adjusted R Squared = .976)

Appendix 3.9 Effect of Pepstatin A on cat D knocked down cells at 72 hours.

Between-Subjects Factors

CatD KD			Value Label	N
Presence	PepA	1	Presence	3
		2	Absent	3
Absent	PepA	1	Presence	3
		2	Absent	3

Tests of Between-Subjects Effects

Dependent Variable: MFI

CatD KD	Source	Type III Sum of Squares	df	Mean Square	F	Sig.
Presence	Corrected Model	1514951011.000[a]	1	1514951011.000	2.095	.221
	Intercept	861646695423.784	1	861646695423.784	1191.834	.000
	PepA	1514951011.000	1	1514951011.000	2.095	.221
	Error	2891834064.268	4	722958516.067		
	Total	866053480499.053	6			
	Corrected Total	4406785075.269	5			
Absent	Corrected Model	123588375830.780[b]	1	123588375830.780	81.003	.001
	Intercept	1534360319973.282	1	1534360319973.282	1005.657	.000
	PepA	123588375830.780	1	123588375830.780	81.003	.001
	Error	6102914228.887	4	1525728557.222		
	Total	1664051610032.950	6			
	Corrected Total	129691290059.667	5			

a. R Squared = .344 (Adjusted R Squared = .180)

b. R Squared = .953 (Adjusted R Squared = .941)

Appendix 4.1: Pep A does not accumulate the Iichain in KG-1 cells

Between-Subjects Factors

		Value Label	N
Type	1	untreated	6
	2	vehicle control	6
	3	Pep A	6

Tests of Between-Subjects Effects

Dependent Variable: MFI

Source	Type III Sum of Squares	df	Mean Square	F	Sig.
Corrected Model	163740942.005[a]	2	81870471.002	1.388	.280
Intercept	12167323489.403	1	12167323489.403	206.338	.000
Type	163740942.005	2	81870471.002	1.388	.280
Error	884518034.424	15	58967868.962		
Total	13215582465.832	18			
Corrected Total	1048258976.429	17			

a. R Squared = .156 (Adjusted R Squared = .044)

Appendix 4.2: Accumulation of L243 reactive DR molecules in Pep A treated KG-1 cells

Between-Subjects Factors

		Value Label	N
Type	1	untreated	6
	2	vehicle control	6
	3	Pep A	6

Tests of Between-Subjects Effects

Dependent Variable: MFI

Source	Type III Sum of Squares	df	Mean Square	F	Sig.
Corrected Model	79212857090.717[a]	2	39606428545.359	18.169	.000
Intercept	723690545127.793	1	723690545127.793	331.983	.000
Type	79212857090.717	2	39606428545.359	18.169	.000
Error	32698510328.399	15	2179900688.560		
Total	835601912546.909	18			
Corrected Total	111911367419.116	17			

a. R Squared = .708 (Adjusted R Squared = .669)

Appendix 4.3 No accumulation of Iichain in KG-1 cells treated with Pep-A using GlutaMAX media

Between-Subjects Factors

		Value Label	N
Type	1	Vehicle control	15
	2	Pep A	15
Hour	3	3 hour	6
	6	6 hour	6
	24	24 hours	6
	48	48 hours	6
	72	72 hour	6

Tests of Between-Subjects Effects

Dependent Variable: MFI

Source	Type III Sum of Squares	df	Mean Square	F	Sig.
Corrected Model	447039641.460[a]	9	49671071.273	21.126	.000
Intercept	13324479075.675	1	13324479075.675	5667.135	.000
Type	290807.518	1	290807.518	.124	.729
Hour	426282129.384	4	106570532.346	45.326	.000
Type * Hour	20466704.559	4	5116676.140	2.176	.109
Error	47023689.379	20	2351184.469		
Total	13818542406.515	30			
Corrected Total	494063330.840	29			

a. R Squared = .905 (Adjusted R Squared = .862)

Appendix 5.1 Raw MFI values from the flow cytometry for HTCs from experiment 1

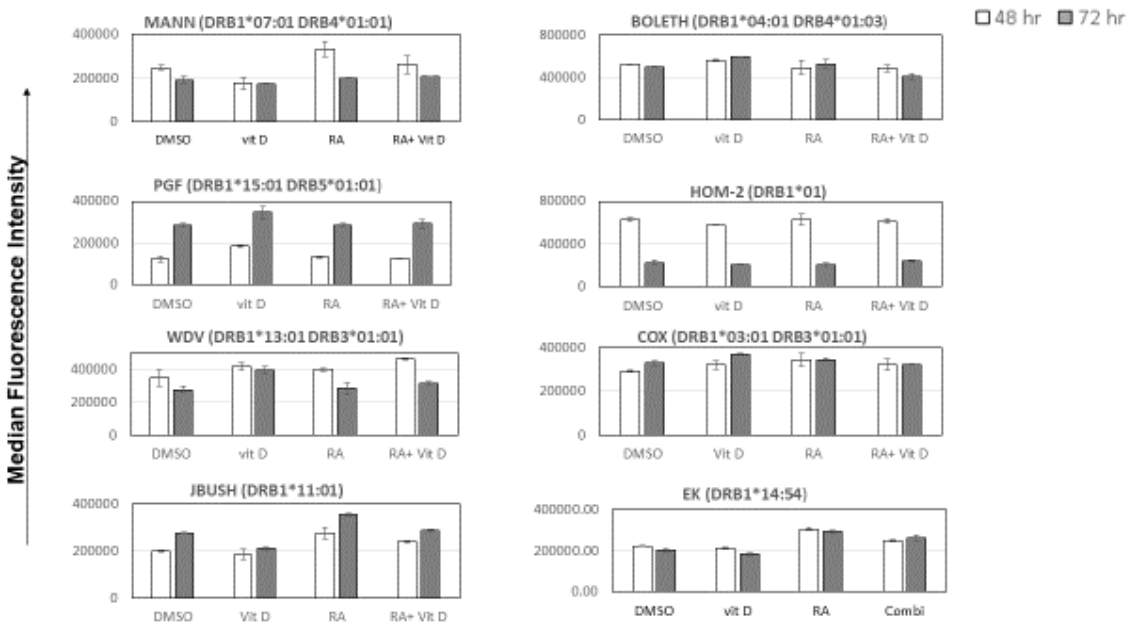

Effect of vitamin D and RA on total HLA DR expression in HTCs: EBV transformed homozygous typing cell lines containing six of the most common allele found in the UK cohort (White/Irish) and two alleles present in KG-1 cells were treated with 10 nM VitD and /or 1 µM RA. DMSO treated cells were used as a vehicle control. L243-FITC antibody was used to stain the DR molecules. Cells were analysed after fixation and permeabilization at 48 and 72 hours post treatment. Staining was quantified by flow cytometry and is reported as mean fluorescence intensities (MFI; mean+- S.D. of triplicate cultures).

Appendix 5.2 Raw MFI values from the flow cytometry for HTCs from experiment 2

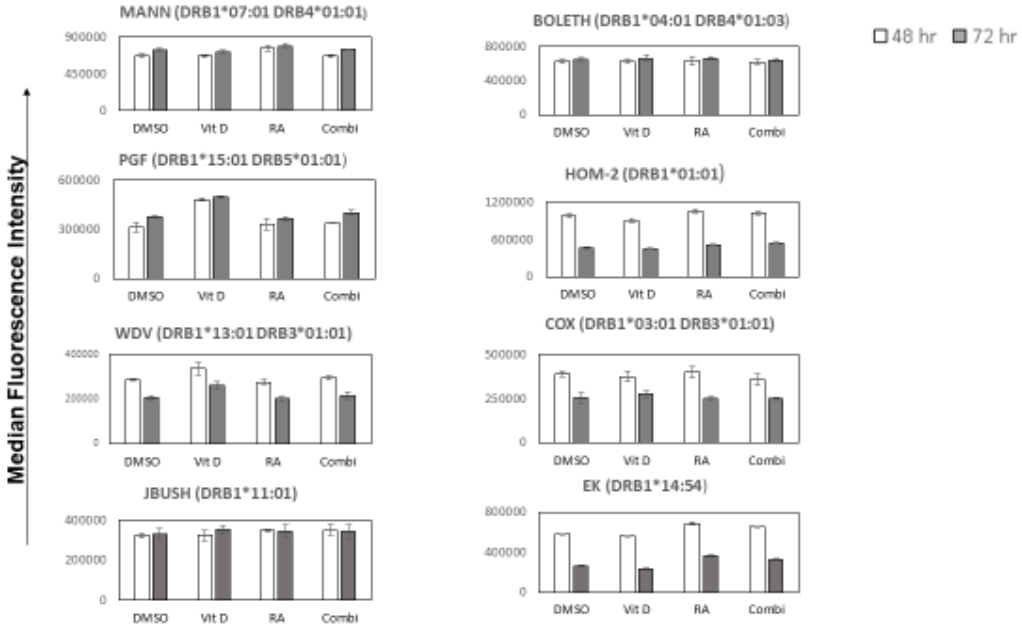

Effect of vitamin D and RA on total HLA DR expression in HTCs: EBV transformed homozygous typing cell line containing six of the most common allele found in the UK cohort (White/Irish) and two alleles present in KG-1 cells were treated with 10 nM VitD and/ or 1 µM RA. DMSO treated cells were used as a vehicle control. L243-FITC antibody was used to stain the DR molecules. Cells were analysed after fixation and permeabilization at 48 and 72 hours post treatment. Staining was quantified by flow cytometry and is reported as mean fluorescence intensities (MFI; mean+- S.D. of triplicate cultures).

Appendix 5.3: Effect of vitamin D on Live KG-1 cells.

Between-Subjects Factors

		Value Label	N
Type	1	untreated	9
	2	vehicle control	9
	3	Vitamin D	9
Hour	24	24 hours	9
	48	48 hours	9
	72	72 hours	9

Tests of Between-Subjects Effects

Dependent Variable: MFI

Source	Type III Sum of Squares	df	Mean Square	F	Sig.
Corrected Model	470991200.243[a]	8	58873900.030	48.967	.000
Intercept	21513386451.551	1	21513386451.551	17893.346	.000
Type	9280106.797	2	4640053.398	3.859	.040
Hour	427496371.178	2	213748185.589	177.781	.000
Type * Hour	34214722.268	4	8553680.567	7.114	.001
Error	21641617.728	18	1202312.096		
Total	22006019269.521	27			
Corrected Total	492632817.970	26			

a. R Squared = .956 (Adjusted R Squared = .937)

Appendix 5.4 Effect of Vitamin D on fixed and permeabilized KG-1 cells

Between-Subjects Factors

		Value Label	N
Type	1	untreated	9
	2	vehicle control	9
	3	Vitamin D	9
Hour	24	24 hours	9
	48	48 hours	9
	72	72 hours	9

Tests of Between-Subjects Effects

Dependent Variable: MFI

Source	Type III Sum of Squares	df	Mean Square	F	Sig.
Corrected Model	335595337.677[a]	8	41949417.210	29.362	.000
Intercept	33463719158.235	1	33463719158.235	23422.316	.000
Type	51308035.327	2	25654017.664	17.956	.010
Hour	264634371.494	2	132317185.747	92.613	.000
Type * Hour	19652930.855	4	4913232.714	3.439	.030
Error	25716797.169	18	1428710.954		
Total	33825031293.081	27			
Corrected Total	361312134.846	26			

a. R Squared = .929 (Adjusted R Squared = .897)

Appendix 5.5 Effect of vitamin D, RA on KG-1 cells at 24 hours

Between-Subjects Factors

		Value Label	N
Vitamin-D	1	Presence	6
	2	Absent	6
RA	1	Presence	6
	2	Absent	6

Tests of Between-Subjects Effects

Dependent Variable: MFI

Source	Type III Sum of Squares	df	Mean Square	F	Sig.
Corrected Model	144294435.417[a]	3	48098145.139	18.213	.001
Intercept	80183180074.083	1	80183180074.083	30362.351	.000
Vitamin-D	16426800.000	1	16426800.000	6.220	.166
RA	27809985.333	1	27809985.333	10.531	.084
Vitamin-D * RA	100057650.083	1	100057650.083	37.888	.000
Error	21127002.000	8	2640875.250		
Total	80348601511.500	12			
Corrected Total	165421437.417	11			

a. R Squared = .872 (Adjusted R Squared = .824)

Appendix 5.6 Effect of vitamin D, RA on KG-1 cells at 48 hours

Between-Subjects Factors

		Value Label	N
Vitamin D	1	Presence	6
	2	Absent	6
RA	1	Presence	6
	2	Absent	6

Tests of Between-Subjects Effects

Dependent Variable: MFI

Source	Type III Sum of Squares	df	Mean Square	F	Sig.
Corrected Model	1287913985.550[a]	3	429304661.850	17.709	.001
Intercept	107998275744.513	1	107998275744.513	4454.975	.000
Vitamin-D	183383777.548	1	183383777.548	7.565	.025
RA	210655686.164	1	210655686.164	8.690	.018
Vitamin-D * RA	893874521.839	1	893874521.839	36.873	.000
Error	193937368.810	8	24242171.101		
Total	109480127098.873	12			
Corrected Total	1481851354.360	11			

a. R Squared = .869 (Adjusted R Squared = .820)

Appendix 5.7 Effect of vitamin D, RA on KG-1 cells at 72 hours

Between-Subjects Factors

		Value Label	N
Vitamin-D	1	Presence	6
	2	Absent	6
RA	1	Presence	6
	2	Absent	6

Tests of Between-Subjects Effects

Dependent Variable: MFI

Source	Type III Sum of Squares	df	Mean Square	F	Sig.
Corrected Model	619196681.583[a]	3	206398893.861	30.729	.000
Intercept	61920189666.750	1	61920189666.750	9218.651	.000
Vitamin-D	253285596.750	1	253285596.750	17.709	.000
RA	146629234.083	1	146629234.083	21.830	.002
Vitamin-D * RA	219281850.750	1	219281850.750	32.647	.000
Error	53734708.667	8	6716838.583		
Total	62593121057.000	12			
Corrected Total	672931390.250	11			

a. R Squared = .920 (Adjusted R Squared = .890)

Appendix 6.1 Reduction in total HLA-DR in SILAC labelled KG-1 cells

ANOVA

MFI

	Sum of Squares	df	Mean Square	F	Sig.
Between Groups	1746282071.036	1	1746282071.036	484.994	.000
Within Groups	14402502.598	4	3600625.649		
Total	1760684573.634	5			

Appendix 6.2 Effect of media switching on the alleles

Between-Subjects Factors

		Value Label	N
Allele	3	DRB3	8
	11	DRB1*11	8
	14	DRB1*14	8
Type	1	RPMI vs SILAC RPMI	12
	2	IMDM vs SILAC RPMI	12

Tests of Between-Subjects Effects

Dependent Variable: SILACvalue

Source	Type III Sum of Squares	df	Mean Square	F	Sig.
Corrected Model	243.330[a]	5	48.666	101.430	.000
Intercept	148991.890	1	148991.890	310529.158	.000
Allele	95.236	2	47.618	99.245	.000
Type	116.689	1	116.689	243.203	.000
Allele * Type	31.406	2	15.703	32.728	.000
Error	8.636	18	.480		
Total	149243.857	24			
Corrected Total	251.967	23			

a. R Squared = .966 (Adjusted R Squared = .956)

Type * Allele

Dependent Variable: SILACvalue

Type	Allele	Mean	Std. Error	95% Confidence Interval	
				Lower Bound	Upper Bound
RPMI vs SILAC RPMI	DRB3	77.743	.346	77.015	78.470
	DRB1*11	76.378	.346	75.650	77.105
	DRB1*14	75.638	.346	74.910	76.365
IMDM vs SILAC RPMI	DRB3	85.385	.346	84.657	86.113
	DRB1*11	79.293	.346	78.565	80.020
	DRB1*14	78.310	.346	77.582	79.038

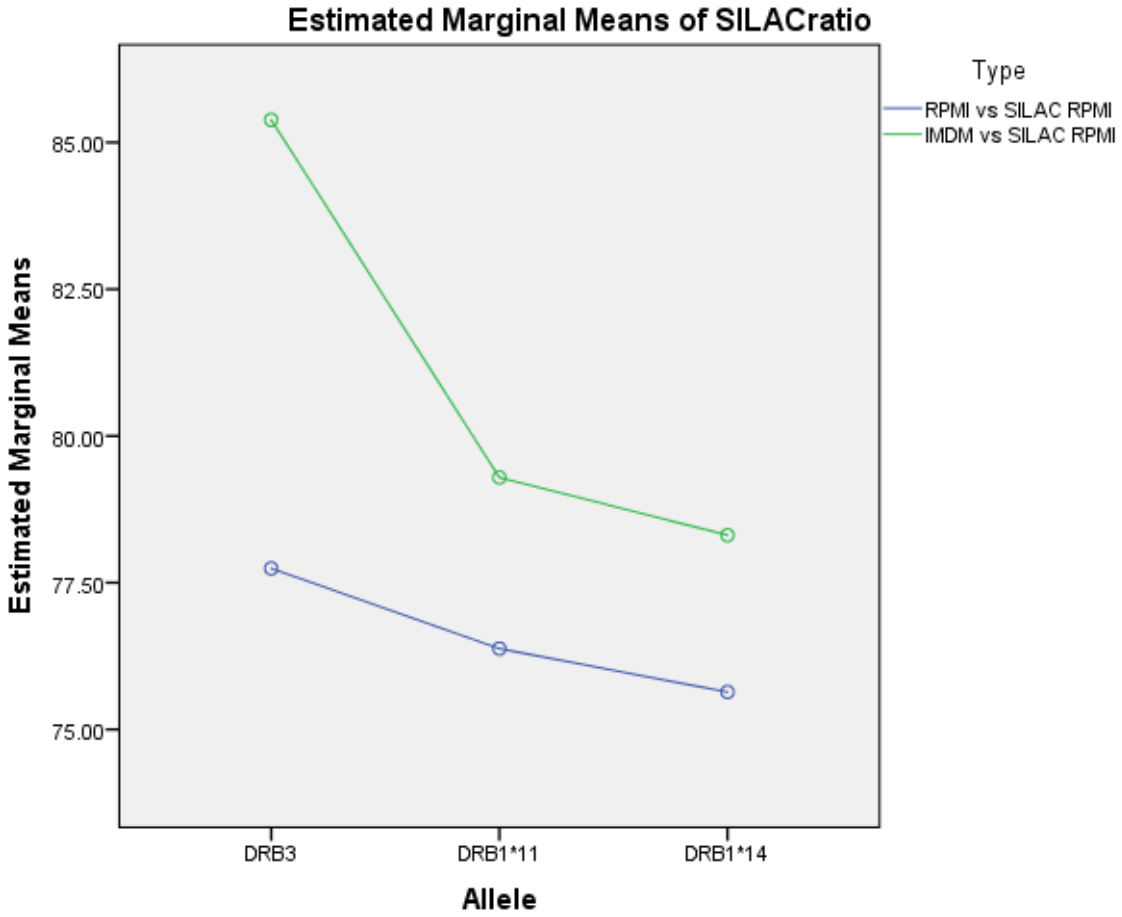

Post Hoc Tests

Multiple Comparisons

Dependent Variable: SILACratio

Tukey HSD

(I) Allele	(J) Allele	Mean Difference (I-J)	Std. Error	Sig.	95% Confidence Interval	
					Lower Bound	Upper Bound
DRB3	DRB1*11	3.7287*	.34634	.000	2.8448	4.6127
	DRB1*14	4.5900*	.34634	.000	3.7061	5.4739
DRB1*11	DRB3	-3.7287*	.34634	.000	-4.6127	-2.8448
	DRB1*14	.8612	.34634	.057	-.0227	1.7452
DRB1*14	DRB3	-4.5900*	.34634	.000	-5.4739	-3.7061
	DRB1*11	-.8612	.34634	.057	-1.7452	.0227

Based on observed means.

The error term is Mean Square(Error) = .480.

*. The mean difference is significant at the 0.05 level.

SILACratio

Tukey HSD[a,b]

Allele	N	Subset 1	Subset 2
DRB1*14	8	76.9738	
DRB1*11	8	77.8350	
DRB3	8		81.5638
Sig.		.057	1.000

Means for groups in homogeneous subsets are displayed.

Based on observed means.

The error term is Mean Square (Error) = .480.

a. Uses Harmonic Mean Sample Size = 8.000.

b. Alpha = 0.05.

Appendix 6.3 Baseline analysis of different alleles of KG-1

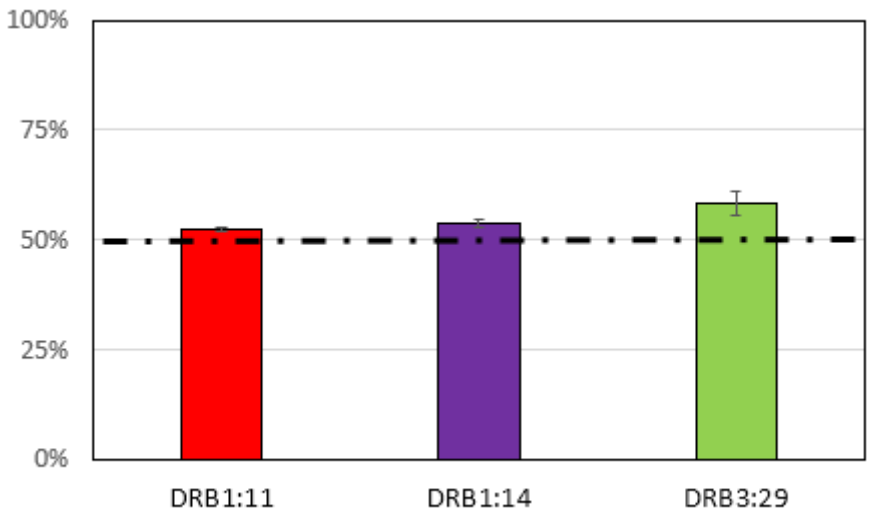

As described in Figure 6.16, KG-1 cultures (n=4) were treated with DMSO for 72 hours in light media. Extracts were mixed 1:1 (by protein content) with SILAC labelled KG-1cells. Mean % light ratios of the allele-specific DR β peptide sets were quantified from the SILAC ratios obtained after LC-MS. The colour coding is as per the Figure 6.7 and Table 6.1. The result describes that at baseline, DRB3 specific peptides had a slightly higher % light value than that of the DRB1 derived peptides

Appendix 6.4 Relative quantification of the effects of vitamin D and/or RA on HLA-DR alleles in KG-1 cells

Between-Subjects Factors

		Value Label	N
Allele	3	DRB3	16
	11	DRB1*11	16
	14	DRB1*14	16
Type	1	DMSO	12
	2	Vit D	12
	3	RA	12
	4	RA + Vit D	12

Tests of Between-Subjects Effects

Dependent Variable: SILAC ratio

Source	Type III Sum of Squares	df	Mean Square	F	Sig.
Corrected Model	6377.729[a]	11	579.794	263.376	.000
Intercept	106126.021	1	106126.021	48208.666	.000
Allele	57.792	2	28.896	13.126	.000
Type	5768.563	3	1922.854	873.473	.000
Allele * Type	551.375	6	91.896	41.744	.000
Error	79.250	36	2.201		
Total	112583.000	48			
Corrected Total	6456.979	47			

a. R Squared = .988 (Adjusted R Squared = .984)

Post Hoc Tests

Allele

Multiple Comparisons

Dependent Variable: SILAC ratio

Tukey HSD

(I) Allele	(J) Allele	Mean Difference (I-J)	Std. Error	Sig.	95% Confidence Interval Lower Bound	95% Confidence Interval Upper Bound
DRB3	DRB1*11	2.6250*	.52457	.000	1.3428	3.9072
	DRB1*14	1.8125*	.52457	.004	.5303	3.0947
DRB1*11	DRB3	-2.6250*	.52457	.000	-3.9072	-1.3428
	DRB1*14	-.8125	.52457	.281	-2.0947	.4697
DRB1*14	DRB3	-1.8125*	.52457	.004	-3.0947	-.5303
	DRB1*11	.8125	.52457	.281	-.4697	2.0947

Based on observed means.

The error term is Mean Square (Error) = 2.201.

*. The mean difference is significant at the 0.05 level.

Homogeneous Subsets

SILACratio

Tukey HSD[a,b]

Allele	N	Subset 1	Subset 2
DRB1*11	16	45.8750	
DRB1*14	16	46.6875	
DRB3	16		48.5000
Sig.		.281	1.000

Means for groups in homogeneous subsets are displayed.

Based on observed means.

The error term is Mean Square(Error) = 2.201.

a. Uses Harmonic Mean Sample Size = 16.000.

b. Alpha = 0.05.

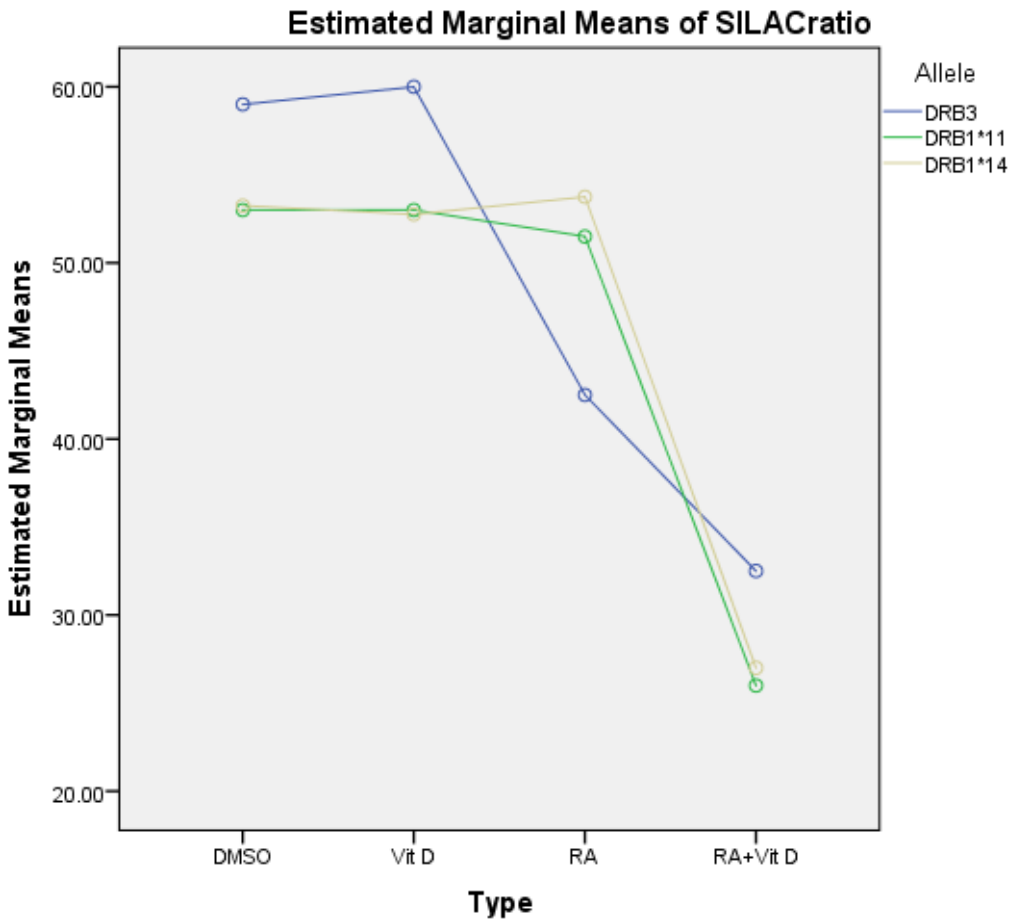
Estimated Marginal Means of SILACratio
Allele
DRB3
DRB1*11
DRB1*14
60.00
50.00
40.00
30.00
20.00
Estimated Marginal Means
DMSO
Vit D
RA
RA+Vit D
Type

Quality control of peptide presentation by MHC class II molecules: Selective degradation of empty molecules by an aspartyl protease

Nakul Shah[a], Sarah McDonald*[b], Alessandra De Riva[b], Michael J. Deery[c], Amin Oomatia[b], J.S. Hill Gaston[b], Robert Busch[a,b]* (* joint first authors)

[a] Dept of Life Sciences, University of Roehampton, London, UK; Depts of [b] Medicine and [c] Biochemistry (Cambridge Centre for Proteomics), University of Cambridge, Cambridge, UK

Introduction

- MHC class II (MHCII) molecules bind antigenic peptides in endosomes and present them on antigen-presenting cell (APC) surfaces for recognition by CD4⁺ T cells.[1]
- MHCII degradation is less well-characterised than synthesis and maturation (**Fig. 1**).[1] Ubiquitination targets MHCII molecules to endosomes/lysosomes for degradation,[2] yet nascent molecules acquire peptides in these compartments without being degraded.[1]
- The protease(s) that degrade MHCII remain unknown. Previous work suggests only a minor role for cysteine proteases [3] and no contribution from the serine protease, cathepsin G (CatD).[4]
- The role of aspartyl proteases in MHCII protein degradation has not yet been studied.
- Whether aspartyl proteases initiate degradation of MHCII-associated invariant chain (Ii)[5] has been disputed.[6]

Fig. 1. MHCII protein fate

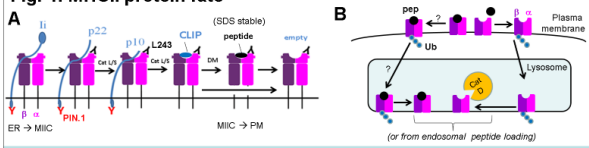

(A) Steps in MHCII maturation. HLA-DR reactivity with PIN.1 and L243 mAbs is indicated. (B) Selective degradation of empty mature DR by CatD. (The cleavage site may also be protected by Ii or DM.)

Objectives

1. To determine whether the lysosomal aspartyl proteases, cathepsin D (CatD) and/or cathepsin E (CatE) mediate MHCII protein degradation in APCs.

2. To determine which MHCII conformations are targeted for degradation.

Methods

- *In vitro* digestion of MHCII with CatD/E, SDS-PAGE and LC-MS/MS analysis
- CatD/E detection by Western blot
- CTSD/CTSE mRNA detection by RT-PCR
- Culture of APCs with pepstatin A (PepA), an aspartyl protease inhibitor, and analysis of rescued MHCII molecules by flow cytometry and Western blot

Fig. 2. MHCII proteins are rescued from degradation by pepstatin A (PepA)

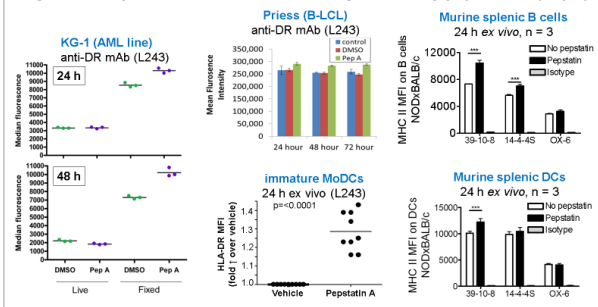

Cells were treated with 20 uM PepA, vehicle control (DMSO), or nothing, cultured for 24-72 h, fixed and permeabilised (unless specified), stained with MHCII-specific mAb-FITC, and analysed by flow cytometry.

Fig. 3. Expression of lysosomal aspartyl cathepsins D and E in Priess and KG-1 cells

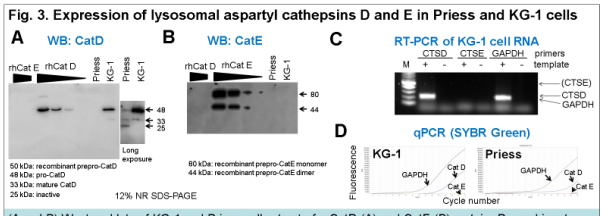

(A and B) Western blots of KG-1 and Priess cell extracts for CatD (A) and CatE (B) protein. Recombinant prepro-CatD and E were used as quantitative standards and specificity controls. (C) Agarose gels of CTSD, CTSE, and GAPDH RT-PCR products from KG-1 cells. (D) Quantitative RT-PCR amplification curves.

Conclusion 1: CatD initiates HLA-DR degradation

- PepA, a specific inhibitor of the lysosomal aspartyl proteases, CatD and CatE, rescued intracellular HLA-DR molecules from degradation in immature MoDC and in KG-1 acute myeloid leukaemia cells (**Fig 2**).
- There was less rescue by PepA, or none, in cells known [7] to have low DR protein turnover (LPS-activated MoDC or Priess B-LCL; **Fig 2**).
- Some mouse MHCII alleles were rescued by PepA (**Fig 2**).
- KG-1 cells expressed CTSD mRNA and CatD protein, but no evidence for CTSE mRNA or CatE protein expression was found (**Fig 3**).
- Formal proof that CatD mediates HLA-DR degradation will require genetic ablation of CatD expression (ongoing work).
- Partial digestion of soluble recombinant HLA-DR with CatD *in vitro* produced defined fragments, with initial cleavage between αPhe54 and αGlu55, a highly conserved, surface-accessible site (**Fig. 4**).

Fig. 4. CatD cleaves HLA-DRα at the peptide-binding groove

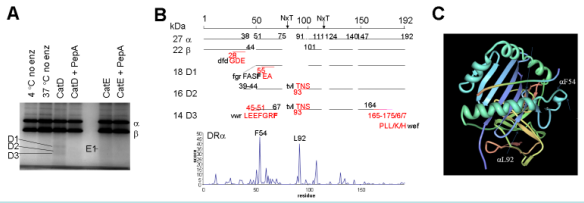

(A) SDS-PAGE analysis of recombinant soluble HLA-DR molecules after digestion with recombinant human CatD or CatE with or without PepA. (B) Mapping of intact DR chains and CatD fragments of DRα by Orbitrap LC-MS/MS analysis of tryptic digests, compared with cleavage preferences predicted from the MEROPS database. (C) Key cleavage sites in the crystal structure of HLA-DR. The CatD cleavage site of the largest (D1) fragment at αF54/αE55 is exposed but would be protected by peptide, DM, or Ii binding.

Conclusion 2: Empty mature HLA-DR is degraded by CatD

- CatD cleavage *in vitro* mapped to a site in DRα that interacts with bound peptide and changes conformation when peptides bind (**Fig. 4**).
- PepA rescued conformationally mature (L243-reactive) DR molecules, which accumulated slowly (**Fig. 5**)
- PepA did not rescue Ii or its fragments in KG-1 cells (**Fig. 5**), despite previous claims.[5] Thus, immature Ii/DR complexes are not targeted by CatD. CLIP/DR was not detected in KG-1 cells (not shown).
- In KG-1 cells, PepA rescued SDS-unstable DR molecules but had no effect on SDS-stable DR levels (**Fig. 5**), suggesting that DR molecules lacking stably bound peptides are selectively degraded.

Fig. 5. Rescue of SDS-unstable, Ii-non-associated HLA-DR by Pep A in KG-1 cells

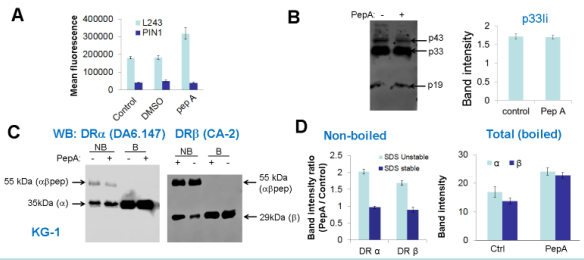

KG-1 cells were treated with 20 μM PepA or vehicle for 48h and analysed. (A) Rescue of different HLA-DR-associated epitopes (cf. Fig. 1A) measured by flow cytometry in fixed, permeabilised cells. L243 reacts poorly with immature, Ii-associated DR , but well with all other forms of DR. PIN.1 reacts with the cytoplasmic tail of intact Ii and Ii degradation intermediates. (B) Western blot for Ii (PIN.1) confirms the lack of PepA effect on levels of Ii and its degradation intermediates. (C) Selective rescue of SDS-unstable HLA-DR molecules by PepA. Cell extracts were made in RIPA buffer, resolved by SDS-PAGE with or without boiling, and probed with antibodies to DRα or β. (D) Quantification of (C).

Funded by:

- Arthritis Research UK
- University of Roehampton
- MS Society (UK)
- MS International Federation

References

1. Busch & Mellins (1996) *Curr Opin Immunol* **8:** 51; Neefjes (2011) *Nat Immunol* **11**:823
2. Shin et al. (2006) *Nature* **444**:115
3. Herrmann et al. (2007) *J Leukoc Biol* **82**:686
4. Burster et al. (2010) *Immunology* **130:** 436
5. Maric et al. (1994) *PNAS* **91**:2171
6. Villadangos et al. (1997) *J Exp Med* **186**:549; Deussing et al. (1998) *PNAS* **95:** 4516
7. De Riva et al. (2010) *Anal Biochem* **403**:1; Prevosto et al. (2016) *PLoS One* 11: e0161011

Bibliography

2006. RIPA buffer (05-01). *Cold Spring Harbor Protocols,* 2006**,** pdb.rec10617.

2007. Genome-wide association study of 14,000 cases of seven common diseases and 3,000 shared controls. *Nature,* 447**,** 661-678.

ACKERMAN, A. L. & CRESSWELL, P. 2003. Regulation of MHC class I transport in human dendritic cells and the dendritic-like cell line KG-1. *J Immunol,* 170**,** 4178-88.

ADAMSON, P. C. 1996. All-Trans-Retinoic Acid Pharmacology and Its Impact on the Treatment of Acute Promyelocytic Leukemia. *The Oncologist,* 1**,** 305-314.

ALBERT, L. J. & INMAN, R. D. 1999. Molecular mimicry and autoimmunity. *N Engl J Med,* 341**,** 2068-74.

ALCINA, A., ABAD-GRAU MDEL, M., FEDETZ, M., IZQUIERDO, G., LUCAS, M., FERNANDEZ, O., NDAGIRE, D., CATALA-RABASA, A., RUIZ, A., GAYAN, J., DELGADO, C., ARNAL, C. & MATESANZ, F. 2012. Multiple sclerosis risk variant HLA-DRB1*1501 associates with high expression of DRB1 gene in different human populations. *PLoS One,* 7**,** e29819.

ALROY, I., TOWERS, T. L. & FREEDMAN, L. P. 1995. Transcriptional repression of the interleukin-2 gene by vitamin D3: direct inhibition of NFATp/AP-1 complex formation by a nuclear hormone receptor. *Mol Cell Biol,* 15**,** 5789-99.

ALVAREZ, D., VOLLMANN, E. H. & VON ANDRIAN, U. H. 2008. Mechanisms and Consequences of Dendritic Cell Migration. *Immunity,* 29**,** 325.

ANAND, P. K., KAUL, D. & SHARMA, M. 2008. Synergistic action of vitamin D and retinoic acid restricts invasion of macrophages by pathogenic mycobacteria. *J Microbiol Immunol Infect,* 41**,** 17-25.

ANDERSSON, G. 1998. Evolution of the human HLA-DR region. *Front Biosci,* 3**,** d739-45.

ANDERSSON, G., SVENSSON, A.-C., SETTERBLAD, N. & RASK, L. Retroelements in the human MHC class II region. *Trends in Genetics,* 14**,** 109-114.

ANDERSSON, G., SVENSSON, A.-C., SETTERBLAD, N. & RASK, L. 1998. Retroelements in the human MHC class II region. *Trends in Genetics,* 14**,** 109-114.

ANDERTON, S. M. 2004. Post-translational modifications of self antigens: implications for autoimmunity. *Curr Opin Immunol,* 16**,** 753-8.

ARANDA, A. & PASCUAL, A. 2001. Nuclear hormone receptors and gene expression. *Physiol Rev,* 81**,** 1269-304.

ASCHERIO, A. 2013. Environmental factors in multiple sclerosis. *Expert Rev Neurother,* 13**,** 3-9.

ASCHERIO, A., MUNGER, K. L., LENNETTE, E. T., SPIEGELMAN, D., HERNAN, M. A., OLEK, M. J., HANKINSON, S. E. & HUNTER, D. J. 2001. Epstein-Barr virus antibodies and risk of multiple sclerosis: a prospective study. *JAMA,* 286**,** 3083-8.

BAKDASH, G., VAN CAPEL, T. M., MASON, L. M., KAPSENBERG, M. L. & DE JONG, E. C. 2014. Vitamin D3 metabolite calcidiol primes human dendritic cells to promote the development of immunomodulatory IL-10-producing T cells. *Vaccine,* 32**,** 6294-302.

BAKER, D. & AMOR, S. 2014. Experimental autoimmune encephalomyelitis is a good model of multiple sclerosis if used wisely. *Mult Scler Relat Disord,* 3**,** 555-64.

BALDWIN, M. A. 2004. Protein identification by mass spectrometry: issues to be considered. *Mol Cell Proteomics,* 3**,** 1-9.

BALLERINI, C., GUERINI, F. R., ROMBOLA, G., ROSATI, E., MASSACESI, L., FERRANTE, P., CAPUTO, D., TALAMANCA, L. F., NALDI, P., LIGUORI, M., ALIZADEH, M., MOMIGLIANO-RICHIARDI, P. & D'ALFONSO, S. 2004. HLA-multiple sclerosis association in continental Italy and correlation with disease prevalence in Europe. *J Neuroimmunol,* 150**,** 178-85.

BALLOW, M., XIANG, S., WANG, W. & BRODSKY, L. 1996. The effects of retinoic acid on immunoglobulin synthesis: role of interleukin 6. *J Clin Immunol,* 16**,** 171-9.

BALTIMORE, D. 1970. RNA-dependent DNA polymerase in virions of RNA tumour viruses. *Nature,* 226**,** 1209-11.

BANTSCHEFF, M., SCHIRLE, M., SWEETMAN, G., RICK, J. & KUSTER, B. 2007. Quantitative mass spectrometry in proteomics: a critical review. *Anal Bioanal Chem,* 389**,** 1017-31.
BARBER, H. R. 1980. Introduction to immunology. *Mt Sinai J Med,* 47**,** 427-37.
BARRAGAN, M., GOOD, M. & KOLLS, J. K. 2015. Regulation of Dendritic Cell Function by Vitamin D. *Nutrients,* 7**,** 8127-51.
BARRETT, J. C., HANSOUL, S., NICOLAE, D. L., CHO, J. H., DUERR, R. H., RIOUX, J. D., BRANT, S. R., SILVERBERG, M. S., TAYLOR, K. D., BARMADA, M. M., BITTON, A., DASSOPOULOS, T., DATTA, L. W., GREEN, T., GRIFFITHS, A. M., KISTNER, E. O., MURTHA, M. T., REGUEIRO, M. D., ROTTER, J. I., SCHUMM, L. P., STEINHART, A. H., TARGAN, S. R., XAVIER, R. J., THE, N. I. B. D. G. C., LIBIOULLE, C., SANDOR, C., LATHROP, M., BELAICHE, J., DEWIT, O., GUT, I., HEATH, S., LAUKENS, D., MNI, M., RUTGEERTS, P., VAN GOSSUM, A., ZELENIKA, D., FRANCHIMONT, D., HUGOT, J. P., DE VOS, M., VERMEIRE, S., LOUIS, E., THE BELGIAN-FRENCH, I. B. D. C., THE WELLCOME TRUST CASE CONTROL, C., CARDON, L. R., ANDERSON, C. A., DRUMMOND, H., NIMMO, E., AHMAD, T., PRESCOTT, N. J., ONNIE, C. M., FISHER, S. A., MARCHINI, J., GHORI, J., BUMPSTEAD, S., GWILLAM, R., TREMELLING, M., DELOUKAS, P., MANSFIELD, J., JEWELL, D., SATSANGI, J., MATHEW, C. G., PARKES, M., GEORGES, M. & DALY, M. J. 2008. Genome-wide association defines more than thirty distinct susceptibility loci for Crohn's disease. *Nature genetics,* 40**,** 955-962.
BASTIE, J. N., BALITRAND, N., GUIDEZ, F., GUILLEMOT, I., LARGHERO, J., CALABRESSE, C., CHOMIENNE, C. & DELVA, L. 2004. 1 alpha,25-dihydroxyvitamin D3 transrepresses retinoic acid transcriptional activity via vitamin D receptor in myeloid cells. *Mol Endocrinol,* 18**,** 2685-99.
BEN-NUN, A., KAUSHANSKY, N., KAWAKAMI, N., KRISHNAMOORTHY, G., BERER, K., LIBLAU, R., HOHLFELD, R. & WEKERLE, H. 2014. From classic to spontaneous and humanized models of multiple sclerosis: impact on understanding pathogenesis and drug development. *J Autoimmun,* 54**,** 33-50.
BENES, P., VETVICKA, V. & FUSEK, M. 2008. CATHEPSIN D – MANY FUNCTIONS OF ONE ASPARTIC PROTEASE. *Critical reviews in oncology/hematology,* 68**,** 12-28.
BERGES, C., NAUJOKAT, C., TINAPP, S., WIECZOREK, H., HÖH, A., SADEGHI, M., OPELZ, G. & DANIEL, V. 2005. A cell line model for the differentiation of human dendritic cells. *Biochemical and Biophysical Research Communications,* 333**,** 896-907.
BISCHOFF-FERRARI, H. A., DAWSON-HUGHES, B., STOCKLIN, E., SIDELNIKOV, E., WILLETT, W. C., EDEL, J. O., STAHELIN, H. B., WOLFRAM, S., JETTER, A., SCHWAGER, J., HENSCHKOWSKI, J., VON ECKARDSTEIN, A. & EGLI, A. 2012. Oral supplementation with 25(OH)D3 versus vitamin D3: effects on 25(OH)D levels, lower extremity function, blood pressure, and markers of innate immunity. *J Bone Miner Res,* 27**,** 160-9.
BLOMHOFF, H. K., SMELAND, E. B., ERIKSTEIN, B., RASMUSSEN, A. M., SKREDE, B., SKJONSBERG, C. & BLOMHOFF, R. 1992. Vitamin A is a key regulator for cell growth, cytokine production, and differentiation in normal B cells. *J Biol Chem,* 267**,** 23988-92.
BLOMHOFF, R. & BLOMHOFF, H. K. 2006. Overview of retinoid metabolism and function. *J Neurobiol,* 66**,** 606-30.
BLUM, J. S., WEARSCH, P. A. & CRESSWELL, P. 2013. Pathways of Antigen Processing. *Annual review of immunology,* 31**,** 443-473.
BONIFACINO, J. S. & DELL'ANGELICA, E. C. 2001. Immunoprecipitation. *Current Protocols in Cell Biology.* John Wiley & Sons, Inc.
BONILLA, F. A. & OETTGEN, H. C. 2010. Adaptive immunity. *J Allergy Clin Immunol,* 125**,** S33-40.
BRACHET, V., RAPOSO, G., AMIGORENA, S. & MELLMAN, I. 1997. Ii Chain Controls the Transport of Major Histocompatibility Complex Class II Molecules to and from Lysosomes. *The Journal of Cell Biology,* 137**,** 51-65.
BRIX, K. 2005. Lysosomal Proteases. *In:* SAFTIG, P. (ed.) *Lysosomes.* Boston, MA: Springer US.
BRODSKY, F. M., PARHAM, P., BARNSTABLE, C. J., CRUMPTON, M. J. & BODMER, W. F. 1979. Monoclonal antibodies for analysis of the HLA system. *Immunol Rev,* 47**,** 3-61.

BROUX, B., STINISSEN, P. & HELLINGS, N. 2013. Which immune cells matter? The immunopathogenesis of multiple sclerosis. *Crit Rev Immunol,* 33**,** 283-306.
BROWN, J. H., JARDETZKY, T. S., GORGA, J. C., STERN, L. J., URBAN, R. G., STROMINGER, J. L. & WILEY, D. C. 1993. 3-DIMENSIONAL STRUCTURE OF THE HUMAN CLASS-II HISTOCOMPATIBILITY ANTIGEN HLA-DR1. *Nature,* 364**,** 33-39.
BRUBAKER, S. W., BONHAM, K. S., ZANONI, I. & KAGAN, J. C. 2015. Innate Immune Pattern Recognition: A Cell Biological Perspective. *Annual review of immunology,* 33**,** 257-290.
BSCHEIDER, M. & BUTCHER, E. C. 2016. Vitamin D immunoregulation through dendritic cells. *Immunology,* 148**,** 227-236.
BURSTER, T., BECK, A., TOLOSA, E., MARIN-ESTEBAN, V., ROTZSCHKE, O., FALK, K., LAUTWEIN, A., REICH, M., BRANDENBURG, J., SCHWARZ, G., WIENDL, H., MELMS, A., LEHMANN, R., STEVANOVIC, S., KALBACHER, H. & DRIESSEN, C. 2004. Cathepsin G, and not the asparagine-specific endoprotease, controls the processing of myelin basic protein in lysosomes from human B lymphocytes. *J Immunol,* 172**,** 5495-503.
BURSTER, T., MACMILLAN, H., HOU, T. Y., SCHILLING, J., TRUONG, P., BOEHM, B. O., ZOU, F., LAU, K., STROHMAN, M., SCHAFFERT, S., BUSCH, R. & MELLINS, E. D. 2010. Masking of a cathepsin G cleavage site in vivo contributes to the proteolytic resistance of major histocompatibility complex class II molecules. *Immunology,* 130**,** 436-446.
BUSCH, R., CLOUTIER, I., SEKALY, R. P. & HAMMERLING, G. J. 1996. Invariant chain protects class II histocompatibility antigens from binding intact polypeptides in the endoplasmic reticulum. *Embo Journal,* 15**,** 418-428.
BUSCH, R. & DE RIVA, A. 2013. MHC Class II Protein Turnover In vivo and Its Relevance for Autoimmunity in Non-Obese Diabetic Mice. *Frontiers in Immunology,* 4.
BUSCH, R., DE RIVA, A., HADJINICOLAOU, A. V., JIANG, W., HOU, T. & MELLINS, E. D. 2012. On the perils of poor editing: Regulation of peptide loading by HLA-DQ and H2-A molecules associated with celiac disease and type 1 diabetes. *Expert reviews in molecular medicine,* 14**,** e15-e15.
BUSCH, R., DOEBELE, R. C., VON SCHEVEN, E., FAHRNI, J. & MELLINS, E. D. 1998. Aberrant intermolecular disulfide bonding in a mutant HLA-DM molecule: implications for assembly, maturation, and function. *J Immunol,* 160**,** 734-43.
BUSCH, R. & MELLINS, E. D. 1996. Developing and shedding inhibitions: How MHC class II molecules reach maturity. *Current Opinion in Immunology,* 8**,** 51-58.
BUSCH, R., RINDERKNECHT, C. H., ROH, S., LEE, A. W., HARDING, J. J., BURSTER, T., HORNELL, T. M. & MELLINS, E. D. 2005. Achieving stability through editing and chaperoning: regulation of MHC class II peptide binding and expression. *Immunol Rev,* 207**,** 242-60.
BUSTIN, S. A. 2002. Quantification of mRNA using real-time reverse transcription PCR (RT-PCR): trends and problems. *J Mol Endocrinol,* 29**,** 23-39.
CALLIS, J. 2014. The Ubiquitination Machinery of the Ubiquitin System. *The Arabidopsis Book / American Society of Plant Biologists,* 12**,** e0174.
CALVO, M. S., WHITING, S. J. & BARTON, C. N. 2005. Vitamin D Intake: A Global Perspective of Current Status. *The Journal of Nutrition,* 135**,** 310-316.
CANNING, M. O., GROTENHUIS, K., DE WIT, H., RUWHOF, C. & DREXHAGE, H. A. 2001. 1-alpha,25-Dihydroxyvitamin D3 (1,25(OH)(2)D(3)) hampers the maturation of fully active immature dendritic cells from monocytes. *Eur J Endocrinol,* 145**,** 351-7.
CHAIN, B. M., FREE, P., MEDD, P., SWETMAN, C., TABOR, A. B. & TERRAZZINI, N. 2005. The expression and function of cathepsin E in dendritic cells. *J Immunol,* 174**,** 1791-800.
CHAMBERS, E. S. & HAWRYLOWICZ, C. M. 2011. The impact of vitamin D on regulatory T cells. *Curr Allergy Asthma Rep,* 11**,** 29-36.
CHAPLIN, D. D. 2006. 1. Overview of the human immune response. *Journal of Allergy and Clinical Immunology,* 117**,** S430-S435.
CHAPLIN, D. D. 2010. Overview of the Immune Response. *The Journal of allergy and clinical immunology,* 125**,** S3-23.
CHEN, J. J., HOLLENBACH, J. A., TRACHTENBERG, E. A., JUST, J. J., CARRINGTON, M., RONNINGEN, K. S., BEGOVICH, A., KING, M. C., MCWEENEY, S., MACK, S. J.,

ERLICH, H. A. & THOMSON, G. 1999. Hardy-Weinberg testing for HLA class II (DRB1, DQA1, DQB1, and DPB1) loci in 26 human ethnic groups. *Tissue Antigens,* 54**,** 533-42.
CHEN, S., SIMS, G. P., CHEN, X. X., GU, Y. Y., CHEN, S. & LIPSKY, P. E. 2007. Modulatory effects of 1,25-dihydroxyvitamin D3 on human B cell differentiation. *J Immunol,* 179**,** 1634-47.
CHICZ, R. M., URBAN, R. G., LANE, W. S., GORGA, J. C., STERN, L. J., VIGNALI, D. A. & STROMINGER, J. L. 1992. Predominant naturally processed peptides bound to HLA-DR1 are derived from MHC-related molecules and are heterogeneous in size. *Nature,* 358**,** 764-8.
CHOKKATHUKALAM, A., KIM, D. H., BARRETT, M. P., BREITLING, R. & CREEK, D. J. 2014. Stable isotope-labeling studies in metabolomics: new insights into structure and dynamics of metabolic networks. *Bioanalysis,* 6**,** 511-24.
CHOO, S. Y. 2007. The HLA System: Genetics, Immunology, Clinical Testing, and Clinical Implications. *Yonsei Medical Journal,* 48**,** 11-23.
CHRISTEN, U., BENDER, C. & VON HERRATH, M. G. 2012. Infection as a cause of type 1 diabetes? *Current opinion in rheumatology,* 24**,** 417-423.
CLARK, D. P. & PAZDERNIK, N. J. 2013. Chapter e15 - Proteomics: The Global Analysis of Proteins. *Molecular Biology (Second Edition)*. Boston: Academic Press.
CLEMENS, T. L., ADAMS, J. S., HENDERSON, S. L. & HOLICK, M. F. 1982. Increased skin pigment reduces the capacity of skin to synthesise vitamin D3. *Lancet,* 1**,** 74-6.
COCCO, E., MELONI, A., MURRU, M. R., CORONGIU, D., TRANQUILLI, S., FADDA, E., MURRU, R., SCHIRRU, L., SECCI, M. A., COSTA, G., ASUNIS, I., CUCCU, S., FENU, G., LOREFICE, L., CARBONI, N., MURA, G., ROSATELLI, M. C. & MARROSU, M. G. 2012. Vitamin D Responsive Elements within the HLA-DRB1 Promoter Region in Sardinian Multiple Sclerosis Associated Alleles. *PLOS ONE,* 7**,** e41678.
COCCO, E., MURRU, R., COSTA, G., KUMAR, A., PIERONI, E., MELIS, C., BARBERINI, L., SARDU, C., LOREFICE, L., FENU, G., FRAU, J., COGHE, G., CARBONI, N. & MARROSU, M. G. 2013. Interaction between HLA-DRB1-DQB1 Haplotypes in Sardinian Multiple Sclerosis Population. *PLOS ONE,* 8**,** e59790.
COLBERT JEFF, D., MATTHEWS STEPHEN, P., MILLER, G. & WATTS, C. 2009. Diverse regulatory roles for lysosomal proteases in the immune response. *European Journal of Immunology,* 39**,** 2955-2965.
COLE, D. K. 2013. Re-directing CD4+ T cell responses with the flanking residues of MHC class II-bound peptides: the core is not enough. *Frontiers in Immunology,* 4.
COMPSTON, A. & COLES, A. 2002. Multiple sclerosis. *Lancet,* 359**,** 1221-31.
CORREALE, J. & FAREZ, M. F. 2013. Modulation of multiple sclerosis by sunlight exposure: role of cis-urocanic acid. *J Neuroimmunol,* 261**,** 134-40.
COSSON, P. & BONIFACINO, J. S. 1992. Role of transmembrane domain interactions in the assembly of class II MHC molecules. *Science,* 258**,** 659-62.
COSTANTINO, C. M., HANG, H. C., KENT, S. C., HAFLER, D. A. & PLOEGH, H. L. 2008. Lysosomal cysteine and aspartic proteases are heterogeneously expressed and act redundantly to initiate human invariant chain degradation. *J Immunol,* 180**,** 2876-85.
COX, J. & MANN, M. 2008. MaxQuant enables high peptide identification rates, individualized p.p.b.-range mass accuracies and proteome-wide protein quantification. *Nat Biotechnol,* 26**,** 1367-72.
CRESSWELL, P. 1996. Invariant chain structure and MHC class II function. *Cell,* 84**,** 505-7.
DANG, Z. C. & LOWIK, C. W. 2005. Removal of serum factors by charcoal treatment promotes adipogenesis via a MAPK-dependent pathway. *Mol Cell Biochem,* 268**,** 159-67.
DANKERS, W., COLIN, E. M., VAN HAMBURG, J. P. & LUBBERTS, E. 2016. Vitamin D in Autoimmunity: Molecular Mechanisms and Therapeutic Potential. *Front Immunol,* 7**,** 697.
DARMANIN, S., CHEN, J., ZHAO, S., CUI, H., SHIRKOOHI, R., KUBO, N., KUGE, Y., TAMAKI, N., NAKAGAWA, K., HAMADA, J., MORIUCHI, T. & KOBAYASHI, M. 2007. All-trans retinoic acid enhances murine dendritic cell migration to draining lymph nodes via the balance of matrix metalloproteinases and their inhibitors. *J Immunol,* 179**,** 4616-25.

DASGUPTA, R. & FOWLER, C. J. 2003. Bladder, bowel and sexual dysfunction in multiple sclerosis: management strategies. *Drugs,* 63**,** 153-66.
DAUSSET, J. 1981. The major histocompatibility complex in man. *Science,* 213**,** 1469-74.
DAVIS, M. M. & BJORKMAN, P. J. 1988. T-cell antigen receptor genes and T-cell recognition. *Nature,* 334**,** 395-402.
DE GASSART, A., CAMOSSETO, V., THIBODEAU, J., CEPPI, M., CATALAN, N., PIERRE, P. & GATTI, E. 2008. MHC class II stabilization at the surface of human dendritic cells is the result of maturation-dependent MARCH I down-regulation. *Proc Natl Acad Sci U S A,* 105**,** 3491-6.
DE GASSART, A., DE ANGELIS RIGOTTI, F. & GATTI, E. 2013. MHC-II Ubiquitination. *In:* VAN ENDERT, P. (ed.) *Antigen Processing: Methods and Protocols.* Totowa, NJ: Humana Press.
DE RIVA, A., DEERY, M. J., MCDONALD, S., LUND, T. & BUSCH, R. 2010. Measurement of protein synthesis using heavy water labeling and peptide mass spectrometry: Discrimination between major histocompatibility complex allotypes. *Anal Biochem,* 403**,** 1-12.
DE RIVA, A., VARLEY, M. C., BLUCK, L. J., COOKE, A., DEERY, M. J. & BUSCH, R. 2013. Accelerated turnover of MHC class II molecules in NOD mice is developmentally and environmentally regulated in vivo and dispensable for autoimmunity(). *Journal of immunology (Baltimore, Md. : 1950),* 190**,** 5961-5971.
DEFACQUE, H., COMMES, T., SEVILLA, C., ROCHETTEEGLY, C. & MARTI, J. 1994. Synergistic Differentiation of U937 Cells by All-Trans Retinoic Acid and 1α,25-Dihydroxyvitamin D3 Is Associated with the Expression of Retinoid X Receptor α. *Biochemical and Biophysical Research Communications,* 203**,** 272-280.
DELENDA, C. 2004. Lentiviral vectors: optimization of packaging, transduction and gene expression. *J Gene Med,* 6 Suppl 1**,** S125-38.
DEMBINSKI, T. C., LEUNG, C. K. & SHIU, R. P. 1985. Evidence for a novel pituitary factor that potentiates the mitogenic effect of estrogen in human breast cancer cells. *Cancer Res,* 45**,** 3083-9.
DENDROU, C. A., FUGGER, L. & FRIESE, M. A. 2015. Immunopathology of multiple sclerosis. *Nat Rev Immunol,* 15**,** 545-558.
DENZIN, L. K. & CRESSWELL, P. 1995. HLA-DM INDUCES CLIP DISSOCIATION FROM MHC CLASS-II ALPHA-BETA DIMERS AND FACILITATES PEPTIDE LOADING. *Cell,* 82**,** 155-165.
DEROSSI, D., CALVET, S., TREMBLEAU, A., BRUNISSEN, A., CHASSAING, G. & PROCHIANTZ, A. 1996. Cell internalization of the third helix of the Antennapedia homeodomain is receptor-independent. *J Biol Chem,* 271**,** 18188-93.
DEROSSI, D., JOLIOT, A. H., CHASSAING, G. & PROCHIANTZ, A. 1994. The third helix of the Antennapedia homeodomain translocates through biological membranes. *J Biol Chem,* 269**,** 10444-50.
DEUSSING, J., ROTH, W., SAFTIG, P., PETERS, C., PLOEGH, H. L. & VILLADANGOS, J. A. 1998. Cathepsins B and D are dispensable for major histocompatibility complex class II-mediated antigen presentation. *Proceedings of the National Academy of Sciences of the United States of America,* 95**,** 4516-4521.
DISANTO, G., MORAHAN, J. M., BARNETT, M. H., GIOVANNONI, G. & RAMAGOPALAN, S. V. 2012. The evidence for a role of B cells in multiple sclerosis. *Neurology,* 78**,** 823-832.
DOLATI, S., BABALOO, Z., JADIDI-NIARAGH, F., AYROMLOU, H., SADREDDINI, S. & YOUSEFI, M. 2017. Multiple sclerosis: Therapeutic applications of advancing drug delivery systems. *Biomedicine & Pharmacotherapy,* 86**,** 343-353.
DUAN, S., LV, Z., FAN, X., WANG, L., HAN, F., WANG, H. & BI, S. 2014. Vitamin D status and the risk of multiple sclerosis: a systematic review and meta-analysis. *Neurosci Lett,* 570**,** 108-13.
DUNCKLEY, H. 2012. HLA typing by SSO and SSP methods. *Methods Mol Biol,* 882**,** 9-25.
DYMENT, D. A., EBERS, G. C. & DESSA SADOVNICK, A. 2004. Genetics of multiple sclerosis. *The Lancet Neurology,* 3**,** 104-110.

EDER, J., HOMMEL, U., CUMIN, F., MARTOGLIO, B. & GERHARTZ, B. 2007. Aspartic proteases in drug discovery. *Curr Pharm Des,* 13**,** 271-85.
ELIUK, S. & MAKAROV, A. 2015. Evolution of Orbitrap Mass Spectrometry Instrumentation. *Annu Rev Anal Chem (Palo Alto Calif),* 8**,** 61-80.
EMERSON, M. R., GALLAGHER, R. J., MARQUIS, J. G. & LEVINE, S. M. 2009. Enhancing the ability of experimental autoimmune encephalomyelitis to serve as a more rigorous model of multiple sclerosis through refinement of the experimental design. *Comp Med,* 59**,** 112-28.
ERCOLINI, A. M. & MILLER, S. D. 2009. The role of infections in autoimmune disease. *Clinical and Experimental Immunology,* 155**,** 1-15.
ERICKSON, R. P. 1987. Natural history of the major histocompatibility complex. *American Journal of Human Genetics,* 40**,** 468-469.
ERKELENS, M. N. & MEBIUS, R. E. 2017. Retinoic Acid and Immune Homeostasis: A Balancing Act. *Trends Immunol,* 38**,** 168-180.
FAGNANI, C., NEALE, M. C., NISTICO, L., STAZI, M. A., RICIGLIANO, V. A., BUSCARINU, M. C., SALVETTI, M. & RISTORI, G. 2015. Twin studies in multiple sclerosis: A meta-estimation of heritability and environmentality. *Mult Scler,* 21**,** 1404-13.
FERNANDO, M. M., STEVENS, C. R., WALSH, E. C., DE JAGER, P. L., GOYETTE, P., PLENGE, R. M., VYSE, T. J. & RIOUX, J. D. 2008. Defining the role of the MHC in autoimmunity: a review and pooled analysis. *PLoS Genet,* 4**,** e1000024.
FERRANTE, A. 2013. For Many But Not For All: How The Conformational Flexibility Of The Peptide/Mhcii Complex Shapes Epitope Selection. *Immunologic research,* 56**,** 85-95.
FINLEY, E. M. & KORNFELD, S. 1994. Subcellular localization and targeting of cathepsin E. *J Biol Chem,* 269**,** 31259-66.
FOGDELL, A., HILLERT, J., SACHS, C. & OLERUP, O. 1995. The multiple sclerosis- and narcolepsy-associated HLA class II haplotype includes the DRB5*0101 allele. *Tissue Antigens,* 46**,** 333-336.
FOWLER, S. D., KAY, J., DUNN, B. M. & TATNELL, P. J. 1995. Monomeric human cathepsin E. *FEBS Letters,* 366**,** 72-74.
FREEDMAN, D. M., DOSEMECI, M. & ALAVANJA, M. C. 2000. Mortality from multiple sclerosis and exposure to residential and occupational solar radiation: a case-control study based on death certificates. *Occup Environ Med,* 57**,** 418-21.
FRIEDRICHS, B., TEPEL, C., REINHECKEL, T., DEUSSING, J., VON FIGURA, K., HERZOG, V., PETERS, C., SAFTIG, P. & BRIX, K. 2003. Thyroid functions of mouse cathepsins B, K, and L. *Journal of Clinical Investigation,* 111**,** 1733-1745.
FURLEY, A. J., REEVES, B. R., MIZUTANI, S., ALTASS, L. J., WATT, S. M., JACOB, M. C., VAN DEN ELSEN, P., TERHORST, C. & GREAVES, M. F. 1986. Divergent molecular phenotypes of KG1 and KG1a myeloid cell lines. *Blood,* 68**,** 1101-7.
FURUTA, K., WALSENG, E. & ROCHE, P. A. 2013. Internalizing MHC class II-peptide complexes are ubiquitinated in early endosomes and targeted for lysosomal degradation. *Proc Natl Acad Sci U S A,* 110**,** 20188-93.
GADEOCK, S., PUPOVAC, A., SLUYTER, V., SPILDREJORDE, M. & SLUYTER, R. 2012. P2X7 receptor activation mediates organic cation uptake into human myeloid leukaemic KG-1 cells. *Purinergic Signal,* 8**,** 669-76.
GAMAZON, E. R. & STRANGER, B. E. 2015. The impact of human copy number variation on gene expression. *Briefings in Functional Genomics,* 14**,** 352-357.
GAN, C. S., CHONG, P. K., PHAM, T. K. & WRIGHT, P. C. 2007. Technical, experimental, and biological variations in isobaric tags for relative and absolute quantitation (iTRAQ). *J Proteome Res,* 6**,** 821-7.
GARRELS, J. I. 2001. Proteome A2 - Brenner, Sydney. *In:* MILLER, J. H. (ed.) *Encyclopedia of Genetics.* New York: Academic Press.
GEISSMANN, F., REVY, P., BROUSSE, N., LEPELLETIER, Y., FOLLI, C., DURANDY, A., CHAMBON, P. & DY, M. 2003. Retinoids regulate survival and antigen presentation by immature dendritic cells. *J Exp Med,* 198**,** 623-34.
GIOVANNONI, G. & EBERS, G. 2007. Multiple sclerosis: the environment and causation. *Curr Opin Neurol,* 20**,** 261-8.

GODOVAC-ZIMMERMANN, J. & BROWN, L. R. 2001. Perspectives for mass spectrometry and functional proteomics. *Mass Spectrom Rev,* 20**,** 1-57.
GONDI, C. S. & RAO, J. S. 2013. Cathepsin B as a Cancer Target. *Expert opinion on therapeutic targets,* 17**,** 281-291.
GORER, P. A. 1937. The genetic and antigenic basis of tumour transplantation. *The Journal of Pathology and Bacteriology,* 44**,** 691-697.
GORER, P. A. & SCHÜTZE, H. 1938. Genetical studies on immunity in mice: II. Correlation between antibody formation and resistance. *Epidemiology and Infection,* 38**,** 647-662.
GORGA, J. C., BROWN, J. H., JARDETZKY, T., WILEY, D. C. & STROMINGER, J. L. 1991. CRYSTALLIZATION OF HLA-DR ANTIGENS. *Research in Immunology,* 142**,** 401-407.
GRANUCCI, F., VIZZARDELLI, C., VIRZI, E., RESCIGNO, M. & RICCIARDI-CASTAGNOLI, P. 2001. Transcriptional reprogramming of dendritic cells by differentiation stimuli. *European Journal of Immunology,* 31**,** 2539-2546.
HALL, J. A., GRAINGER, J. R., SPENCER, S. P. & BELKAID, Y. 2011. The Role of Retinoic Acid in Tolerance and Immunity. *Immunity,* 35**,** 13-22.
HAMMOND, S. R., ENGLISH, D. R. & MCLEOD, J. G. 2000. The age-range of risk of developing multiple sclerosis: evidence from a migrant population in Australia. *Brain,* 123 (Pt 5)**,** 968-74.
HANDEL, A. E., HANDUNNETTHI, L., EBERS, G. C. & RAMAGOPALAN, S. V. 2009. Type 1 diabetes mellitus and multiple sclerosis: common etiological features. *Nature Reviews Endocrinology,* 5**,** 655.
HANDEL, A. E., SANDVE, G. K., DISANTO, G., BERLANGA-TAYLOR, A. J., GALLONE, G., HANWELL, H., DRABLOS, F., GIOVANNONI, G., EBERS, G. C. & RAMAGOPALAN, S. V. 2013. Vitamin D receptor ChIP-seq in primary CD4+ cells: relationship to serum 25-hydroxyvitamin D levels and autoimmune disease. *BMC Med,* 11**,** 163.
HANDUNNETTHI, L., RAMAGOPALAN, S. V. & EBERS, G. C. 2010a. Multiple sclerosis, vitamin D, and HLA-DRB1*15. *Neurology,* 74**,** 1905-10.
HANDUNNETTHI, L., RAMAGOPALAN, S. V., EBERS, G. C. & KNIGHT, J. C. 2010b. Regulation of major histocompatibility complex class II gene expression, genetic variation and disease. *Genes Immun,* 11**,** 99-112.
HAQUE, M. A., LI, P., JACKSON, S. K., ZAROUR, H. M., HAWES, J. W., PHAN, U. T., MARIC, M., CRESSWELL, P. & BLUM, J. S. 2002. Absence of gamma-interferon-inducible lysosomal thiol reductase in melanomas disrupts T cell recognition of select immunodominant epitopes. *Journal of Experimental Medicine,* 195**,** 1267-1277.
HARRISON, E. H. 2005. Mechanisms of digestion and absorption of dietary vitamin A. *Annu Rev Nutr,* 25**,** 87-103.
HARSHA, H. C., MOLINA, H. & PANDEY, A. 2008. Quantitative proteomics using stable isotope labeling with amino acids in cell culture. *Nat Protoc,* 3**,** 505-16.
HAUPTMANN, G. & BAHRAM, S. 2004. Genetics of the central MHC. *Curr Opin Immunol,* 16**,** 668-72.
HAUSER, S. L., WAUBANT, E., ARNOLD, D. L., VOLLMER, T., ANTEL, J., FOX, R. J., BAR-OR, A., PANZARA, M., SARKAR, N., AGARWAL, S., LANGER-GOULD, A. & SMITH, C. H. 2008. B-cell depletion with rituximab in relapsing-remitting multiple sclerosis. *N Engl J Med,* 358**,** 676-88.
HAUSMANN, M., OBERMEIER, F., SCHREITER, K., SPOTTL, T., FALK, W., SCHOLMERICH, J., HERFARTH, H., SAFTIG, P. & ROGLER, G. 2004. Cathepsin D is up-regulated in inflammatory bowel disease macrophages. *Clin Exp Immunol,* 136**,** 157-67.
HAUSSLER, M. R., HAUSSLER, C. A., JURUTKA, P. W., THOMPSON, P. D., HSIEH, J. C., REMUS, L. S., SELZNICK, S. H. & WHITFIELD, G. K. 1997. The vitamin D hormone and its nuclear receptor: molecular actions and disease states. *J Endocrinol,* 154 Suppl**,** S57-73.
HEENEMAN, S., DEUTZ, N. E. P. & BUURMAN, W. A. 1993. The concentrations of glutamine and ammonia in commercially available cell culture media. *Journal of Immunological Methods,* 166**,** 85-91.

HEINE, G., NIESNER, U., CHANG, H. D., STEINMEYER, A., ZUGEL, U., ZUBERBIER, T., RADBRUCH, A. & WORM, M. 2008. 1,25-dihydroxyvitamin D(3) promotes IL-10 production in human B cells. *Eur J Immunol,* 38**,** 2210-8.

HEMMER, B., KERSCHENSTEINER, M. & KORN, T. 2015. Role of the innate and adaptive immune responses in the course of multiple sclerosis. *Lancet Neurol,* 14**,** 406-19.

HENSIEK, A., SAWCER, S., FEAKES, R., DEANS, J., MANDER, A., AKESSON, E., ROXBURGH, R., CORADDU, F., SMITH, S. & COMPSTON, D. 2002. HLA-DR 15 is associated with female sex and younger age at diagnosis in multiple sclerosis. *Journal of Neurology, Neurosurgery, and Psychiatry,* 72**,** 184-187.

HERRMANN, T. L., AGRAWAL, R. S., CONNOLLY, S. F., MCCAFFREY, R. L., SCHLOMANN, J. & KUSNER, D. J. 2007. MHC Class II levels and intracellular localization in human dendritic cells are regulated by calmodulin kinase II. *J Leukoc Biol,* 82**,** 686-99.

HEWISON, M., FREEMAN, L., HUGHES, S. V., EVANS, K. N., BLAND, R., ELIOPOULOS, A. G., KILBY, M. D., MOSS, P. A. & CHAKRAVERTY, R. 2003. Differential regulation of vitamin D receptor and its ligand in human monocyte-derived dendritic cells. *J Immunol,* 170**,** 5382-90.

HEWITT, E. W., TREUMANN, A., MORRICE, N., TATNELL, P. J., KAY, J. & WATTS, C. 1997. Natural processing sites for human cathepsin E and cathepsin D in tetanus toxin: implications for T cell epitope generation. *J Immunol,* 159**,** 4693-9.

HOEDT, E., ZHANG, G. & NEUBERT, T. A. 2014. Stable isotope labeling by amino acids in cell culture (SILAC) for quantitative proteomics. *Adv Exp Med Biol,* 806**,** 93-106.

HOFFMAN, W., LAKKIS, F. G. & CHALASANI, G. 2016. B Cells, Antibodies, and More. *Clinical Journal of the American Society of Nephrology : CJASN,* 11**,** 137-154.

HOFFMANN, J. & AKIRA, S. 2013. Innate immunity. *Curr Opin Immunol,* 25**,** 1-3.

HOLICK, M. F. 1981. The cutaneous photosynthesis of previtamin D3: a unique photoendocrine system. *J Invest Dermatol,* 77**,** 51-8.

HOLICK, M. F. 2014. Sunlight, ultraviolet radiation, vitamin D and skin cancer: how much sunlight do we need? *Adv Exp Med Biol,* 810**,** 1-16.

HOLLING, T. M., SCHOOTEN, E. & VAN DEN ELSEN, P. J. 2004. Function and regulation of MHC class II molecules in T-lymphocytes: of mice and men. *Hum Immunol,* 65**,** 282-90.

HOLMØY, T. 2007. Immunopathogenesis of multiple sclerosis: concepts and controversies. *Acta Neurologica Scandinavica,* 115**,** 39-45.

HOR, S., ZIV, T., ADMON, A. & LEHNER, P. J. 2009. Stable isotope labeling by amino acids in cell culture and differential plasma membrane proteome quantitation identify new substrates for the MARCH9 transmembrane E3 ligase. *Mol Cell Proteomics,* 8**,** 1959-71.

HORIKOSHI, T., ARANY, I., RAJARAMAN, S., CHEN, S. H., BRYSK, H., LEI, G., TYRING, S. K. & BRYSK, M. M. 1998. Isoforms of cathepsin D and human epidermal differentiation. *Biochimie,* 80**,** 605-12.

HORTON, R., GIBSON, R., COGGILL, P., MIRETTI, M., ALLCOCK, R. J., ALMEIDA, J., FORBES, S., GILBERT, J. G. R., HALLS, K., HARROW, J. L., HART, E., HOWE, K., JACKSON, D. K., PALMER, S., ROBERTS, A. N., SIMS, S., STEWART, C. A., TRAHERNE, J. A., TREVANION, S., WILMING, L., ROGERS, J., DE JONG, P. J., ELLIOTT, J. F., SAWCER, S., TODD, J. A., TROWSDALE, J. & BECK, S. 2008. Variation analysis and gene annotation of eight MHC haplotypes: The MHC Haplotype Project. *Immunogenetics,* 60**,** 1-18.

HORTON, R., WILMING, L., RAND, V., LOVERING, R. C., BRUFORD, E. A., KHODIYAR, V. K., LUSH, M. J., POVEY, S., TALBOT, C. C., JR., WRIGHT, M. W., WAIN, H. M., TROWSDALE, J., ZIEGLER, A. & BECK, S. 2004. Gene map of the extended human MHC. *Nat Rev Genet,* 5**,** 889-99.

HOWSON, J. M. M., WALKER, N. M., SMYTH, D. J., TODD, J. A. & THE TYPE, I. D. G. C. 2009. Analysis of 19 genes for association with type I diabetes in the Type I Diabetes Genetics Consortium families. *Genes and immunity,* 10**,** S74-S84.

HSIEH, C. S., DEROOS, P., HONEY, K., BEERS, C. & RUDENSKY, A. Y. 2002. A role for cathepsin L and cathepsin S in peptide generation for MHC class II presentation. *J Immunol,* 168**,** 2618-25.

HSING, L. C. & RUDENSKY, A. Y. 2005. The lysosomal cysteine proteases in MHC class II antigen presentation. *Immunological Reviews,* 207**,** 229-241.
IM, E. & KAZLAUSKAS, A. 2007. The role of cathepsins in ocular physiology and pathology. *Exp Eye Res,* 84**,** 383-8.
IMITOLA, J., CHITNIS, T. & KHOURY, S. J. 2005. Cytokines in multiple sclerosis: from bench to bedside. *Pharmacol Ther,* 106**,** 163-77.
ISHIDA, Y., NAYAK, S., MINDELL, J. A. & GRABE, M. 2013. A model of lysosomal pH regulation. *The Journal of General Physiology,* 141**,** 705-720.
ISRANI, N., GOSWAMI, R., KUMAR, A. & RANI, R. 2009. Interaction of Vitamin D Receptor with HLA DRB1*0301 in Type 1 Diabetes Patients from North India. *PLOS ONE,* 4**,** e8023.
ISSA, L. L., LEONG, G. M. & EISMAN, J. A. 1998. Molecular mechanism of vitamin D receptor action. *Inflamm Res,* 47**,** 451-75.
JABBOUR, M., CAMPBELL, E. M., FARES, H. & LYBARGER, L. 2009. Discrete domains of MARCH1 mediate its localization, functional interactions, and posttranscriptional control of expression. *J Immunol,* 183**,** 6500-12.
JANIK, S., NOWAK, U., ŁASZKIEWICZ, A., SATYR, A., MAJKOWSKI, M., MARCHWICKA, A., ŚNIEŻEWSKI, Ł., BERKOWSKA, K., GABRYŚ, M., CEBRAT, M. & MARCINKOWSKA, E. 2017. Diverse Regulation of Vitamin D Receptor Gene Expression by 1,25-Dihydroxyvitamin D and ATRA in Murine and Human Blood Cells at Early Stages of Their Differentiation. *International Journal of Molecular Sciences,* 18**,** 1323.
JARDETZKY, T. S., GORGA, J. C., BUSCH, R., ROTHBARD, J., STROMINGER, J. L. & WILEY, D. C. 1990. Peptide binding to HLA-DR1: a peptide with most residues substituted to alanine retains MHC binding. *Embo j,* 9**,** 1797-803.
JARDETZKY, T. S., LANE, W. S., ROBINSON, R. A., MADDEN, D. R. & WILEY, D. C. 1991. Identification of self peptides bound to purified HLA-B27. *Nature,* 353**,** 326-9.
JEFFERY, L. E., WOOD, A. M., QURESHI, O. S., HOU, T. Z., GARDNER, D., BRIGGS, Z., KAUR, S., RAZA, K. & SANSOM, D. M. 2012. Availability of 25-hydroxyvitamin D(3) to APCs controls the balance between regulatory and inflammatory T cell responses. *J Immunol,* 189**,** 5155-64.
JESENBERGER, V. & JENTSCH, S. 2002. Deadly encounter: ubiquitin meets apoptosis. *Nature Reviews Molecular Cell Biology,* 3**,** 112.
JOHNSON, D. E. & REDNER, R. L. 2015. An ATRActive future for differentiation therapy in AML. *Blood reviews,* 29**,** 263-268.
JOYNER, A. L. & BERNSTEIN, A. 1983. Retrovirus transduction: generation of infectious retroviruses expressing dominant and selectable genes is associated with in vivo recombination and deletion events. *Mol Cell Biol,* 3**,** 2180-90.
KAMPMAN, M. T. & BRUSTAD, M. 2008. Vitamin D: a candidate for the environmental effect in multiple sclerosis - observations from Norway. *Neuroepidemiology,* 30**,** 140-6.
KAMRADT, T. & MITCHISON, N. A. 2001. Tolerance and autoimmunity. *N Engl J Med,* 344**,** 655-64.
KAMRADT, T., SOLOWAY, P. D., PERKINS, D. L. & GEFTER, M. L. 1991. Pertussis toxin prevents the induction of peripheral T cell anergy and enhances the T cell response to an encephalitogenic peptide of myelin basic protein. *J Immunol,* 147**,** 3296-302.
KAMWERU, P. K. & TINDIBALE, E. L. 2016. Vitamin D and Vitamin D from Ultraviolet-Irradiated Mushrooms (Review). *Int J Med Mushrooms,* 18**,** 205-14.
KAUFMAN, J. F., AUFFRAY, C., KORMAN, A. J., SHACKELFORD, D. A. & STROMINGER, J. 1984. The class II molecules of the human and murine major histocompatibility complex. *Cell,* 36**,** 1-13.
KAYE, J. F., RICHARDSON, J. H. & LEVER, A. M. 1995. cis-acting sequences involved in human immunodeficiency virus type 1 RNA packaging. *J Virol,* 69**,** 6588-92.
KIM, C. H. 2011. Retinoic acid, immunity, and inflammation. *Vitam Horm,* 86**,** 83-101.
KIRA, J., KANAI, T., NISHIMURA, Y., YAMASAKI, K., MATSUSHITA, S., KAWANO, Y., HASUO, K., TOBIMATSU, S. & KOBAYASHI, T. 1996. Western versus Asian types of multiple sclerosis: immunogenetically and clinically distinct disorders. *Ann Neurol,* 40**,** 569-74.

KLEIN, J. & SATO, A. 2000. The HLA system. First of two parts. *N Engl J Med,* 343**,** 702-9.
KLEIN, L., KYEWSKI, B., ALLEN, P. M. & HOGQUIST, K. A. 2014. Positive and negative selection of the T cell repertoire: what thymocytes see and don't see. *Nature reviews. Immunology,* 14**,** 377-391.
KNEZEVIC, S. Z., JENS, C. S. & CHRISTIAN, R. 2007. Utilizing R Software Package for Dose-Response Studies: The Concept and Data Analysis. *Weed Technology,* 21**,** 840-848.
KOCH, N., ZACHARIAS, M., KONIG, A., TEMME, S., NEUMANN, J. & SPRINGER, S. 2011. Stoichiometry of HLA Class II-Invariant Chain Oligomers. *Plos One,* 6.
KOEFFLER, H. P. & GOLDE, D. W. 1978. Acute myelogenous leukemia: a human cell line responsive to colony-stimulating activity. *Science,* 200**,** 1153-4.
KOJIMA, H., AIZAWA, Y., YANAI, Y., NAGAOKA, K., TAKEUCHI, M., OHTA, T., IKEGAMI, H., IKEDA, M. & KURIMOTO, M. 1999. An essential role for NF-kappa B in IL-18-induced IFN-gamma expression in KG-1 cells. *J Immunol,* 162**,** 5063-9.
KORNEK, B. & LASSMANN, H. 2003. Neuropathology of multiple sclerosis-new concepts. *Brain Res Bull,* 61**,** 321-6.
KRAGT, J., VAN AMERONGEN, B., KILLESTEIN, J., DIJKSTRA, C., UITDEHAAG, B., POLMAN, C. & LIPS, P. 2009. Higher levels of 25-hydroxyvitamin D are associated with a lower incidence of multiple sclerosis only in women. *Mult Scler,* 15**,** 9-15.
KROPSHOFER, H., ARNDT, S. O., MOLDENHAUER, G., HAMMERLING, G. J. & VOGT, A. B. 1997. HLA-DM acts as a molecular chaperone and rescues empty HLA-DR molecules at lysosomal pH. *Immunity,* 6**,** 293-302.
KROPSHOFER, H., VOGT, A. B., MOLDENHAUER, G., HAMMER, J., BLUM, J. S. & HÄMMERLING, G. J. 1996. Editing of the HLA-DR-peptide repertoire by HLA-DM. *The EMBO Journal,* 15**,** 6144-6154.
KROPSHOFER, H., VOGT, A. B., STERN, L. J. & HAMMERLING, G. J. 1995. SELF-RELEASE OF CLIP IN PEPTIDE LOADING OF HLA-DR MOLECULES. *Science,* 270**,** 1357-1359.
KUMMER, J. A., KAMP, A. M., CITARELLA, F., HORREVOETS, A. J. & HACK, C. E. 1996. Expression of human recombinant granzyme A zymogen and its activation by the cysteine proteinase cathepsin C. *J Biol Chem,* 271**,** 9281-6.
KYEWSKI, B. & KLEIN, L. 2006. A central role for central tolerance. *Annu Rev Immunol,* 24**,** 571-606.
LAEMMLI, U. K. 1970. Cleavage of Structural Proteins during the Assembly of the Head of Bacteriophage T4. *Nature,* 227**,** 680-685.
LAMPIS, R., MORELLI, L., DE VIRGILIIS, S., CONGIA, M. & CUCCA, F. 2000. The distribution of HLA class II haplotypes reveals that the Sardinian population is genetically differentiated from the other Caucasian populations. *Tissue Antigens,* 56**,** 515-21.
LAMPSON, L. A. & LEVY, R. 1980. 2 POPULATIONS OF IA-LIKE MOLECULES ON A HUMAN B-CELL LINE. *Journal of Immunology,* 125**,** 293-299.
LAPAQUE, N., JAHNKE, M., TROWSDALE, J. & KELLY, A. P. 2009. The HLA-DRalpha chain is modified by polyubiquitination. *J Biol Chem,* 284**,** 7007-16.
LEIBUNDGUT-LANDMANN, S., WALDBURGER, J. M., KRAWCZYK, M., OTTEN, L. A., SUTER, T., FONTANA, A., ACHA-ORBEA, H. & REITH, W. 2004. Mini-review: Specificity and expression of CIITA, the master regulator of MHC class II genes. *Eur J Immunol,* 34**,** 1513-25.
LEVER, A. M. L., STRAPPE, P. M. & ZHAO, J. 2004. Lentiviral Vectors. *Journal of Biomedical Science,* 11**,** 439-449.
LI, F., VIJAYASANKARAN, N., SHEN, A., KISS, R. & AMANULLAH, A. 2010. Cell culture processes for monoclonal antibody production. *mAbs,* 2**,** 466-477.
LI, W. & YE, Y. 2008. Polyubiquitin chains: functions, structures, and mechanisms. *Cellular and molecular life sciences : CMLS,* 65**,** 2397-2406.
LINCOLN, M. R., MONTPETIT, A., CADER, M. Z., SAARELA, J., DYMENT, D. A., TIISLAR, M., FERRETTI, V., TIENARI, P. J., SADOVNICK, A. D., PELTONEN, L., EBERS, G. C. & HUDSON, T. J. 2005. A predominant role for the HLA class II region in the association of the MHC region with multiple sclerosis. *Nat Genet,* 37**,** 1108-12.

LINCOLN, M. R., RAMAGOPALAN, S. V., CHAO, M. J., HERRERA, B. M., DELUCA, G. C., ORTON, S.-M., DYMENT, D. A., SADOVNICK, A. D. & EBERS, G. C. 2009. Epistasis among HLA-DRB1, HLA-DQA1, and HLA-DQB1 loci determines multiple sclerosis susceptibility. *Proceedings of the National Academy of Sciences,* 106**,** 7542-7547.

LIU, P. T., SCHENK, M., WALKER, V. P., DEMPSEY, P. W., KANCHANAPOOMI, M., WHEELWRIGHT, M., VAZIRNIA, A., ZHANG, X., STEINMEYER, A., ZÜGEL, U., HOLLIS, B. W., CHENG, G. & MODLIN, R. L. 2009. Convergence of IL-1β and VDR Activation Pathways in Human TLR2/1-Induced Antimicrobial Responses. *PLOS ONE,* 4**,** e5810.

LIU, P. T., STENGER, S., LI, H., WENZEL, L., TAN, B. H., KRUTZIK, S. R., OCHOA, M. T., SCHAUBER, J., WU, K., MEINKEN, C., KAMEN, D. L., WAGNER, M., BALS, R., STEINMEYER, A., ZUGEL, U., GALLO, R. L., EISENBERG, D., HEWISON, M., HOLLIS, B. W., ADAMS, J. S., BLOOM, B. R. & MODLIN, R. L. 2006. Toll-like receptor triggering of a vitamin D-mediated human antimicrobial response. *Science,* 311**,** 1770-3.

LOIS, C., HONG, E. J., PEASE, S., BROWN, E. J. & BALTIMORE, D. 2002. Germline transmission and tissue-specific expression of transgenes delivered by lentiviral vectors. *Science,* 295**,** 868-72.

LOVELOCK, J. E. & BISHOP, M. W. 1959. Prevention of freezing damage to living cells by dimethyl sulphoxide. *Nature,* 183**,** 1394-5.

LUCCHINETTI, C., BRUCK, W., PARISI, J., SCHEITHAUER, B., RODRIGUEZ, M. & LASSMANN, H. 2000. Heterogeneity of multiple sclerosis lesions: implications for the pathogenesis of demyelination. *Ann Neurol,* 47**,** 707-17.

LUZIO, J. P., PRYOR, P. R. & BRIGHT, N. A. 2007. Lysosomes: fusion and function. *Nat Rev Mol Cell Biol,* 8**,** 622-32.

MACKAY, C. R. & VON ANDRIAN, U. H. 2001. Immunology. Memory T cells--local heroes in the struggle for immunity. *Science,* 291**,** 2323-4.

MACLAUGHLIN, J. & HOLICK, M. F. 1985. Aging decreases the capacity of human skin to produce vitamin D3. *J Clin Invest,* 76**,** 1536-8.

MAHMOOD, T. & YANG, P.-C. 2012. Western Blot: Technique, Theory, and Trouble Shooting. *North American Journal of Medical Sciences,* 4**,** 429-434.

MAK, T. W. & SAUNDERS, M. E. 2006. 10 - MHC: The Major Histocompatibility Complex. *The Immune Response.* Burlington: Academic Press.

MANJUNATH, N., WU, H., SUBRAMANYA, S. & SHANKAR, P. 2009. Lentiviral delivery of short hairpin RNAs. *Adv Drug Deliv Rev,* 61**,** 732-45.

MANN, M. 2006. Functional and quantitative proteomics using SILAC. *Nat Rev Mol Cell Biol,* 7**,** 952-8.

MANOURY, B., HEWITT, E. W., MORRICE, N., DANDO, P. M., BARRETT, A. J. & WATTS, C. 1998. An asparaginyl endopeptidase processes a microbial antigen for class II MHC presentation. *Nature,* 396**,** 695-9.

MARIC, M., ARUNACHALAM, B., PHAN, U. T., DONG, C., GARRETT, W. S., CANNON, K. S., ALFONSO, C., KARLSSON, L., FLAVELL, R. A. & CRESSWELL, P. 2001. Defective antigen processing in GILT-free mice. *Science,* 294**,** 1361-1365.

MARIĆ, M. A., TAYLOR, M. D. & BLUM, J. S. 1994. Endosomal aspartic proteinases are required for invariant-chain processing. *Proceedings of the National Academy of Sciences of the United States of America,* 91**,** 2171-2175.

MARROSU, M. G., MURRU, R., MURRU, M. R., COSTA, G., ZAVATTARI, P., WHALEN, M., COCCO, E., MANCOSU, C., SCHIRRU, L., SOLLA, E., FADDA, E., MELIS, C., PORRU, I., ROLESU, M. & CUCCA, F. 2001. Dissection of the HLA association with multiple sclerosis in the founder isolated population of Sardinia. *Human Molecular Genetics,* 10**,** 2907-2916.

MARSH, S. G., ALBERT, E. D., BODMER, W. F., BONTROP, R. E., DUPONT, B., ERLICH, H. A., FERNANDEZ-VINA, M., GERAGHTY, D. E., HOLDSWORTH, R., HURLEY, C. K., LAU, M., LEE, K. W., MACH, B., MAIERS, M., MAYR, W. R., MULLER, C. R., PARHAM, P., PETERSDORF, E. W., SASAZUKI, T., STROMINGER, J. L.,

SVEJGAARD, A., TERASAKI, P. I., TIERCY, J. M. & TROWSDALE, J. 2010. Nomenclature for factors of the HLA system, 2010. *Tissue Antigens,* 75**,** 291-455.
MARUOTTI, N. & CANTATORE, F. P. 2010. Vitamin D and the immune system. *J Rheumatol,* 37**,** 491-5.
MASCIULLI, R., TESTA, U., BARBERI, T., SAMOGGIA, P., TRITARELLI, E., PUSTORINO, R., MASTROBERARDINO, G., CAMAGNA, A. & PESCHLE, C. 1995. Combined vitamin D3/retinoic acid induction of human promyelocytic cell lines: enhanced phagocytic cell maturation and hybrid granulomonocytic phenotype. *Cell Growth Differ,* 6**,** 493-503.
MASTERMAN, T., LIGERS, A., OLSSON, T., ANDERSSON, M., OLERUP, O. & HILLERT, J. 2000. HLA-DR15 is associated with lower age at onset in multiple sclerosis. *Ann Neurol,* 48**,** 211-9.
MASTERNAK, K., MUHLETHALER-MOTTET, A., VILLARD, J., ZUFFEREY, M., STEIMLE, V. & REITH, W. 2000. CIITA is a transcriptional coactivator that is recruited to MHC class II promoters by multiple synergistic interactions with an enhanceosome complex. *Genes Dev,* 14**,** 1156-66.
MATSUKI, Y., OHMURA-HOSHINO, M., GOTO, E., AOKI, M., MITO-YOSHIDA, M., UEMATSU, M., HASEGAWA, T., KOSEKI, H., OHARA, O., NAKAYAMA, M., TOYOOKA, K., MATSUOKA, K., HOTTA, H., YAMAMOTO, A. & ISHIDO, S. 2007. Novel regulation of MHC class II function in B cells. *EMBO J,* 26**,** 846-54.
MCDONALD, W. I., COMPSTON, A., EDAN, G., GOODKIN, D., HARTUNG, H. P., LUBLIN, F. D., MCFARLAND, H. F., PATY, D. W., POLMAN, C. H., REINGOLD, S. C., SANDBERG-WOLLHEIM, M., SIBLEY, W., THOMPSON, A., VAN DEN NOORT, S., WEINSHENKER, B. Y. & WOLINSKY, J. S. 2001. Recommended diagnostic criteria for multiple sclerosis: guidelines from the International Panel on the diagnosis of multiple sclerosis. *Ann Neurol,* 50**,** 121-7.
MCGRANE, M. M. 2007. Vitamin A regulation of gene expression: molecular mechanism of a prototype gene. *J Nutr Biochem,* 18**,** 497-508.
MCMICHAEL, A. J. & HALL, A. J. 1997. Does immunosuppressive ultraviolet radiation explain the latitude gradient for multiple sclerosis? *Epidemiology,* 8**,** 642-5.
MELLMAN, I., TURLEY, S. J. & STEINMAN, R. M. 1998. Antigen processing for amateurs and professionals. *Trends Cell Biol,* 8**,** 231-7.
MICHALSKI, A., DAMOC, E., HAUSCHILD, J.-P., LANGE, O., WIEGHAUS, A., MAKAROV, A., NAGARAJ, N., COX, J., MANN, M. & HORNING, S. 2011. Mass Spectrometry-based Proteomics Using Q Exactive, a High-performance Benchtop Quadrupole Orbitrap Mass Spectrometer. *Molecular & Cellular Proteomics : MCP,* 10**,** M111.011015.
MILLER, D. H., MCDONALD, I. & SMITH, K. J. 2005. The diagnosis of multiple sclerosis. *In:* WEKERLE, H. (ed.) *McAlpine's Multiple Sclerosis.* Unknown Publisher.
MINDELL, J. A. 2012. Lysosomal acidification mechanisms. *Annu Rev Physiol,* 74**,** 69-86.
MODIN, H., OLSSON, W., HILLERT, J. & MASTERMAN, T. 2004. Modes of action of HLA-DR susceptibility specificities in multiple sclerosis. *Am J Hum Genet,* 74**,** 1321-2.
MOFFAT, J. M., MINTERN, J. D. & VILLADANGOS, J. A. 2013. Control of MHC II antigen presentation by ubiquitination. *Current Opinion in Immunology,* 25**,** 109-114.
MOORE, C. B., GUTHRIE, E. H., HUANG, M. T.-H. & TAXMAN, D. J. 2010. Short Hairpin RNA (shRNA): Design, Delivery, and Assessment of Gene Knockdown. *Methods in molecular biology (Clifton, N.J.),* 629**,** 141-158.
MORA, J. R., IWATA, M. & VON ANDRIAN, U. H. 2008. Vitamin effects on the immune system: vitamins A and D take centre stage. *Nature reviews. Immunology,* 8**,** 685-698.
MORGAN, J. W., KOUTTAB, N., FORD, D. & MAIZEL, A. L. 2000. Vitamin D-Mediated Gene Regulation in Phenotypically Defined Human B Cell Subpopulations*. *Endocrinology,* 141**,** 3225-3234.
MORRIS, G. P. & ALLEN, P. M. 2012. How the TCR balances sensitivity and specificity for the recognition of self and pathogens. *Nature Immunology,* 13**,** 121-128.
MUNGALL, A. J., PALMER, S. A., SIMS, S. K., EDWARDS, C. A., ASHURST, J. L., WILMING, L., JONES, M. C., HORTON, R., HUNT, S. E., SCOTT, C. E., GILBERT, J. G. R., CLAMP, M. E., BETHEL, G., MILNE, S., AINSCOUGH, R., ALMEIDA, J. P., AMBROSE, K. D.,

ANDREWS, T. D., ASHWELL, R. I. S., BABBAGE, A. K., BAGGULEY, C. L., BAILEY, J., BANERJEE, R., BARKER, D. J., BARLOW, K. F., BATES, K., BEARE, D. M., BEASLEY, H., BEASLEY, O., BIRD, C. P., BLAKEY, S., BRAY-ALLEN, S., BROOK, J., BROWN, A. J., BROWN, J. Y., BURFORD, D. C., BURRILL, W., BURTON, J., CARDER, C., CARTER, N. P., CHAPMAN, J. C., CLARK, S. Y., CLARK, G., CLEE, C. M., CLEGG, S., COBLEY, V., COLLIER, R. E., COLLINS, J. E., COLMAN, L. K., CORBY, N. R., COVILLE, G. J., CULLEY, K. M., DHAMI, P., DAVIES, J., DUNN, M., EARTHROWL, M. E., ELLINGTON, A. E., EVANS, K. A., FAULKNER, L., FRANCIS, M. D., FRANKISH, A., FRANKLAND, J., FRENCH, L., GARNER, P., GARNETT, J., GHORI, M. J. R., GILBY, L. M., GILLSON, C. J., GLITHERO, R. J., GRAFHAM, D. V., GRANT, M., GRIBBLE, S., GRIFFITHS, C., GRIFFITHS, M., HALL, R., HALLS, K. S., HAMMOND, S., HARLEY, J. L., HART, E. A., HEATH, P. D., HEATHCOTT, R., HOLMES, S. J., HOWDEN, P. J., HOWE, K. L., HOWELL, G. R., HUCKLE, E., HUMPHRAY, S. J., HUMPHRIES, M. D., HUNT, A. R., JOHNSON, C. M., JOY, A. A., KAY, M., KEENAN, S. J., KIMBERLEY, A. M., KING, A., LAIRD, G. K., LANGFORD, C., LAWLOR, S., LEONGAMORNLERT, D. A., LEVERSHA, M., et al. 2003. The DNA sequence and analysis of human chromosome 6. *Nature,* 425**,** 805-811.

MUNGER, K. L., LEVIN, L. I., HOLLIS, B. W., HOWARD, N. S. & ASCHERIO, A. 2006. Serum 25-hydroxyvitamin D levels and risk of multiple sclerosis. *JAMA,* 296**,** 2832-8.

MUTO, A., KIZAKI, M., YAMATO, K., KAWAI, Y., KAMATA-MATSUSHITA, M., UENO, H., OHGUCHI, M., NISHIHARA, T., KOEFFLER, H. P. & IKEDA, Y. 1999. 1,25-Dihydroxyvitamin D₃ Induces Differentiation of a Retinoic Acid–Resistant Acute Promyelocytic Leukemia Cell Line (UF-1) Associated With Expression of p21^{WAF1/CIP1} and p27^{KIP1}. *Blood,* 93**,** 2225-2233.

NAGPAL, S., NA, S. & RATHNACHALAM, R. 2005. Noncalcemic actions of vitamin D receptor ligands. *Endocr Rev,* 26**,** 662-87.

NAGY, Z. A., HUBNER, B., LOHNING, C., RAUCHENBERGER, R., REIFFERT, S., THOMASSEN-WOLF, E., ZAHN, S., LEYER, S., SCHIER, E. M., ZAHRADNIK, A., BRUNNER, C., LOBENWEIN, K., RATTEL, B., STANGLMAIER, M., HALLEK, M., WING, M., ANDERSON, S., DUNN, M., KRETZSCHMAR, T. & TESAR, M. 2002. Fully human, HLA-DR-specific monoclonal antibodies efficiently induce programmed death of malignant lymphoid cells. *Nat Med,* 8**,** 801-7.

NAKAJIMA, H., KIZAKI, M., UENO, H., MUTO, A., TAKAYAMA, N., MATSUSHITA, H., SONODA, A. & IKEDA, Y. 1996. All-trans and 9-cis retinoic acid enhance 1,25-dihydroxyvitamin D3-induced monocytic differentiation of U937 cells. *Leukemia Research,* 20**,** 665-676.

NALDINI, L., BLOMER, U., GALLAY, P., ORY, D., MULLIGAN, R., GAGE, F. H., VERMA, I. M. & TRONO, D. 1996. In vivo gene delivery and stable transduction of nondividing cells by a lentiviral vector. *Science,* 272**,** 263-7.

NATARAJAN, K., LI, H., MARIUZZA, R. A. & MARGULIES, D. H. 1999a. MHC class I molecules, structure and function. *Rev Immunogenet,* 1**,** 32-46.

NATARAJAN, S. K., STERN, L. J. & SADEGH-NASSERI, S. 1999b. Sodium dodecyl sulfate stability of HLA-DR1 complexes correlates with burial of hydrophobic residues in pocket 1. *J Immunol,* 162**,** 3463-70.

NEEFJES, J., JONGSMA, M. L. M., PAUL, P. & BAKKE, O. 2011. Towards a systems understanding of MHC class I and MHC class II antigen presentation. *Nature Reviews Immunology,* 11**,** 823-836.

NEUMANN, J. & KOCH, N. 2005. Assembly of major histocompatibility complex class II subunits with invariant chain. *FEBS Letters,* 579**,** 6055-6059.

NIINO, M., FUKAZAWA, T., KIKUCHI, S. & SASAKI, H. 2008. Therapeutic potential of vitamin D for multiple sclerosis. *Curr Med Chem,* 15**,** 499-505.

NING, J., MORGAN, D. & PAMPHILON, D. 2011. A Rapid Culture Technique Produces Functional Dendritic-Like Cells from Human Acute Myeloid Leukemia Cell Lines. *Journal of Biomedicine and Biotechnology,* 2011**,** 9.

NISHIOKU, T., HASHIMOTO, K., YAMASHITA, K., LIOU, S. Y., KAGAMIISHI, Y., MAEGAWA, H., KATSUBE, N., PETERS, C., VON FIGURA, K., SAFTIG, P., KATUNUMA, N., YAMAMOTO, K. & NAKANISHI, H. 2002. Involvement of cathepsin E in exogenous antigen processing in primary cultured murine microglia. *J Biol Chem,* 277**,** 4816-22.

NOMURA, T. & KATUNUMA, N. 2005. Involvement of cathepsins in the invasion, metastasis and proliferation of cancer cells. *J Med Invest,* 52**,** 1-9.

OH, J. & SHIN, J. S. 2015. Molecular mechanism and cellular function of MHCII ubiquitination. *Immunol Rev,* 266**,** 134-44.

OHMURA-HOSHINO, M., MATSUKI, Y., AOKI, M., GOTO, E., MITO, M., UEMATSU, M., KAKIUCHI, T., HOTTA, H. & ISHIDO, S. 2006. Inhibition of MHC class II expression and immune responses by c-MIR. *J Immunol,* 177**,** 341-54.

ONG, S.-E. & MANN, M. 2007a. A practical recipe for stable isotope labeling by amino acids in cell culture (SILAC). *Nat. Protocols,* 1**,** 2650-2660.

ONG, S. E., BLAGOEV, B., KRATCHMAROVA, I., KRISTENSEN, D. B., STEEN, H., PANDEY, A. & MANN, M. 2002. Stable isotope labeling by amino acids in cell culture, SILAC, as a simple and accurate approach to expression proteomics. *Mol Cell Proteomics,* 1**,** 376-86.

ONG, S. E. & MANN, M. 2005. Mass spectrometry-based proteomics turns quantitative. *Nat Chem Biol,* 1**,** 252-62.

ONG, S. E. & MANN, M. 2006. A practical recipe for stable isotope labeling by amino acids in cell culture (SILAC). *Nat Protoc,* 1**,** 2650-60.

ONG, S. E. & MANN, M. 2007b. Stable isotope labeling by amino acids in cell culture for quantitative proteomics. *Methods Mol Biol,* 359**,** 37-52.

OPARA, J. A., JARACZ, K. & BROLA, W. 2010. Quality of life in multiple sclerosis. *J Med Life,* 3**,** 352-8.

OZTURK, S. S. & PALSSON, B. O. 1990. Chemical Decomposition of Glutamine in Cell Culture Media: Effect of Media Type, pH, and Serum Concentration. *Biotechnology Progress,* 6**,** 121-128.

PACHNER, A. R. & STEINER, I. 2009. The multiple sclerosis severity score (MSSS) predicts disease severity over time. *J Neurol Sci,* 278**,** 66-70.

PAINTER, C. A., NEGRONI, M. P., KELLERSBERGER, K. A., ZAVALA-RUIZ, Z., EVANS, J. E. & STERN, L. J. 2011. Conformational lability in the class II MHC 3(10) helix and adjacent extended strand dictate HLA-DM susceptibility and peptide exchange. *Proceedings of the National Academy of Sciences of the United States of America,* 108**,** 19329-19334.

PAINTER, C. A. & STERN, L. J. 2012. Conformational variation in structures of classical and non-classical MHCII proteins and functional implications. *Immunol Rev,* 250**,** 144-57.

PAUL, P., VAN DEN HOORN, T., JONGSMA, MARLIEKE L. M., BAKKER, MARK J., HENGEVELD, R., JANSSEN, L., CRESSWELL, P., EGAN, DAVID A., VAN HAM, M., TEN BRINKE, A., OVAA, H., BEIJERSBERGEN, RODERICK L., KUIJL, C. & NEEFJES, J. 2011. A Genome-wide Multidimensional RNAi Screen Reveals Pathways Controlling MHC Class II Antigen Presentation. *Cell,* 145**,** 268-283.

PENN, D. J. & ILMONEN, P. 2001. Major Histocompatibility Complex (MHC). *eLS.* John Wiley & Sons, Ltd.

PENNA, G., RONCARI, A., AMUCHASTEGUI, S., DANIEL, K. C., BERTI, E., COLONNA, M. & ADORINI, L. 2005. Expression of the inhibitory receptor ILT3 on dendritic cells is dispensable for induction of CD4+Foxp3+ regulatory T cells by 1,25-dihydroxyvitamin D3. *Blood,* 106**,** 3490-7.

PFEIFER, A., IKAWA, M., DAYN, Y. & VERMA, I. M. 2002. Transgenesis by lentiviral vectors: lack of gene silencing in mammalian embryonic stem cells and preimplantation embryos. *Proc Natl Acad Sci U S A,* 99**,** 2140-5.

PICKART, C. M. 2001. Mechanisms underlying ubiquitination. *Annu Rev Biochem,* 70**,** 503-33.

PIERROT-DESEILLIGNY, C. 2009. Clinical implications of a possible role of vitamin D in multiple sclerosis. *J Neurol,* 256**,** 1468-79.

PIERROT-DESEILLIGNY, C. & SOUBERBIELLE, J.-C. 2013. Contribution of vitamin D insufficiency to the pathogenesis of multiple sclerosis. *Therapeutic Advances in Neurological Disorders,* 6**,** 81-116.

PIKE, J. W. & MEYER, M. B. 2010. The vitamin D receptor: new paradigms for the regulation of gene expression by 1,25-dihydroxyvitamin D(3). *Endocrinol Metab Clin North Am,* 39**,** 255-69, table of contents.

PINO-LAGOS, K., BENSON, M. J. & NOELLE, R. J. 2008. Retinoic acid in the immune system. *Ann N Y Acad Sci,* 1143**,** 170-87.

PLUDOWSKI, P., HOLICK, M. F., PILZ, S., WAGNER, C. L., HOLLIS, B. W., GRANT, W. B., SHOENFELD, Y., LERCHBAUM, E., LLEWELLYN, D. J., KIENREICH, K. & SONI, M. 2013. Vitamin D effects on musculoskeletal health, immunity, autoimmunity, cardiovascular disease, cancer, fertility, pregnancy, dementia and mortality-a review of recent evidence. *Autoimmun Rev,* 12**,** 976-89.

POLMAN, C. H., REINGOLD, S. C., BANWELL, B., CLANET, M., COHEN, J. A., FILIPPI, M., FUJIHARA, K., HAVRDOVA, E., HUTCHINSON, M., KAPPOS, L., LUBLIN, F. D., MONTALBAN, X., O'CONNOR, P., SANDBERG-WOLLHEIM, M., THOMPSON, A. J., WAUBANT, E., WEINSHENKER, B. & WOLINSKY, J. S. 2011. Diagnostic criteria for multiple sclerosis: 2010 Revisions to the McDonald criteria. *Annals of Neurology,* 69**,** 292-302.

POLMAN, C. H., REINGOLD, S. C., EDAN, G., FILIPPI, M., HARTUNG, H. P., KAPPOS, L., LUBLIN, F. D., METZ, L. M., MCFARLAND, H. F., O'CONNOR, P. W., SANDBERG-WOLLHEIM, M., THOMPSON, A. J., WEINSHENKER, B. G. & WOLINSKY, J. S. 2005. Diagnostic criteria for multiple sclerosis: 2005 revisions to the "McDonald Criteria". *Ann Neurol,* 58**,** 840-6.

PONCHEL, F., TOOMES, C., BRANSFIELD, K., LEONG, F. T., DOUGLAS, S. H., FIELD, S. L., BELL, S. M., COMBARET, V., PUISIEUX, A., MIGHELL, A. J., ROBINSON, P. A., INGLEHEARN, C. F., ISAACS, J. D. & MARKHAM, A. F. 2003. Real-time PCR based on SYBR-Green I fluorescence: An alternative to the TaqMan assay for a relative quantification of gene rearrangements, gene amplifications and micro gene deletions. *BMC Biotechnology,* 3**,** 18.

POS, W., SETHI, D. K., CALL, M. J., SCHULZE, M.-S. E. D., ANDERS, A.-K., PYRDOL, J. & WUCHERPFENNIG, K. W. 2012. Crystal Structure of the HLA-DM - HLA-DR1 Complex Defines Mechanisms for Rapid Peptide Selection. *Cell,* 151**,** 1557-1568.

POTTS, W., BOWYER, J., JONES, H., TUCKER, D., FREEMONT, A. J., MILLEST, A., MARTIN, C., VERNON, W., NEERUNJUN, D., SLYNN, G., HARPER, F. & MACIEWICZ, R. 2004. Cathepsin L-deficient mice exhibit abnormal skin and bone development and show increased resistance to osteoporosis following ovariectomy. *International Journal of Experimental Pathology,* 85**,** 85-96.

PREVOSTO, C., USMANI, M. F., MCDONALD, S., GUMIENNY, A. M., KEY, T., GOODMAN, R. S., GASTON, J. S. H., DEERY, M. J. & BUSCH, R. 2016. Allele-Independent Turnover of Human Leukocyte Antigen (HLA) Class Ia Molecules. *PLOS ONE,* 11**,** e0161011.

PROCHIANTZ, A. 1999. Homeodomain-derived peptides. In and out of the cells. *Ann N Y Acad Sci,* 886**,** 172-9.

PROSSER, D. E. & JONES, G. 2004. Enzymes involved in the activation and inactivation of vitamin D. *Trends Biochem Sci,* 29**,** 664-73.

PUGLIATTI, M., HARBO, H. F., HOLMOY, T., KAMPMAN, M. T., MYHR, K. M., RIISE, T. & WOLFSON, C. 2008. Environmental risk factors in multiple sclerosis. *Acta Neurol Scand Suppl,* 188**,** 34-40.

PUIZDAR, V., ZAJC, T., ŽEROVNIK, E., RENKO, M., PIEPER, U., ESWAR, N., ŠALI, A., DOLENC, I. & TURK, V. 2012. Biochemical characterization and structural modeling of human cathepsin E variant 2 in comparison to the wild-type protein. *Biological chemistry,* 393**,** 177-186.

PULENDRAN, B. 2005. Variegation of the immune response with dendritic cells and pathogen recognition receptors. *J Immunol,* 174**,** 2457-65.

RAMAGOPALAN, S. V., DELUCA, G. C., DEGENHARDT, A. & EBERS, G. C. 2008. The genetics of clinical outcome in multiple sclerosis. *J Neuroimmunol,* 201-202**,** 183-99.
RAMAGOPALAN, S. V. & EBERS, G. C. 2009. Multiple sclerosis: major histocompatibility complexity and antigen presentation. *Genome Medicine,* 1**,** 105-105.
RAMAGOPALAN, S. V., HEGER, A., BERLANGA, A. J., MAUGERI, N. J., LINCOLN, M. R., BURRELL, A., HANDUNNETTHI, L., HANDEL, A. E., DISANTO, G., ORTON, S. M., WATSON, C. T., MORAHAN, J. M., GIOVANNONI, G., PONTING, C. P., EBERS, G. C. & KNIGHT, J. C. 2010. A ChIP-seq defined genome-wide map of vitamin D receptor binding: associations with disease and evolution. *Genome Res,* 20**,** 1352-60.
RAMAGOPALAN, S. V., MAUGERI, N. J., HANDUNNETTHI, L., LINCOLN, M. R., ORTON, S.-M., DYMENT, D. A., DELUCA, G. C., HERRERA, B. M., CHAO, M. J., SADOVNICK, A. D., EBERS, G. C. & KNIGHT, J. C. 2009. Expression of the Multiple Sclerosis-Associated MHC Class II Allele HLA-DRB1*1501 Is Regulated by Vitamin D. *PLOS Genetics,* 5**,** e1000369.
RAMMENSEE, H. G. 1995. CHEMISTRY OF PEPTIDES ASSOCIATED WITH MHC CLASS-I AND CLASS-II MOLECULES. *Current Opinion in Immunology,* 7**,** 85-96.
RAYCHAUDHURI, S. 2010. Recent advances in the genetics of rheumatoid arthritis. *Current opinion in rheumatology,* 22**,** 109-118.
RECHE, P. A. & REINHERZ, E. L. 2003. Sequence variability analysis of human class I and class II MHC molecules: functional and structural correlates of amino acid polymorphisms. *J Mol Biol,* 331**,** 623-41.
REICH, M., ZOU, F., SIENCZYK, M., OLEKSYSZYN, J., BOEHM, B. O. & BURSTER, T. 2011. Invariant chain processing is independent of cathepsin variation between primary human B cells/dendritic cells and B-lymphoblastoid cells. *Cellular Immunology,* 269**,** 96-103.
REINHECKEL, T., PETERS, C., KRÜGER, A., TURK, B. & VASILJEVA, O. 2012. Differential Impact of Cysteine Cathepsins on Genetic Mouse Models of De novo Carcinogenesis: Cathepsin B as Emerging Therapeutic Target. *Frontiers in Pharmacology,* 3**,** 133.
RIESE, R. J. & CHAPMAN, H. A. 2000. Cathepsins and compartmentalization in antigen presentation. *Current Opinion in Immunology,* 12**,** 107-113.
RIESE, R. J., WOLF, P. R., BROMME, D., NATKIN, L. R., VILLADANGOS, J. A., PLOEGH, H. L. & CHAPMAN, H. A. 1996. Essential role for cathepsin S in MHC class II-associated invariant chain processing and peptide loading. *Immunity,* 4**,** 357-66.
RIGBY, W. F., WAUGH, M. & GRAZIANO, R. F. 1990. Regulation of human monocyte HLA-DR and CD4 antigen expression, and antigen presentation by 1,25-dihydroxyvitamin D3. *Blood,* 76**,** 189-97.
ROBINSON, J., SOORMALLY, A. R., HAYHURST, J. D. & MARSH, S. G. 2016. The IPD-IMGT/HLA Database - New developments in reporting HLA variation. *Hum Immunol,* 77**,** 233-7.
ROCHE, P. A. & CRESSWELL, P. 1990. Invariant chain association with HLA-DR molecules inhibits immunogenic peptide binding. *Nature,* 345**,** 615-618.
ROCHE, P. A. & CRESSWELL, P. 2011. Proteolysis of the class II-associated invariant chain generates a pepetide binding site in intracellular HLA-DR molecules. *Journal of Immunology,* 187**,** 3150-3154.
ROCHE, P. A., MARKS, M. S. & CRESSWELL, P. J. 1991. Formation of a nine-subunit complex by HLA class II glycoproteins and the invariant chain. *Nature,* 354**,** 392.
ROLF, L., MURIS, A. H., HUPPERTS, R. & DAMOISEAUX, J. 2014. Vitamin D effects on B cell function in autoimmunity. *Ann N Y Acad Sci,* 1317**,** 84-91.
ROSSER, E. C. & MAURI, C. 2016. A clinical update on the significance of the gut microbiota in systemic autoimmunity. *J Autoimmun,* 74**,** 85-93.
ROVARIS, M., BARKHOF, F., CALABRESE, M., DE STEFANO, N., FAZEKAS, F., MILLER, D. H., MONTALBAN, X., POLMAN, C., ROCCA, M. A., THOMPSON, A. J., YOUSRY, T. A. & FILIPPI, M. 2009. MRI features of benign multiple sclerosis: toward a new definition of this disease phenotype. *Neurology,* 72**,** 1693-701.
ROXBURGH, R. H., SEAMAN, S. R., MASTERMAN, T., HENSIEK, A. E., SAWCER, S. J., VUKUSIC, S., ACHITI, I., CONFAVREUX, C., COUSTANS, M., LE PAGE, E., EDAN,

G., MCDONNELL, G. V., HAWKINS, S., TROJANO, M., LIGUORI, M., COCCO, E., MARROSU, M. G., TESSER, F., LEONE, M. A., WEBER, A., ZIPP, F., MITERSKI, B., EPPLEN, J. T., OTURAI, A., SORENSEN, P. S., CELIUS, E. G., LARA, N. T., MONTALBAN, X., VILLOSLADA, P., SILVA, A. M., MARTA, M., LEITE, I., DUBOIS, B., RUBIO, J., BUTZKUEVEN, H., KILPATRICK, T., MYCKO, M. P., SELMAJ, K. W., RIO, M. E., SA, M., SALEMI, G., SAVETTIERI, G., HILLERT, J. & COMPSTON, D. A. 2005. Multiple Sclerosis Severity Score: using disability and disease duration to rate disease severity. *Neurology,* 64**,** 1144-51.

RUNIA, T. F., HOP, W. C., DE RIJKE, Y. B., BULJEVAC, D. & HINTZEN, R. Q. 2012. Lower serum vitamin D levels are associated with a higher relapse risk in multiple sclerosis. *Neurology,* 79**,** 261-6.

RYAN, K. J. P., DANIEL, Z. C. T. R., CRAGGS, L. J. L., PARR, T. & BRAMELD, J. M. 2013. Dose-dependent effects of vitamin D on transdifferentiation of skeletal muscle cells to adipose cells. *The Journal of Endocrinology,* 217**,** 45-58.

SADEGH-NASSERI, S., NATARAJAN, S., CHOU, C.-L., HARTMAN, I. Z., NARAYAN, K. & KIM, A. 2010. Conformational heterogeneity of MHC class II induced upon binding to different peptides is a key regulator in antigen presentation and epitope selection. *Immunologic research,* 47**,** 56-64.

SALLUSTO, F. & LANZAVECCHIA, A. 2002. The instructive role of dendritic cells on T-cell responses. *Arthritis Research,* 4**,** S127-S132.

SALZER, J., HALLMANS, G., NYSTROM, M., STENLUND, H., WADELL, G. & SUNDSTROM, P. 2012. Vitamin D as a protective factor in multiple sclerosis. *Neurology,* 79**,** 2140-5.

SANTAMBROGIO, L., SATO, A. K., CARVEN, G. J., BELYANSKAYA, S. L., STROMINGER, J. L. & STERN, L. J. 1999. Extracellular antigen processing and presentation by immature dendritic cells. *Proceedings of the National Academy of Sciences of the United States of America,* 96**,** 15056-15061.

SAURER, L., MCCULLOUGH, K. C. & SUMMERFIELD, A. 2007. In vitro induction of mucosa-type dendritic cells by all-trans retinoic acid. *J Immunol,* 179**,** 3504-14.

SAWCER, S., HELLENTHAL, G., PIRINEN, M., SPENCER, C. C., PATSOPOULOS, N. A., MOUTSIANAS, L., DILTHEY, A., SU, Z., FREEMAN, C., HUNT, S. E., EDKINS, S., GRAY, E., BOOTH, D. R., POTTER, S. C., GORIS, A., BAND, G., OTURAI, A. B., STRANGE, A., SAARELA, J., BELLENGUEZ, C., FONTAINE, B., GILLMAN, M., HEMMER, B., GWILLIAM, R., ZIPP, F., JAYAKUMAR, A., MARTIN, R., LESLIE, S., HAWKINS, S., GIANNOULATOU, E., D'ALFONSO, S., BLACKBURN, H., MARTINELIIBONESCHI, F., LIDDLE, J., HARBO, H. F., PEREZ, M. L., SPURKLAND, A., WALLER, M. J., MYCKO, M. P., RICKETTS, M., COMABELLA, M., HAMMOND, N., KOCKUM, I., MCCANN, O. T., BAN, M., WHITTAKER, P., KEMPPINEN, A., WESTON, P., HAWKINS, C., WIDAA, S., ZAJICEK, J., DRONOV, S., ROBERTSON, N., BUMPSTEAD, S. J., BARCELLOS, L. F., RAVINDRARAJAH, R., ABRAHAM, R., ALFREDSSON, L., ARDLIE, K., AUBIN, C., BAKER, A., BAKER, K., BARANZINI, S. E., BERGAMASCHI, L., BERGAMASCHI, R., BERNSTEIN, A., BERTHELE, A., BOGGILD, M., BRADFIELD, J. P., BRASSAT, D., BROADLEY, S. A., BUCK, D., BUTZKUEVEN, H., CAPRA, R., CARROLL, W. M., CAVALLA, P., CELIUS, E. G., CEPOK, S., CHIAVACCI, R., CLERGET-DARPOUX, F., CLYSTERS, K., COMI, G., COSSBURN, M., COURNU-REBEIX, I., COX, M. B., COZEN, W., CREE, B. A., CROSS, A. H., CUSI, D., DALY, M. J., DAVIS, E., DE BAKKER, P. I., DEBOUVERIE, M., D'HOOGHE M, B., DIXON, K., DOBOSI, R., DUBOIS, B., ELLINGHAUS, D., ELOVAARA, I., ESPOSITO, F., et al. 2011. Genetic risk and a primary role for cell-mediated immune mechanisms in multiple sclerosis. *Nature,* 476**,** 214-9.

SCHASCHL, H., AITMAN, T. J. & VYSE, T. J. 2009. Copy number variation in the human genome and its implication in autoimmunity. *Clinical and Experimental Immunology,* 156**,** 12-16.

SCHMIDT, H., WILLIAMSON, D. & ASHLEY-KOCH, A. 2007. HLA-DR15 haplotype and multiple sclerosis: a HuGE review. *Am J Epidemiol,* 165**,** 1097-109.

SESTAK, A. L., FÜRNROHR, B. G., HARLEY, J. B., MERRILL, J. T. & NAMJOU, B. 2011. The genetics of systemic lupus erythematosus and implications for targeted therapy. *Annals of the Rheumatic Diseases,* 70**,** i37-i43.

SHIN, J. S., EBERSOLD, M., PYPAERT, M., DELAMARRE, L., HARTLEY, A. & MELLMAN, I. 2006. Surface expression of MHC class II in dendritic cells is controlled by regulated ubiquitination. *Nature,* 444**,** 115-8.

SILVERBERG, M. S., CHO, J. H., RIOUX, J. D., MCGOVERN, D. P., WU, J., ANNESE, V., ACHKAR, J. P., GOYETTE, P., SCOTT, R., XU, W., BARMADA, M. M., KLEI, L., DALY, M. J., ABRAHAM, C., BAYLESS, T. M., BOSSA, F., GRIFFITHS, A. M., IPPOLITI, A. F., LAHAIE, R. G., LATIANO, A., PARE, P., PROCTOR, D. D., REGUEIRO, M. D., STEINHART, A. H., TARGAN, S. R., SCHUMM, L. P., KISTNER, E. O., LEE, A. T., GREGERSEN, P. K., ROTTER, J. I., BRANT, S. R., TAYLOR, K. D., ROEDER, K. & DUERR, R. H. 2009. Ulcerative colitis-risk loci on chromosomes 1p36 and 12q15 found by genome-wide association study. *Nat Genet,* 41**,** 216-20.

SIMPSON, S., JR., TAYLOR, B., BLIZZARD, L., PONSONBY, A. L., PITTAS, F., TREMLETT, H., DWYER, T., GIES, P. & VAN DER MEI, I. 2010. Higher 25-hydroxyvitamin D is associated with lower relapse risk in multiple sclerosis. *Ann Neurol,* 68**,** 193-203.

SINGER, O. & VERMA, I. M. 2008. Applications of Lentiviral Vectors for shRNA Delivery and Transgenesis. *Current gene therapy,* 8**,** 483-488.

SLIVAC, I., BLAJIĆ, V., RADOŠEVIĆ, K., KNIEWALD, Z. & GAURINA SRČEK, V. 2010. Influence of different ammonium, lactate and glutamine concentrations on CCO cell growth. *Cytotechnology,* 62**,** 585-594.

SLOAN, V. S., CAMERON, P., PORTER, G., GAMMON, M., AMAYA, M., MELLINS, E. & ZALLER, D. M. 1995. MEDIATION BY HLA-DM OF DISSOCIATION OF PEPTIDES FROM HLA-DR. *Nature,* 375**,** 802-806.

SMITH, D. A. & GERMOLEC, D. R. 1999. Introduction to immunology and autoimmunity. *Environmental Health Perspectives,* 107**,** 661-665.

SMITH, P. K., KROHN, R. I., HERMANSON, G. T., MALLIA, A. K., GARTNER, F. H., PROVENZANO, M. D., FUJIMOTO, E. K., GOEKE, N. M., OLSON, B. J. & KLENK, D. C. 1985. Measurement of protein using bicinchoninic acid. *Anal Biochem,* 150**,** 76-85.

SMOLDERS, J. & DAMOISEAUX, J. 2011. Vitamin D as a T-cell modulator in multiple sclerosis. *Vitam Horm,* 86**,** 401-28.

SNELL, G. D. 1948. Methods for the study of histocompatibility genes. *J Genet,* 49**,** 87-108.

SOCHOROVA, K., BUDINSKY, V., ROZKOVA, D., TOBIASOVA, Z., DUSILOVA-SULKOVA, S., SPISEK, R. & BARTUNKOVA, J. 2009. Paricalcitol (19-nor-1,25-dihydroxyvitamin D2) and calcitriol (1,25-dihydroxyvitamin D3) exert potent immunomodulatory effects on dendritic cells and inhibit induction of antigen-specific T cells. *Clin Immunol,* 133**,** 69-77.

SODERSTROM, M., YA-PING, J., HILLERT, J. & LINK, H. 1998. Optic neuritis: prognosis for multiple sclerosis from MRI, CSF, and HLA findings. *Neurology,* 50**,** 708-14.

STOECKLE, C., SOMMANDAS, V., ADAMOPOULOU, E., BELISLE, K., SCHIEKOFER, S., MELMS, A., WEBER, E., DRIESSEN, C., BOEHM, B. O., TOLOSA, E. & BURSTER, T. 2009. Cathepsin G is differentially expressed in primary human antigen-presenting cells. *Cell Immunol,* 255**,** 41-5.

STOKA, V., TURK, V. & TURK, B. 2016. Lysosomal cathepsins and their regulation in aging and neurodegeneration. *Ageing Research Reviews,* 32**,** 22-37.

STOKKERS, P., REITSMA, P., TYTGAT, G. & VAN DEVENTER, S. J. H. 1999. HLA-DR and -DQ phenotypes in inflammatory bowel disease: a meta-analysis. *Gut,* 45**,** 395-401.

SZECSI, P. B. 1992. The aspartic proteases. *Scand J Clin Lab Invest Suppl,* 210**,** 5-22.

TANG, J. & WONG, R. N. 1987. Evolution in the structure and function of aspartic proteases. *J Cell Biochem,* 33**,** 53-63.

TAVERA-MENDOZA, L., WANG, T. T., LALLEMANT, B., ZHANG, R., NAGAI, Y., BOURDEAU, V., RAMIREZ-CALDERON, M., DESBARATS, J., MADER, S. & WHITE, J. H. 2006. Convergence of vitamin D and retinoic acid signalling at a common hormone response element. *EMBO Rep,* 7**,** 180-5.

TEN BROEKE, T., DE GRAAFF, A., VAN'T VELD ESTHER, M., WAUBEN MARCA, H. M., STOORVOGEL, W. & WUBBOLTS, R. 2010. Trafficking of MHC Class II in Dendritic Cells is Dependent on but Not Regulated by Degradation of Its Associated Invariant Chain. *Traffic,* 11**,** 324-331.

TEN BROEKE, T., WUBBOLTS, R. & STOORVOGEL, W. 2013. MHC Class II Antigen Presentation by Dendritic Cells Regulated through Endosomal Sorting. *Cold Spring Harbor Perspectives in Biology,* 5**,** a016873.

THIBODEAU, J., BOURGEOIS-DAIGNEAULT, M. C., HUPPE, G., TREMBLAY, J., AUMONT, A., HOUDE, M., BARTEE, E., BRUNET, A., GAUVREAU, M. E., DE GASSART, A., GATTI, E., BARIL, M., CLOUTIER, M., BONTRON, S., FRUH, K., LAMARRE, D. & STEIMLE, V. 2008. Interleukin-10-induced MARCH1 mediates intracellular sequestration of MHC class II in monocytes. *Eur J Immunol,* 38**,** 1225-30.

THOMPSON, A. J., BANWELL, B. L., BARKHOF, F., CARROLL, W. M., COETZEE, T., COMI, G., CORREALE, J., FAZEKAS, F., FILIPPI, M., FREEDMAN, M. S., FUJIHARA, K., GALETTA, S. L., HARTUNG, H. P., KAPPOS, L., LUBLIN, F. D., MARRIE, R. A., MILLER, A. E., MILLER, D. H., MONTALBAN, X., MOWRY, E. M., SORENSEN, P. S., TINTORÉ, M., TRABOULSEE, A. L., TROJANO, M., UITDEHAAG, B. M. J., VUKUSIC, S., WAUBANT, E., WEINSHENKER, B. G., REINGOLD, S. C. & COHEN, J. A. 2018. Diagnosis of multiple sclerosis: 2017 revisions of the McDonald criteria. *The Lancet Neurology,* 17**,** 162-173.

THOMPSON, P. D., HSIEH, J. C., WHITFIELD, G. K., HAUSSLER, C. A., JURUTKA, P. W., GALLIGAN, M. A., TILLMAN, J. B., SPINDLER, S. R. & HAUSSLER, M. R. 1999. Vitamin D receptor displays DNA binding and transactivation as a heterodimer with the retinoid X receptor, but not with the thyroid hormone receptor. *J Cell Biochem,* 75**,** 462-80.

THOMPSON, P. D., JURUTKA, P. W., HAUSSLER, C. A., WHITFIELD, G. K. & HAUSSLER, M. R. 1998. Heterodimeric DNA binding by the vitamin D receptor and retinoid X receptors is enhanced by 1,25-dihydroxyvitamin D3 and inhibited by 9-cis-retinoic acid. Evidence for allosteric receptor interactions. *J Biol Chem,* 273**,** 8483-91.

THORSBY, E. 2009. A short history of HLA. *Tissue Antigens,* 74**,** 101-16.

TIOSANO, D., WILDBAUM, G., GEPSTEIN, V., VERBITSKY, O., WEISMAN, Y., KARIN, N. & EZTIONI, A. 2013. The role of vitamin D receptor in innate and adaptive immunity: a study in hereditary vitamin D-resistant rickets patients. *J Clin Endocrinol Metab,* 98**,** 1685-93.

TRAPP, B. D. & NAVE, K. A. 2008. Multiple sclerosis: an immune or neurodegenerative disorder? *Annu Rev Neurosci,* 31**,** 247-69.

TRAVIS, J. 2009. Origins. On the origin of the immune system. *Science,* 324**,** 580-2.

TROWSDALE, J. 1993. Genomic structure and function in the MHC. *Trends in Genetics,* 9**,** 117-122.

TROWSDALE, J. & KNIGHT, J. C. 2013. Major Histocompatibility Complex Genomics and Human Disease. *Annual review of genomics and human genetics,* 14**,** 301-323.

TURK, B., TURK, D. & TURK, V. 2000. Lysosomal cysteine proteases: more than scavengers. *Biochim Biophys Acta,* 1477**,** 98-111.

TURK, V., STOKA, V., VASILJEVA, O., RENKO, M., SUN, T., TURK, B. & TURK, D. 2012. Cysteine cathepsins: From structure, function and regulation to new frontiers. *Biochimica et Biophysica Acta (BBA) - Proteins and Proteomics,* 1824**,** 68-88.

TURK, V., TURK, B. & TURK, D. 2001. Lysosomal cysteine proteases: facts and opportunities. *The EMBO Journal,* 20**,** 4629-4633.

TURVEY, S. E. & BROIDE, D. H. 2010. Chapter 2: Innate Immunity. *The Journal of allergy and clinical immunology,* 125**,** S24-S32.

TZE, L. E., HORIKAWA, K., DOMASCHENZ, H., HOWARD, D. R., ROOTS, C. M., RIGBY, R. J., WAY, D. A., OHMURA-HOSHINO, M., ISHIDO, S., ANDONIOU, C. E., DEGLI-ESPOSTI, M. A. & GOODNOW, C. C. 2011. CD83 increases MHC II and CD86 on dendritic cells by opposing IL-10-driven MARCH1-mediated ubiquitination and degradation. *J Exp Med,* 208**,** 149-65.

VÄLIKANGAS, T., SUOMI, T. & ELO, L. L. 2017. A comprehensive evaluation of popular proteomics software workflows for label-free proteome quantification and imputation. *Briefings in Bioinformatics***,** bbx054-bbx054.

VAN DER MEI, I. A., PONSONBY, A. L., DWYER, T., BLIZZARD, L., TAYLOR, B. V., KILPATRICK, T., BUTZKUEVEN, H. & MCMICHAEL, A. J. 2007. Vitamin D levels in people with multiple sclerosis and community controls in Tasmania, Australia. *J Neurol,* 254**,** 581-90.

VAN KASTEREN, S. I. & OVERKLEEFT, H. S. 2014. Endo-lysosomal proteases in antigen presentation. *Current Opinion in Chemical Biology,* 23**,** 8-15.

VAN LITH, M., MCEWEN-SMITH, R. M. & BENHAM, A. M. 2010. HLA-DP, HLA-DQ, and HLA-DR have different requirements for invariant chain and HLA-DM. *J Biol Chem,* 285**,** 40800-8.

VAN LUIJN, M. M., WESTERS, T. M., CHAMULEAU, M. E., VAN HAM, S. M., OSSENKOPPELE, G. J. & VAN DE LOOSDRECHT, A. A. 2011. Class II-associated invariant chain peptide expression represents a novel parameter for flow cytometric detection of acute promyelocytic leukemia. *Am J Pathol,* 179**,** 2157-61.

VAN NIEL, G., WUBBOLTS, R., TEN BROEKE, T., BUSCHOW, S. I., OSSENDORP, F. A., MELIEF, C. J., RAPOSO, G., VAN BALKOM, B. W. & STOORVOGEL, W. 2006. Dendritic cells regulate exposure of MHC class II at their plasma membrane by oligoubiquitination. *Immunity,* 25**,** 885-94.

VANTOUROUT, P. & HAYDAY, A. 2013. Six-of-the-best: unique contributions of γδ T cells to immunology(). *Nature reviews. Immunology,* 13**,** 88-100.

VELDURTHY, V., WEI, R., OZ, L., DHAWAN, P., JEON, Y. H. & CHRISTAKOS, S. 2016. Vitamin D, calcium homeostasis and aging. *Bone Research,* 4**,** 16041.

VILLADANGOS, J. A., RIESE, R. J., PETERS, C., CHAPMAN, H. A. & PLOEGH, H. L. 1997. Degradation of Mouse Invariant Chain: Roles of Cathepsins S and D and the Influence of Major Histocompatibility Complex Polymorphism. *The Journal of Experimental Medicine,* 186**,** 549-560.

VOGT, A. B., ARNDT, S. O., HAMMERLING, G. J. & KROPSHOFER, H. 1999. Quality control of MHC class II associated peptides by HLA-DM/H2-M. *Semin Immunol,* 11**,** 391-403.

VOJDANI, A., POLLARD, K. M. & CAMPBELL, A. W. 2014. Environmental Triggers and Autoimmunity. *Autoimmune Diseases,* 2014**,** 798029.

WALSENG, E., FURUTA, K., GOLDSZMID, R. S., WEIH, K. A., SHER, A. & ROCHE, P. A. 2010. Dendritic cell activation prevents MHC class II ubiquitination and promotes MHC class II survival regardless of the activation stimulus. *J Biol Chem,* 285**,** 41749-54.

WALSH, C. & CEPKO, C. 1988. Clonally related cortical cells show several migration patterns. *Science,* 241**,** 1342-1345.

WANG, B., SHI, G. P., YAO, P. M., LI, Z., CHAPMAN, H. A. & BROMME, D. 1998. Human cathepsin F. Molecular cloning, functional expression, tissue localization, and enzymatic characterization. *J Biol Chem,* 273**,** 32000-8.

WANG, T. T., DABBAS, B., LAPERRIERE, D., BITTON, A. J., SOUALHINE, H., TAVERA-MENDOZA, L. E., DIONNE, S., SERVANT, M. J., BITTON, A., SEIDMAN, E. G., MADER, S., BEHR, M. A. & WHITE, J. H. 2010. Direct and indirect induction by 1,25-dihydroxyvitamin D3 of the NOD2/CARD15-defensin beta2 innate immune pathway defective in Crohn disease. *J Biol Chem,* 285**,** 2227-31.

WARRINGTON, R., WATSON, W., KIM, H. L. & ANTONETTI, F. R. 2011. An introduction to immunology and immunopathology. *Allergy, Asthma, and Clinical Immunology : Official Journal of the Canadian Society of Allergy and Clinical Immunology,* 7**,** S1-S1.

WATTS, C. 2012. The endosome–lysosome pathway and information generation in the immune system(). *Biochimica et Biophysica Acta,* 1824**,** 14-21.

WEATHERBY, S. J. M., THOMSON, W., PEPPER, L., DONN, R., WORTHINGTON, J., MANN, C. L. A., DAVIES, M. B., FRYER, A. A., BOGGILD, M. D., YOUNG, C. A., JONES, P. W., STRANGE, R. C., OLLIER, W. E. R. & HAWKINS, C. P. 2001. HLA-DRB1 and disease outcome in multiple sclerosis. *Journal of Neurology,* 248**,** 304-310.

WESTBERG, M., FEYCHTING, M., JONSSON, F., NISE, G. & GUSTAVSSON, P. 2009. Occupational exposure to UV light and mortality from multiple sclerosis. *Am J Ind Med,* 52**,** 353-7.

WHERRY, E. J. & MASOPUST, D. 2016. Chapter 5 - Adaptive Immunity: Neutralizing, Eliminating, and Remembering for the Next Time A2 - Katze, Michael G. *In:* KORTH, M. J., LAW, G. L. & NATHANSON, N. (eds.) *Viral Pathogenesis (Third Edition)*. Boston: Academic Press.

WHITE, J. H. 2004. Profiling 1,25-dihydroxyvitamin D3-regulated gene expression by microarray analysis. *The Journal of Steroid Biochemistry and Molecular Biology,* 89-90**,** 239-244.

WILKINS, M. R., LINDSKOG, I., GASTEIGER, E., BAIROCH, A., SANCHEZ, J. C., HOCHSTRASSER, D. F. & APPEL, R. D. 1997. Detailed peptide characterization using PEPTIDEMASS--a World-Wide-Web-accessible tool. *Electrophoresis,* 18**,** 403-8.

WILKINS, M. R., SANCHEZ, J. C., GOOLEY, A. A., APPEL, R. D., HUMPHERY-SMITH, I., HOCHSTRASSER, D. F. & WILLIAMS, K. L. 1996. Progress with proteome projects: why all proteins expressed by a genome should be identified and how to do it. *Biotechnol Genet Eng Rev,* 13**,** 19-50.

WILLER, C. J., DYMENT, D. A., RISCH, N. J., SADOVNICK, A. D. & EBERS, G. C. 2003. Twin concordance and sibling recurrence rates in multiple sclerosis. *Proc Natl Acad Sci U S A,* 100**,** 12877-82.

WILSON, N. S., EL-SUKKARI, D. & VILLADANGOS, J. A. 2004. Dendritic cells constitutively present self antigens in their immature state in vivo and regulate antigen presentation by controlling the rates of MHC class II synthesis and endocytosis. *Blood,* 103**,** 2187.

WOOLLEY, C. F., HAYES, M. A., MAHANTI, P., DOUGLASS GILMAN, S. & TAYLOR, T. 2015. Theoretical limitations of quantification for noncompetitive sandwich immunoassays. *Analytical and bioanalytical chemistry,* 407**,** 8605-8615.

WRIGHT, M. H., BERLIN, I. & NASH, P. D. 2011. Regulation of endocytic sorting by ESCRT-DUB-mediated deubiquitination. *Cell Biochem Biophys,* 60**,** 39-46.

WRZOSEK, M., LUKASZKIEWICZ, J., WRZOSEK, M., JAKUBCZYK, A., MATSUMOTO, H., PIATKIEWICZ, P., RADZIWON-ZALESKA, M., WOJNAR, M. & NOWICKA, G. 2013. Vitamin D and the central nervous system. *Pharmacol Rep,* 65**,** 271-8.

YATES, J. R., RUSE, C. I. & NAKORCHEVSKY, A. 2009. Proteomics by mass spectrometry: approaches, advances, and applications. *Annu Rev Biomed Eng,* 11**,** 49-79.

YOSHIMURA, S., ISOBE, N., YONEKAWA, T., MATSUSHITA, T., MASAKI, K., SATO, S., KAWANO, Y., YAMAMOTO, K., KIRA, J.-I. & THE SOUTH JAPAN MULTIPLE SCLEROSIS GENETICS, C. 2012. Genetic and Infectious Profiles of Japanese Multiple Sclerosis Patients. *PLOS ONE,* 7**,** e48592.

YOUNG, L. J., WILSON, N. S., SCHNORRER, P., PROIETTO, A., TEN BROEKE, T., MATSUKI, Y., MOUNT, A. M., BELZ, G. T., O'KEEFFE, M., OHMURA-HOSHINO, M., ISHIDO, S., STOORVOGEL, W., HEATH, W. R., SHORTMAN, K. & VILLADANGOS, J. A. 2008. Differential MHC class II synthesis and ubiquitination confers distinct antigen-presenting properties on conventional and plasmacytoid dendritic cells. *Nat Immunol,* 9**,** 1244-52.

ZAIDI, N., BURSTER, T., SOMMANDAS, V., HERRMANN, T., BOEHM, B. O., DRIESSEN, C., VOELTER, W. & KALBACHER, H. 2007. A novel cell penetrating aspartic protease inhibitor blocks processing and presentation of tetanus toxoid more efficiently than pepstatin A. *Biochemical and Biophysical Research Communications,* 364**,** 243-249.

ZHAO, J. & LEVER, A. M. L. 2007. Lentivirus-Mediated Gene Expression. *In:* ZHANG, J. & ROKOSH, G. (eds.) *Cardiac Gene Expression: Methods and Protocols.* Totowa, NJ: Humana Press.

ZHU, J. & PAUL, W. E. 2010. Heterogeneity and plasticity of T helper cells. *Cell Res,* 20**,** 4-12.

ZHU, J. G., OCHALEK, J. T., KAUFMANN, M., JONES, G. & DELUCA, H. F. 2013. CYP2R1 is a major, but not exclusive, contributor to 25-hydroxyvitamin D production in vivo. *Proc Natl Acad Sci U S A,* 110**,** 15650-5.